THE DEVELOPMENT OF METAL COMPLEXES AS HYDROLYTIC AND OXIDATIVE CATALYSTS

A thesis presented by Thomas Clifford to the University of St. Andrews in application for the degree of Doctor of Philosophy (March 1996)

Declaration

I, Thomas Clifford, hereby certify that this thesis has been composed by myself, that it is a record of my work and it has not been accepted in partial or complete fulfillment of any other degree or professional qualification.

Signed_ ___ date 20th March 96

I was admitted to the Faculty of Science of the University of St. Andrews under Ordinance General No.12 on the 1st of October 1992 and as a candidate for the Degree of Ph.D. on the 1st of October 1992.

Signed_ _ date 20th March 96

I hereby certify that the candidate has fulfilled the conditions of the Resolution and Regulations appropriate to the Degree of Ph.D

Signed___ ____ date 20/3/96.

Supervisor, R.W.Hay

Copyright

In submitting this thesis to the University of St.Andrews, I understand that I am giving permission for it to be made available for its use in accordance with the regulations of the University library for the time being in force, subject to any copyright vested in the work not being affected thereby. I also understand that the title and abstract will be published, and that a copy of the work may also be made and supplied to any *bona fide* library or research worker.

Dedication

To Mum and Dad

and the Ringers of St.Pauls, Dundee

Acknowledgments

I wish to acknowledge the MOD for funding this project, and the British council for a visit to Heidelburg.

I would like to express my gratitude to Professor R.W.Hay for three years of wise advice and entertaining lunch time conversation. Thanks also go to Dr.N.Govan (MOD) handling the nasties, Dr.Hassan for teaching me the ways of potentiometric titrations and Dr.P.Gans for patience in getting HYPERQUAD debugged and running. I would also like to thank Professor P.Comba and Dr. D.T.Richens for organising a brief working visit to Heidelburg and Dr.P.Lightfoot for determining all the crystal structures in this project.

Finally, thanks to the Ringers of St. Pauls Cathedral, especially Christina and Norma for an escape from chemistry.

List of Abbreviations

[B]	mmols of base
[L]	mmols of ligand
$[T_L]$	molar concentration of ligand
$[T_M]$	molar concentration of metal ion
a	activity
acac	pentane-2,4-dione (acetylacetonate)
β	gross or cumulative equilibrium constant
br	broad
Brij	polyether surfactant ($CH_3(CH_2)_7CH{=}CH(CH_2)_8(OCH_2CH_2)_{10}OH$)
cm	centimeters
δ	bending vibration (IR spectroscopy)
dd	doublet of doublets (NMR)
decomp.	decompose
δ oop	out of plane bending vibration (IR spectroscopy)
dien	1,5-diamino-3-azapentane (diethylenetriamine)
dm	decimeter
DMB	3,7-diazabicyclo[3.3.1]nonane (dimethyl bispidine)
dmbipy	6.11-dimethylbipyridine
dmdach	N,N'-dimethyl-1,4-diazacyclohexane
dmdaco	N,N'-dimethyl-1,5-diazacyclooctane
DMF	dimethylformamide
DMSO	dimethylsulphoxide
dmtpt	2,6,10-triaminododecane

DNPDEP	1,4-dinitrophenol diethylphosphate
ε	extinction cefficient
ether	diethylether
EtOH	ethanol
FTIR	Fourier transform infrared
γ	wagging vibration (IR spectroscopy)
GCMS	Gas chromatographic mass spectroscopy
H	hydrogen ion
HD	*bis*-(2-chloroethyl)sulphide (mustard)
hpnp	2-hydroxypropyl-4-nitrophenyl phosphate
I	ionic strength
IR	infrared, infrared spectroscopy
imid.	imidazole
K	stepwise or consecutive equilibrium constant
k_{obs}	observed pseudo first order rate constant
Λ_M	molar conductivity
λ_{max}	wavelength at maximum ε
MEA	1,4,7,16,19,22-hexaaza[9.9]metacyclophane
MeOH	methanol
MES	morpholine ethane sulphonate
MHz	Mega Hertz
MPA	1,5,9,18,22,26-hexaaza[11.11]metacyclophane
mustard	*bis*-(2-chloroethyl)sulphide (HD)
NMR	nuclear magnetic resonance
O/W	oil in water
PEA	4,7,16,19,22-hexaaza[9.9]paracyclophane
pH	$-\log[H^+]$
pK_a	-logK
PPA	1,5,9,18,22,26-hexaaza[11.11]paracyclophane

Pydpa	5-(2'-pyridylmethyl)-1,5,9-triazanonane
Q	equilibrium quotient
R	gas constant
S	siemens
s	second
σ	standard deviation
SDS	sodium dodecyl sulphate
T	temperature
tt	triplet of triplets (NMR)
tmen	N,N'-2,4-dimethyl-2,4-diazapentane (tetramethylethylenediamine
TMS	tetramethylsilane
tosyl	toluene sulphonate
tren	ligand 2,2',2"-Triaminotriethylamine
trpn	2,2',2"-Triaminotriethylamine
ν	bond streching (IR spectroscopy)
UV	ultraviolet
Uvis	ultraviolet/visible
vw	very weak
W/O	water in oil
wt	weight

Abstract

Abstract

The activity of benzimidazole copper(II) and zinc(II) complexes were accessed and found to be poor catalysts for the hydrolysis of phosphotriesters. The solution chemistry, in a mixed methanol-water solvent system indicates this is partially due to low formation constants for the hydroxy-aqua complexes.

A number of metal complexes of 3,3',3''-triaminotripropylamine (trpn) and 5-(2'-pyridylmethyl)-1,5,9-triazanonane (pydpa) have been synthesised and characterised. The equilibrium constants for the formation of complexes between 3,3',3''-triaminotriethylamine (tren) and pydpa and the metal ions cobalt(II), nickel(II), copper(II) and zinc(II) have been determined in aqueous solution and comparisons made with the ligand trpn.

The cobalt(II), nickel(II), copper(II) and zinc(II) complexes of a range of *para-* and *meta-*cyclophanes have been synthesised and characterised. The equilibrium constants for the copper complexes have been determined in aqueous solution. The dicopper complexes of 1,4,7,16,19,22-hexaaza[9.9]paracyclophane (PEA) and 1,4,7,16,19,22-hexaaza[9.9]metacyclophane (MEA) have been investigated for activity towards 2, dinitrophenol diethyl phosphate and found to be moderately active. The crystal structures for the complexes indicate that the copper centres are too far apart for a mechanism involving attack of bound hydroxide on one metal centre at phosphate bound on the other.

An attempt has been made to rationally design new catalysts for the hydrolysis of phosphate esters. Using the MM+ forcefield in HYPERCHEM a number of ligands were investigated and the most promising ligand [N,N'-dimethyl 3,7-diazabicyclo[3.3.1]nonane (DMB)] was synthesised. The copper complex was found to have unusually slow dissociation kinetics, but was unstable at neutral pH.

Oxidation catalysts have been investigated to find new decontaminants for the chemical warfare agent mustard [*bis*-(2-chloroethyl)sulphide]. The complexes $VO(acac)_2$ and $[Mn_2(III)L_2(CH_3CO_2)_2\mu(O)]^{2+}$ (L=1, 4, 7 trimethyl-1, 4, 7 triazacyclononane) in microemulsions were found to catalyse the oxidation of mustard by t-butyl hydroperoxide. $[Mn_2(III)L_2(CH_3CO_2)_2\mu(O)]^{2+}$ catalysed the rapid oxidation to the sulphone and $VO(acac)_2$ to the sulphoxide. Since the sulphone is physiologically active the manganese complex is not

a suitable catalyst. The vanadyl catalyst may prove to be an effective, cheap, and selective catalyst for the decontamination of mustard (HD).

Binucleating Hexaaza Macrocycle(1,4,7,16,19,22-hexaaza[9.9]paracyclophane (PEA) and its Methylated Derivative 1,4,7,16,19,22-Hexamethyl-1,4,7,16,19,22-hexaaza[9.9]paracyclophane (Me6PEA) and Its Copper(II) and Zinc(II) Complexes, Synthesis, and Solution Chemistry of The Copper Complex.

Chapter 1

Introduction

Introduction

Current Decontamination Techniques

The nerve agent group of Chemical Warfare Agents (Figure 1) produce their physiological effects by inhibiting the enzyme acetylcholinesterase which hydrolyses acetylcholine.

Diagram of a synaps inhibited by a nerve agent.

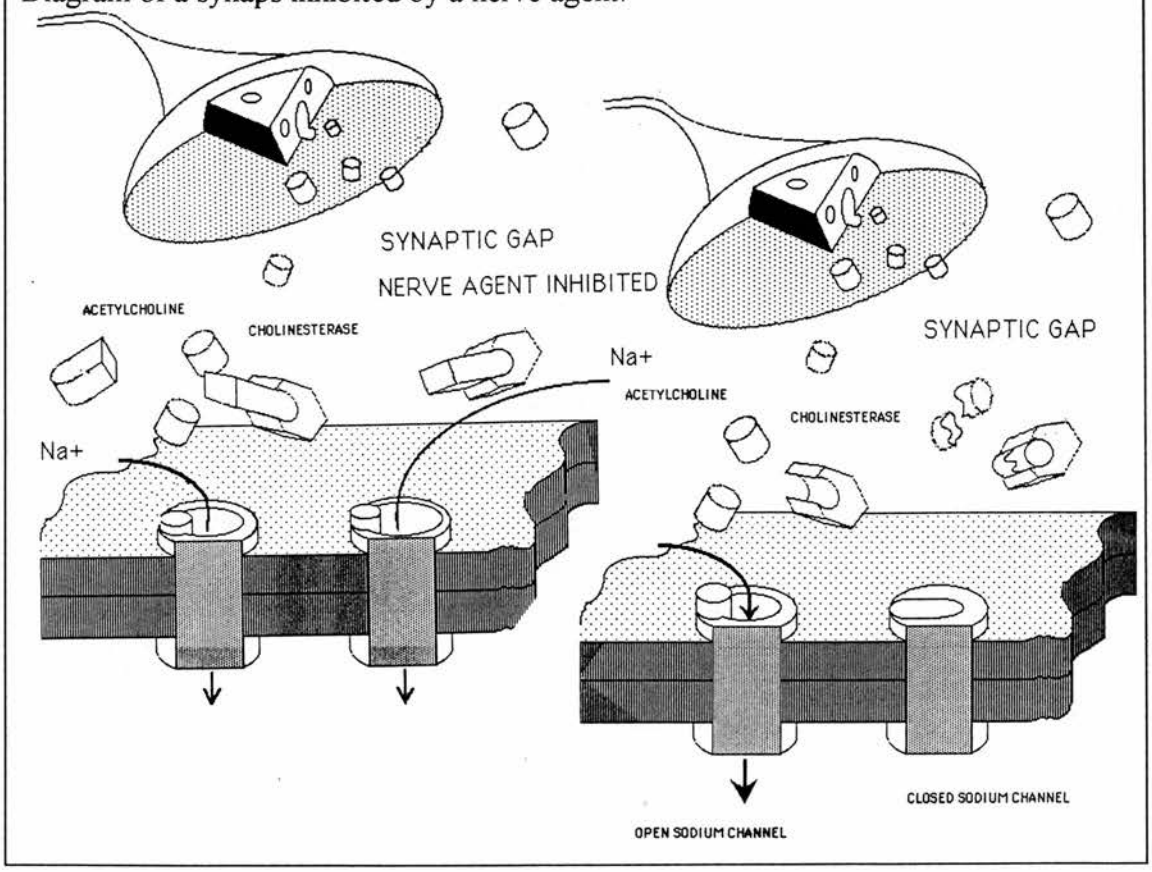

Acetylcholine thus remains available to continuously trigger nerve impulses, resulting in overstimulation of muscle cells.

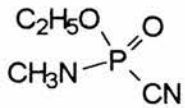

Tabun (GA)

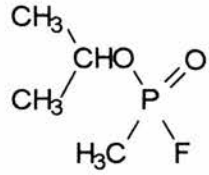

Sarin (GB)

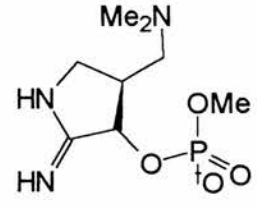

ANATOXIN-A(S)

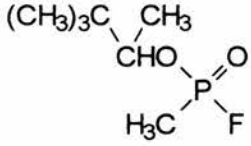

Soman (GD)

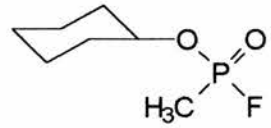

(GF)

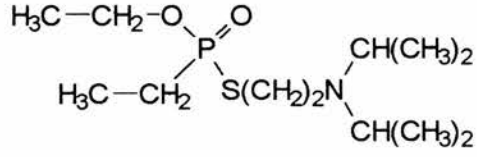

Agent VX

Figure 1

Cholinesterase is inhibited by the irreversible phosphorylation of serine, Figure 2.

Figure 2

Release of fluoride is irreversible and the active site of the enzyme is blocked. Decontamination of these CW agents may be achieved by breaking of the P-F bond or P-O bond, or by an oxidative route. P-F or P-O bond breaking occurs by nucleophilic substitution and a variety of nucleophiles have been used for decontamination purposes:

Nucleophilic Attack

a) Water and Hydroxide.- Use of water as a decontaminant (Figure 3) is unsophisticated but effective in many cases. Aqueous basic solutions (NaOH or $Ca(OH)_2$ slurry) are used regularly for the small scale decontamination of laboratory equipment and glassware. Their effectiveness depends largely on the solubility of the agent in water. As GB and GD are both water soluble they can be effectively destroyed by this method. An added benefit of using $Ca(OH)_2$ is that fluoride is removed from solution as insoluble CaF_2.

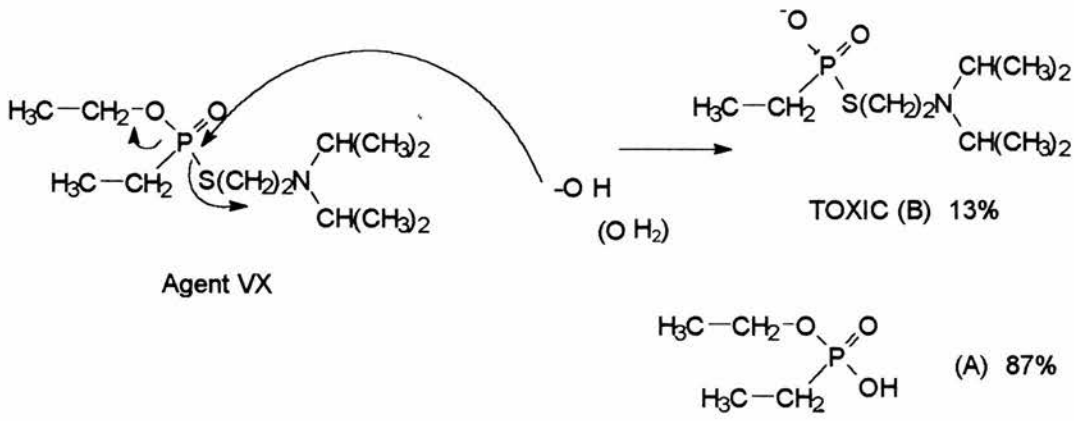

Figure 3

The agent VX, has a lower solubility in alkaline media, and is not as quickly destroyed as GB or GD. Base hydrolysis is some 10^{-4} times slower than that of GB or GD. A toxic thiolate anion is formed (Figure 4). This ion is destroyed by 5M NaOH at elevated temperature (90-80°C). Addition of MeOH improves the solubility of VX in water, resulting in an improvement in its rate of destruction.

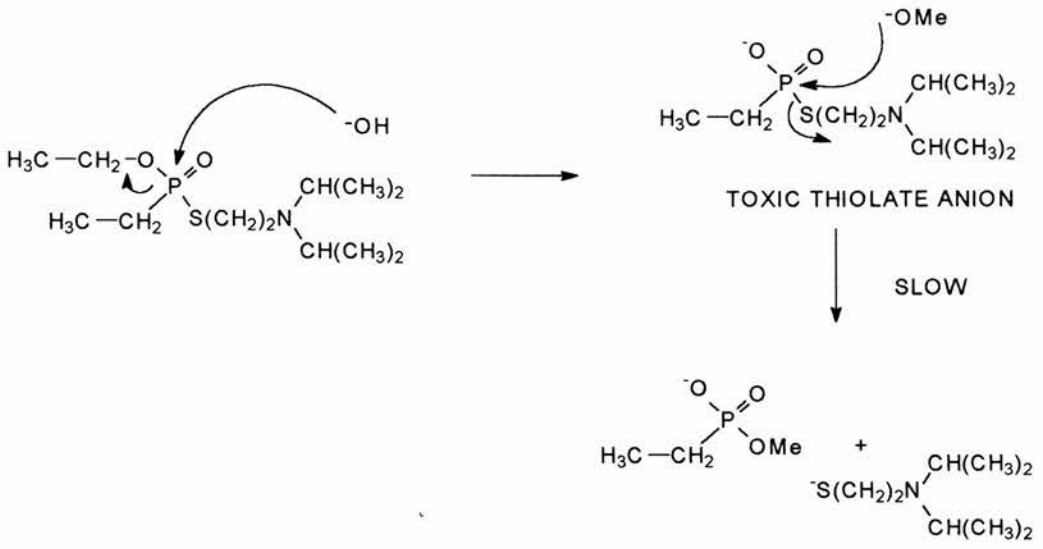

Figure 4

b)*Alcohol Solvents.*- 7M KOH solutions can be made up with absolute methanol to give a concentrated source of methoxide. G agents react rapidly to form diesters at room

Figure 5

temperature e.g GB, Figure 5

Hydrolysis of VX is rather slower and forms a short lived thioester in a side reaction, Figure 6.

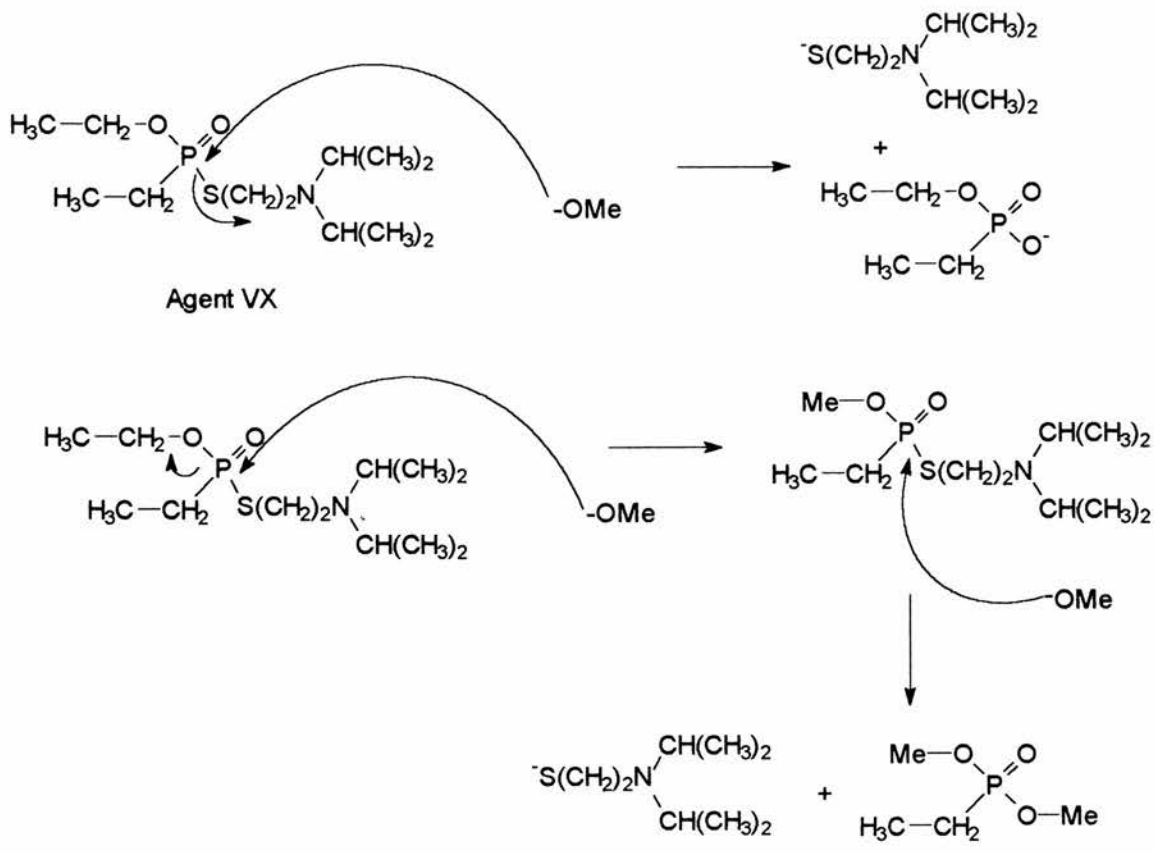

Figure 6

The presence of water must be minimised (<10%) to prevent the formation of the long lived toxic thiolate anion.

c) Hydroperoxide anion HO_2^-. Hydrogen peroxide with a pK_a of 11.0 will form the anion in the presence of sodium hydroxide (Figure 7). The hydroperoxide anion is a particularly active nucleophile against VX, breaking the P-S bond some 40 times faster than hydroxide. The sulfide leaving group is subsequently oxidised to sulfate.

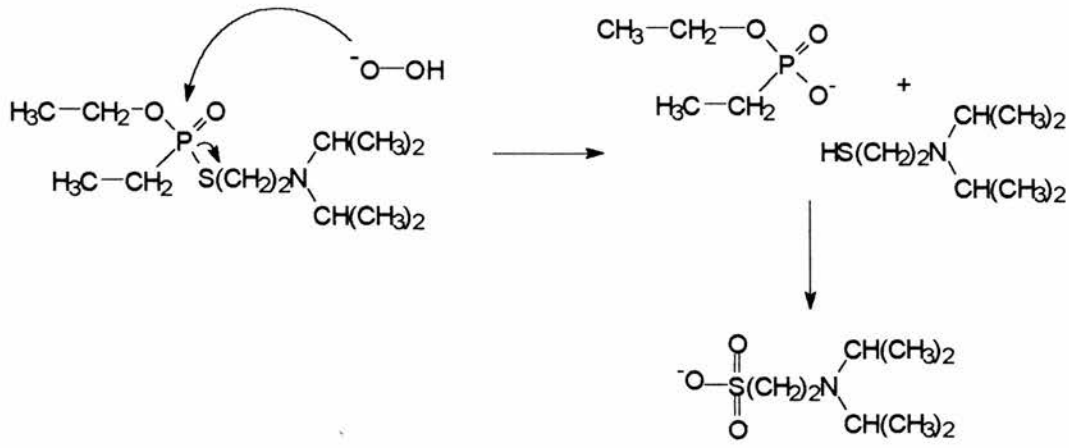

Figure 7

Hydrogen peroxide is attractive as a decontaminant as it generates no solid wastes and hydrogen peroxide is readily decomposed to water.

d) Ethanolamine.- Ethanolamine is an active nucleophile towards the G agents displacing

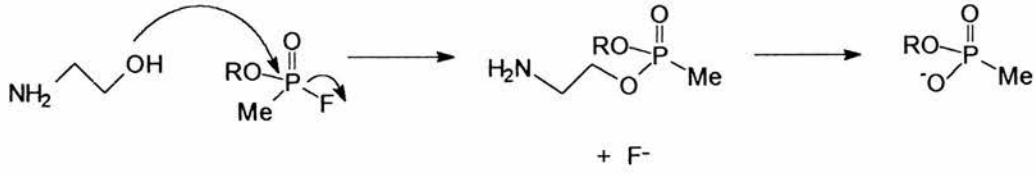

Figure 8

fluoride, (Figure 8) the hydroxyl group acting as the nucleophile.

The agent VX reacts more slowly and is attacked by both the hydroxyl and amino groups of ethanolamine (Figure 9). In the presence of water these products hydrolyse further.

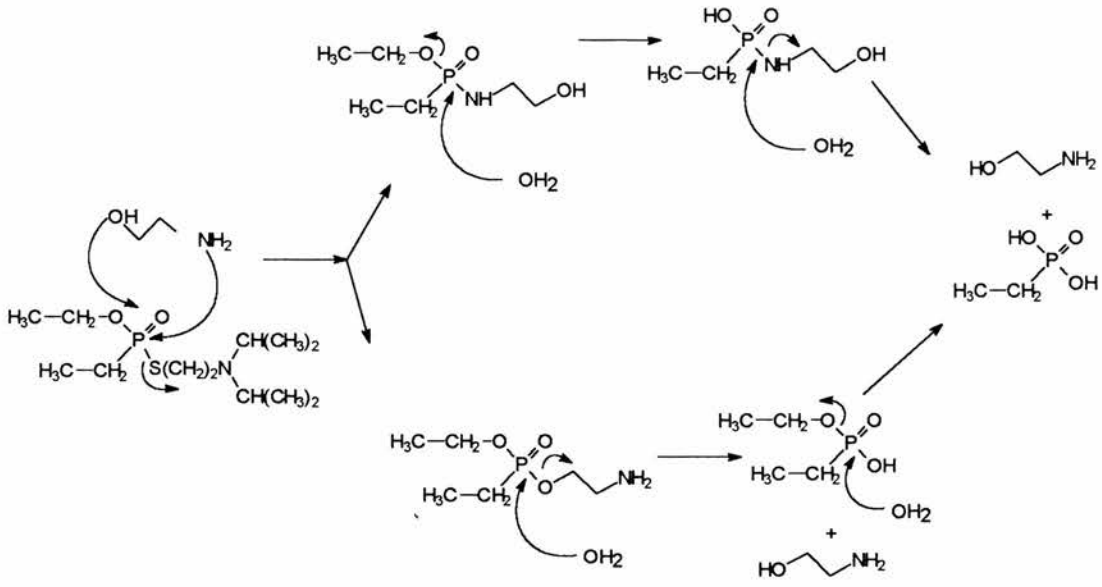

Figure 9

The rate of the decontamination can be increased by addition of aqueous NaOH to the solution. This forms the stronger alkoxide nucleophile, Figure 10

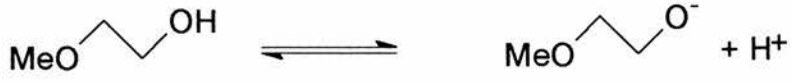

Figure 10

e)85%(wt) H_3PO_4 in ethylene glycol.-Ethylene glycol acts as a solvent for VX and phosphoric acid and does not play an active role as previously reported. Unfortunately

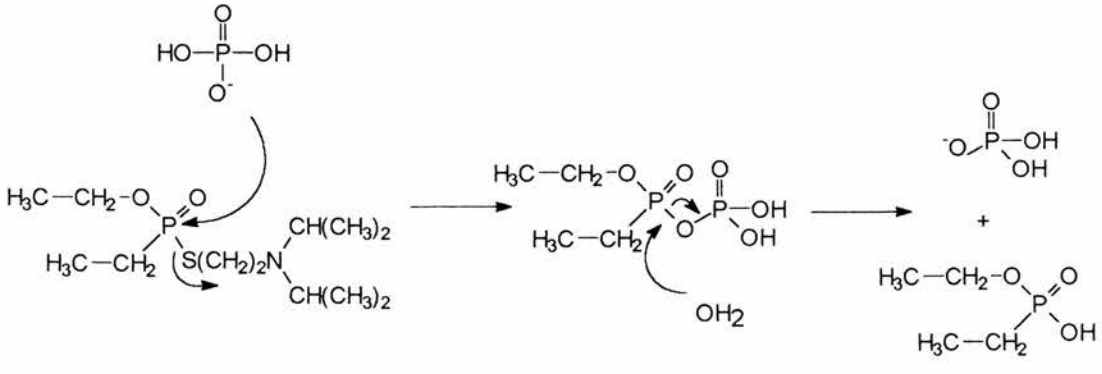

Figure 11

the reaction is slow so that elevated temperatures (~140°C) are required for practical use. This decontaminant has been used for the destruction of Russian stocks of CW agents.

f) Ethylene glycol monomethyl ether.-This reagent is used in the military decontaminant DS2 (dien70%, ethylene glycol monomethyl ether 28%, and NaOH 2%) under these

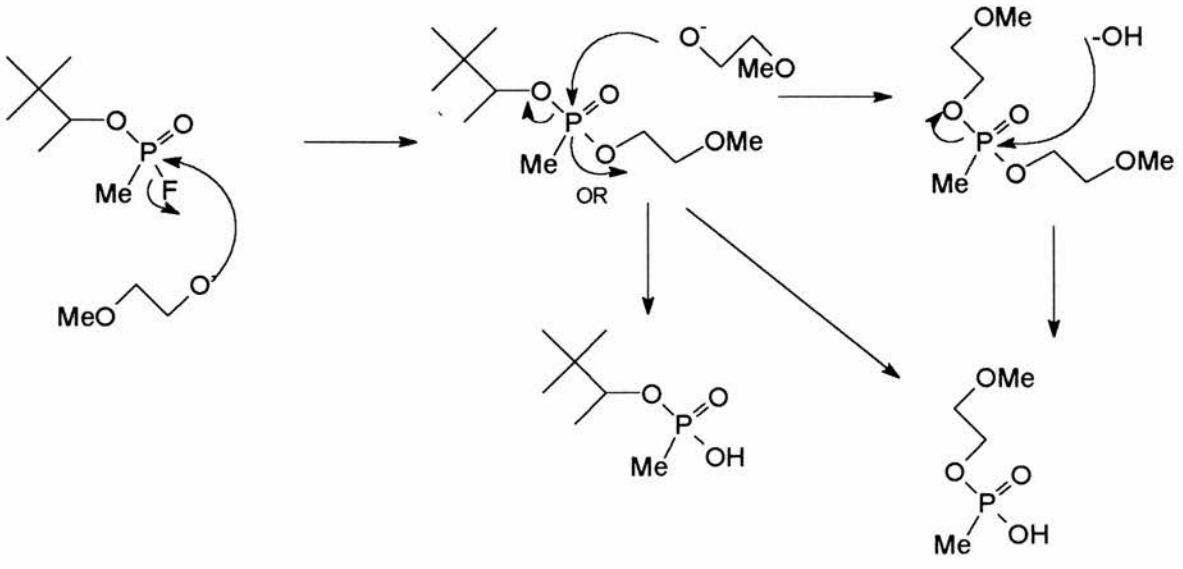

Figure 12

basic conditions the alcohol deprotonates to provide a powerful nucleophile.

The G agents are rapidly attacked to form initially, a diester, then over longer periods of time, monoesters are formed by OH^- attack, Figure 12.

In a similar manner VX is destroyed by hydrolysis of the P-S bond.

g) Phenol.- The phenolate ion may be used as a nucleophile towards phosphorus. Phenol is the active ingredient in the Soviet system (later used by the US). In this formulation a fabric wad, soaked in ethanol (72%), phenol (5%) ammonia (0.2%) and water is effective against the G agents.

Although these methods of decontamination have been effectively put to use in the large scale destruction of nerve agents, there are some disadvantages to these systems. These problems are summarised below.

1)Corrosive properties.- Most of these decontamination techniques require high pH to generate the nucleophiles. Unfortunately these conditions degrade rubbers plastics paints and skin. In addition the personal decontaminant DS2 contains dien which has been shown to be a teratogen in rats.

2)Deactivation of the solution.- The high pH required leads to absorption of CO_2 from the atmosphere, resulting in the formation of carbonate salts. The pH is lowered as a result, so that the relevant nucleophile is not generated. The decontaminants age and must therefore be freshly prepared to be effective.

3) Stoichiometry.- Most of these decontaminants require a stoichiometric amount of reagent rather than a catalytic quantity. Any system which reduces the weight of the decontaminant will always be an advantage in an emergency situation.

4)Solubility.- A major problem associated with decontamination is getting the reagent and the CW agent together for hydrolysis to occur. The rate of decontamination is related to the solubility of the CW agent in the decontaminant.

Mechanism For Nucleophilic Attack at Phosphorus

Three main reaction types are found for phosphorus:

1) *Associative attack of a nucleophile* resulting in a discrete, pentavalent phosphorane intermediate Figure 13.

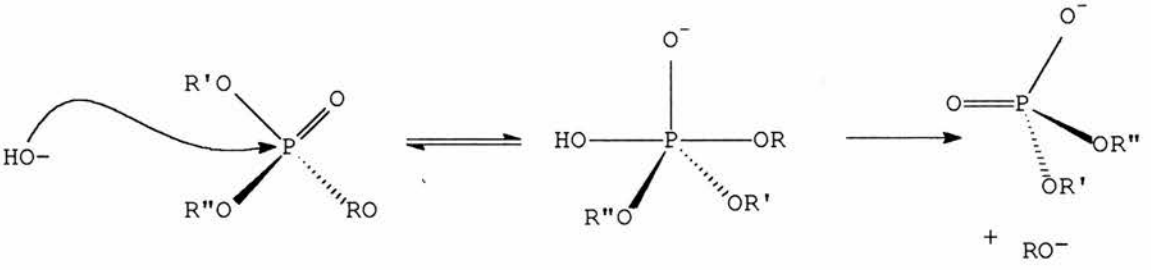

Figure 13

2) *Dissociative mechanism* resulting in a trivalent intermediate Figure 14.

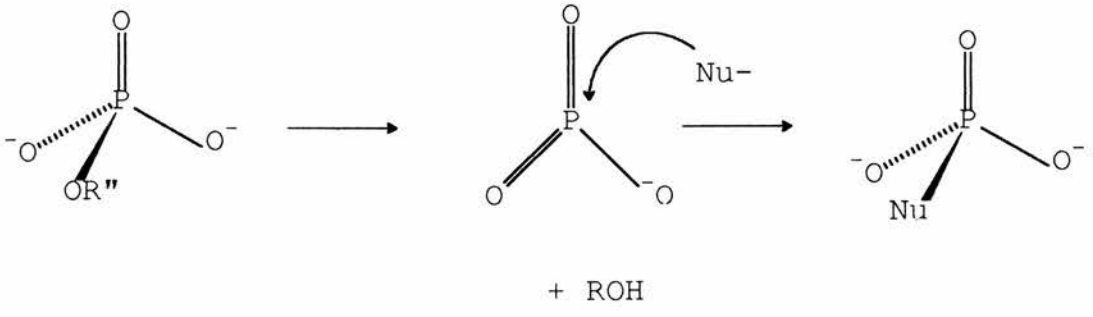

Figure 14

3) *S_N2 reaction*, Figure 15

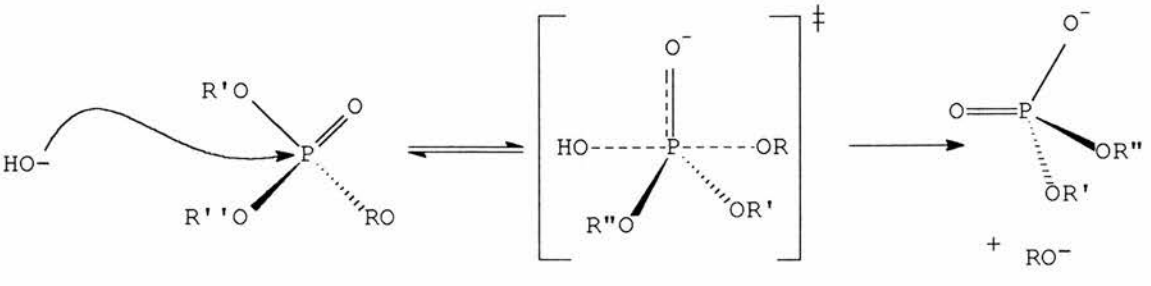

Figure 15

The associative and dissociative mechanisms describe the boundaries of a *continuous* spectrum of possible transition states and to describe mechanisms that do not fit either extreme. The range of possible functionalisation, and degree of protonation at the phosphoryl oxygens results in a range of mechanisms within this spectrum. Even triesters have been shown to have some degree of dissociative character.

Work by Cleland[1] *et al* in recent years, using secondary isotope effects, has been of great value in determining the degree of dissociation or association in the transition state of the activated complex in those reactions assigned an S_N2 mechanism.

Dissociative [$S_N1(P)$]

The elimination of an alcohol results in the formation of a metaphosphate intermediate. The metaphosphate subsequently reacts with a nucleophile to reform a tetrahedral phosphate. As might be expected the rate of reaction depends upon the nature of the leaving group. Good leaving groups such as phenols eliminate the phenolate ion, maximum rate is found where the dianion is the major species in solution, but poor leaving groups such as aliphatic alcohols require protonation to become effective leaving groups. In this case the reaction procedes fastest when the major phosphate species is the monoanion. Presumably the elimination reaction occurs with the concomitant transfer of H^+ from a phosphoryl oxygen to the leaving group, the protonated alkyl alcohol being a much better leaving group.

Direct evidence for the involvment of metaphosphate in ester hydrolysis has been found in trapping experiments and mass spectrometry. No direct evidence has been found in aqueous systems. In protic solvents, at least the metaphosphate intermediate must be a short lived species.

Associative [$S_N2(P)$]

Phosphate diesters, triesters and neutral diprotonated monoesters are thought to react in this manner. NMR studies and X-ray crystal structures confirm the formation of a discrete phosphorane, particularly in the case of cyclic phosphates. Interestingly cyclic

diphosphates hydrolyse much faster than their acyclic analogs. Early work by Westheimer[2] suggested that relief of strain in cyclic phosphates moving to a pentacoordinate transition state may explain their greater rates of hydrolysis. The ring strain hypothesis (supported by calorimetric measurments of ring strains) led to Westheimer's rules dealing with rates of hydrolysis of cyclic esters. Modern calorimetric measurements have led to Kluger[3] *et al* to propose that, although Westheimer's theory that rate enhancement is due to relief of ring strain is correct, the enhanced hydrolysis rate is too great to be explained on these grounds alone. Steric crowding of the acyclic esters may destabilise the phosphoranes of acyclic esters even more than their cyclic counterparts. *Ab initio*[4] studies also indicate that differences in solvation between the acyclic and cyclic phosphate transition states may lead to a significant contribution towards lowering the energy of the cyclic phosphorane intermediate relative to the acyclic phosphorane.

Normally all triesters hydrolyse via a phosphorane intermediate or transition state[5]. The mechanism for the hydrolysis of (1) has been investigated using primary and secondary ^{18}O isotope effects[6]. Evidence is given for significant bond order changes in the phosphoryl oxygen and phenolic leaving group P-O bond lengths. There is about 25% bond cleavage in the transition state.

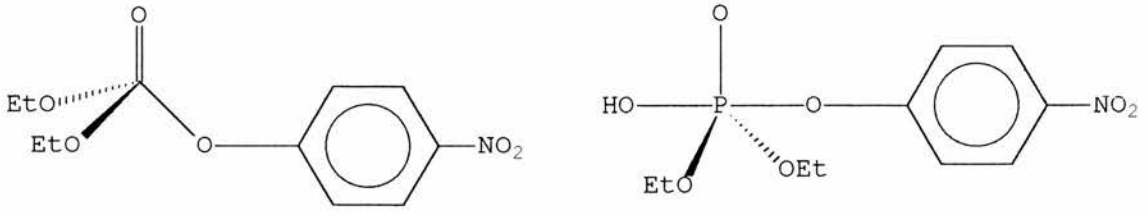

PARAOXON (1) PHOSPHORANE TRANSITION STATE

Figure 16

It is argued that the large isotope effect shows that although the activated complex will involve pentavalent phosphorus, a *discrete* phosphorane intermediate (Figure 16) is unlikely and that the reaction proceeds by a S_N2 process. The enzymatic process catalysed by a phosphotriesterase has also been investigated[7] and it has been found that

there is a lower isotope effect, and here the enzyme may stabilise the phosphorane intermediate. As yet, these studies have not been extended to metal-ion-catalysed reactions. Weak nucleophiles and leaving groups that are weaker acids than the nucleophile have been shown to exhibit a general base mechanism[4,8].

Phosphonate ester hydrolysis.

Phosphonate esters lie structurally between phosphate triesters and phosphinate. There has to be an awareness of possible differences between the nerve agent simulant (mainly triesters) and the nerve agents themselves (mainly phosphonates). Investigations into differences between the reactivity of phosphate triesters[9] and phosphonates have an important bearing on research into new decontaminants.

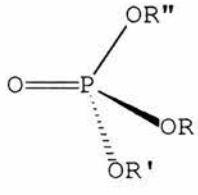

PHOSPHATE ESTER

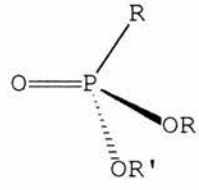

PHOSPHONATE ESTER

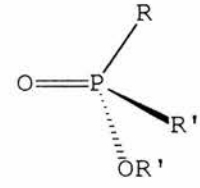

PHOSPHINATE ESTER

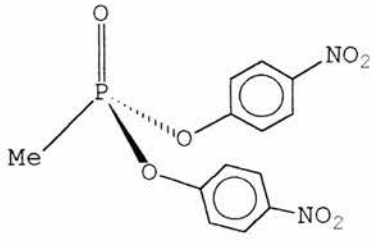

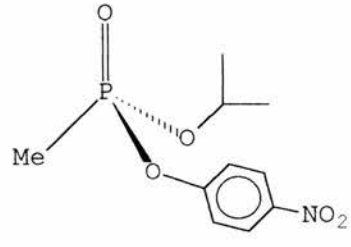

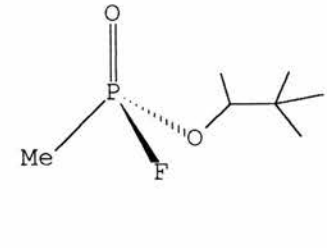

Figure 17

An investigation into the chemical reactivity of the above phosphonate esters has been made[10]. There is a decrease in positive charge on the phosphorus atom and increased steric crowding in moving from the phosphate to the phosphinate. It might therefore be expected, that there is a decrease in the tendency for the phosphorus centre to undergo nucleophilic attack and this effect is observed. For example imidazole acts as a

nucleophile towards phosphate esters but with 4-nitrophenyl diphenyl phosphinate[11], imidazole acts as a general base catalyst. As the phosphonates lie between these two extremes it might be expected that the phosphonates might exhibit both modes of catalysis and this is indeed found.

Solvent isotope effects indicate that P-O bond formation is rate determining and the reaction is essentially associative in character. It is also found that imidazole acts as a general base catalyst (the transition state is found to occur early on in the reaction profile and a significant part of the process is a single proton transferring from water to imidazole). The hydroxide ion acts as a nucleophile.

In summary, triesters are normally hydrolysed by nucleophilic attack at phosphorus in a S_N2 process with associative character but no discrete phosphorane exists. Enzymes may stabilise a phosphorane intermediate.

Weak nucleophiles hydrolyse the ester through general base mechanisms and strong nucleophiles operate by a nucleophilic mechanism. Phosphonate esters are more likely to undergo hydrolysis by a general base mechanism because of greater steric crowding and the lower charge at phosphorus.

Metal Ion Catalysed Hydrolysis

There are four mechanisms by which metal ions can promote phosphate ester hydrolysis.

1) A metal ion can bring a phosphoryl group and a nucleophile together in a favourable orientation for an intramolecular reaction (template effect).

2)Charge neutralisation (mono and diesters only). Shielding of the negative charge of the phosphoryl group lowers the electrostatic barrier towards attack by nucleophiles. This will not be an important consideration for the neutral triesters and phosphonate esters.

3) P=O bond polarisation. Increasing the positive charge at phosphorus by coordination at the phosphoryl oxygen[12].

4) Leaving group stabilisation.

The proposed mechanism for [Cu(dpa)(OH)(OH_2)] (dpa = 2,2'-dipyridylamine) catalysed hydrolysis of a phosphotriester is shown in Figure 18. The reaction involves the formation of a ternary complex in which the P=O group displaces the labile water molecule and hydrolysis occurs by intramolecular attack of coordinated hydroxide on the bound ester.

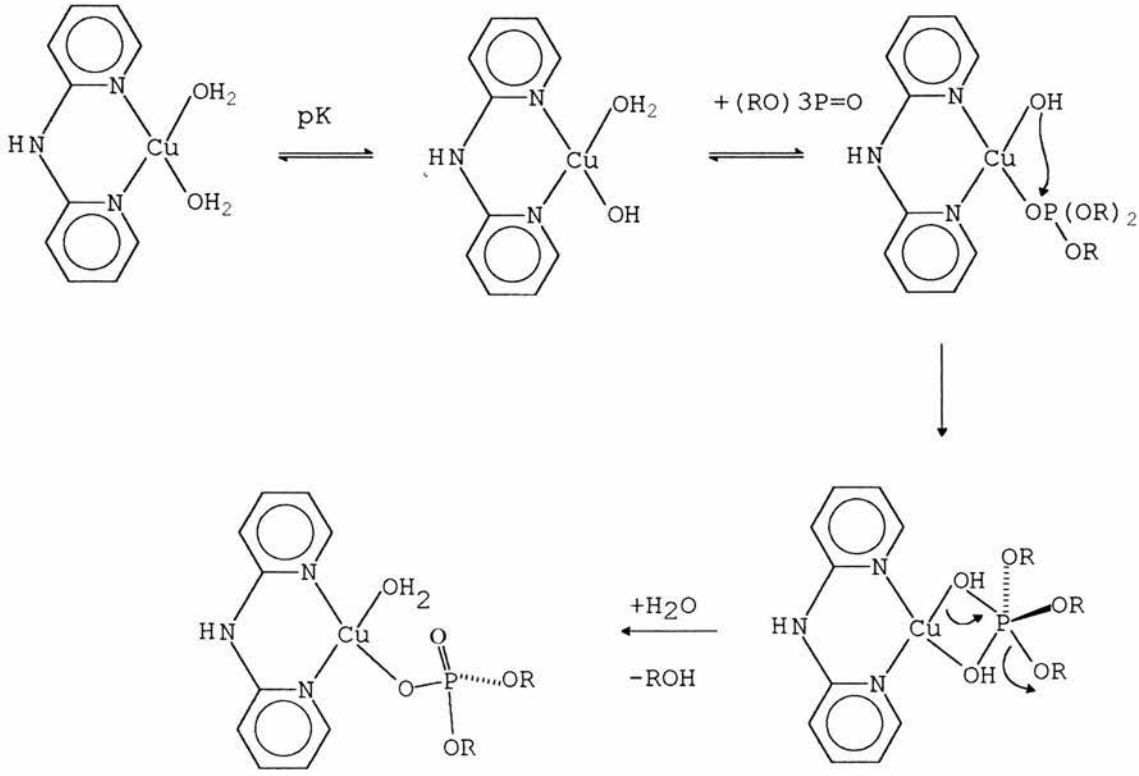

Figure 18

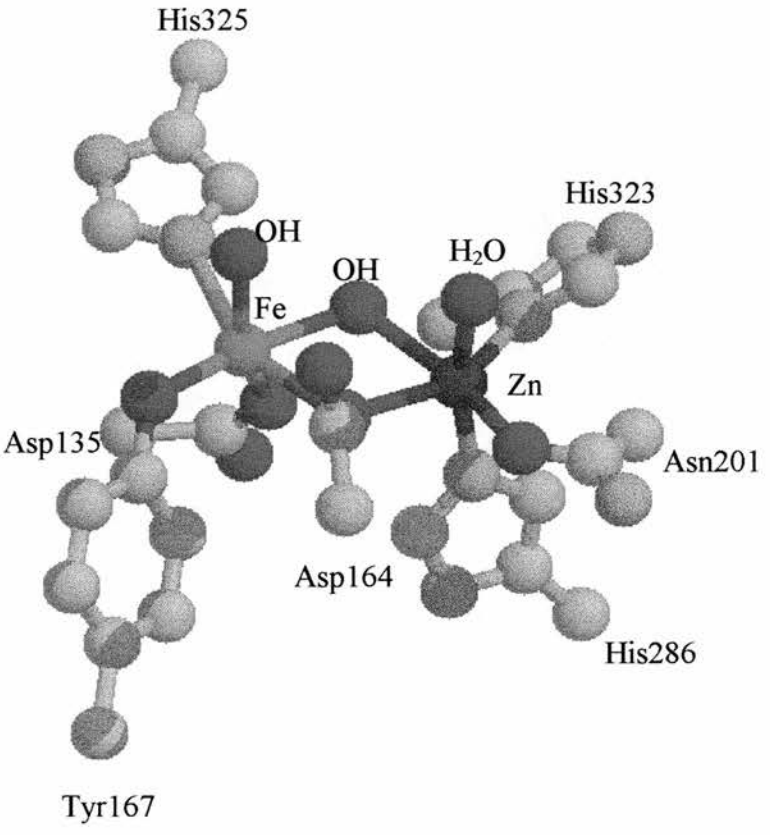

View of the active site of red kidney bean purple acid phosphatase

The Hydroxy-aqua Mechanism. Some hydroxy-aqua complexes which are active in the hydrolysis of phosphate esters are shown in Figure 19. The enzymes alkaline phosphatase and Red kidney bean purple acid phosphatase catalyse the hydrolysis of phosphate esters as do a number of cobalt(III), nickel(II) copper(II) and zinc(II) complexes.

These complexes act by forming a mixed ligand complex with the phosphate ester and hydrolysis occurs by intramolecular attack by coordinated hydroxide. The aquo ligand is substitutionally labile and provides a position for phosphoryl coordination and the hydroxyl moiety is located for attack on the phosphorus atom.

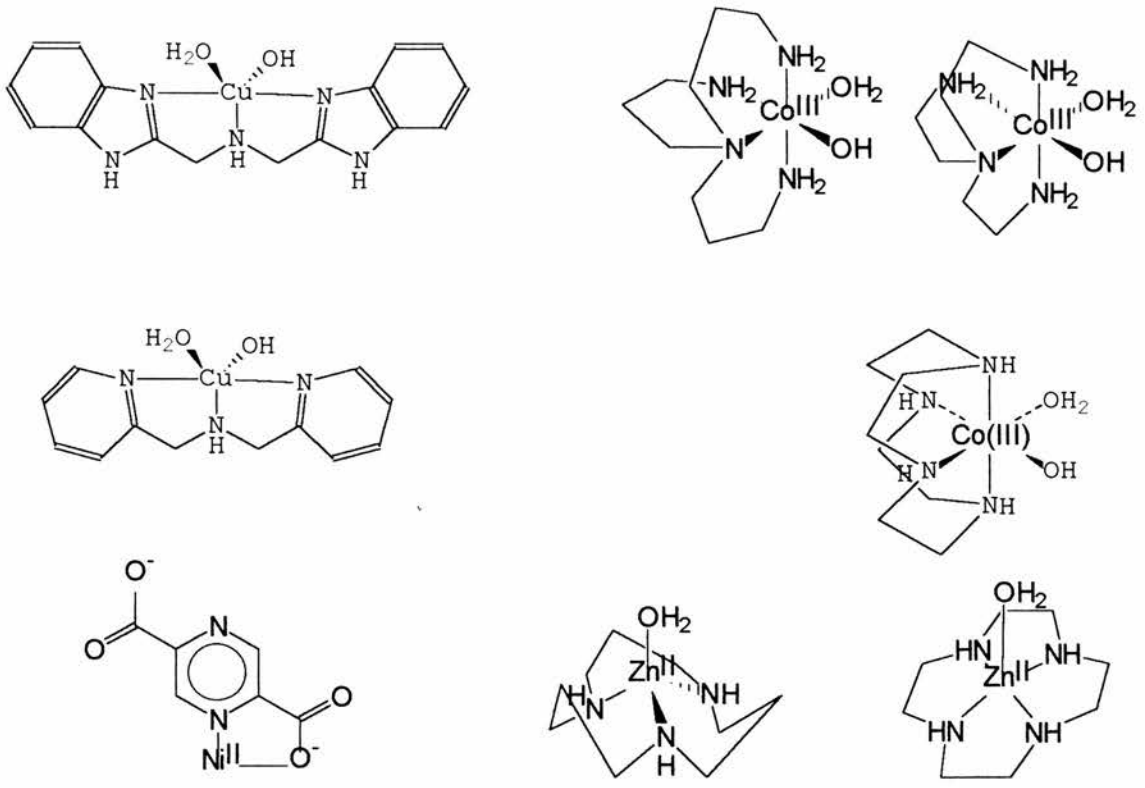

Figure 19

A example of this mechanism may be found in the hydrolysis of 2,4-nitrophenyl diethyl-phosphate (DNPDEP) by the complex[13] $[Cu(dpa)OH(OH_2)]^+$ (Figure 18). The pH-rate profile may be explained on the basis of an active hydroxy aquo complex, and an inactive hydroxy dimer at higher pH. ^{18}O labelling shows that P-O fission not C-O fission occurs. There is no direct evidence for P=O coordination to the metal ions, but the rate enhancements achieved with *cis* hydroxy-aquo complexes is compelling evidence for this mechanism.

A way to overcome the problem of identifying the active metal ion-phosphate species and to obtain an insight into the reactive processes during the catalytic cycle, is to use well characterised non-labile, metal [Co(III), Cr(III) and Ir(III)].

Enhancing Hydrolysis by Providing a Source of Nucleophile at Neutral pH (Figure 20).

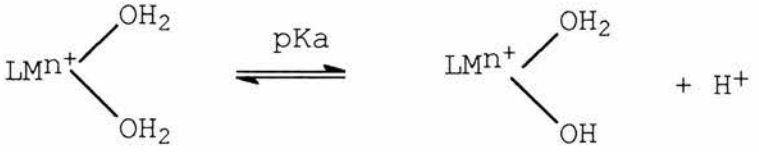

Figure 20

Hydroxide is a good nucleophile but at neutral pH the concentration is so low that the pseudo first order rate constants for phosphate esters and phosphonates[14] are in the range 10^{-6} to 10^{-8} s^{-1}. The coordination of water to a metal ion drastically reduces its pK_a and the metal bound hydroxide is sufficiently nucleophilic to attack a phosphorus centre. A similar effect is seen with hydroxy allyl[15] or oxime[16] groups.

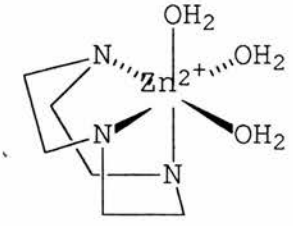

Figure 21

A wide variety of *cis* hydroxy aquo complexes have been investigated. Copper (II) complexes dominate the literature, giving rise to large rate enhancements. The tendency of copper to form square planar complexes means that its Lewis acidity is high (formation of the hydroxy aquo species at neutral pH results in catalytic activity at neutral pH). The requirement of high Lewis acidity, and the discovery of a relation ship between pKa of the coordinated water molecule had been discussed recently for zinc amine complexes[17]. The high $pK_{a's}$ of the coordinated water of Zn([9]aneN_3) (pK_{a1} 10.9, pK_{a2} 12.3) has been connected to its octahedral geometry[18] (Figure 21) resulting in a low Lewis acidity (the greater the number of σ donors the greater the electron density around the metal centre thus the lower the polarisation of the O-H bond resulting in a higher pKa). However, the closely related macrocycle [12]aneN_3 forms tetrahedral zinc complexes[19] and the aquo complex has a low pK_a (7.3)[20] and is active against phosphate triesters[21].It is interesting to note that zinc is found with a low coordination number (four coordinate) in enzymes which operate by a zinc-hydroxide mechanism[22].

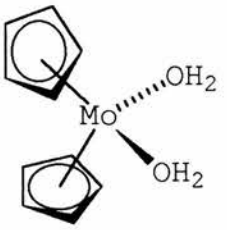

Figure 22

There has been some interesting recent work on molybdenum *bis*-cyclopentadienyl binding to DNA[23]. Figure 22 shows the structure of the complex. The *cis* coordinated aquo ligands have pKa's of 5.5 and 8.5. Cp_2Mo is quite stable to C-Mo bond rupture in aqueous solution pH 7.4. The complex may thus be a useful organometalic derivative for catalytic studies.

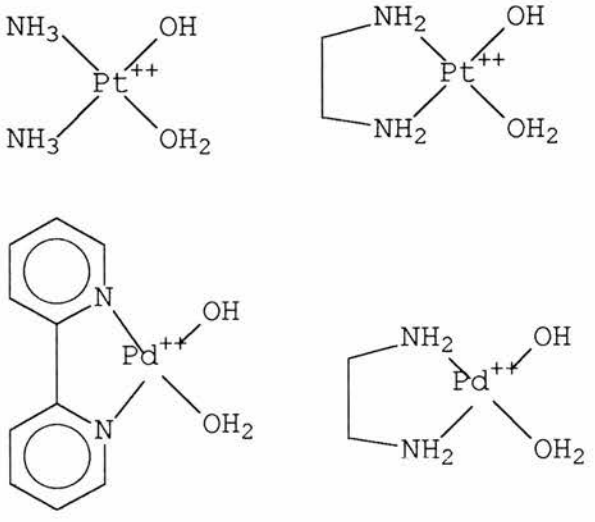

Figure 23

A number of planar platinum(II) complexes, Figure 23 have been studied[24]. These compounds were not tested for activity against triesters but the kinetics of hydrolysis of an activated diester were investigated. Turnover was not observed due to strong product binding. The activity of the palladium complexes at high pH was drastically reduced by the formation of hydroxy bridged dimers.

The palladium complexes were found to be much more active than the platinum complexes. A second important requirment is the presence of a labile site *cis* to the coordinated nucleophile. The lower lability of the platinum complexes makes them poorer catalysts.

Importance of a Labile site Cis *to The Bound Nucleophile* (Figure 24).

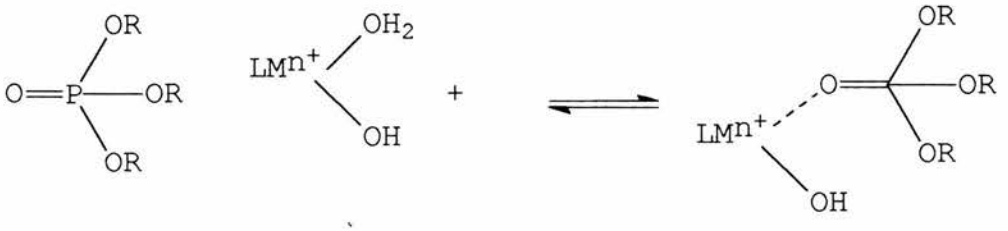

Figure 24

An early study[25] established that the complex $[Co(NH_3)_5PO_4(CH_3)_3]^{3+}$ undergoes fast base catalysed hydrolysis with Co-O bond cleavage. No solid complex could be isolated. O-C bond fission was found to occur[26] when non basic nucleophiles such as SCN^-, I^-, and $S_2O_3^-$ were used (about 150 fold rate enhancements). The iridium(III) complex $[Ir(NH_3)_5OP(OR)]$ has been prepared[27] and its hydrolysis in basic solution studied. Only P-OR cleavage occurred. In general the coordination of an ester to the metal centre results in a several hundred fold increase in rate compared with the uncoordinated ester. This increase may be assigned to the electrophilic activation of co-ordinating the P=O group to a metal centre. As enzymes lead to a 10^{11} fold rate enhancement[28] (ie E.Coli alkaline phosphatase) an 400 fold rate increase does not provide an adequate explanation for the rate enhancement. Other factors must contribute to the rate enhancement, in particular the proximity effect.

*Attack of Coordinated Hydroxide: the Proximity Effect (*Figure 25*).*

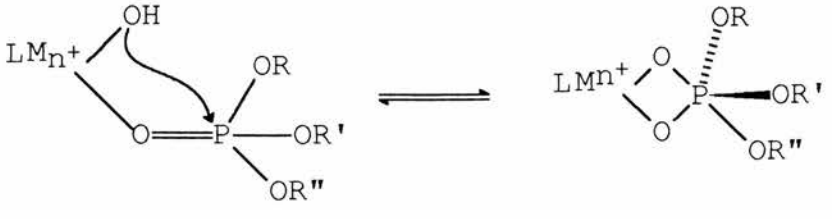

Figure 25

Intramolecular attack of hydroxide has been investigated primarily with the inert metal ions cobalt(III) and iridium(III). Hydrolysis of the ester (4-nitrophenyl)phosphate (NPP) coordinated to cobalt(III), Figure 26, showed that hydrolysis occurs exclusively by intramolecular attack of coordinated hydroxide ion on the phosphorus centre (18O tracer studies)[29].

Recent studies have dealt with the less labile $[Ir(en)_2(OH)(BNPP)]$ system[30]

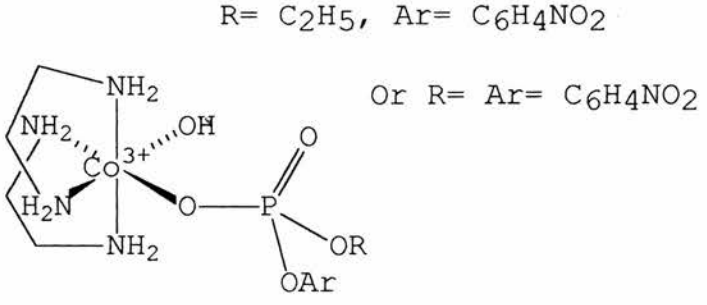

Figure 26

Between pH 8 to 12 the rate constant for the production of nitrophenyl phosphate was about 10^{-3} s^{-1} (greater than 10^5 fold faster than uncoordinated phosphate at pH 9). This indicated that even though the basicity was reduced 10^7 to 10^8 fold, the nucleophilic efficiency increased 10^5-10^6 fold. However the rate enhancement by *E.Coli* alkaline phosphatase[31] is approximately 10^{11}. So the rate enhancement by enzymes cannot be explained solely by the proximity effect.

References

[1] A.C.Hengge and W.W.Cleland, *J.Am.Chem.Soc.*, 1991, *113*, 5835.

[2] F.H.Westheimer, *Acc.Chem.Res.*, 1968, **1**, 70

[3] S.D.Taylor and R.Kluger, *J.Am.Chem.Soc.*, 1992, **114**, 3067.

[4] A.Dejaegere and M.Karplus, *J.Am.Chem.Soc.*, 1993, **115**, 5317..

[5] P.Hendry and A.M.Sargeson, *Progress in Inorganic Chemistry: Bioinorganic Chemistry*, 1990, **38**, 202.

[6]S.R.Caldwell, F.M.Raushel, P.M.Weiss and W.W.Cleland, *J.Am.Chem.Soc*, 1991, **113**, 730.

[7]D.P.Dumas, S.R.Caldwell. J.R.Wild and F.M.Raushel, *J.Biol.Chem.*, 1990, **264**, 19659.

[8]R.K.Osterheld, *"Topics in Phosphorus Chemistry"* (Ed. E.J.Griffith, M.Grayson) **7**, 206.

[9]AWilliams, *Acc.Chem.Res.*, 1989, **22**, 387; S.A. Ba-Saif, M.A.Waring, *J.Am.Chem.Soc.*, 1990, **112**, 8115; D.Herschlag, and W.P.Jencks, *J.Am.Chem.Soc*, 1989, **111**, 7587; M.T.Skoog and W.P.Jencks, *J.Am.Chem.Soc.*, 1984, **106**, 7597.

[10]I.M.Korvach, A.J.Bennet, J.A.Bibbs and Q.Zhao, *J.Am.Chem.Soc.*, 1993, **115**, 5138.

[11]A.Williams and R.A.Naylor *J.Chem.Soc.(B)*, 1971, 1967.

[12].G.J.Lloyd, C.M.Hsu and B.S.Cooperman, *J.Am.Chem.Soc.*, 1971, **93**, 4889; T.G.Spiro *"Inorganic Biochemistry"* G.L.Eichhorn, Ed. in press.

[13].T.R.Morrow and W.C.Trogler,1989, **28**, 2330.

[14].J.Emsley and D.A.Hall, *"The Chemistry of Phosphorus"* Wiley, NY 1976, 494.

[15].D.S.Sigman and C.T.Jorgensen, *J.Am.Chem.Soc.* 1970, **92**, 1075.

[16].R.Breslow and D.Chapman, *J.Am.Chem.Soc.*, 1965, **87**, 4195.; K.Ogino,K.Shindo, T.Miniami, W.Tagoki and T.Eiki, *Bull.Chem.Soc.Jpn.*, 1983, **56**, 1101.

[17].Y.Fujii, T.Itoh. K.Onodera and T.Tada, *Chem.Lett.*, 1995, 305.

[18].G.C.Silver, P.Gantzel and W.C.Trogler, *Inorg.Chem.*, 1995, **34**, 2487.

[19].P.M.Schaber, J.C.Feltinger, M.R.Churchill, D.Nalewajek and K.Fries, *Inorg.Chem.*, 1988, **27**, 1641.

[20].E.Kimura, T.Shiota, T.Koike, M.Shiro and M.Kodama, *J.Am.Chem.Soc.*, 1990, **112**, 5805.

[21].T.Koike and E.Kimura, *J.Am.Chem.Soc.*, 1991, **113**, 8935.

[22].E.E.Kim and H.W.Wycoff, *J.Mol.Biology*, 1992, **218**, 449.

[23].L.Y.Kuo, M.G.Kanatzidio, M.Sabat, A.L.Tipton and T.J.Marks, *J.Am.Chem.Soc.*, 1991, **113**, 9027.

[24].M.A.Rosch and W.C.Trogler, *Inorg.Chem.*, 1990, **29**, 2409.

[25].W.Schmidt and H.Taube, *Inorg.Chem.*, 1963, **2**, 698.

[26].W.G.Jackson and B.C.McGregor, *Inog.Chim.Acta.*, 1984, **83**, 115.

[27].P.Hendry, and A.M.Sargeson, *Aust.J.Chem.*, 1986, **39**, 1177.

[28].E.J.Coleman and P.Gettins, *Adv.Enzymol.Relat.Areas Mol.Biol.*, 1983, **55**, 453.

[29].D.R.Jones, L.F.Lindoy and A.M.Sargeson, *J.Am.Chem.Soc.*, 1983, **105**, 7327.

[30] P.Hendry and A.M.Sargeson, *Inorg.Chem.*, 1989, *111*, 2521.

[31] E.J.Coleman and P.Gettins, *Adv.Enzymol.Relat.Areas Mol.Biol.*, 1983, *55*, 453.

Chapter 2

N,N-bis(benzimidazole-2-ylmethyl)amine and its Copper(II) and Zinc(II) Complexes

Investigation of a N,N-Bis(benzimidazole-2-ylmethyl)amine Copper(II) and Zinc(II) Complex for the Hydrolysis of Phosphate Triesters.

Abstract

The copper(II) and zinc(II) complexes of N,N-bis(benzimidazole-2-ylmethyl)amine (L) have been prepared and the crystal structure of $[Zn(L)Cl_2].MeOH$ determined by X-ray diffraction and found to have a structure[1] analogous to that of $[Cu(L)Cl_2]$. The stability constants, in 50% MeOH/H_2O (wt. %), have been obtained for a variety of copper and zinc(II) complexes. The stepwise protonation constants for the ligand [$\log K_{lh}$] are: $\log K_{11}$, 5.638(3) and $\log K_{12}$, 10.12(1) and the stability constants [$\log \beta_{lmh}$] for Cu^{2+} are: $\log \beta_{120}$, 10.64(3); $\log \beta_{110}$, 6.34(2); $\log \beta_{11-1}$, -0.97(7); $\log \beta_{11-2}$, 10.07(6); $\log \beta_{121}$, 15.05(5) and for Zn^{2+}: $\log \beta_{120}$, 8.97(8); $\log \beta_{110}$, 5.96(2); $\log \beta_{11-1}$, -2.33(6)). The copper(II) complex is a moderately active catalyst for the hydrolysis of the phosphotriester 2,4-dinitrophenyl diethylphosphate.

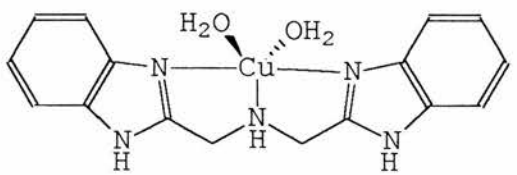

[1]

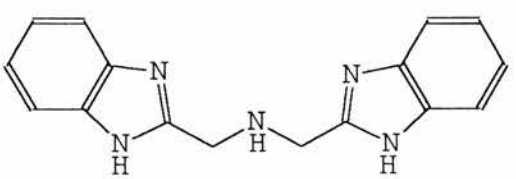

[L]

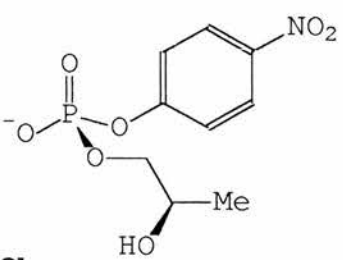

[2]

Introduction

The diaquabisbenzimidazole complex [1] has been found to be active in the transesterification of hpnp ([2] = 2-hydroxypropyl-4-nitrophenyl phosphate)[1], which has been used as an RNA model[2].

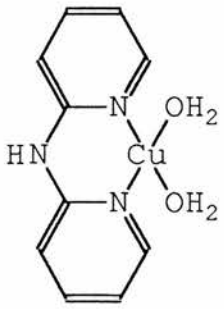

[4]

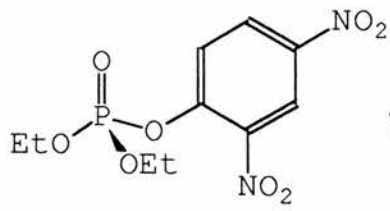

DNPDEP

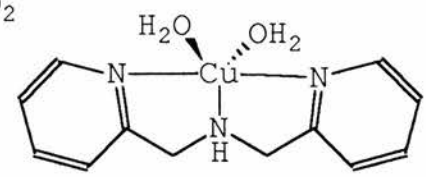

[3]

Figure 1

The activity of complex [1] towards hpnp was compared with that of [3] and [4] which are also known to be active against 2,4-dinitrophenyl diethylphosphate. Complex [1] was shown to be more reactive at high concentrations unlike [3] and [4] in which the rate is lowered at high concentrations. It was proposed that steric bulk of the benzene rings of [1] prevented the formation of an inactive dihydroxy bridged species, but allowed a highly active monohydroxy dimer to form [5].

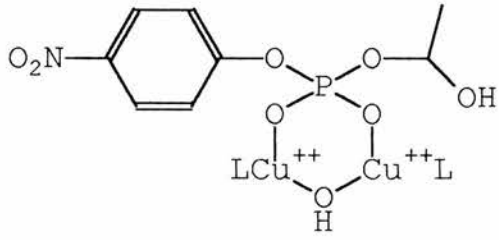

[5]

We are interested in developing catalysts for destruction of phosphate esters, which are active over a wider range of concentrations than are currently available. On-site formulation of decontaminants in an emergency must not require accurate preparation of solutions.

Experimental

Measurements. Infrared spectra were recorded on a Perkin Elmer 1710 Infrared Fourier Transform Spectrometer as KBr discs. Melting points were obtained using a Gallenkamp melting point apparatus and were uncorrected. UV/Visible spectra were recorded on a

Lambda 14P Spectrometer. The NMR spectra were obtained using a 200MHz Varian Gemini FT spectrometer.

Preparation of the Ligand and Complexes.-

(a) N,N-bis(benzimidazole-2-ylmethyl)amine.3HCl (L.3HCl)

The ligand was prepared as described by Berend and Stephan[3].

Iminodiaceticacid (108.1g, 1mol) and *o*-phenylenediamine (108g, 1.2mol) were refluxed in 6mol dm^{-3} aqueous HCl for 72 hours. On cooling a blue powder formed. The powder was filtered off, washed with acetone and recrystallised from 40-60 (v/v) water/acetone (62g, 16%)

(b) N,N-bis(benzimidazole-2-ylmethyl)amine($L.H_2O$)

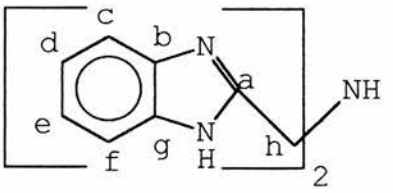

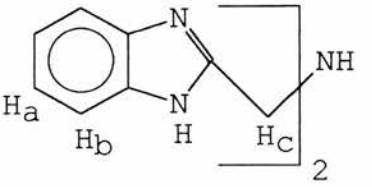

The HCl salt prepared above (5.72g, 14.8mmol) was dissolved in water ($100cm^3$) and sodium hydrogen carbonate (3.73g, 44.5mmol) added in portions, to give a pale lilac precipitate. The precipitate was filtered off, refluxed in methanol with activated charcoal for two hours and filtered hot. The pale yellow filtrate gave pale-mauve needles on cooling (yield 3.95g, 81%). (Found: C, 64.99; H, 6.05; N, 23.80; Calc. for $C_{16}H_{17}N_5O$: C, 65.10; H, 5.81; N, 23.73%); i.r./cm^{-1} 3433s, br (O-H ν); 3224, 3206, (imid. N-H ν); 3052s (sec. N-H ν); 2960, 2928, 2905m (C-H ν); 1624w (O-H δ); 1590vw (imid. N-H δ), 1531w, 1479w, br (N-H δ); 1455s, 1438s, 1428s, 1384w (C-N imidazole ν); 1310m, 1332m, 1273s, 1223m, 1099m, 1014m, 876m, 843m, 769w, 749, 735s, 621, 534, 481w; δ_H(200MHz; solvent CD_3OD; standard reference TMS) 7.58 [4H, m, $J(H_a, H_b)$ 6.5Hz], Hb, 7.24 H_a[4H, m, $J(H_b, H_c)$ 3.2Hz], 4.41 H_c(4H, s); δc 157 *a*, 141.3 *b, g*, 126 *d,e*, 118*c, f*, 50 *h*.

(c) N,N-bis(benzimidazole-2-ylmethyl)amine dihydrochloride.(L.2HCl)

N,N-bis(benzimidazole-2-ylmethyl)amine (2.71g, 9.18mmol) was dissolved in hot methanol ($50cm^3$) and HCl (35%) added dropwise until pH <2. A white precipitate formed

immediately on addition of the HCl. The precipitate was filtered off, washed with ethanol(2x20cm^3) and finally with diethyl ether (2x30cm^3), then dried at reduced pressure. yield (2.51g, 78%)

(Found: C, 54.86; H, 4.79; N, 19.98. Calc. for $C_{16}H_{17}N_5Cl_2$: C, 54.87; H, 4.89; N, 20.00%); i.r./cm^{-1} 3431s br (O-H ν); 3245s (N-H ν); 2960, 2909, 2850, 2803, 2713, 2583, 2519s br (C-H and NR_2H-H^+ ν); 1685w br (O-H δ); 1620s (RHN^+-H δ); 1575m (N-H δ); 1518w, 1488w br (N-H δ); 1459s, 1441s, 1390m, 1371w (C-N imid. ν); 1314m, 1220s, 878m br, 759s, 746s, 623m, 576vw, 548vw, 481w;

The crude product is blue in colour, however, the hydrochloride salt of the purified free base was obtained as colourless needles. Titration studies confirmed that the halide salts are diprotonated and not triprotonated.

(d) N,N-bis(benzimidazole-2-ylmethyl)amine dihydrobromide.(L.2HBr)

This compound was prepared in a similar manner to the hydrochloride salt, except that hydrobromic acid was used in the acidification of the free base (3.2g, 10.8mmol) to give the amine dihydrobromide as a white powder (4.43g, 93%).

(Found: C, 43.84; H, 4.30; N, 15.90. Calc. for $C_{16}H_{17}N_5Br_2$: C, 43.76; H, 3.90; N, 15.95%); i.r./cm^{-1} 3433s br (O-H ν); 3243s (N-H ν); 3014, 2957, 2792, 2716, 2632, 2596, 2505s br (C-H and NR_2H-H^+ ν); 1685w sh (O-H δ); 1620s (RHN^+-H δ); 1564m (N-H δ); 1516w, 1484w br (N-H δ); 1457s, 1438s, 1338m, 1356w (C-N imidazole ν); 842m br, 739s, 624m, 577vw, 475w;

(e) Dichloro N,N-bis(benzimidazole-2-ylmethyl)amine copper(II).MeOH.[$CuLCl_2$].MeOH

N,N-bis(benzimidazole-2-ylmethyl)amine(0.5g, 1.8mmol) in MeOH (50cm^3) was added rapidly to a hot solution of copper (II) chloride (0.307g, 1.80mmol) in MeOH (20cm^3) to give a blue-green solution from which a blue precipitate formed on standing. The complex was filtered off, washed with ethanol (2x10cm^3) and dried *in vacuo*.

(Found: C, 46.12; H, 4.20; N, 15.99. Calc. for $C_{17}H_{19}N_5OCuCl_2$: C, 45.43; H, 4.87; N, 14.72%); λmax/nm(H_2O) 683.6 (ε/dm^3 mol^{-1} cm^{-1} 97.4); i.r./cm^{-1} 3373s br (O-H ν); 3107, 3063 (imid. N-H ν), 2916s (sec N-H ν); 2787m (C-H ν); 1626w (O-H δ); 1594w (imid. N-H δ), 1548w, 1493w br (N-H δ); 1476s, 1455s, 1441s, 1390w (C-N imid.ν);

326m, 1295m, 1279s, 1226m, 1056m, 1013m, 1005m, 954w, 907w, 847w, 747s, 496w; Λ_M /S cm^2 mol^{-1} (H_2O) 221.

(f) Dichloro N,N-bis(benzimidazole-2-ylmethyl)amine zinc(II).EtOH. [$ZnLCl_2$].EtOH N,N-bis(benzimidazole-2-ylmethyl)amine (2.5g, 8.47mmol) in EtOH (50cm^3) was added rapidly to a hot solution of zinc (II) chloride (1.23g, 4.24mmol) in EtOH (20cm^3) to give a colourless solution from which a colourless plates formed. The complex was filtered off, washed with ethanol(2x10cm^3) and dried *in vacuo* (3.40g, 82%).
(Found: C, 46.97; H, 4.35; N, 15.16. Calc. for $C_{18}H_{22}N_5OZnCl_2$: C, 47.03; H, 4.60; N, 15.23%); i.r./cm^{-1} 3370s br (O-H ν); 3286, 3062 (imid. N-H ν), 3062s (sec N-H ν); 2972, 2914, 2782s (C-H ν); 1626w (O-H δ); 1596w (imid. N-H δ), 1540w, 1492w (N-H δ); 1472s, 1456s, 1431s, 1386w (C-N imid. ν); 1333m, 1278m, 1046m, 1034m, 1004w, 935w, 916w, 769, 761, 750s, 502, 490w; Λ_M /S cm^2 mol^{-1} (H_2O) 213.

Colourless crystals suitable for X-ray diffraction were prepared by vapour diffusion of diethylether into a solution of the complex in MeOH/H_2O (0.96g).

Crystal Data.-- $C_{17}H_{19}N_5ZnCl_2O$, (the methanolate) M = 445.66, Primitive orthorhombic, a = 14.642(1), b = 18.357(2), c = 13.962(4) Å, U = 3752.8(9) $Å^3$ (by least-squares refinement on diffractometer angles for 25 automatically centred reflections, in the range 32.17<2θ<34.77° λ = 0.71069 Å), space group *Pbca*(#61), Z = 8, D_c = 1.577 g cm^{-3}, F(000) = 1824.00. Pale block crystal. Approximate crystal dimensions 0.50 x 0.40 x 0.30 mm, μ(Mo-K_α) = 16.10 cm^{-1}.

Data Collection and Processing.--Rigaku AFC7S diffractometer, ω-2θ scan type with ω scan width = (1.47 + 0.35 tan θ)°, ω scan speed 16.00° min-1 (up to 4 scans), graphite monochromated MoKα radiation; 3724 reflections measured (max 2θ = 50.0°), 3718 unique (R_{int} = 0.74). No decay correction, or absorption correction was required. Corrections were made for Lorentz and polarisation effects.

Structure Analysis and Refinement.-- Direct methods[4] were employed and expanded using Fourier techniques[5] Some non-hydrogen atoms were refined anisotropically, while

the rest were refined isotropically. Hydrogen's were included but not refined. The final cycle of full-matrix least-squares refinement[6] was based on 2245 observed reflections ($I>3.00\sigma(I)$) and 235 variable parameters and converged with unweighted agreement factors of:

$$R = \sum \| Fo| - |Fc| \| / \sum |Fo| = 0.036$$

$$R_w = \sqrt{\left(\sum \left(|Fo| - |Fc| \right)^2 / \sum wFo^2 \right)} = 0.034$$

The standard deviation of an observation of unit weight[7] was 2.17. The weighting scheme was based on counting statistics and included a factor (p = 0.005) to downweight the intense reflections. Plots of $w(\Sigma |Fo| - |Fc|)^2$ versus $|Fo|$, reflection order in data collection, $\sin\theta/\lambda$ and various classes of indices showed no unusual trends. The maximum and minimum peaks on the final difference Fourier map correspond to 0.45 and -0.41 $e^- Å^{-3}$, respectively. The secondary nitrogen N1 was initially refined anisotropically, but after finding large anisotropy perpendicular to the plane of the complex at this position, the model was replaced with one with the nitrogen partially occupying two positions (designated as N1 and N6). All calculations were performed using the TEXSAN[8] crystallographic software package of the Molecular Structure Corporation.

Potentiometric Titrations.- Potentiometric pH measurements and computation of the protonation constants and stability constants were carried out by procedures described in detail in appendix I. Solutions were made up with 50% wt aqueous methanol and the ionic strength adjusted to 0.1mol dm^{-3} with KNO_3. Details of the concentrations of the components in the titration are given in Table 1.

Table 1 Summary of experimental parameters for the system Cu(II)-L, and Zn(II)-L (L = N,N-bis(benzimidazole-2-ylmethyl)amine)

Solution composition	
$[T_L]$ range/mol dm^{-3}	$3.6x10^{-3}$ - $1.5x10^{-4}$
$[T_M]$ range/mol dm^{-3}	Cu^{2+} $4x10^{-4}$ - $1.2x10^{-3}$
	Zn^{2+} $8x10^{-4}$-$1x10^{-4}$
I/mol dm^{-3}, electrolyte	0.1, KNO_3
pH Range	Cu 3-10.5
	Zn 3-7
Experimental method	pH Titration, calibrated
	by standard buffers
T/°C	25±0.1
Total number of data points	
Protonation	205 (5 curves)
Copper complexation	351 (5 curves)
Zinc complexation	204 (4 curves)
Method of calculation	SUPERQUAD

In total five titration curves were used in the calculation (350 datapoints) with metal concentrations over the range $1.58x10^{-3}$ to $4.0x10^{-4}$ mol dm^{-3} The glass electrode was calibrated and checked for linearity with the borax and potassium hydrogen phthalate buffers in aqueous solution. The presence of CO_3^{2-} was checked using a Gran plot and Kw determined for the solvent system (see Appendix I).

Although adjustments have not been made to compensate for the methanol-water junction potential, a correction value of 0.1236 pH units can be subtracted from the pH instrument

readings as suggested by R.G.Bates[9] *et al.* This enables a comparison to be made with measurements in aqueous media.

Hydrolysis of 2,4-dinitrophenyl diethyl phosphate (DNPDEP).- Hydrolysis of the triester was monitored by the production of 2,4-dinitrophenolate at 360nm with a Lambda 14P Spectrometer. The temperature was maintained at 25°C by a Perkin Elmer Peltier System. Solutions were buffered at the required pH with MES (pH 5.0-6.0), HEPES (6.5-7.5.0) and TAPS (8.0-9.0) buffers at 0.05 mol dm^{-3}. The ionic strength was adjusted to 0.1mol dm^{-3} with KNO_3. To prevent formation of insoluble copper hydroxo complexes the ligand was present in a three fold excess.

Results and Discussion.

The Crystal Structure of [ZnLCl$_2$].MeOH.-

In the zinc(II) complex the benzimidazole ligand is coordinated via the two pyridine-type nitrogens of the imidazole moieties. The secondary amino group and two chlorides complete the coordination sphere to form a distorted square pyramidal coordination geometry. The benzimidazole nitrogen- zinc bond distances are as expected for imidazole derivatives, but the bond to the secondary nitrogen is a little longer than expected (2.188Å is the average Zn-N distance found in the Daresbury database). The benzimidazole donors and one chloride form the base to the pyramid (the zinc atom is approximately 0.65 Å above this plane) and the other chloride occupies the apical position. The structure also contains one molecule of methanol which is hydrogen bonded to an imidazole nitrogen(N5).

The imidazole ligand is remarkably planar. A plane described by the two benzene rings indicates a deviation from the plane of only ca 0.02Å (with zinc sitting approximately 0.4Å above) and may be caused, in part, by stacking of the aromatic rings (see the diagram showing the two complexes in the structure). This packing arrangement may also explain the square pyramidal geometry of the complex. One would imagine that the basal chloride (Cl2) experiences considerable steric hindrance from the hydrogens (H10 and H3) of the benzene ring. However relief of strain, by moving the chloride further beneath the ligand plane might disrupt the stacking arrangement.

It was found that there are two conformations of the secondary amine nitrogen (N1). Two positions were refined, N1 and N6, with a total occupancy equal to one. Refined occupancies were 0.68 and 0.32 corresponding to *trans* and *cis* conformations respectively (presumably the *trans* arrangement is sterically favoured).

Table 2. Selected bond lengths and angles of[$ZnLCl_2$].MeOH

Zn(1)-N(1)	2.300(5)	N(1)-Zn(1)-N(2)	72.6(2)
Zn(1)-N(2)	2.079(3)	N(1)-Zn(1)-N(3)	98.3(3)
Zn(1)-N(4)	2.078(3)	N(1)-Zn(1)-N(4)	73.1(2)
Zn(1)-Cl(1)	2.316(1)	N(4)-Zn(1)-N(2)	143.5(1)
Zn(1)-Cl(2)	2.304(7)	N(1)-Zn(1)-Cl(2)	144.1(2)
O(1)-N(5)	2.827(4)	N(1)-Zn(1)-Cl(1)	109.4(2)
		Cl(1)-Zn(1)-Cl(2)	106.51(5)

ORTEP diagram of the complex N,N-bis(benzimidazole-2-ylmethyl)amine zinc(II).EtOH and packing diagram.

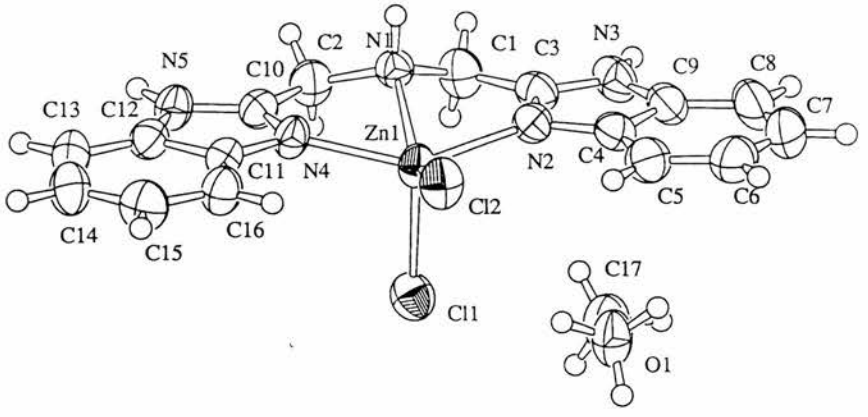

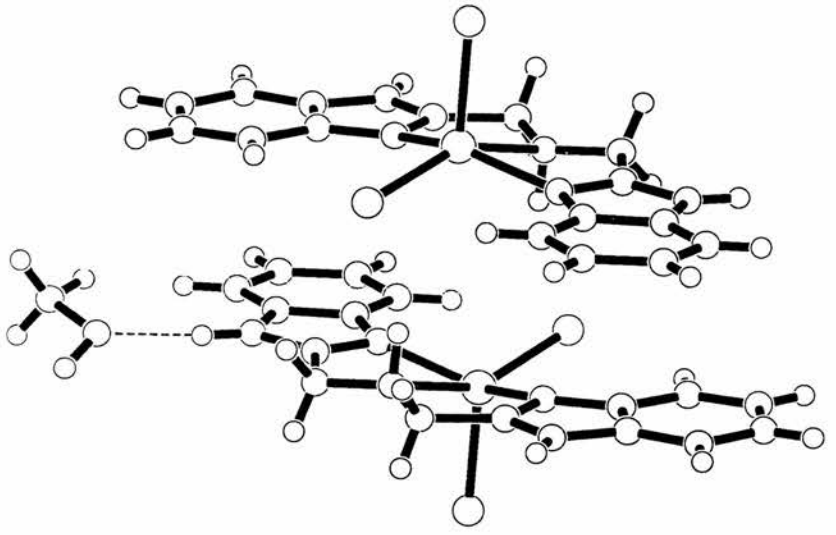

Activity of the Zinc(II) and Copper (II) Complexes in the Hydrolysis of Phosphate Triesters.- The hydrolysis of the phosphotriester, 2,4-dinitrophenyl phosphate in the presence of the copper(II) complex was studied. The reaction was monitored at 360nm (λ_{max} for 2,4-dinitrophenol) over a pH range, Table 3.

Table 3. pH-Rate Profile for the Hydrolysis of 2,4-dinitrophenyl diethylphosphate in the presence of $[ZnL(OH_2)_2]^{2+}$ at 25°C

pH	10^5 k s^{-1}
6.7	1.839(25)
6.5	0.239(12)
6.3	0.435(17)

In a typical run 2μL of phosphate stock solution was added to 2cm^3 of buffer (MES, 0.05 mol dm^{-3}) and 1 cm^3 of MeOH and the reaction initiated by addition of a DMF solution of the complex.

The reactions were carried out in MES buffer and the ionic strength adjusted to 0.1 mol dm^{-3} with KNO_3.

Precipitation occurred at higher pH and the rather low rates of reaction indicate that only small concentrations of the hydroxy complexes exist in solution even at the highest pH (6.7).

In order to determine the conditions over which the complexes were stable, a potentiometric study was carried out. Titration of the complexes ($1x10^{-3}$ mol dm^{-3}) in 0.1 mol dm^{-3} KNO_3 resulted in formation of precipitates at approximately pH 6.8. Even in the absence of KNO_3 precipitates formed at about pH 7.0. To obtain data over the higher pH range, an excess of the ligand had to be used. However, due to the low solubility of the ligand free base, a water-methanol solvent system had to be used.

Table 4. pH-Rate Profile for the Hydrolysis of 2,4-dinitrophenyl diethylphospate, (DNPDEP) $10^6 k_{obs}$ (s^{-1}) at 25°C

pH	Buffer and ligand only	Cu^{2+} and L[(a)]	Zn^{2+} and L[(b)]
8.5	9.2	15.4	-
8.0	6.6	9.6	-
7.5	6.0	6.5	-
7.0	5.1	4.8	8.8
6.6	4.4	3.7	5.6
6.0	-	-	4.0
5.5	-	-	3.5
5.0	-	-	3.2

[(a)]These values are the average of two runs (standard deviation was found to be between 0.01 and 0.06 s.

[(b)]These values are obtained from one run only. The standard deviation computed from the fitted absorbence-time curves was found to be between 0.009 and 0.002 s^{-1}.

Hydrolysis of DNPDEP.- The hydrolysis of the triester was studied at a number of pH's to identify the catalytically active metal complex, Table 4. For both the zinc and copper systems the rate increases at higher pH. Only small catalytic effects are observed in the system with the metal complexes.

The potentiometric data enables the concentration of various species to be determined at each of the pH's examined. An inspection of the speciation curves shows that the only species increasing in concentration over the experimental pH range was the hydroxy aquo complex. Figure 2 shows that values of k_{obs} correlates quite closely with the concentration of the hydroaquo species.

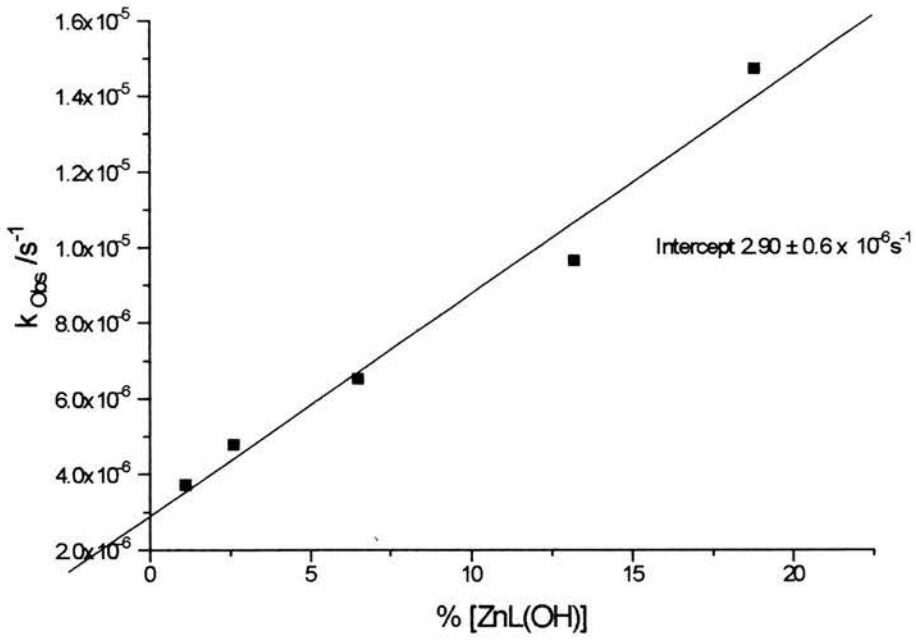

Figure 2

Potentiometry.- The titration curve, Figure 3 for the ligand only shows a buffer region corresponding to the loss of two protons then a sharp inflexion point after addition of two equivalents of base. The solution behaviour is best modelled by assuming that the hydrochloride salt is a di-acid; the log β values are given in Table 5.

Table 5 Protonation constants and stability constants for Copper(II), Zinc(II) complexes

Protonation constants (ligand = H_2L, errors as σ)

$\log \beta_{HL}$	$H^+ + L = HL^+$	5.638 ± 0.003
$\log \beta_{H2L}$	$2H^+ + L = H_2L^{2+}$	10.12 ± 0.01

Copper(II) stability constants

$\log \beta_{Cu2L}$	$Cu^{2+} + 2L = CuL_2^{2+}$	10.64 ± 0.03
$\log \beta_{CuL}$	$Cu^{2+} + L = CuL^{2+}$	6.34 ± 0.02
$\log \beta_{Cu(OH)L}$	$Cu^{2+} + OH^- + L = Cu(OH)L^+$	-0.97 ± 0.07
$\log \beta_{Cu(OH)2L}$	$Cu^{2+} + 2OH^- + L = Cu(OH)_2L^+$	-10.07 ± 0.06
$\log \beta_{CuHL2}$	$Cu^{2+} + 2L^+ + H^+ = L_2CuH^{3+}$	15.05 ± 0.05

Zinc(II) stability constants

$\log \beta_{ZnL}$	$Zn^{2+} + L = ZnL^{2+}$	5.96 ± 0.02
$\log \beta_{ZnL2}$	$Zn^{2+} + 2L = ZnL_2^{2+}$	8.97 ± 0.08
$\log \beta_{ZnLOH}$	$Zn^{2+} + +OH- L = ZnL^{2+}$	-2.33 ± 0.06

The logβ values for the protonation of the free ligand equate to a pKa of 4.48(1) for the removal of the first proton and 5.638(2) for the second. Both pKa's are rather low, indicating that the protonation sites are the imidazole nitrogen's rather than the secondary amine nitrogen. A secondary amine would be expected to have a much higher pKa (e.g. dibenzylamine hydrochloride has a pKa of 8.08[10] in 50% EtOH).

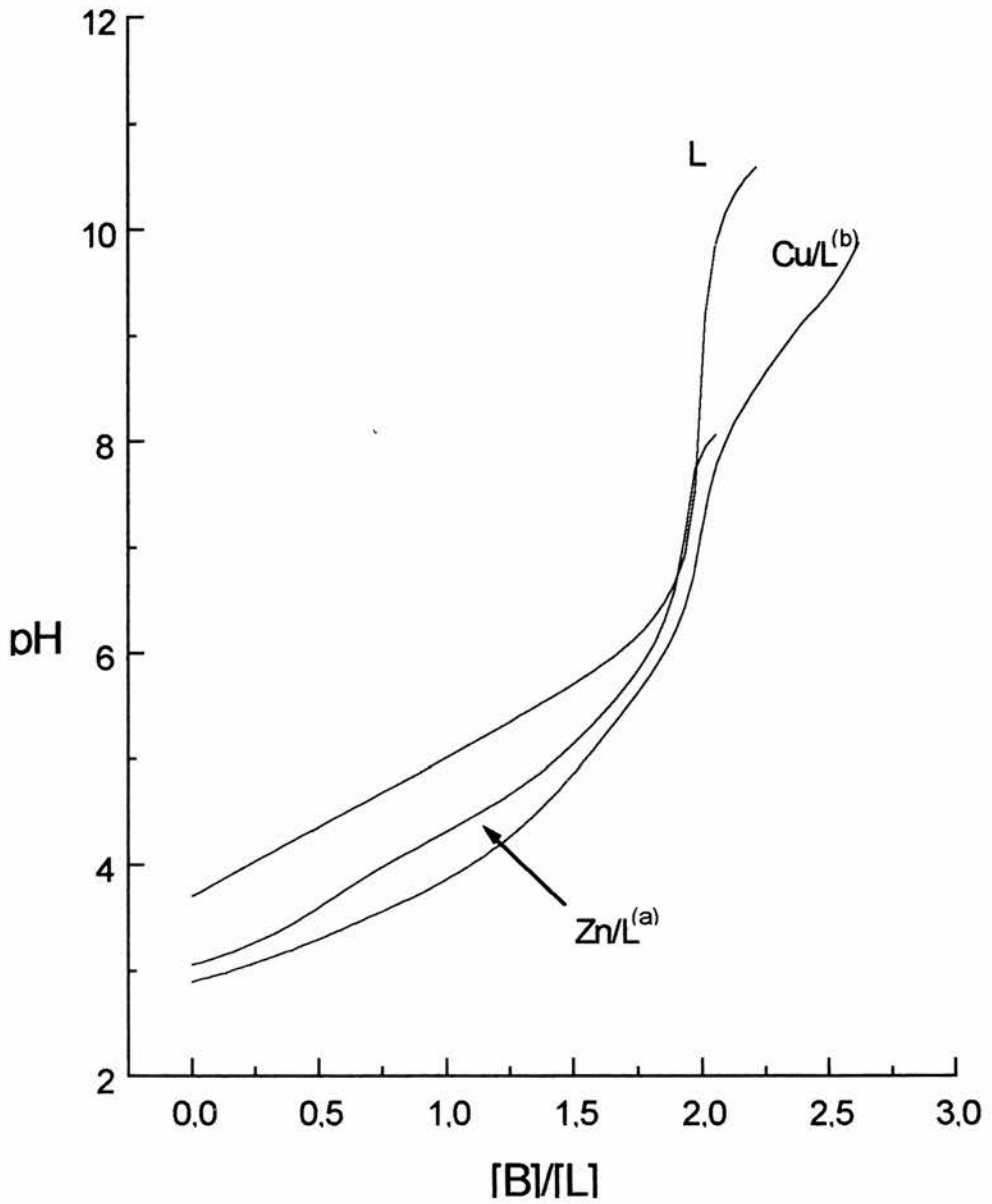

Figure 3

Protonation at the pyridine-type nitrogen of the imidazole is probably favoured as this minimises electrostatic repulsion between the charges in the dication LH_2^{2+}

The titrations in the presence of copper(II) shows an inflexion point after addition of two equivalents of base indicating the formation of mono ligand complexes. The three fold excess of ligand over the metal makes the formation of bis ligand complexes likely. A slight rise at approximately one equivalent of base indicates the presence of a protonated complex. The system also shows the presence of titratable protons at more than two equivalents of base indicating hydroxy complexes. In Chin's kinetic work the presence of a μ hydroxy dimer was proposed so the binuclear hydroxy species were also included in the calculation.

The program HYPERQUAD easily identified the presence of the bis complex (210), mono complex(110) and a minor protonated bis ligand complex species (211)at low pH (pH<6). At high pH the dominant complexes are the mono ligand hydroxy complexes (11-1 and 11-2). Using the β values in Table 5 the following pKa's could be calculated for the coordinated water molecules:

$CuL(OH_2)_2 = CuL(OH_2)OH^+ + H^+$ $\log K_1$ 7.31(7)

$[CuL(OH_2)OH]^+ = CuL(OH)_2 + H^+$ $\log K_2$ 9.10(5)

The speciation curves, Figure 4, indicate that the ML species disappears before the MLOH complex is formed and that the major species in solution is the bis complex ML_2.

It is likely that the monohydroxy complex is formed, not from the deprotonation of a coordinated water molecule, but hydroxide displacement of a benzimidazole ligand:

$CuL_2^{2-} + OH^- = CuL(OH)^+ + L$

Figure 4. speciation curves for Cu(II)-L

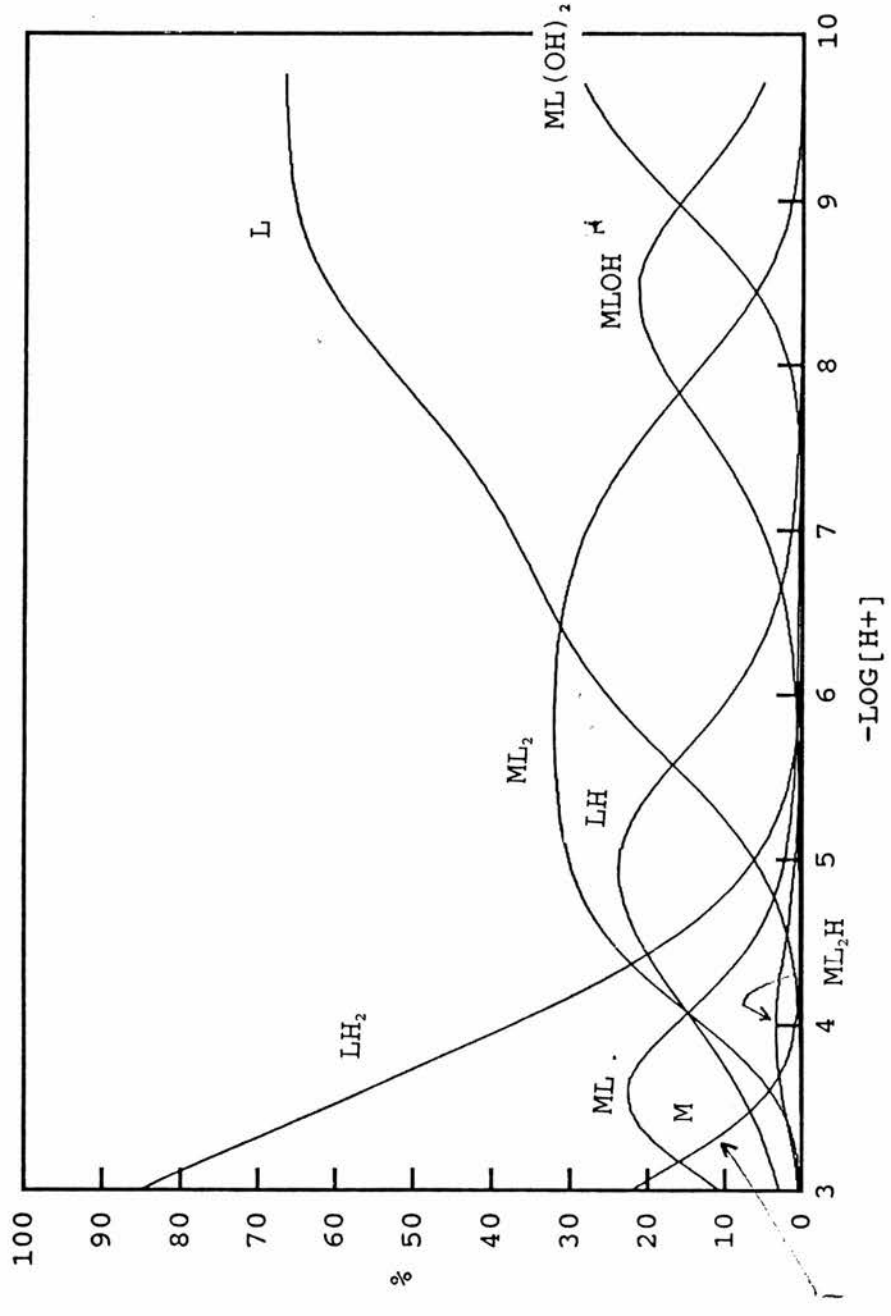

Titration in the presence of zinc(II) resulted in a similar curve to that obtained in the presence of copper, except that in the alkaline region (pH > 7) precipitates formed. The same species model was run with the zinc data. It was found that the dihydroxy complex 11-2 was rejected by SUPERQUAD, as was the minor protonated complex found in the copper(II) system. Unfortunately the monohydroxy complex seems to be formed at a pH where precipitation occurs. The monohydroxy complex must be included in the model but inspection of the speciation curves indicate that formation of this complex is only begining as precipitation takes place. The stability constant for the 11-1 species and the calculated pK_a of the zinc bound water molecule (8.29 ± 0.06) can only be regarded as estimates.

Although three of the titrations were run at double the concentration no evidence for polynuclear complexes could be found under these experimental conditions.

Our findings cast some doubt on the results published in the communication by Chin[1] where the transesterification experiments on hnpn were carried out at pH 7. Such solutions would precipitate copper(II) hydroxide, preventing accurate monitoring of the reaction by spectrophotometric means. Under our experimental conditions (three fold excess of ligand) the speciation curves show full complexation of copper by pH 6.5 and we are confident that, even in the presence of 0.05 mol dm^{-3} buffer, no precipitates formed below pH 6.5.

Investigation of the solution chemistry enabled the study to be extended to zinc(II).The precipitation of hydroxide species in the copper(II) system occurred above pH 7.3 even in the presence of a three fold excess of the ligand over the metal ion.

References

[1].D.Wahnon, R.C.Hynes and J.Chin; *J.C.S. Chem. Commun.*, 1994, 1441.

[2].V.Jubian,R.P.Dixon and A.Hamilton, *J.Am.Chem.Soc.*, 1992, **112**, 3686; J.R.Morrow, L.A.Buttrey, V.M.Shelton and K.A.Berback, *J.Am.Chem.Soc.*, 1992, **114**, 1903; R.Breslow, D.Berger and D.-L.Huang, *J.Am.Chem.Soc.*, 1990, **112**, 3686.

[3].H.P.Berends and D.W.Stephan, *Inorg.Chim.Act.*,1984,**93**, 173.

[4].*SIR92:* A.Altomare, M.C.Burla, M.Camalli, M.Cascarano, C.Giacovazzo, A.Guagliardi, and G.Polidori, **(1994)**, *J.Appl.Cryst.*, in preparation.

[5].DIRDIF94: P.T.Beurskens, G.Admiraal, G.Beurskens, W.P.Bosman, R. de Gelder, R.Israel and J.M.M.Smits **(1994)**. *The DIRDIF-94 program system,* Technical Report of the Crystallography Laboratory, University of Nijmegen, The Netherlands.

[6].Least-Squares:

Function minimised: $\Sigma w(|Fo| - |Fc|)^2$ where $w = 1/\sigma^2(Fo) = 4Fo^2/\sigma^2(Fo^2)$

$\sigma^2(Fo^2) = S^2(C+R^2B)+(pFo^2)^2/Lp^2$

S = Scan speed

C = Total integrated peak count

R = Ratio of scan time to background counting time

B = Total background count

Lp = Lorentz-polarization factor

p = p-factor

[7].Standard deviation of an observation of unit weight:

$$\sqrt{\sum w\left(|Fo| - |Fc|\right)^2 / (No - Nv)}$$

where: No = number of observations

Nv = number of variables

[8].*Crystal Structure Analysis Package,* Molecular Structure Corporation (1985& 1992)

[9].R.G.Bates, M.Paabo and R.A.Robinson, *J.Phys.Chem,* 1963, **67**, 1833.

[10]*Stability Constants*, Special Publication No.17, L.G.Sillen and A.E.Martell, *The Chemical Society* **(1964)**

Chapter 3

Tripodal Ligands

The Preparation of Transition metal complexes of 3,3',3''-triaminotripropylamine (trpn) and the Crystal Structure of $[Ni(trpn)CO_3]NaClO_4.5H_2O$.

Abstract

The synthesis of the polyamine ligand 3,3',3''-triaminotripropylamine is described. A variety of copper(II), nickel(II), cobalt(II), chromium(III) and zinc(II) complexes have been prepared and characterised. I.r., UVis spectra, magnetic and conductivity measurements are described. The crystal structure of the carbonato complex, $[Ni(trpn)CO_3]NaClO_4$ has been determined. The four protonation constants of trpn have been determined at I= 0.1 mol dm^{-3} at 25°C as $logK_{11}$ 10.56, $logK_{12}$ 9.96, $logK_{13}$ 9.37 and $logK_{14}$ 5.70. Formation constants for complexes with Cu(II), Ni(II), Zn(II) and Co(II) have also been determined by potentiometric and spectrophotometric methods.

Introduction

The ligand 3,3',3''-triaminotripropylamine (trpn=1) was first synthesised by Mann and Pope in 1926[1], who also characterised several solid nickel(II) complexes. Thermochemical and spectroscopic studies of aqueous solutions of M(II) complexes have indicated that Co(II) and Cu(II) are five coordinate, Ni(II) is octahedral and Zn(II) tetrahedral[2,3]. Shafer and Raymond [4] subsequently established by x-ray crystallography that [Co(trpn)Br]Br.0.5EtOH has a trigonal bipyramidal structure with axial and equatorial Co-N bond lengths of 2.194 and 2.055 Å respectively. The unusually long Co-N bond length is cited as evidence towards four coordinate geometry.

Complexes of trpn have attracted considerable attention in recent years as the cobalt(III) complex $[Co(trpn)(OH)(OH_2)]^{2+}$ catalyses the hydrolysis of unactivated carboxylic esters such as methyl acetate[5] phosphate diesters[6] and polyphosphates[7]. As a result we have been interested in various aspects of the chemistry of this flexible tripodal ligand. The present work describes the preparation and characterisation of a variety of copper(II), nickel(II), cobalt(III), chromium(III), cobalt(III) and zinc(II) complexes. Formation constants have also been determined for the metal(II) complexes at I= 0.1mol dm^{-3}, 25°C.

Experimental

Synthesis.- All I.r spectra were obtained with a Perkin Elmer 1710 FTIR spectrometer and recorded on a Hewlett Packard colourpro plotter. KBr discs were used for all solid specimens and a thin film between NaCl plates for the free base trpn.

Preparation of the Ligand.-(a) 3,3',3"-triaminotripropylamine (trpn).- The amine was synthesised by catalytic hydrogenation[6b] of *tris*-(2-cyanoethyl)amine prepared by the reaction of ammonia with acrylonitrile[8]. *Tris*-(2-cyanoethyl)amine (6.13g) and KOH (3.37g) were added to absolute ethanol (30 cm^3) in a glass hydrogenation vessel (600cm^3) containing a magnetic stirrer bar. Raney nickel (6.6g, 50% aqueous slurry) was added to the hydrogenation vessel with ethanol (50 cm^3). The vessel was pressurised to 30p.s.i with hydrogen and the mixture stirred vigorously at room temperature. Uptake of hydrogen ceased after six repressurisations over a period of three days. The catalyst was filtered off and washed with ethanol. The filtrate and washings were treated with HBr (12.1g, 48%) to remove KOH. The precipitated KBr was filtered off and the filtrate dried over $MgSO_4$. The ethanol was removed on a rotary evaporator to give a pale yellow residue which was vacuum distilled to give trpn as a colourless oil. I.r./cm^{-1} 3354, 3279s (N-H ν); 2932, 2860m (C-H ν); 1600s, br; 1304, 1381 (C-N ν); 1113 (ClO_4^-); 898, 844 (CH_2 γ).

*(b)*Trpn.4HBr.0.5H_2O.- Trpn (7.0g, 0.0486mol) was dissolved in ethanol (20cm^3) and the solution acidified with HBr (4.5 cm^3, 48%) with cooling in an ice bath. The white crystalline solid precipitated overnight and was filtered off and recrystallised from ethanol-H_2O (70-30;v/v) to give white crystals (12g, 62%).(Found: C, 20.28, H, 5.68, N, 10.54. Calc. for $C_9H_{29}N_4O_{0.5}Br_4$: C, 20.75, H, 5.68, N, 10.54%).

Preparation of the Transition Metal Complexes.-

(a) [Zn(trpn)Cl]Cl.0.75H_2O. Zinc(II)chloride (0.38g, 6.16mmol) was dissolved in ethanol (10cm^3) and the solution heated with rapid stirring. The free base ligand (0.53g,

2.82mmol) in ethanol ($10cm^3$) was added dropwise. A white precipitate formed almost immediately. Methanol (*ca.*$30cm^3$) was added until the precipitate dissolved (traces of $Zn(OH)_2$ were filtered off and discarded). The solvent was removed on a rotary evaporator to give the colourless complex which was recrystallised from *iso*-PrOH (yield 0.45g, 23%). (Found: C, 31.92; H, 7.82; N, 16.67%. Calc. for $C_9H_{24}N_4(H_2O)_{0.75}Cl_2Zn$: C, 31.97; H, 7.60; N, 16.57%); i.r./cm^{-1} 3387s, br (O-H ν); 3320, 3122s (N-H ν); 2965, 2934, 2892, 2861m (C-H ν); 1596s, br (N-H δ); 1408, 1552m, 1314w, 1292m (C-N ν); 954, 911, 896, 854 (CH_2 γ); 741m (C-H δ); 620, 525, 490, 463w N-M ν; Λ_M /S cm^2 mol^{-1} 47.

(b)[Ni(trpn)(CO_3)]$NaClO_4.5H_2O$. Trpn (0.75g, 4mmol) in water ($10cm^3$) was adjusted to pH 9.5 with sodium hydroxide and added to nickel(II) perchlorate hexahydrate (1.46g, 4mmol) to produce a pale-green, gelatinous precipitate. Over three days the solution partially cleared and blue, block crystals formed. After one week all the precipitate had dissolved and many large dark blue crystals had formed. The product was filtered off, washed with ice cold water ($2x3cm^3$) and dried over silica gel. (yield 1.32g, 86%). (Found: C, 23.20; H, 6.58; N, 10.74%; $C_{10}H_{24}N_4O_7ClNaNi.5H_2O$ requires: C, 23.12; H, 6.60; N, 10.78%); λmax/nm (DMSO) 365 (ε/dm^3 mol^{-1} cm^{-1} 43), 580 (5.3); i.r./cm^{-1} 3594s (O-H ν); 3354s, 3336s, 3330vs, 3320s, and 3186s (N-H ν), 2981w, 2964w, 2943w, 2885w, and 2857w (C-H ν), 1659w, 1626s, and 1609s (O-H δ), 1435vs (C-Oν and N-H), 1332w, 1308w (C-O ν), 1284w, 1268w, 1201-1011vs (ClO_4^- ν), 626s, 535w; Λ_M /S cm^2mol^{-1} 37.

(c)[Ni(trpn)OH_2]ClO_4. A solution of nickel(II)perchlorate hexahydrate (1.07g, 2.93mmol) in ethanol was gently heated with rapid stirring. To this was added, dropwise, a solution of trpn (0.55g, 2.93mmol) in methanol (*ca.*$10cm^3$) Some precipitates formed initially on mixing, but over a period of 15min the solution cleared to give a blue green solution. On cooling a green complex crystallised. The precipitate was filtered off and washed with ethanol ($2x1cm^3$) and dried *in vacuo* (yield 0.81g, 62%). (Found: C, 23.51; H, 5.23; N, 11.98%. Calc. for $C_9H_{26}N_4O_9Cl_2Ni$: C, 23.30; H, 5.65; N, 12.07%) i.r./cm^{-1}

3388s (O-H ν); 3292s, 3238s, 3159vs, and 3320s, (N-H ν), 2965m, 2927m, and 2885m, (C-H ν), 1623w (O-H δ), 1598m, sh (N-H δ), 1329w, 1371w, 1396w, 1272w, (C-N ν) 1201-1011vs, br (ClO_4^- ν), 957w, 923w, 885w, 860w, (CH_2 γ); λmax/nm (DMSO) 371(ε/dm^3 mol^{-1} cm^{-1} 27), 597(15); Λ_M /S cm^2 mol^{-1} 74.

(d)[Cu(trpn)Cl]Cl. $0.5CH_3OH$. $2.5H_2O$. Trpn (0.43g, 2.29mmol) in ethanol ($10cm^3$) and $CuCl_2.2H_2O$ (0.38g, 2.29mmol) in ethanol ($10cm^3$) were heated to boiling then rapidly mixed to form a blue green suspension. The mixture was boiled until a deep blue solution was obtained. The solution was left to cool. The blue solid, which separated from solution was filtered off and washed with ethanol ($2x2cm^3$). (yield 0.63, 85%) (Found: C, 29.87; H, 7.40; N, 14.64%. Calc. for $C_9H_{26}N_4O_9Cl_2Cu$: C, 29.73; H, 8.14; N, 14.60%); λ_{max}/nm (DMSO) 498 (ε/dm^3 mol^{-1} cm^{-1} 29), 677(178); i.r./cm^{-1} 3400s br (O-H ν); 3209, 3123s (N-H ν); 2957, 2938, 2885m (C-H ν); 1589s (N-H δ); 1469m, 1400, 1375, 1337w, 1289, 1369m (C-N ν); 748 (CH_2 γ); 517w (N-M ν); Λ_M /S cm^2 mol^{-1} 28.

(e)[Cu(trpn)Cl]ClO_4. [Cu(trpn)Cl]Cl was dissolved in a minimum amount of water, to which was added a saturated solution of sodium perchlorate. Over a period of a few hours dark green blades formed. The crystals were filtered off and washed with water ($2x1cm^3$) then ethanol ($1x10cm^3$) then dried *in vacuo*. (Found: C, 26.96; H, 6.85; N, 13.60%: Calc. for $C_9H_{26}N_4O_4Cl_2Cu$: C, 26.71; H, 6.47; N, 13.84%); λmax/nm (DMSO) 700 (ε/dm^3 mol^{-1} cm^{-1} 121), 889 (114); i.r./cm^{-1} 3435s, br (O-H ν); 3340, 3287, 3231, 3138s (N-H ν); 2928, 2877m, (C-H ν); 1593s (N-H δ); 1411w, 1390w, 1338w, 1306w, 1265m (C-N ν); 1096 (ClO_4^-); 953, 893, 906 (CH γ); 741m (C-H δ); 626 (ClO_4^-), 524, 506m (N-M ν); Λ_M /S cm^2 mol^{-1} 54.

(g)[Cu(trpn) OH_2]$(NO_3)_2$. Trpn (0.28, 1.49mmol) in ethanol ($10cm^3$) and $Cu(NO_3)_2.2H_2O$ (0.36g, 1.49mmol) in ethanol ($10cm^3$) were heated to boiling then rapidly mixed. A gelatinous precipitate immediately formed. On further heating a dark blue oil formed. Addition of methanol ($20cm^3$) and prolonged heating (*ca.* 30min) dissolved the oil and on cooling a deep blue precipitate formed. The complex was filtered off and washed with

ethanol (2x1cm^3) (yield 0.37g, 63%); λ_{max}/nm (DMSO) 400 (sh), 645 (ε/dm^3 mol^{-1} cm^{-1} 83). Λ_M /S cm^2 mol^{-1} 69.

(h)[Cr(trpn)Cl_2]Cl.0.5H_2O. This complex was prepared by a modification of Zip and Madans method[9] for the preparation of Cr(III) amine complexes.
Chromium (III) chloride hexahydrate (0.71g, 2.66mmol) was dissolved in DMF (20cm^3) and the solution boiled for 10-15 min to give [Cr(DMF)$_3Cl_3$] (the solution changes from green to purple as dehydration occurs). The ligand (0.71g) dissolved in boiling DMF (20cm^3) was then added dropwise with stirring. On cooling pale lilac needles formed and were filtered off and washed with copious quantities of *iso*-PrOH, then ether and dried *in vacuo* over silica gel (yield 0.75g, 93%), (Found: C, 30.28; H, 7.44; N, 15.53%. Calc. for $C_9H_{24}N_4Cl_3Cr.0.5H_2O$: C, 30.39; H, 7.08; N, 15.75%); λ_{max}/nm (DMSO) 405 (ε/dm^3 mol^{-1} cm^{-1} 34), 537 (31); i.r./cm^{-1} 3571, 3483m, br (O-H ν); 3181, 3113s (N-H ν); 2977, 2945, 2894m (C-H ν); 1657, 1616m 1578s, br (N-H δ); 1400, 1370, 1330, 1299w, (C-N ν), 940, 920, 884, 861 (CH_2 γ); 750w (C-H δ); 527, 494, 461w (N-M ν); Λ_M /S cm^2 mol^{-1} 30.

(i)[Cr(trpn)$(OH_2)_2$]$(ClO_4)_3$ DMF. To [Cr(trpn)Cl_2]Cl.0.5H_2O. (0.2g, 0.56mmol) in water (50cm^3) was added silver perchlorate (0.35g, 1.68mmol). The solution was gently warmed and left stirring overnight. The pink solution was filtered and the filtrate evaporated to dryness. The pink solid was recrystallized from a minimum volume of hot DMF. (0.27g, 73%); (Found: C, 22.99; H, 5.35; N, 10.40%. Calc. for $C_9H_{24}N_4Cl_3O_{12}Cr.C_3H_7NO$: C, 22.25; H, 5.45; N, 10.81%); λmax/nm (DMSO) 379 (ε/dm^3 mol^{-1} cm^{-1} 42), 379 (44) i.r./cm^{-1} 3436s, br (O-H ν); 3231s (N-H ν); 3057, 3003m (C-H ν); 1551s, 1600m (b), 1556m (N-H δ); 1478w, 1428m, 1387, 1303, 1258m (C-N ν); 1149 (ClO_4^-); 941, 901, 886, 851 (CH_2 γ); 741, 710w (C-H δ); 627 (ClO_4^-); 556, 521, 491w (N-M ν); Λ_M /S cm^2 mol^{-1} 81.

(k)[Co(trpn)Cl_2]Cl 2.7NaCl The ligand tetrahydrochloride (1.9g, 3.71mmol) and $Na_3[Co(CO_3)_3].3H_2O$ (1.06g, 3.71mmol) were heated together as a slurry with water (*ca.*

20 cm^3) on a water bath (*ca.* 1 hr). The mixture turns deep red, and further water (3-4 cm^3) was added and the mixture maintained at 70°C overnight. The sticky residue obtained was dissolved in methanol (10cm^3) and filtered to remove unreacted $Na_3[Co(CO_3)_3].3H_2O$. The solution was reduced by half on a rotary evaporator and HCl (35%) added dropwise until the vigorous effervescence ceased. The bright green complex was filtered off, washed with copious amounts of ethanol then ether and dried *in vacuo* (yield 0.69g) (Found: C, 21.34; H, 4.53; N, 10.58%. Calc. for $C_9H_{24}N_4Cl_{5.7}CrNa_{2.7}$: C, 21.14; H, 4.73; N 10.96%). i.r./cm^{-1} 3436s, br (O-H ν); 3325m, 3293m, 3262m, 3170s (N-H ν); 2951m (C-H ν); 1599m, 1578s, (N-H δ); 1464m, 1438m, 1414m, (C-N ν).

Crystal Data.-- $C_{10}H_{24}NiN_4O_{12}ClNa$, M = 509.46, monoclinic, a = 8.080(2), b = 9.360(3), c = 14.970(3) Å, β = 100.02(3)°, U = 1114.8(5) $Å^3$ (by least-squares refinement on diffractometer angles for 18 automaticaly centred reflections, in the range 8.96°<2θ<13.72° λ = 0.71069 Å), space group $P2_1$(#4), Z = 2, D_c = 1.52 g cm^{-3}, F(000) = 528.00. Blue needle crystal. Aproximate crystal dimensions 1.00 x 0.20 x 0.40 mm, μ(Mo-K_α) = 10.7 cm^{-1}.

Data Collection and Processing.--Rigaku AFC7S diffractometer, ω-2θ scan type with ω scan width = (1.78 + 0.35 tan θ)°, ω scan speed 16.00 min-1 (up to 4 scans), graphite monochromated MoKα radiation; 2254 reflections measured (max 2θ = 50.0°), 2099 unique (R_{int} = 0.023). No decay correction, or absorbtion correction was required. Corrections were made for Lorentz and polarisation effects.

Structure Analysis and Refinement.-- Direct methods[10] were employed and expanded using Fourier techniques[11] Some non-hydrogen atoms were refined anisotropicaly, while the rest were refined isotropicaly. Hydrogens were included but not refined. The final cycle of full-matrix least-squares refinement[12] was based on 2036 observed reflections ($I>3.00\sigma(I)$) and 241 variable parameters and converged with unweighted agreement factors of:

$$R = \sum \| Fo| - |Fc| \| / \sum |Fo| = 0.041$$

$$R_w = \sqrt{\left(\sum \left(|Fo| - |Fc| \right)^2 / \sum wFo^2 \right)} = 0.034$$

The standard deviation of an observation of unit weight[13] was 8.25. The Weighting scheme was based on counting statistics and included a factor (p = 0.002) to downweight the intence reflections. Plots of $w(\Sigma |Fo| - |Fc|)^2$ versus $|Fo|$, reflection order in data collection, sin θ/λ and various classes of indices showed no unusual trends. The maximum and minimum peaks on the final difference Fourier map correspond to 1.59 and -0.87 $e^-Å^{-3}$, respectively. All calculations were performed using the teXsan[14] crystallographic software package of molecular Structure Corporation.

Results and Discussion

Synthesis.- 3,3',3"-triaminotripropylamine (trpn) was prepared by catalytic reduction of tris(2-cyanoethyl)amine. It was found that the brown oil obtained from the preparation of tris(2-cyanoethyl)amine could be induced to crystallise by the addition of an equal volume of crushed ice. GCMS analysis of the brown oil showed considerable contamination with the dialkylated compound. The chemical reduction of similar nitriles with $LiAlH_4$ or $NaBH_4$ has not been successful[15], so other reagents were investigated. The reagents $CoCl_2/NaBH_4$[16] and $LiAlH_4/AlCl_3$[17] gave ill defined products (extractions with CH_2Cl_2 gave only small amounts of tarry material and attempts to isolate the product as the HBr salt produced white solids showing no organic bands in the IR spectrum). Reduction using $NaBH_4$/Raney nickel[18] gave the product in very low yield. Trpn is extremely soluble in water so attempts to extract trpn from aqueous solutions (even from saturated NaOH) with dichloromethane is difficult.

Crystallography.- Description of the structure- $[Ni(trpn)(CO_3)]NaClO_4.5H_2O$. The structure of the nickel complex establishes that the nickel is in a pseudo octahedral environment. Four coordination sites are occupied by the nitrogen donors of trpn and the remaining two sites by chelated carbonate. It was also found that the structure has a sodium ion bonded to four water molecules (average O-Na bond lengths of 2.47(9)Å) and a short bond to a chelating oxygen of the carbonate(O-Na 2.299(8)Å. The charge on sodium is balanced by a perchlorate which is substantially disordered. The fifth water molecule(O12) exists as water of crystallisation.

Table 1.Selected bond lengths (Å) and angles of$[Ni(trpn)(CO_3)]NaClO_4.5H_2O$

Ni(1)-N(1) 2.123(9)	N(1)-Ni(1)-N(2) 92.4(4)
Ni(1)-N(2) 2.12(1)	N(1)-Ni(1)-N(3) 98.3(3)
Ni(1)-N(3) 2.093(8)	N(1)-Ni(1)-N(4) 90.3(4)
Ni(1)-N(4) 2.11(1)	N(1)-Ni(1)-O(1) 104.0(3)
Ni(1)-O(1) 2.164(6)	N(1)-Ni(1)-O(2) 166.2(3)
Ni(1)-O(2) 2.135(7)	O(1)-Ni(1)-O(2) 62.2(2)
Na(1)-O(2) 2.299(8)	O(1)-C(1)-O(2) 117.8(9)
Na(1)-O(8) 2.432(9)	O(1)-C(1)-O(3) 120.8(1)
Na(1)-O(9) 2.61(1)	
Na(1)-O(10) 2.472(9)	
Na(1)-O(11) 2.37(1)	

Examples of mononuclear complexes with chelating carbonate can be found in other transition elements e.g. copper (II)[19] cobalt(III)[20] platinum(II)[21] There are also examples of carbonate acting as a bridge, simultaneously chelating two metal centres[22] or as mixed mono and bidentate bridges[23]

ORTEP diagram of the complex $[Ni(trpn)(CO_3)]NaClO_4.5H_2O$

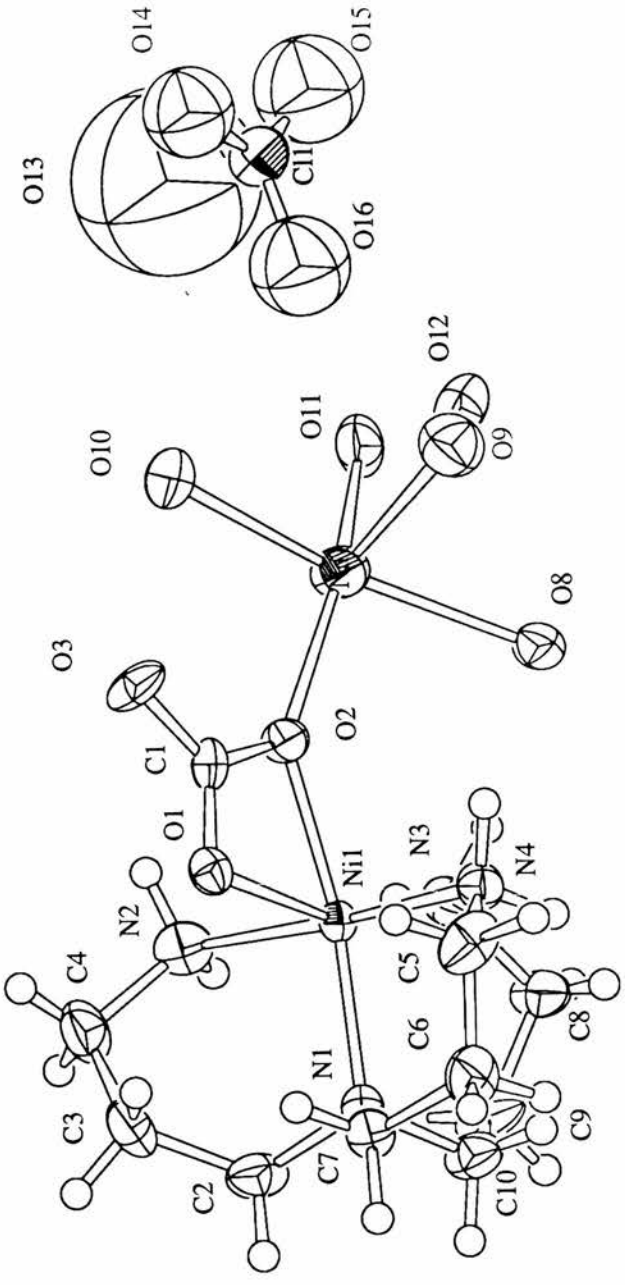

References

[1].F.G.Mann and W.J.Pope, *J.Chem.Soc.*, 1926, **7**, 865.

[2]. A.D.Paoletti and A.Vacca, *Inorg.Chem.*, 1968, **7**, 867.

[3].A.Vacca and P.Paoletti, *J.Chem.Soc.(A)*, 1968, 2378.

[4].J.L.Shafer and K.N.Raymond, *Inorg.Chem.*, 1971, **10**, 1799.

[5].J.Chin and M.Banaszczyk, *J.Am.Chem.Soc.* 1989, **111**, 2724.

[6].a)G.H.Rawji and R.M.Milburn, *Inorg.Chim.Acta*, 1988, **150**, 227;F.Tafesse, S.S.Massoud and R.M.Milburn, *Inorg.Chem.*, 1985, **24**, 2591; (b)J.Chin, M. Banaszczyk, V.Jubian and X.Zou, *J.Am.Chem.Soc.*, 1989, **111**, 186; (c) J.Chin and M. Banaszczyk, *J.Am.Chem.Soc.*, 1989, **111**, 4103;

[7] a) F.Tafesse, *Trans.Met.Chem.*, 1991, **16**, 114; (b) R.J.Geue, A.M.Sargeson and R.Wijesekera, *Austr.J.Chem.*, 1993, **46**, 1021.

[8].J.A.Laurino, S.Knapp and H.J.Schugar, *Inorg.Chem.*, 1978, **17**, 2027

[9].S.G.Zipp and S.K.Madan, *Inorg.Chem.*, 1976, **15**, 587.

[10].*SIR92:* A.Altomare, M.C.Burla, M.Camalli, M.Cascarano, C.Giacovazzo, A.Guagliardi and G.Polidori, (1994).*J.Appl.Cryst.*, in preparation.

[11].DIRDIF94: P.T.Beurskens, G.Admiraal, G.Beurskens, W.P.Bosman, R. de Gelder, R.Israel and J.M.M.Smits(1994). *The DIRDIF-94 program system,* Technical Report of the Crystallography Laboratory, University of Nijmegen, The Netherlands.

[12].Least-Squares:

Function minimised: $\Sigma w(|Fo| - |Fc|)^2$ where $w = 1/\sigma^2(Fo) = 4Fo^2/\sigma^2(Fo^2)$

$\sigma^2(Fo^2) = S^2(C+R^2B)+(pFo^2)^2/Lp^2$

S = Scan speed

C = Total integrated peak count

R = Ratio of scan time to background counting time

B = Total background count

Lp = Lorentz-polarization factor

p = p-factor

[13].Standard deviation of an observation of unit weight:

$$\sqrt{\sum w\left(|Fo| - |Fc|\right)^2 / \left(No - Nv\right)}$$

where: No = number of observations

Nv = number of variables

[14].*Crystal Structure Analysis Package,* Molecular Structure Corporation (1985& 1992)

[15].J.L.Winkel, J.D.McClure, and P.H.Williams, *J.Org.Chem.*, 1966, **31**, 3300.

[16].T.Satoh and S.Suzuki, *Tet.Lett.*, 1969, **52**, 4555; (b)E.Buhleier, W.Wehner, and F.Vogtle, *Synthesis,* 1978, 115.

[17].R.F.Nystrom, *J.Am.Chem.Soc.* 1955, 77, 2544

[18].Egli, *Helv.Chim.Acta*, 1970, **53**, 47

[19].M.H.Meyer, P.Singh, W.E.Hatfield, and D.J.Hodgson, *Acta.Crystallog.Sec.B*, 1972, **28**, 16

[20].G.A.Barclay, and B.F.Hoskins, *J.Chem.Soc*, 1962, 5586.

21.a)F.Cariati, R.Mason, G.B.Rogertson, and R.Ugo, *Chem.Commun.*, 1967, 408, b)T.K.Miyamoto, Y.Suzuki and H.Ichida, Chem.Lett., 1992, **5**, 839.

[22].(a)M.R.Churchill, G.Davies, M.A.El-Sayed, M.F.El-Shazly, J.P.Huchinson, M.W.Rupich, and K.O.Watkins, *Inorg.Chem.*, 1979, **18**, 2296; (b) M.R.Churchill, G.Davies, M.A.El-Sayed and J.P.Huchinson,. *Inorg.Chem.*, 1982, **21**, 1002; (c)A.R.Davies and F.W.B.Einstein, *Inorg.Chem.* 1980, **19**, 1203; (d) H.Harada, M.Kodera, G.Vuckovic, N.Matsumoto and S.Kida, *Inorg.Chem*, 1991, **30**, 1190; (e)S.C.Rawle, C.J.Harding, P.Moore and N.W.Alcock, *J.Chem.Soc, Chem.Commun.*, 1992, 1701.

[23].a) J.Chatt, M.Kuboto, G.J.Leigh, F.C.March, R.Mason and D.J.Yarrow, *J.Chem.Soc.,Chem.Commun*, 1974, 1033. (b) S.Krogstrud, S.Komiga, T.Ito, J.A.Ibers, and A.Yamamoto, *Inorg.Chem*, 1976, **15**, 2798.

Synthesis of the Tripodal Ligand 5-(2'-Pyridylmethyl)-1,5,9-Triazanonane and Characterization of its Transition Metal Complexes. Crystal Structures of $[NiL(MeCN)](ClO_4)_2$ and $[CuLCl]ClO_4$

Abstract

The preparation of the new tripodal ligand 5-(2'-pyridylmethyl)-1,5,9-triazanonane (L) by reaction of 2-aminomethyl pyridine with acrylonitrile followed by reduction of the nitrile is described. Copper(II), nickel(II), zinc(II), cobalt(III), and chromium(III), complexes of the ligand have been prepared and characterised. The crystal structure of the copper(II) complex $[CuLCl]ClO_4$ and the nickel(II) complex $[NiL(MeCN)_2](ClO_4)_2$ has been determined. The copper(II) is five co-ordinate with approximate square pyramidal stereochemistry and the nickel complex octahedral with the *cis* coordination sites occupied by coordinated acetonitrile.

Introduction

There are a limited number of tripodal amine ligands, important examples are tren $[N(CH_2CH_2NH_2)_3]$ and trpn $[N(CH_2CH_2CH_2NH_2)_3]$. Cobalt(III) complexes of trpn have recently attracted considerable attention as the complex $[Co(trpn)(OH_2)(OH)]^{2+}$ promotes the hydrolysis of unactivated carboxylic esters such as methyl acetate[1], and the hydrolysis of phosphate esters[2]. The complex $[Co(tren)(OH)(OH_2)]^{2+}$ is also known to promote the hydrolysis of amino acid esters and peptides[3]. In addition tren and trpn have been used as intermediates in the synthesis of a range of macrocycles and cryptand ligands, such as (1) in which a variety of dialdehydes can be used as "spacers"[4]. For this reason we have been interested in the synthesis of new tripodal amine ligands which may be of value in catalytic studies and as intermediates in the synthesis of macrocyclic ligands. In the present work we describe the synthesis of the new tripodal ligand 5-(2'-pyridylmethyl)-1,5,9-triazanonane (2) and characterisation of some of its transition metal complexes.

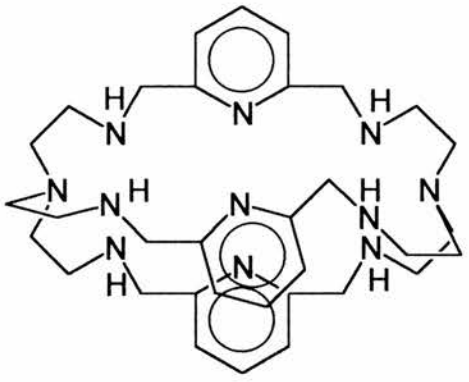

(1)

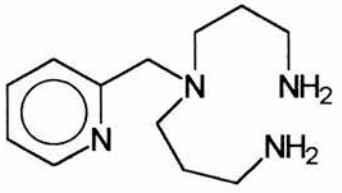

(2) = Pydpa

Experimental

Measurements.- Infrared spectra were recorded on a Perkin Elmer 1710 Infrared Fourier Transform Spectrometer as KBr discs. Melting points were obtained using a Gallenkamp melting point apparatus. UVis spectra were recorded on a Lambda 14P Spectrometer. The NMR spectra were obtained using a 200MHz Varian Gemini FT spectrometer.

Preparation of the ligand and metal complexes.-(a) 4-(2'pyridylmethyl)-4-amino-1,7-heptanedinitrile

2-Aminomethyl pyridine (8g, 0.08 mol) was dissolved in acrylonitrile (92g, 1.72 mol). The solution was heated at reflux under argon for 48hr during which time the solution turned yellow in colour. The excess acrylonitrile was removed under reduced pressure and dichloromethane (150 cm^3) added. The organic solution was washed with ammonia solution (d 0.88, 125 cm^3) then water (3x100 cm^3) and dried over anhydrous magnesium sulphate. After filtration, the solvent was removed to give the product as a pale brown oil (9.8g, 57%). (Found: C, 66.50; H, 7.23; N, 26.62. Calc. for $C_{12}H_{14}N_4$: C, 67.27; H, 6.59; N, 26.15%); ir (thin film)/ cm^{-1}, 2931, 2844 (CH ν); 2248 (CN ν); 1654, 1591, 1570 (CH bend). δ_H (200MHz; solvent $CDCl_3$; standard reference TMS) 8.55 (d, Py H [1H]) , 7.74 (Py H, triplet of doublets [4H]), 7.53 (doublet, Py H [1H]), 7.25 (m, Py H[1H]), 3.10 (s, benzyl H [2H]), 3.00 (t, H of CH_2CH_2-CN [4H]), 2.53 (t, H of

[1H]) , 7.74 (Py H, triplet of doublets [4H]), 7.53 (doublet, Py H [1H]), 7.25 (m, Py H[1H]), 3.10 (s, benzyl H [2H]), 3.00 (t, H of CH_2CH_2-CN [4H]), 2.53 (t, H of CH_2CH_2-CN [4H]); δ_H 118.635, 122.593, 123.109, 136.896, 149.086 (py), 157.951(*C*N), 59.429 (benzyl carbon), 16.761, 49.689 (CH_2CH_2CN);

(b)- 5-(2'-pyridylmethyl)-1,5,9-triazanonane (Pydpa = [2])

The amine was synthesised by catalytic hydrogenation of 4-(2'pyridylmethyl)-4-amino-1,7-heptanedinitrile. 4-(2'pyridylmethyl)-4-amino-1,7-heptanedinitrile (10g, 47mmol) and KOH (3.16g) were added to dry MeOH (60 cm^3) in a glass hydrogenation vessel (600 cm^3) containing a magnetic stirrer bar. W-5 Raney nickel, freshly prepared from 25g of Raney aluminium/nickel alloy[5] was washed in with 50 cm^3 MeOH. The vessel was pressurised to 30 p.s.i. with hydrogen and the mixture vigorously stirred at room temperature. Hydrogen uptake ceased after 12hr. The methanolic solution was decanted from the Raney nickel, and the Raney nickel washed twice with ethanol (the Raney Nickel may be re-used for at least three times without any noticeable drop in activity). The solution and washings were combined and the solvent removed under reduced pressure. Saturated sodium hydroxide solution (25 cm^3) was then added to the oil and the mixture extracted with dichloromethane (5x30 cm^3). After the combined extracts had been dried over anhydrous magnesium sulphate and filtered, the solvent was removed to give the crude amine as a pale yellow oil.

The oil was purified by distillation at 0.05mmHg, 153-154°C discarding a forererun at 105°C of the monoalkylated product.(yield 7.15g, 68.5%) (Found: C, 64.04; H, 10.22; N, 24.02. Calc. for $C_{12}H_{22}N_4$: C, 64.83; H, 9.97; N, 25.20%); i.r. (thin film)/cm^{-1}, 3360, 3287 (NH ν); 3009, 2934, 2859, 2363 (CH ν); 1590, 1569 (NH δ); 1473, 1434 (CH δ); 760 (ArH δ oop). δ_H(200MHz; solvent $CDCl_3$; standard reference TMS) 8.52 (1H, d, Py H), 7.64 (Py-H, triplet of doublets [4H]), 7.27 (s, Py-H [1H]), 7.13 (triplet of doublets, Py H [1H]), 3.70 (s, benzyl H [2H]), 2.72 (t, H of $CH_2CH_2CH_2$-NH_2 [4H]), 2.53 (t, CH_2CH_2-NH_2 [4H]), 1.65 (p, $CH_2CH_2CH_2$-NH_2 [4H]); δ_C 148.672, 147.525, 147.303,

130.974, 130.024 (py), 57.662 (benzyl methylene), 53.363, 39.094, 24.395 (propyl methylenes).

(c)- 5-(2'-pyridylmethyl)-1,5,9-triazanonane tetrahydrobromide (Pydpa.4HBr)
5-(2'-pyridylmethyl)-1,5,9-triazanonane (1g, 4.5 mmol) was dissolved in ethanol and HBr (38% added dropwise until the solution showed acidic by pH indicator paper. *Iso*-propyl alcohol was added until the solution became slightly turbid. On standing an oil separated from solution from which square colourless plates formed overnight. The crystals were filtered off, washed with MeOH (3cm^3) then twice with diethylether (5 cm^3).
The crystals crumbled to a fine white powder on drying at reduced pressure at 60°C (yield 1.03g, 42%). Mp 260°C (decomp.). (Found: C, 26.30; H, 4.70; N, 10.25.. Calc. for $C_{12}H_{26}N_4Br_4$: C, 26.40; H, 4.80; N, 10.26%); i.r. (KBr pellet)/cm^{-1}, 2700-2300 (NH_3^+ ν); 2986, 2901 (CH ν); 3392 (NH^+ δ).

(d) [Cu(Pydpa)Cl]ClO_4.- Pydpa (0.5g,2.25 mmol) dissolved in ethanol (10 cm^3) was added to copper(II) chloride dihydrate (0.383g, 2.25 mmol). A sticky solid formed on addition of *iso*-propyl alcohol. The solid was dissolved in the minimum of hot ethanol (*ca* 10 cm^3) and sodium perchlorate (0.5g, 3.56 mmol) in ethanol (20 cm^3) added. Immediately a pale blue precipitate formed. The complex was filtered off washed with ethanol (2x20 cm^3) then diethylether (10 cm^3). The complex was recrystallized from boiling acetonitrile (yield 0.42g, 39%); Mp. 166°C (decomp.). (Found: C, 34.73; H, 5.17; N, 13.48. Calc. for $C_{12}H_{22}N_4O_4Cl_2Cu$: C, 34.25; H, 5.27; N, 13.31%); i.r. (KBr)/cm^{-1}, 3327, 3286 (NH ν); 2929, 2886 (NH ν); 1694, 1608 (NH δ); 1508, 1458 (CH δ); 1087 (ClO_4^- ν); 624 (ArH δ oop). Λ_M / S cm^2 mol^{-1} 116 (nitromethane); λ_{max}/nm (ε_{max}/dm^{3}mol^{-1}cm^{-1}) 736(98), 822(100) water, 721(121), sh 849(108) acetonitrile

(e) [Zn(Pydpa)]$(ClO_4)_2$.- A boiling solution of pydpa (0.30g, 1.35mmol) in ethanol (10 cm^3) was added dropwise to a solution of zinc(II)perchlorate hexahydrate (0.503g, 1.35mmol) in boiling ethanol (5 cm^3). On cooling a small amount of oil separated from

the solution then colourless blades formed. The product was filtered off and washed with ethanol. The complex was further purified by recrystallization from a minimum volume of boiling ethanol (10cm^3) (yield 0.488g, 74%). Mp. 232-3°C. (Found: C, 29.61; H, 4.04; N, 11.34. Calc. for $C_{12}H_{22}N_4O_8Cl_2Zn$: C, 29.62; H, 4.56; N, 11.51%); i.r.(KBr)/cm^{-1}, 3313, 3268 (NH ν); 2962 (CH ν); 1612 (NH δ); 1450 (CH δ); 1106 (ClO_4^- ν); 625 (ArH γ); Λ_M / S cm^{2}mol^{-1} 193 (nitromethane)

(f) $[Ni(Pydpa)(CH_3CN)_2](ClO_4)_2$. -A boiling solution of pydpa (0.30g, 1.35mmol) in ethanol (10 cm^3) was added dropwise to a solution of nickel(II)perchlorate hexahydrate (0.494g, 1.35mmol) in boiling ethanol (5 cm^3). The green nickel solution turned blue on addition to the amine. On cooling a blue oil formed from which no solid could be isolated. The oil was redissolved in boiling acetonitrile (15 cm^{-3}), which, on cooling, gave purple blocks (yield 0.558g, 82%). Mp. 194-5°C. (Found: C, 31.96; H, 4.63; N, 13.11. Calc. for $C_{14}H_{28}N_6O_8Cl_2Ni$: C, 34.19; H, 5.02; N, 14.95%); i.r. (KBr)/cm^{-1}, (NH ν) 3335, 3288; 2940, 2311, 2283 (CH ν); 1609 (NH δ); 1478, 1449 (CH δ); 1086 (ClO_4^- ν); 775 (ArH δ oop); Λ_M / S cm^{2}mol^{-1} 227 (nitromethane); λ_{max}/nm (ε_{max}/dm^{3}mol^{-1}cm^{-1}) 524(11), 888(8) acetonitrile, 569(8), sh 900(7) water.

(g) $[Co(pydpa)Br_2]Br$ - The cobalt (III) complex was prepared from triscarbonato cobaltate(III)[6] without the isolation of the carbonato complex. Pydpa.4HBr (1g) as ground together with $Na_3[Co(CO_3)_3].3H_2O$ (0.663g). Water (1 cm^3) was added and after the vigorous effervescence had subsided, the mixture was heated on a hot plate (19min.) to give a burgundy red solution. Heating was continued until most of the water had evaporated. The sticky red solid was dissolved in methanol (10 cm^3) and HBr added with gentle heating until the solution became brown-green. *Iso*-propyl alcohol (25 cm^3) was added giving a pale green brown precipitate. This was dissolved by addition of a little methanol (ca. 10 cm^3) and gentle heating. Dark drown crystals formed on cooling. The crystals were filtered off and washed with ethanol (1 cm^3) then diethylether (2x2 cm^3) (yield 0.5g). Mp. 260°C (decomp.); (Found: C, 27.47; H, 3.87; N, 10.52. Calc. for

$C_{12}H_{22}N_4Br_3Co$: C,27.67; H, 4.26; N, 10.75%); i.r. (KBr)/cm^{-1}, 3155, 3084 (NH ν); 2267 (CH ν); 1609 ,1576 (NH δ); 1485, 1450 (CH δ); 1086, 775 (ArH δ oop). Λ_M/ S cm^2mol^{-1} 421 (water); λ_{max}/nm (ε_{max}/$dm^3mol^{-1}cm^{-1}$) 468 (567) methanol.

(h)- [Cr(pydpa)Cl_2]Cl - Pydpa (1g, 4.5 cm^3) and chromium trichloride hexahydrate were both dissolved separately in DMF (20 cm^3) and brought to the boil on a hot plate. After boiling for 20min the chromium trichloride (which becomes rose pink when fully dehydrated) is added dropwise to the boiling solution of pydpa. A dark brown solution is formed from which a purple powder was collected by filtration. Removal of half the solvent at reduced pressure yielded more of the purple precipitate. The crude product was recrystallized from a 1M HCl solution (5 cm^3). Mp.260°C. (Found: C, 37.38; H, 5.82; N, 14.59. Calc. for $C_{12}H_{22}N_4Cl_3Cr$: C, 37.86; H, 5.82; N, 14.72%); i.r.(KBr)/cm^{-1}, 3259, 3166, 3079 (NH ν); 2311, 2283 (CN ν); 1660, 1610, 15.85 (NH δ); 14.69, 1446; Λ_M/ S cm^2mol^{-1} 98 (water); λ_{max}/nm (ε_{max}/$dm^3mol^{-1}cm^{-1}$) 404 (72), 541 (59) water.

Crystal Data.-- $C_{12}H_{22}N_4CuCl_2O_4$, M = 420.78, Primitive orthorhombic, a = 9.172(2), b = 23.090(2), c = 8.270(1) Å, U = 1751.4(4) $Å^3$ (by least-squares refinement on diffractometer angles for 25 automatically centred reflections, in the range 27.2<2θ<33.4° λ = 0.71069 Å), space group $P2_12_12_1$ (#19), Z = 4, D_c = 1.596 g cm^{-3}, F(000) = 868.00. Blue block crystal (grown by vapor diffusion of diethylether into methanol). Approximate crystal dimensions 0.20 x 0.150 x 0.30 mm, μ(Mo-K_α) = 15.75 cm^{-1}.

$C_{16}H_{28}N_6NiCl_2O_8$, M = 562.04, Primitive orthorhombic, a = 15.974(3), b = 8.054(4), c = 19.371(4) Å, U = 2491(2) $Å^3$ (by least-squares refinement on diffractometer angles for 15 automatically centred reflections, in the range 6.62<2θ<11.15° λ = 0.71069 Å), space group $Pna2_1$(#33), Z = 4, D_c = 1.498 g cm^{-3}, F(000) = 1168.00. Purple block crystal crystal (grown by slow recrystallization from methanol). Approximate crystal dimensions 0.20 x 0.10 x 0.30 mm, μ(Mo-K_α) = 10.44 cm^{-1}.

Data Collection and Processing.- [Cu(Pydpa)Cl]ClO_4. Rigaku AFC7S diffractometer, ω-2θ scan type with ω scan width = (0.89 + 0.35 tan θ)°, ω scan speed 16.00° min-1 (up to 4 scans), graphite monochromated MoKα radiation; 1809 reflections measured (max 2θ = 50.0°). No decay correction was made, but an absorption correction was required (*trans. factors*: 0.8653- 1.0000). Corrections were made for Lorentz and polarisation effects.

[Ni(Pydpa)$(CH_3CN)_2$]$(ClO_4)_2$ Rigaku AFC7S diffractometer, ω-2θ scan type with ω scan width = (0.84 + 0.35 tan θ)°, ω scan speed 16.00° min-1 (up to 4 scans), graphite monochromated MoKα radiation; 2532 reflections measured (max 2θ = 50.0°). No decay correction was made, but an absorption correction was required (*trans. factors*: 0.9057-1.0000). Corrections were made for Lorentz and polarisation effects.

Structure Analysis and Refinement.- [Cu(Pydpa)Cl]ClO_4- Direct methods[7] and expanded using Fourier techniques[8] Some non-hydrogen atoms were refined anisotropically, while the rest were refined isotropically. Hydrogen's were included but not refined. The final cycle of full-matrix least-squares refinement[9] was based on 2245 observed reflections (I>3.00σ(I)) and 235 variable parameters and converged with unweighted agreement factors of:

$$R = \sum \| Fo| - |Fc| \| / \sum |Fo| = 0.045$$

$$R_w = \sqrt{\left(\sum \left(|Fo| - |Fc| \right)^2 / \sum wFo^2 \right)} = 0.040$$

The standard deviation of an observation of unit weight[10] was 2.96. The Weighting scheme was based on counting statistics and included a factor (p = 0.003) to downweight the intense reflections. Plots of $w(\Sigma |Fo| - |Fc|)^2$ versus $|Fo|$, reflection order in data collection, sin θ/λ and various classes of indices showed no unusual trends. The maximum and minimum peaks on the final difference Fourier map correspond to 0.56 and -0.45 $e^-Å^{-3}$, respectively. The perchlorate anion was refined anisotropically, and inspection of the ortep thermal ellipsoids indicated considerable disorder of the

perchlorate oxygen atoms. Attempts to model the disorder on the basis of a number of partially occupied positions around the chlorine atom, did not produce a significant reduction in the *R* value. All calculations were performed using the TEXSAN[11] crystallographic software package of the Molecular Structure Corporation.

$[Ni(Pydpa)(CH_3CN)_2](ClO_4)_2$ - As for $[Cu(Pydpa)Cl]ClO_4$ direct methods[7] were used and expanded using Fourier techniques.[8] Some non-hydrogen atoms were refined anisotropically, while the rest were refined isotropically. Hydrogen's were included but not refined. The final cycle of full-matrix least-squares refinement[9] was based on 1633 observed reflections ($I>3.00\sigma(I)$) and 277 variable parameters and converged with unweighted agreement factors of $R = 0.072$ and $Rw = 0.061$.

The standard deviation of an observation of unit weight[10] was 3.94. The Weighting scheme was based on counting statistics and included a factor (p = 0.001) to downweight the intense reflections. Plots of $w(\Sigma |Fo| - |Fc|)^2$ versus $|Fo|$, reflection order in data collection, sin θ/λ and various classes of indices showed no unusual trends. The maximum and minimum peaks on the final difference Fourier map correspond to 0.64 and -0.57 $e^-Å^{-3}$, respectively. The perchlorate anions were refined anisotropically, and inspection of the ortep thermal ellipsoids indicated considerable disorder of the perchlorate oxygen atoms. Attempts to model the disorder on the basis of a number of partially occupied positions around the chlorine atom, did not produce a significant reduction in the *R*. value. All calculations were performed using the TEXSAN[11] crystallographic software package of Molecular Structure Corporation.

Results and Discussion

Synthesis. The tripodal ligand 5-(2'-pyridylmethyl)-1,5,9-triazanonane (2 = L) was readily prepared by the reactions outlined in the scheme 1.

SCHEME 1

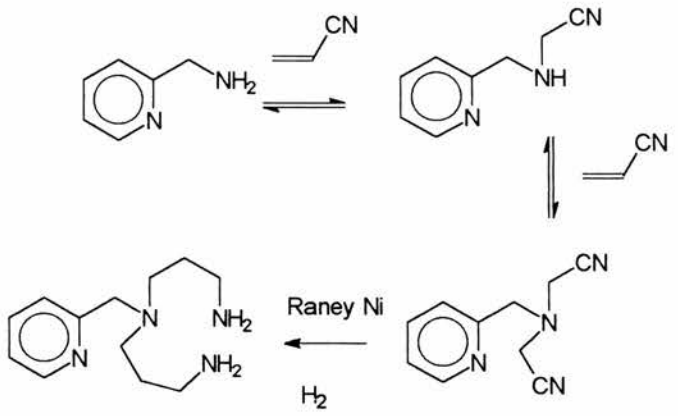

It was found that the cyanoethylation of aminomethyl pyridine does not require the presence of an acid catalyst and that even under the reaction conditions chosen (large excess of acrylonitrile) there was still contamination with a mono alkylated species. The cyanoethylated product was not purified further (distillation could not be achieved without appreciable decomposition). However the monoalkylated compound could easily be separated by distillation after reduction.

Description of the Crystal Structure of [Cu(Pydpa)Cl]ClO_4.-The $[Cu(pydpa)Cl]^+$ cation is five co-ordinate with an N_4Cl donor set which is best described as distorted square pyramidal. It might be expected that pydpa, like the symmetrical tripodal ligand tren, would form a copper(II) complex with trigonal bipyramidal geometry[12]. However, instead of the expected 120, 120, 120° angles of the trigonal plane, there is a particularly large N4-Cu-N2 bond angle of 151.5 and particularly acute angles of 106.3 and 101.4 for N4-Cu1-N3 and N3-Cu1-N2 respectively. These angles suggest that square pyramidal geometry best describes this complex. N1, N2, N4, and Cl1 may be thought of as forming the base of the pyramid with the copper sitting a little above the plane (ca 0.5 Å) and N3 occupying the apical position. Of the two possible isomers with square pyramidal geometry (Figure 1) isomer I is found in this structure.

The primary amine in the apical position (N3) has a slightly longer bond (2.192A) to copper than the in plane amine (2.004A). The pyridine copper bond length is not unusual for pyridine donors (often found to be approximately 1.98A) and the Cu-Cl distance also falls within expected limits for five co-ordinate complexes. The pyridine ring is planar

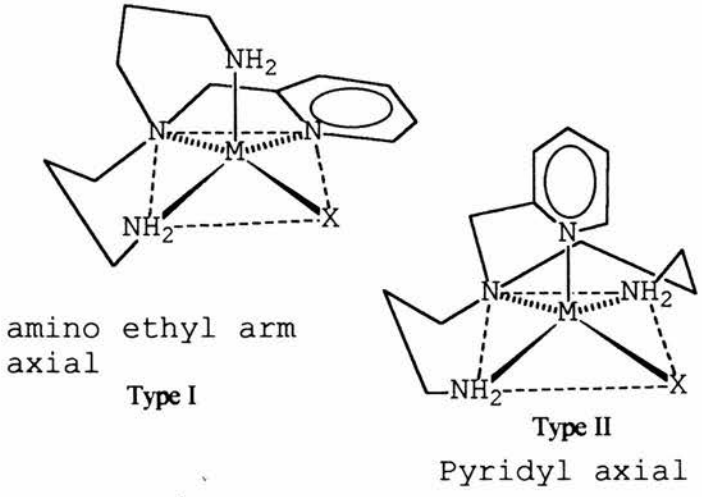

Figure 1

(torsional angles for the pyridine moiety are 0.3°±2°) and the carbon-carbon distances in the alkyl chains show no unusual features (1.51± 0.02Å)

ORTEP diagram of the complex $[Cu(Pydpa)Cl]ClO_4$

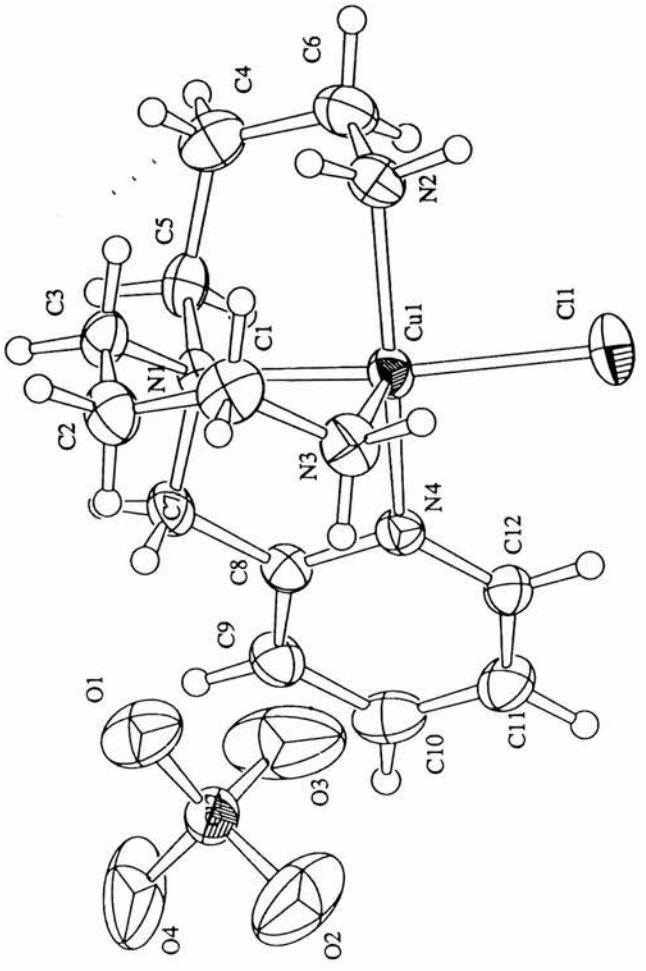

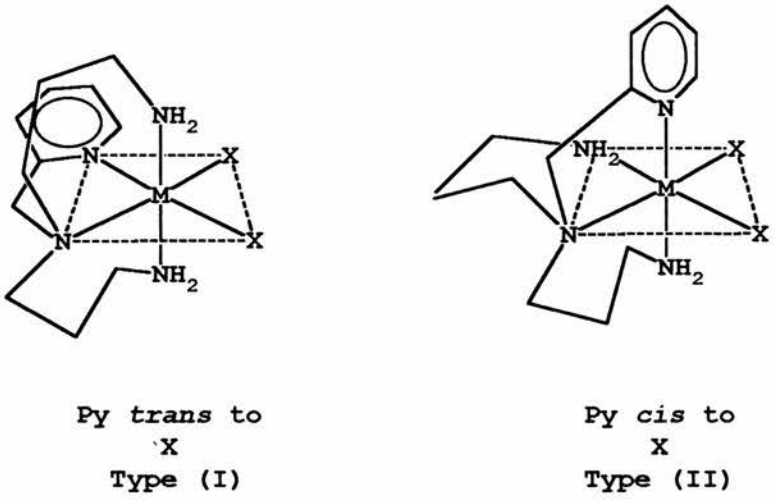

Py *trans* to X
Type (I)

Py *cis* to X
Type (II)

Figure 2

Table 1. Selected bond lengths and angles for [Cu(Pydpa)Cl]ClO_4

Cu(1)-N(1) 2.069(6)	N(1)-Cu(1)-N(2) 89.2(3)
Cu(1)-N(2) 2.004(6)	N(3)-Cu(1)-N(1) 93.6(3)
Cu(1)-N(3) 2.192(7)	N(1)-Cu(1)-N(4) 82.2(3)
Cu(1)-N(4) 2.033(6)	N(3)-Cu(1)-N(2) 101.4(3)
Cu(1)-Cl(1) 2.300(2)	N(1)-Cu(1)-Cl(1) 166.0(2)
	N(3)-Cu(1)-Cl(1)100.4(2)
	N(2)-Cu(1)-N(4) 151.5(3)
	N(3)-Cu(1)-N(4) 106.3(3)

Description of the Crystal Structure of $[Ni(Pydpa)(CH_3CN)_2](ClO_4)_2$ - The nickel complex is six co-ordinate with octahedral geometry. Four of the co-ordinating groups belong to Pydpa and the remaining coordination sites are occupied by acetonitrile. The structure also has two disordered perchlorate counter ions. Of the two possible isomers that could be formed from a M(Pydpa)X2 complex, this structure shows type (I) geometry (Figure 2) with the pyridyl donor *trans* to an acetonitrile.

The nickel amine and pyridyl bond distances are all fairly similar (2.10[4] is the average Ni-N bond distance) with slightly shorter bonds to the tertiary nitrogen and pyridine

(presumably a consequence of the smaller bite angle of the five membered chelate ring). The Ni-N bond distances of the acetonitrile ligands are close to the average bond lengths found in previously published structures[13] and the Ni-N-C angle (167° and 156°) is slightly bent away from 180° in these complexes. The acetonitrile C-N bond lengths of 1.17 and 1.19 are comparable to literature values for coordinated acetonitrile. The bond length for free acetonitrile[14] is (1.157 Å).

Table 2. Selected bond lengths and angles of $[Ni(Pydpa)(CH_3CN)_2](ClO_4)_2$

Ni(1)-N(1)	2.02(1)	N(1)-Ni(1)-N(2)	82.3(5)
Ni(1)-N(2)	2.09(1)	N(1)-Ni(1)-N(3)	95.5(6)
Ni(1)-N(3)	2.07(1)	N(1)-Ni(1)-N(4)	90.1(5)
Ni(1)-N(4)	2.15(1)	N(1)-Ni(1)-N(5)	174.8(6)
Ni(1)-N(5)	2.10(2)	N(1)-Ni(1)-N(6)	96.3(6)
Ni(1)-N(6)	2.14(2)	N(3)-Ni(1)-N(4)	168.0(6)
N(6)-C(15)	1.17(2)	N(5)-Ni(1)-N(6)	86.8(6)
N(5)-C(13)	1.19(2)	Ni(1)-N(6)-C(15)	156(1)
		Ni(1)-N(5)-C(13)	167(1)

ORTEP diagram of the complex $[Ni(Pydpa)(CH_3CN)_2](ClO_4)_2$

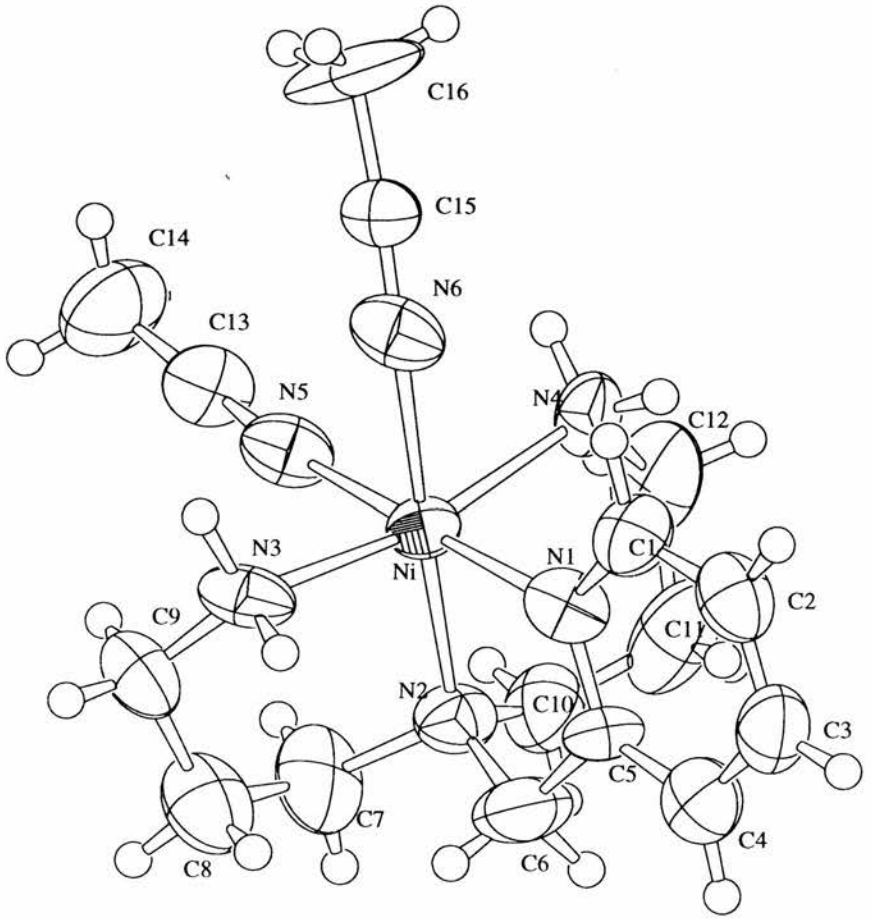

Electronic spectra. The distorted structure of the copper complex is maintained in solution as shown by the partially resolved twin peaks. The twin peak pattern has been observed in the solid state for *bis*-bipyridyl complexes of copper(II) by Hathaway *et al.*[15]

References

[1] J.Chin and M.Banaszczyk, *J.Am.Chem.Soc.*, 1989, **111**, 2724

[2] F.Tafesse, S.S.Massoud and R.M.Milburn, *Inorg.Chem.*, 1985, **24**, 2591; V.Jubian and Xiang Zou, *J.Am.Chem.Soc,* 1989, **111**, 186; G.H.Rawji and R.M.Milburn, *Inorg.Chim.Acta.*, 1988, **150**, 186.

[3] E.Kimura, S.Young and J.P.Collman, *Inorg.Chem.*, **197**, 1183.

[4] M.P.Ngwenya, A.E.Martell, J.Reibenspies, *J.C.S.Chem.Commun.*, 1990, 1207.

[5] H.R.Billica and H.Adkins, *J.Am.Chem.Soc.*, 1948, **70**, 695.

[6] H.F.Bauer, W.C.Drinkard, *J.Am.Chem.Soc.*,, 1960, **82,** 5031.

[7] *SIR92:* A.Altomare, M.C.Burla, M.Camalli, M.Cascarano, C.Giacovazzo, A.Guagliardi, and G.Polidori, **(1994),** *J.Appl.Cryst.*, in preparation.

[8] DIRDIF94: P.T.Beurskens, G.Admiraal, G.Beurskens, W.P.Bosman, R. de Gelder, R.Israel, and J.M.M.Smits **(1994)**. *The DIRDIF-94 program system,* Technical Report of the Crystallography Laboratory, University of Nijmegen, The Netherlands.

[9] Least-Squares:

Function minimised: $\Sigma w(|Fo| - |Fc|)^2$ where $w = 1/\sigma^2(Fo) = 4Fo^2/\sigma^2(Fo^2)$

$\sigma^2(Fo^2) = S^2(C+R^2B)+(pFo^2)^2/Lp^2$

S = Scan speed

C = Total integrated peak count

R = Ratio of scan time to background counting time

B = Total background count

Lp = Lorentz-polarization factor

p = p-factor

[10] Standard deviation of an observation of unit weight:

$$\sqrt{\sum w\left(|Fo| - |Fc|\right)^2 / \left(No - Nv\right)}$$

where: No = number of observations

Nv = number of variables

[11] *Crystal Structure Analysis Package*, Molecular Structure Corporation (1985& 1992)

[12] P.C.Jain and E.C.Lingafelter, *J.Am.Chem.Soc.*, 1967, **89**, 724.

[13] a)A.J.Jircitano and K.B.Mertes, *Inorg.Chem.*, 1983, **22**, 1828; (b)G.M.Freeman, E.K.Barefield and D.G.Derveer, *Inorg.Chem.*, 1984, **23**, 3092; H.Oshio, *Inorg.Chem.*, 1993, **32**, 4123; c) E.C.Constable, S.M.Elder, J.Healy and D.A.Tocher, *J.Chem.Soc.Dalton Trans.*, 1990, 1669; d)J.Z.Zhuang, N.Matsumoto, H.Okawa and S.Kida, *J.Chem.Soc.Dalton Trans.*, 1989, 2095; (e) B.Adhikary, S.Liu and C.Rhncas, *Inorg.Chem.*, 1993, **32**, 5957.

[14] S.M.Peng and V.L.Goedken, *J.Am.Chem.Soc.*, 1976, **98**, 8021.

[15] W.D.Harrison, D.M.Kennedy, M.Power, R.Sheahan and B.J.Hathaway, *J.Chem.Soc.Dalton Trans.*, 1981, 199.

Complex Formation Equilibria Between Nickel(II), Copper(II), Zinc(II), Cobalt(II) and Hydrogen Ions and The Tripodal Ligand 5-(2'-Pyridylmethyl)-1,5,9-Triazanonane.

Abstract

The reactions of 5-(2'-pyridylmethyl)-1,5,9-triazanonane (pydpa) with Ni(II), Cu(II), Zn(II), Co(II) and H^+ ions have been studied at 25°C in aqueous solutions (0.1M, KNO_3) using potentiometric techniques. The calculation of constants was carried out using SUPERQUAD. The stepwise protonation constants of the ligand are as follows: $\log K_{11}$=2.05(4), $\log K_{12}$ 5.56(1), $\log K_{13}$ 9.757(8), $\log K_{14}$ 10.68(1). It was found that, in addition to forming normal (lmh = 110) complexes with all of the above ions ($\log\beta_{110}$)= 12.951(6), 15.37(3), 11.646(9), 9.569(6), for Ni(II), Cu(II), Zn(II), and Co(II) respectively); protonated species were found for Ni(II), Cu(II), and Co(II) $\log K_{[M^{2+} + HL = MHL^{3+}]}$ 8.228(8), 12.55(1), 5.87(1) respectively. Copper(II) and cobalt(II) were also found to form hydroxo species at high pH, $\log K_{[ML = ML(OH)_1 H^+]}$ determined as 9.52(3) and 11.05(1) for Cu(II) and Co(II) respectively. The stability constants for these metal ions with the tripodal ligand 2,2',2"-triaminotriethylamine (tren) have also been redetermined under the same experimental conditions to enable a comparison to be made between trpn, tren and pydpa.

The presence of a five membered chelate ring in pydpa stabilises the complexes with respect to trpn but the presence of two six membered rings destabilises pydpa complexes with respect to tren.

Introduction

Polyamine ligands have commanded the forefront of transition metal chemistry from the earliest days. Many topologies have been studied and, for example, cyclic polyamines opened up a whole new area of chemistry: that of macrocyclic chemistry.

Although cyclic and linear polyamines have attracted considerable attention, there is a paucity of research into the properties of tripodal amines. Prue and Schwarzenbach[1] determined the

Experimental

Potentiometric titrations.- The ligand (pydpa) HBr salt was prepared as described previously (last section) and the bromide content confirmed by titration against standard silver nitrate (found Br, 58.4 calc. for $C_{12}H_{26}N_4Br_3$: Br, 58.54). The ligand tren was purchased from Aldrich and purified by three recrystallisations of the trihydrobromide salt (found Br, 58.6 calc. for $C_6H_{23}N_4Br_3O$: Br, 58.90) from aqueous methanol. Aqueous solutions of pydpa.4HBr and tren.3HBr were titrated with carbonate free 0.100M NaOH. Details of the experimental procedure are described in Appendix I and a summary of the experimental parameters used in the potentiometric titrations are summarised in Table 1 for tren and in Table 2 for Pydpa.

Table 1. Summary of experimental parameters for the system Ni(II), Cu(II), Zn(II), Co(II)-Tren

Solution composition	
$[T_L]$ range/mol dm^{-3}	$1x10^{-4}$ - $2x10^{-3}$
$[T_M]$ range/mol dm^{-3}	$5x10^{-5}$ - $2x10^{-3}$
I/mol dm^{-3}, electrolyte	0.1, KNO_3
pH Range	3-10.5
Experimental method	pH Titration, calibrated by standard buffers
T/°C	25 ± 0.1
Total number of data points	
Protonation	250 (5 curves)
Copper complexation	153 (3 curves)
Cobalt complexation	219 (3 curves)
Nickel complexation	179 (3 curves)
Zinc complexation	212 (5 curves)
Method of calculation	SUPERQUAD

Table 2. Summary of experimental parameters for the system Ni(II), Cu(II), Zn(II), Co(II)-Pyda

Solution composition	
$[T_L]$ range/mol dm^{-3}	$1x10^{-4}$ - $2x10^{-3}$
$[T_M]$ range/mol dm^{-3}	$5x10^{-5}$ - $2x10^{-3}$
I/mol dm^{-3}, electrolyte	0.1, KNO_3
pH Range	3-10.5
Experimental method	pH Titration, calibrated by standard buffers
T/°C	25.0 ± 0.1
Total number of data points	
Protonation	192 (5 curves)
Copper complexation	250 (5 curves)
Cobalt complexation	275 (5 curves)
Nickel complexation	200 (4 curves)
Zinc complexation	200 (4 curves)
Method of calculation	SUPERQUAD

Results and Discussion

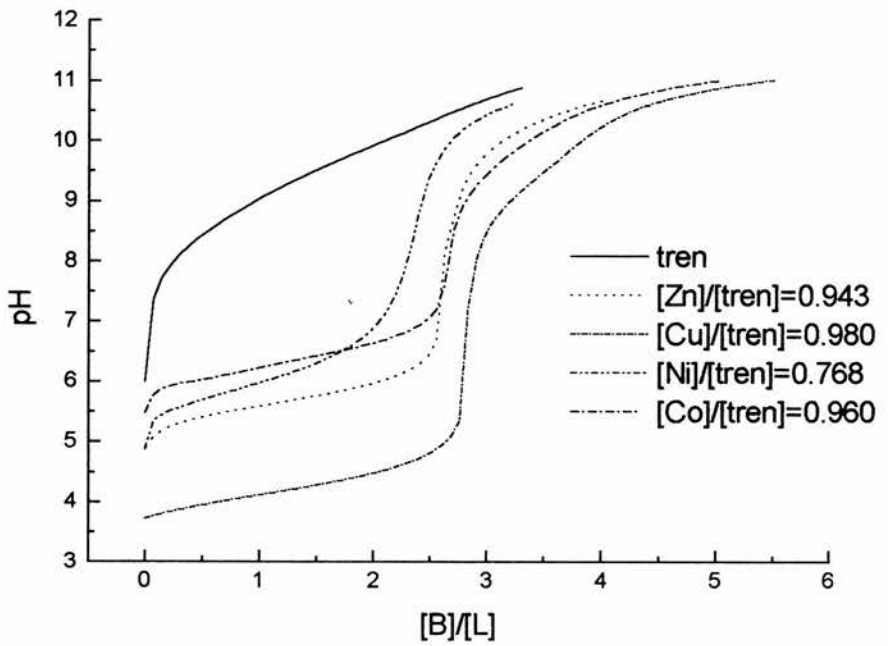

Figure 1. Titration Curves for the Titration of Tren in the Presence of H+, Co(II), Ni(II), Cu(II), and Zn(II)

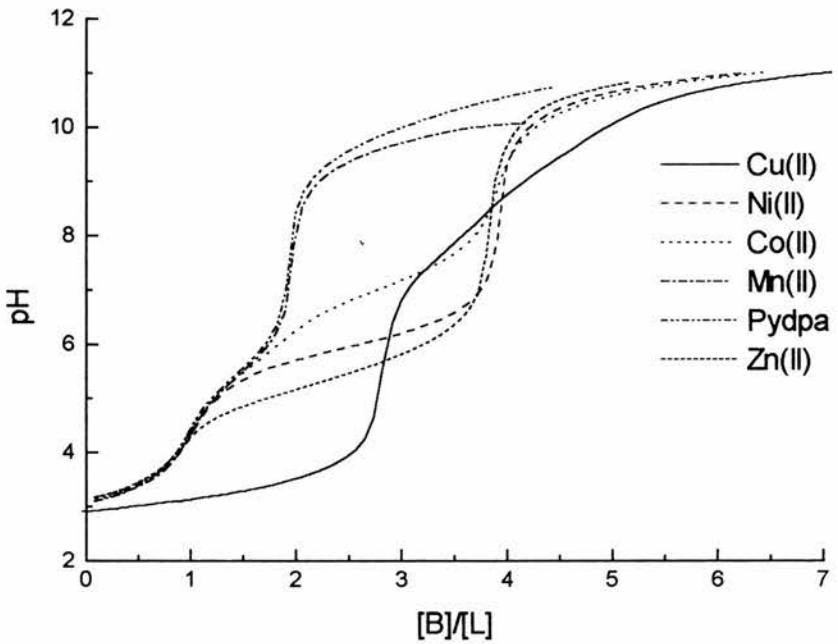

Figure 2. Titration Curves for the Titration of Pydpa in the Presence of H+, Co(II), Ni(II), Cu(II), and Zn(II)

Table 3 Summary of stability constants for the system Ni(II), Cu(II), Zn(II), Co(II)-Pydpa.

Protonation constants (ligand = H_4L, errors as σ)		
$\log \beta_{HL}$	$H^+ + L = HL^+$	10.68 ± 0.01
$\log \beta_{H2L}$	$2H^+ + L = H_2L^{2+}$	20.437 ± 0.008
$\log \beta_{H3L}$	$3H^+ + L = H_3L^{3+}$	26.00 ± 0.01
$\log \beta_{H4L}$	$4H^+ + L = H_4L^{4+}$	28.05 ± 0.05
Copper(II) stability constants		
$\log \beta_{CuHL}$	$Cu^{2+} + H^+ + L = CuHL^{3+}$	23.388 ± 0.01
$\log \beta_{CuL}$	$Cu^{2+} + L = CuL^{2+}$	15.52 ± 0.03
$\log \beta_{Cu(OH)L}$	$Cu^{2+} + OH^- + L = Cu(OH)L^+$	6.01 ± 0.03
Cobalt(II) stability constants		
$\log \beta_{CoHL}$	$Co^{2+} + H^+ + L = CoHL^{3+}$	16.70 ± 0.02
$\log \beta_{CoL}$	$Co^{2+} + L = CoL^{2+}$	9.682 ± 0.007
$\log \beta_{Co(OH)L}$	$Co^{2+} + OH^- + L = Co(OH)L^+$	-1.38 ± 0.04
Nickel(II) stability constants		
$\log \beta_{NiHL}$	$Ni^{2+} + H^+ + L = NiHL^{3+}$	19.057 ± 0.006
$\log \beta_{NiL}$	$Ni^{2+} + L = NiL^{2+}$	13.092 ± 0.006
Zinc(II) stability constants		
$\log \beta_{ZnL}$	$Zn^{2+} + L = ZnL^{2+}$	11.779 ± 0.009

Table 4 Summary of stability constants for the system Ni(II), Cu(II), Zn(II), Co(II)-Tren.

Protonation constants (ligand = H_4L, errors as σ)		
$\log \beta_{HL}$	$H^+ + L = HL^+$	10.54 ± 0.01
$\log \beta_{H2L}$	$2H^+ + L = H_2L^{2+}$	20.036 ± 0.009
$\log \beta_{H3L}$	$3H^+ + L = H_3L^{3+}$	28.59 ± 0.01
$\log \beta_{H4L}$	$4H^+ + L = H_4L^{4+}$	30.47 ± 0.05
Copper(II) stability constants		
$\log \beta_{CuL}$	$Cu^{2+} + L = CuL^{2+}$	19.28 ± 0.01
$\log \beta_{Cu(OH)L}$	$Cu^{2+} + OH^- + L = Cu(OH)L^+$	9.83 ± 0.03
Cobalt(II) stability constants		
$\log \beta_{CoL}$	$Co^{2+} + L = CoL^{2+}$	12.80 ± 0.02
$\log \beta_{Co(OH)L}$	$Co^{2+} + OH^- + L = Co(OH)L^+$	2.04 ± 0.06
Nickel(II) stability constants		
$\log \beta_{NiL}$	$Ni^{2+} + L = NiL^{2+}$	14.20 ± 0.03
Zinc(II) stability constants		
$\log \beta_{ZnL}$	$Zn^{2+} + L = ZnL^{2+}$	14.69 ± 0.01
$\log \beta_{ZnL}$	$OH^- + Zn^{2+} + L = Zn(OH)L^+$	2.04 ± 0.06

Protonation of Pydpa.- The β values for the protonation of pydpa corresponds to the stepwise protonation constants shown below:

$H^+ + L = HL^+$ $\log K_{11} = 10.68 \pm 0.01$

$H^+ + HL^+ = H_2L^{2+}$ $\log K_{12} = 9.757 \pm 0.008$

$H^+ + H_2L^{2+} = H_3L^{3+}$ $\log K_{13} = 5.56 \pm 0.01$

$H^+ + H_3L^{3+} = H_4L^{4+}$ $\log K_{14} = 2.05 \pm 0.04$

Comparison of the pK_a values of pydpa with those of the amine tripodal ligands trpn and tren shows comparable values for the first two pKa's indicating the similar environment of the two primary amine groups. The pK_a of the third protonation constant of pydpa is close to that expected for a pyridine nitrogen (5.45 for pyridine at 25°C 0.5 mol dm^{-3} KNO_3)[5] and so can be assigned to the pyridine moiety. The final protonation may be assigned to the tertiary amine. Electrostatic repulsion between the two protonated primary amine arms account for the low basicity of this amine.

Complexes of Cobalt(II).- The initial model only included the LM complex. However, inspection of the residuals showed a poor fit in the alkaline region. Introduction of a monohydroxy species greatly lowered χ^2 and σ. The χ^2 and σ values could only be further reduced by the inclusion of a monoprotonated species LHM. The final χ^2 and σ were 3.92 and 2.23 respectively. Polynuclear or *bis* ligand species could not be included in the model without seriously affecting χ^2.

As with trpn a hydroxo species was found, however, the pK_a of the coordinated water is significantly different (2.99[4] in trpn and 11.05 in pydpa). The speciation plots for Co(II) with trpn in Paoletti's paper suggest this value may be in error. Dihydroxy complexes were all rejected by SUPERQUAD. The final χ^2 and σ were 15.4 and 1.87 respectively.

Complexes of Nickel(II).- Only the complex ML and a minor protonated species MLH could be included in the model. No evidence was found of hydroxy species.

Complexes of Copper.- The titration of pydpa in the presence of copper lead to a similar set of species as observed for trpn. The best model for the calculation included the monoprotonated, normal, and monohydroxy species. The $\beta_{ML(OH)}$ value corresponding to the equilibrium for the deprotonation of a coordinated water molecule is given below along with the values obtained for tren and trpn-

$[Cu(Pydpa)(OH_2)]^{2+}$	+	OH^- =	$[Cu(Pydpa)(OH)]^+$	logK = 9.51 ± 0.03
$[Cu(Tren)(OH_2)]^{2+}$	+	OH^- =	$[Cu(Tren)(OH)]^+$	logK = 9.45 ± 0.03
$[Cu(Trpn)(OH_2)]^{2+}$	+	OH^- =	$[Cu(Trpn)(OH)]^+$	logK = 9.13 ± 0.02

Complexes of Zinc.- Only a 1:1 complex was observed with zinc (II)

Figure 3 shows a comparison of the stability constants of the copper(II), zinc(II),

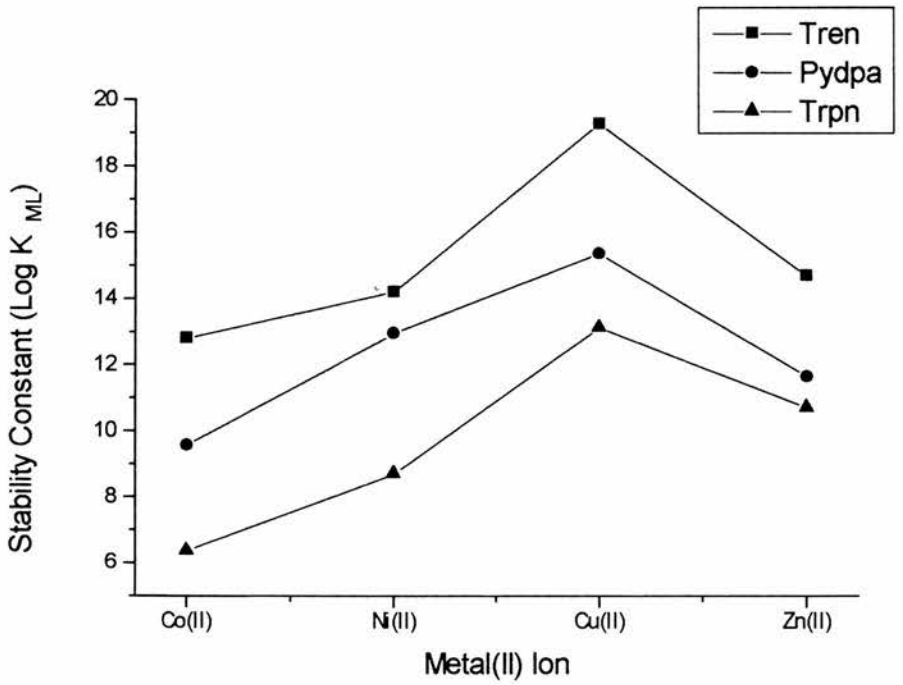

Figure 3. Comparison of the stability constants β_{ML} for the tren, pydpa and trpn ligand.

cobalt(II), and nickel(II) with tren, trpn and pydpa. The same general trend in the stability is followed for the three tripodal ligands, and is commonly found with amine complexes.

The intermediate position of pydpa may best be explained by the presence of one five membered chelate ring (containing the pyridine moiety) and two six membered rings (primary amines). Tren is expected to give complexes of greatest stability as it will form three five membered rings. Trpn gives weaker complexes with three six membered rings.

Pydpa shows a greater propensity to form protonated complexes. Pyda forms protonated complexes with Cu(II), Ni(II) and Co(II). This effect may be due to the extra stability afforded by the five membered pyridine amine chelate ring in pydpa. The primary amine arms can protonate without complete decomplexation.

The zinc complex does not display any tendency to form hydroxy complexes which might indicate the formation of a four co-ordinate complex. Five co-ordinate complexes of aquo-tetramine complexes generally show hydrolytic behaviour of the coordinated water molecule (pKa *ca* 8.5). Since the titration was made up to pH 10.3 the presence of a coordinated water molecule should be observed.

Copper complexes of 5-(2'-Pyridylmethyl)-1,5,9-triazanonane

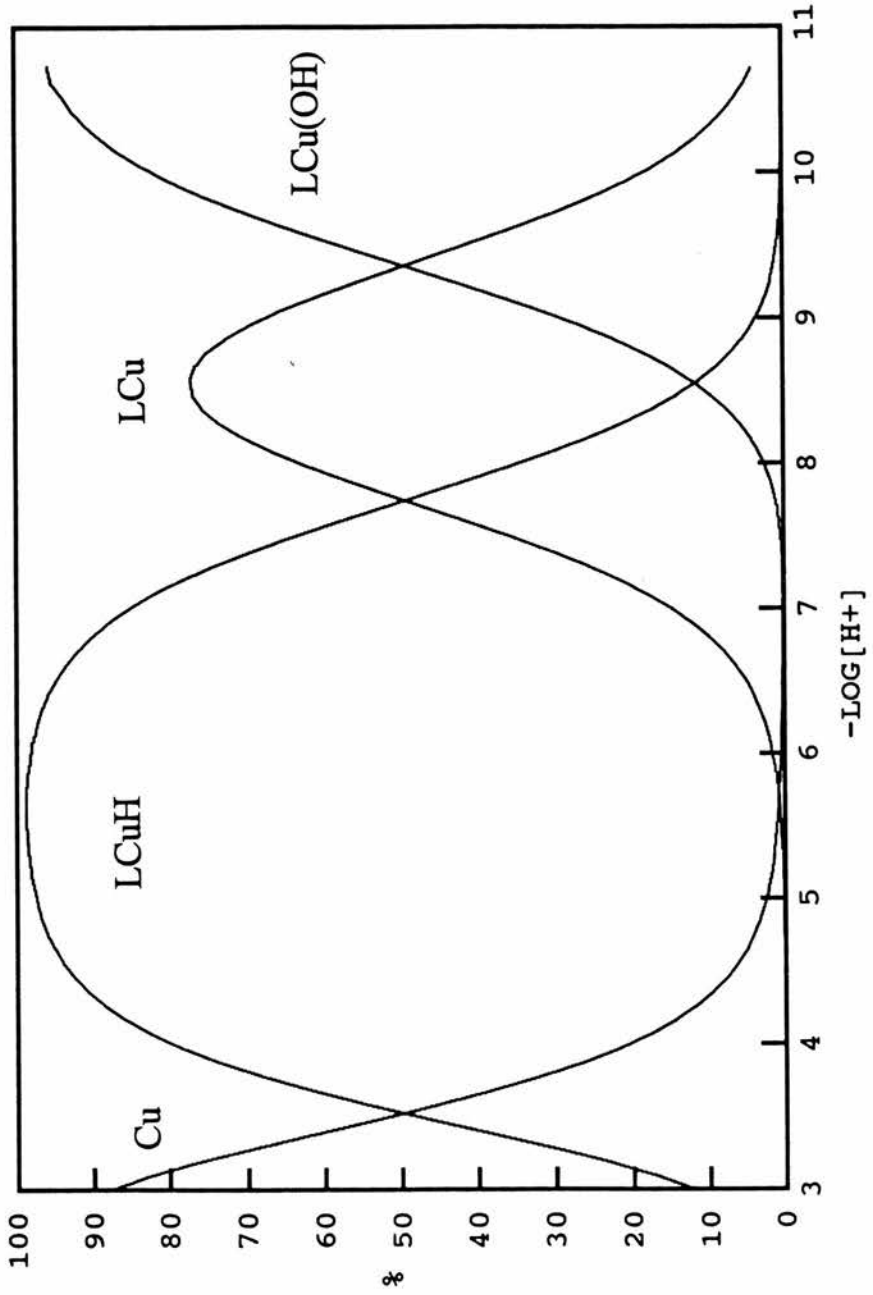

Cobalt complexes of 5-(2'-Pyridylmethyl)-1,5,9-triazanonane

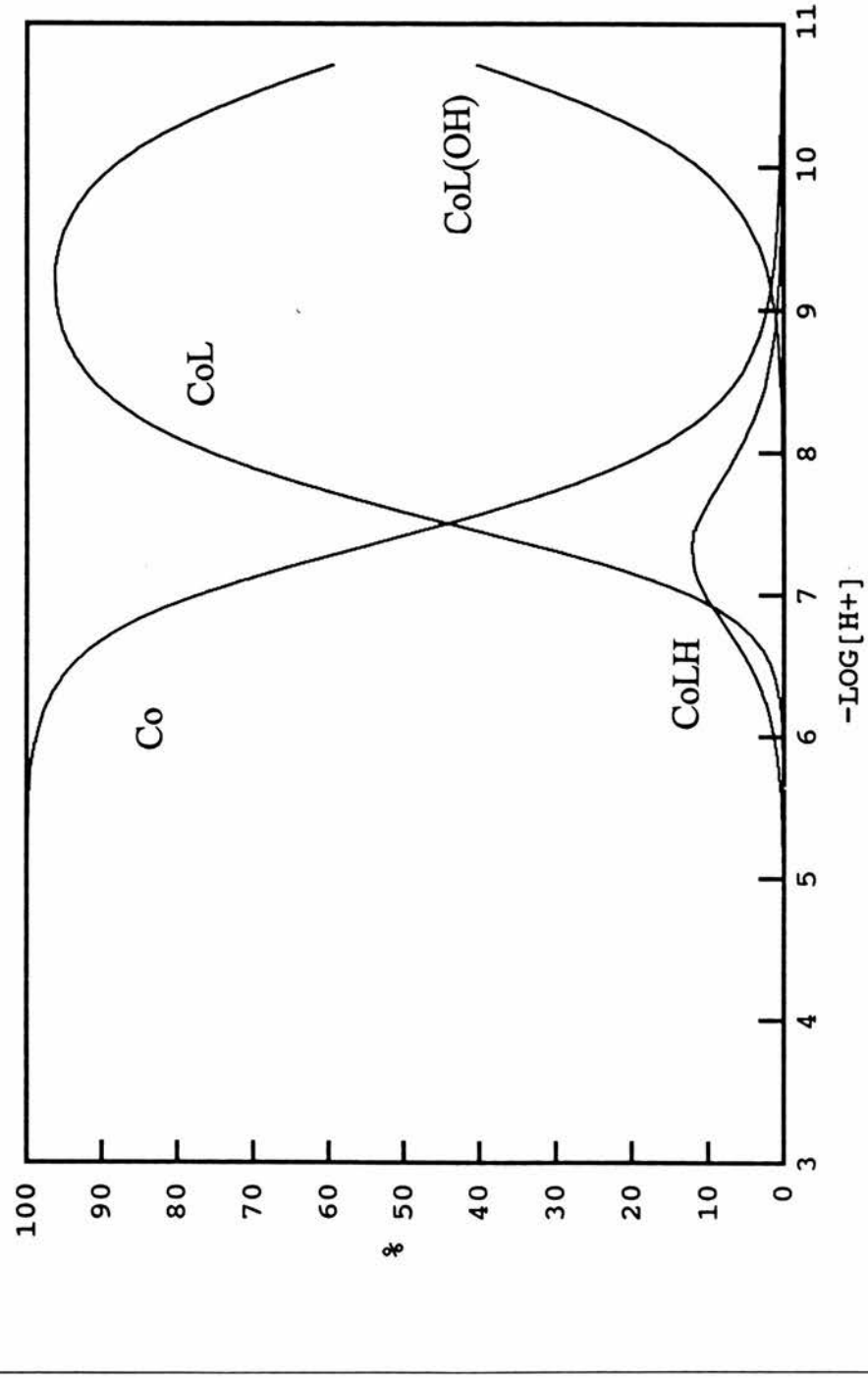

Nickel complexes of 5-(2'-Pyridylmethyl)-1,5,9-triazanonane

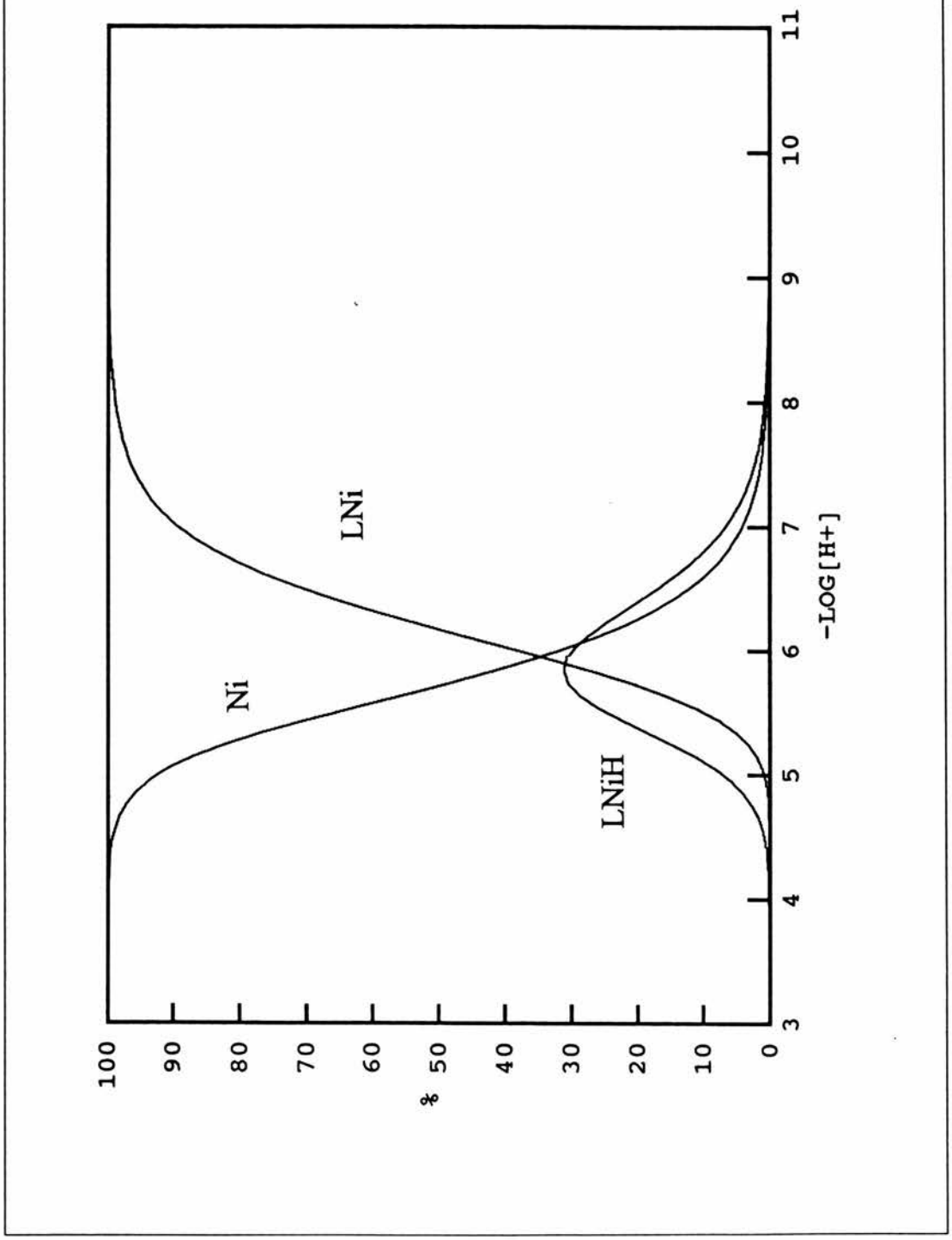

Zinc complexes of 5-(2'-Pyridylmethyl)-1,5,9-triazanonane

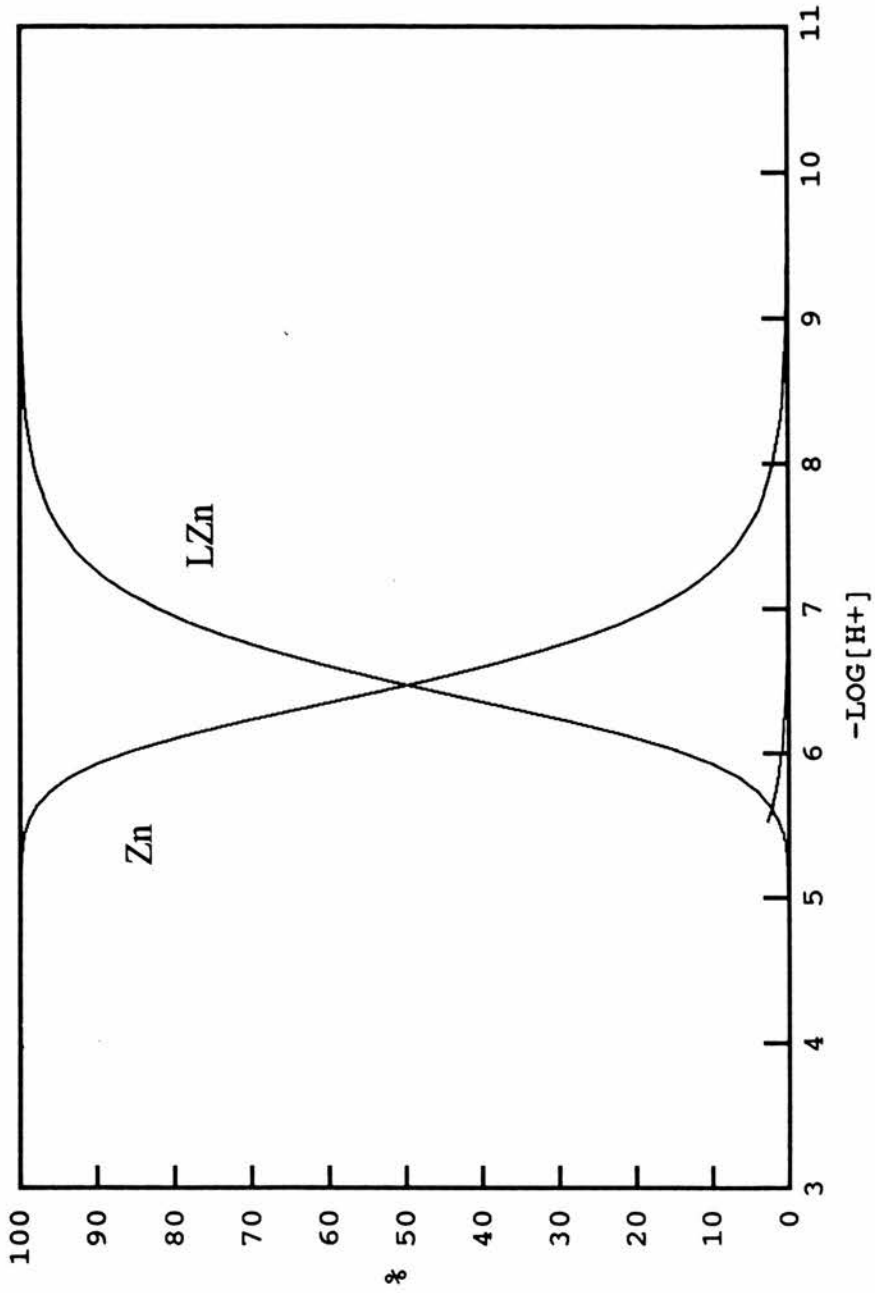

Protonated species of 5-(2'-Pyridylmethyl)-1,5,9-triazanonane

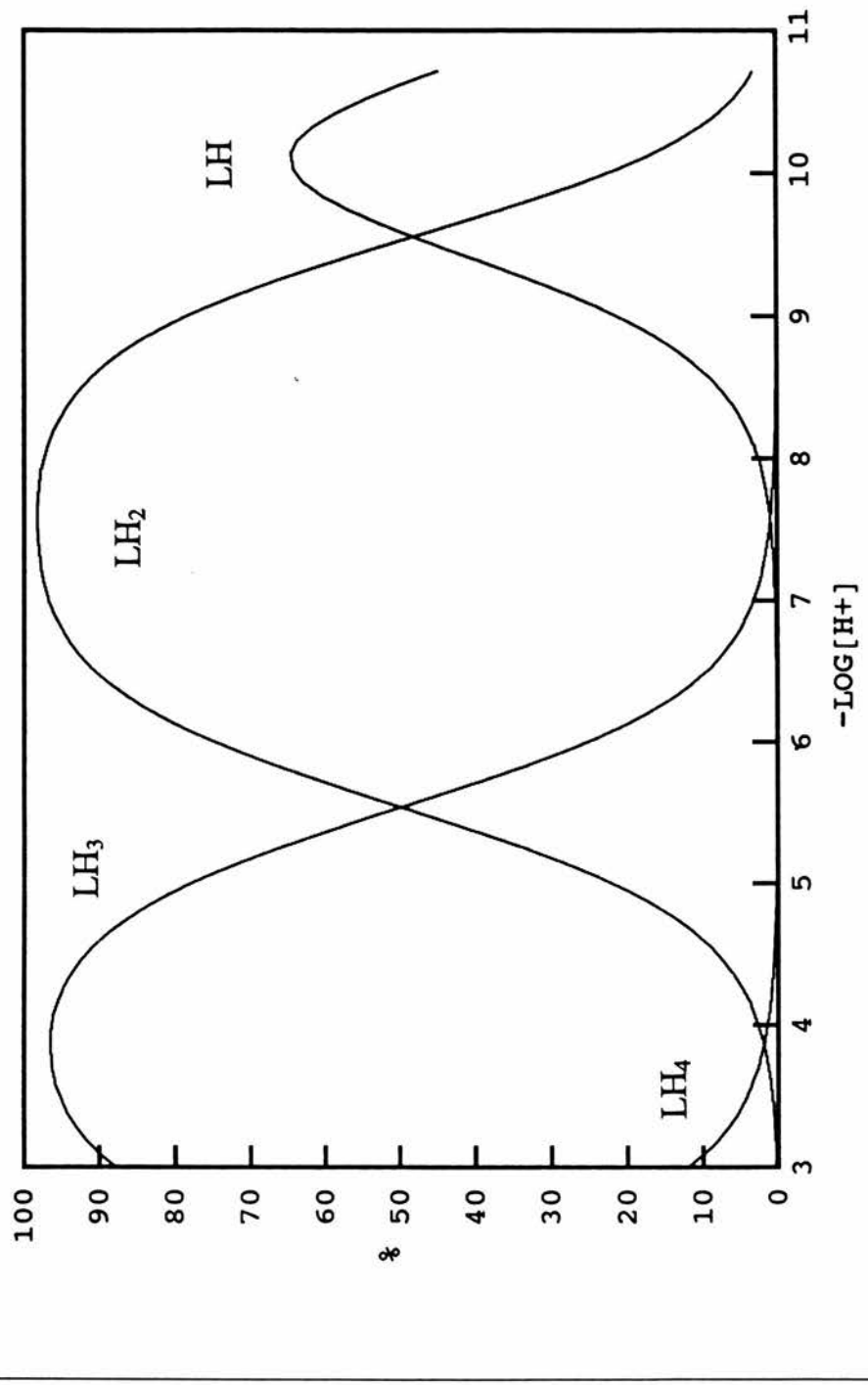

References

[1] J.E.Prue and G.Schwarzenbach, *Helvetica Chim. Acta.*, 1950, **38**, 963.

[2] A.Dei, P.Paoletti and A.Vacca, *Inorg.Chem.*, 1968, **7**, 865.

[3] A.Vacca and P.Paoletti, *J.Chem.Soc.(A)*, 1968, 2378.

[4] a)G.Rawjii, M.Hediger and RM.Milburn, *Inorg.Chim.Acta* 1983, **79**, 247; (b) F.Tafesse, S.S.Massoud and RM.Milburn, *Inorg.Chem.*, 1985, **24**, 2591; (c) F.Tafesse and RM.Milburn, *Inorg.Chim.Acta.*, 1987, **135**, 119; (d) F.Tafesse, S.S.Massoud and R.M.Milburn, *Inorg.Chem.*, 1993, **32**, 1864; (e) J.Chin, *Acc.Chem.Res*, 1991, **24**, 145.

[5] *.Stability Constants of Metal-ion Complexes*, L.G.Sillen and A.E.Martell special publication No17 the Chemical Society,p.440.

Chapter 4

Large Hexaazamacrocycles

Preparation of the Binucleating Hexaaza Macrocycle (1,5,9,18,22,26-hexaaza[11.11]metacyclophane (MPA) and Its Cobalt(II), Nickel(II), Copper(II) and Zinc(II) complexes. The Solution Chemistry of the Copper Complex.

Abstract

The synthesis of the ligand 1,5,9,18,22,26-hexaaza[11.11]metacyclophane (MPA) is described, and complexes of the first row transition metal (II) ions, cobalt, nickel, copper and zinc have been prepared. The stability constants of the copper complexes and the protonation constants of the ligand have been determined in aqueous solution by potentiometry and compared with those of 1,5,9,18,22,26-hexaaza[11.11]paracyclophane (PPA) and its complexes.

Introduction

Binuclear metal sites are common in many biomolecules and enzymes and the topic has been the subject of several recent reviews[1]. For example, the hemocyanins are involved in oxygen-transport in the phyla arthropoda and mollusca. The active site of the oxy protein contains an antiferromagnetically-coupled binuclear copper (II) centre as shown in (1), Figure 1. The nitrogen donors are imidazoles from histidine and the peroxo oxygen is coordinated in μ-η^2:η^2 conformation[2].

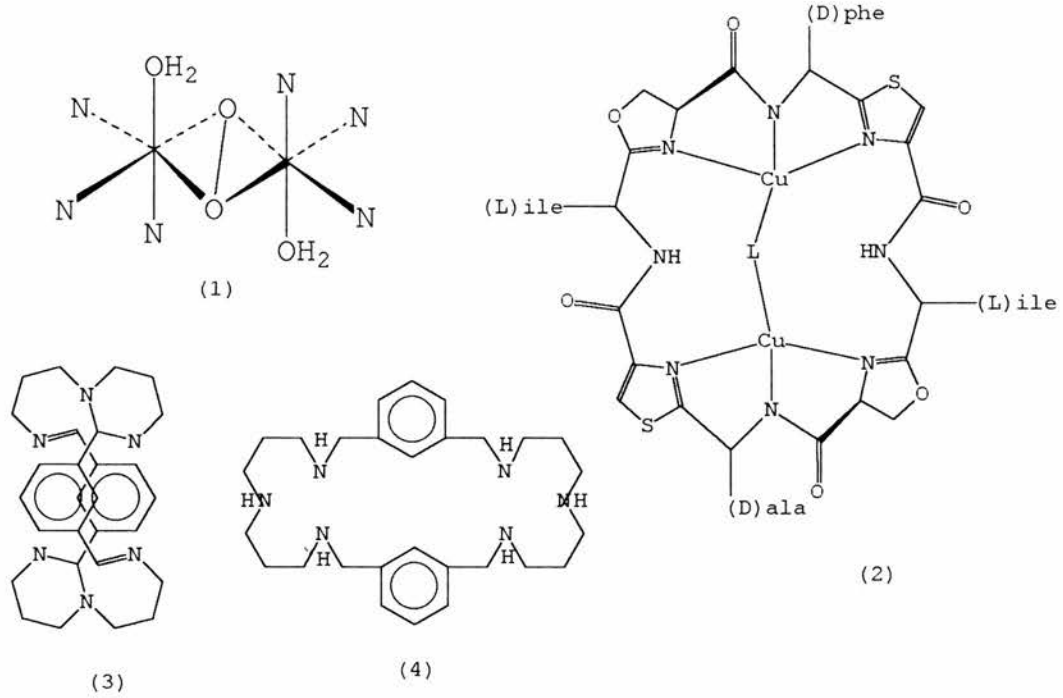

Figure 1

The Cu-Cu separation of 3.6 ± 0.2 is too long for a metal-metal bond and a bridging ligand is required for coupling of the unpaired electron on each copper. Hanson[3] has recently characterised some interesting marine natural products such as ascidiacyclamide and patellamide, which form binuclear metal complexes. A typical example is shown in (2) in which the bridging ligand, L, is CO_3^{2-}. The precise role of these naturally occurring binucleating ligands is currently unknown. Binuclear nickel(II) sites occur in the enzyme urease[4] and binuclear iron sites in purple acid phosphatase[5]. As a result, we have been interested in developing the chemistry of large macrocyclic ligands capable of incorporating two metal atoms. The reaction of *p*-phthalaldehyde or *o*-phthalaldehyde with 1,7-diamino-4-azaheptane (dpt) provides a useful high yield route to 30- (4) and 28- membered rings, respectively via the Schiff base (3). The present work describes[6], the preparation of the ligand (4) and characterisation of a series of binuclear metal complexes. A potentiometric study of the copper(II) complexes in aqueous solution has also been carried out and the results are compared with those recently reported by Martell[7].

Experimental

Measurements.-Infrared spectra were recorded on a Perkin Elmer 1710 Infrared Fourier Transform Spectrometer as KBr pellets. Melting points were obtained using a Gallenkamp

melting point apparatus. UVis spectra were recorded on a Lambda 14P Spectrometer. The NMR spectra were obtained using a 200MHz Varian Gemini in D_2O (reference sodium 2,2-dimethyl-2-sila-pentane-5-sulphonate) or $DCCl_3$ (reference TMS). Chloride and bromide determinations were made by titrating (ABU91 Autoburette) samples of the halide salts of the ligands with standard 0.100N $AgNO_3$ solution in 0.1mol dm^3 HNO_3 (using chloride or bromide selective electrodes). The chloride content of the metal complexes were determined by a similar method.

Materials.-High purity potassium chloride, 1,7-diamino-4-azaheptane (dpt) metal(II) salts, and sodium borohydride were obtained from Aldrich and used without further purification. Terepthalaldehyde was obtained from Avocado.

The concentration of the copper(II) nitrate stock solution was determined by EDTA complexometric titration. Carbonate free stock solutions of NaOH were prepared by dilution of a Rhone Poulenc Volucon ampoule with distilled, boiled out water and then standardised potentiometrically by titrating known weights of potassium hydrogen phthalate. A stock solution of HNO_3 was prepared by diluting concentrated HNO_3. All sample solutions were prepared using freshly boiled out distilled water.

Synthesis.- 1,5,9,18,22,26-hexaaza[11.11]paracyclophane (PPA), was prepared as previously described[8] and purified by recrystallizing once from toluene and twice as the hexahydrochloride salt from water-methanol to give a colourless blocks, which were sufficiently pure for stability constant work. (Found C, 46.69; H, 8.43; N, 10.49%. Calcd. for $C_{28}H_{46}N_6.6HCl.H_2O.3MeOH$: C, 46.57; H, 8.32; N, 10.51%. Chloride analysis: found 26.86%. Calcd. 26.60%).

(a) Macrocyclic Schiff base ([3]). In apparatus sealed to the atmosphere and supplied with nitrogen gas, an acetonitrile solution ($50cm^3$) of isophthalaldehyde (3g,22.4mmol) was dropped slowly (3h) into a rapidly stirred acetonitrile solution ($100cm^3$) of 1,7-diamino-4-azaheptane (dpt) (2.93g, 22.4mmol). After approximately half of the dialdehyde had been added, a fine white precipitate formed. The mixture was left stirring over night before the solid was collected by filtration and dried at reduced pressure at 50°C (yield 4.15g, 80%).

The Schiff base could be recrystallized from toluene or ethylacetate (if the temperature did not exceed 70°C) but the crude product could be used directly in the reduction step.

(b)1,5,9,18,22,26-hexaaza[11.11]metacyclophane (MPA). The Schiff base produced above (4.15g, 8.96mmol) was dissolved in ethanol ($100cm^3$) and cooled in an ice bath. With rapid stirring, sodium borohydride (6g) was added in 0.5g quantities. The mixture was left stirring over night.

The mixture was acidified with concentrated hydrochloric acid (pH < 2) and ethanol added ($30cm^3$). The white precipitate of crude MPA was filtered off and dried at 50°C under reduced pressure.

The ligand was redissolved in water ($100cm^3$) and basified with sodium hydroxide (a white precipitate forms immediately). The mixture was extracted with dichloromethane ($4x20cm^3$) and the extracts combined and dried over anhydrous sodium sulphate. Unlike the *para*-linked isomer PPA the free base of MPA does not form a crystalline solid, but a very sticky viscous oil (yield 3.42g, 82%). (Found C, 65.87; H, 11.06; N, 16.41. Calcd. for $C_{28}H_{46}N_6.2.5\ H_2O$: C, 65.72; H, 10.04; N, 16.42%).

(c)1,5,9,18,22,26-hexaaza[11.11]metacyclophane.6HBr (MPA.6HBr). A methanol solution ($25cm^3$) of the hexamine (1g, 2.14mmol) was acidified with concentrated hydrobromic acid to give a fine white precipitate. The precipitate was filtered off and recrystallized three times from methanol-water to give colourless prisms (yield 0.88g, 60%). (Found C, 35.38; H, 5.75; N, 8.63; Cl, 49.1. Calcd. for $C_{28}H_{46}N_6.6HBr$: C, 35.32; H, 5.75; N, 8.63; Br, 50.35).

The compound was of sufficient pure for potentiometric studies.

(d)$[Cu_2(MPA)Cl_2](CuCl_4).EtOH.2H_2O$. Copper(II) chloride dihydrate (0.738g, 4.33mmol) was dissolved in ethanol ($20cm^3$) and added dropwise to a boiling solution solution of MPA (1.01g, 2.16mmol) in ethanol ($20cm^3$). After half of the copper(II) chloride had been added to the rapidly stirred amine solution, a fine pale dark green precipitate formed. The complex was filtered off, washed with ethanol ($3x10cm^3$) and ether ($1x10cm^3$) and dried at reduced pressure at 50°C (yield 0.790g, 38%). (Found: C, 38.07; H, 5.53; N,

9.00; Cl, 22.1. Calcd. for $C_{28}H_{46}N_6Cu_2Cl_2.CuCl_4.C_2H_5O.2H_2O$: C, 37.84; H, 5.93; N, 8.83; Cl, 22.34%); i.r.(KBr) cm^{-1} 3444s, br (O-H ν); 3181s (N-H ν); 2939, 2875s (C-H ν.); 1612, 1590m (N-H δ); 1447s, (C-N ν); 805, 749, 706m (CH_2 γ). λ_{max}/nm (ε_{max}/$dm^3mol^{-1}cm^{-1}$) 428.6 (226), 732.1 (433) DMF; Λ_M/ S cm^2mol^{-1} 54 (DMF).

(e)[Zn_2(MPA)Cl_2].($ZnCl_4$).EtOH. Anhydrous zinc(II) chloride (0.596, 4.37mmol) was dissolved in ethanol (20cm^3) and added dropwise to a boiling ethanolic solution of MPA (1.02g, 2.19mmol). A flocculant white precipitate immediately formed which cleared after half of the MPA had been added. On near complete addition of MPA, the solution again became cloudy and a white solid separated from the cooled solution. The solid was filtered off, washed with ethanol (3x10cm^3) then ether (1x10cm^3). The complex was then dried *in vacuo* 24h, 50°C (yield 0.980g, 49%). (Found C, 39.17; H, 5.54; N, 9.50; Cl, 23.2. Calcd. for $C_{28}H_{46}N_6Zn_2Cl_2.ZnCl_4.C_2H_6O$: C, 39.10; H, 5.69; N, 9.11; Cl, 23.1); i.r.(KBr)cm^{-1}: 3508s (O-H ν.), 3221s, 3192s (N-H ν); 2942, 2874s (C-H ν.); 1612m (N-H δ); 1454s, 1429s, 1099m, 1086m, 1028s (C-N ν); 960, 894, 799, 764, 698w (CH_2 γ). Λ_M/ S cm^2mol^{-1} 35 (DMF).

(f) [Ni_2(MPA)Cl_4].(0.5$NiCl_2$).(0.5C_2H_5OH).(1.5H_2O). Nickel(II) chloride hexahydrate (1.128g, 4.75mmol) was dissolved in ethanol (20cm^3) and boiled for 10min. An ethanol solution (20cm^3) of MPA (1.107g, 2.37mmol) was boiled and the two solutions quickly mixed and left to cool. A pale green precipitate formed overnight. The crystals were filtered off and washed with cold ethanol (2x10cm^3) then ether (1x10cm^3) then dried *in vacuo* 24h, 50°C (yield 0.895g, 45%). (Found C, 41.37; H, 5.97; N, 9.87; Cl, 20.7. Calcd. for $C_{28}H_{46}N_6Ni_{2.5}Cl_5$. $1.5H_2O.0.5EtOH$: C, 41.43; H, 6.23; N, 10.00; Cl, 21.08%); i.r. (KBr) cm^{-1}: 3412s (O-H ν.), 3250s, 3222w (N-H ν); 2948s, 2928s, 2870s (C-H ν.); 1610m (N-H δ); 1465s (C-N ν); 1103s, 1008s, 995s, (CH_2 γ); 957, 899, 879, 804m. λ_{max}/nm 406, 665, DMF suspension;

(g) [Co_2MPACl_4].(0.5$CoCl_2$).(0.75C_2H_5OH). Anhydrous cobalt(II) chloride (0.686g, 5.28mmol) was dissolved in ethanol (20cm^3) and added dropwise to a boiling ethanolic solution of MPA (1.233g, 2.64mmol). A deep blue precipitate immediately formed which

cleared after half of the MPA was added. On near complete addition of MPA, the solution again became cloudy and a deep blue precipitate formed. The solid was filtered off, washed with ethanol (3x10cm^3) then ether (1x10cm^3). The complex was dried *in vacuo* 24h, 50°C (yield 1.07g, 49%). (Found C, 43.05; H, 6.03; N, 10.28; Cl, 21.6. Calcd. for $C_{28}H_{46}N_6Co_{2.5}Cl_5.(0.75C_2H_5OH)$: C, 42.90; H, 6.16; N, 10.18; Cl, 21.5); i.r. (KBr) cm^{-1}: 3423s (O-H ν.), 3184s (N-H ν); 2934s, 2872 (C-H ν.); 1617w (N-H δ); 1458s, 1163 (C-N ν); 1094m, 1006s (CH_2 γ); 878w, 798, 703m. λ_{max}/nm (ε_{max}/dm^{3}mol^{-1}cm^{-1}) 508 (136), 608 (399), 670 (330) DMF; Λ_M/ S cm^{2}mol^{-1} 31 (DMF).

Potentiometry.- Potentiometric pH measurements and computation of the protonation constants, Cu(II) binding constants, with the large macrocyclic ligands PPA and MPA were carried out by procedures described in Appendix I. Solutions were made up with boiled out water and the ionic strength adjusted to 0.1 with KNO_3. Approximately 1:1 or 1:2 PEA:Cu molar ratios were used. Details of the concentrations of components in the titration are given in Table 1.

Table 1 Summary of experimental parameters for the potentiometric study of the systems Cu(II)- MPA and PPA

Solution composition	MPA	PPA
$[T_L]$ range/mol dm^{-3}	$8.5x10^{-4}$ - $9.6x10^{-4}$	$8.7x10^{-4}$ - $1.2x10^{-3}$
$[T_{Cu}]$ range/mol dm^{-3}	$8.0x10^{-4}$ - $1.5x10^{-3}$	$7.9x10^{-4}$ - $1.4x10^{-3}$
I/mol dm^{-3}, electrolyte	0.1, KNO_3	0.1, KNO_3
pH Range	3 - 10.5	3.5 - 10.5
Experimental method	pH Titration, calibrated by standard buffers	pH Titration, calibrated by standard buffers
T/°C	25±0.1	25±0.1
Total number of data points		
Protonation	466 (7 curves)	263 (4 curves)
Copper complexation	409 (5 curves)	387 (4 curves)
Method of Calculation	SUPERQUAD	SUPERQUAD

* [MPA] / [Cu^{II}] 0.83 - 1.7 and [PPA] / [Cu^{II}] 0.67 - 1.44

The glass electrode was calibrated and checked for linearity with borax and potassium hydrogen phthalate buffers. The presence of CO_3^{2-} was checked by Gran's method (appendix I).

Results and Discussion

Synthesis.- The hexaaza macrocycle was simply made by the reduction of the [2+2] amine-aldehyde condensation product. It should be noted that samples of the free base decomposed over several months to form a resinous material (possibly a carbamate formed from atmospheric CO_2 contamination). MPA should be stored as the hexahalide salt.

Problems were encountered with the preparation of the transition metal complexes. Preparations invariably resulted in fine powders from which we were unable to obtain good crystals by recrystallization. In addition the microanalytical data could not be fitted to a simple binuclear complex structure. The assumption of a high degree of solvation in the complex merely resulted in a poor fit for the hydrogen content. The syntheses were repeated with an excess of metal ion to ensure the formation of binuclear complexes, but poor analytical results were still obtained.

Initially it was difficult to see how the complexes, formed from two analytically pure starting materials, could result in such poor analyses, but the results of the chloride determinations indicate much higher than expected chloride contents. An explanation for this could be that MPA complexes must form structures with more than two metals per ligand. The tetrachlorometalate ion may be participating as an anion in the complex. The copper and zinc complexes give microanalyses that fit well for chlorometalate salts of the metal chloride complexes of MPA. Although zincate salts are well known, examples of chlorocuprates are

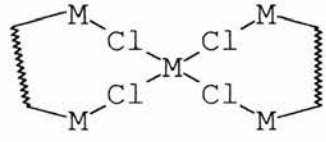

Figure 2

rather less common. An early example is that of a salt of methadone[9] and a Cu_2Cl_2 structure has been observed in a crystal structure of a macrocyclic Schiff base[10].

The nickel and cobalt complexes both analyse for the presence of an additional 0.5 of a metal ion and two chlorides. This result may indicate the presence of bridging of the type shown in Figure 2. The low yield of these complexes is also consistent with the use of 1:2 L:Cu stoichiometries to produce higher metal chloride aggregates. The exact nature of the metal chloride unit can only be ascertained by X-ray diffraction studies.

Potentiometric titration.- Both large macrocycles produce quite similar titration curves, indicating that similar species are formed in solution. Titration of the haloamine salts, in the absence of copper(II), results in two buffer regions (Figure 3 and Figure 4). The first corresponds to the loss of four moderately basic protons, and the second indicates the

removal of strongly basic protons. The behaviour of these two macrocycles differ markedly from the analogues prepared by the [2+2] condensation of dien with *m* or *p*-phthalaldehyde to be discussed later. The large ring macrocycles, containing ethylene bridges display much higher acidity for the first two deprotonations compared with the propyl-bridged macrocycles MPA and PPA. The difference may be explained on the grounds of electrostatic repulsion. In the propyl bridged macrocycle the protonation sites are further apart therefore electrostatic repulsion is less severe than in their ethyl bridged counterparts.

Table 2 Protonation Constants and Cu(II) Stability Constants of PPA and MPA

Reaction	PPA Log β	MPA Log β	symbol
$L + H^+ = LH^+$	10.69 ± 0.07	10.4 0.1(1)	$\log K_1$
$LH^+ + H^+ = LH_2^{2+}$	10.06 ± 0.08	9.64 0.06(6)	$\log K_2$
$LH_2^{2+} + H^+ = LH_3^{3+}$	8.61 ± 0.06	8.48 0.08(8)	$\log K_3$
$LH_3^{3+} + H^+ = LH_4^{4+}$	7.81 ± 0.02	7.86 0.01(1)	$\log K_4$
$LH_4^{4+} + H^+ = LH_5^{4+}$	7.27 ± 0.01	7.29 0.03(3)	$\log K_5$
$LH_5^{4+} + H^+ = LH_6^{6+}$	6.82 ± 0.01	6.80 0.04(4)	$\log K_6$
$2Cu^{2+} + L = [Cu_2(L)]^{4+}$	18.74 ± 0.09	18.31 ± 0.03(3)	$\log \beta_{LM2}$
$2Cu^{2+} + L + H^+ = [Cu_2(L)H]^{5+}$	25.66 ± 0.04	–	$\log \beta_{LM2H}$
$2Cu^{2+} + L + OH^- = [Cu_2(L)OH]^{3+}$	11.83 ± 0.07	10.65 ± 0.03(3)	$\log \beta_{LM2OH}$
$2Cu^{2+} + L + 2OH^- = [Cu_2(L)(OH)_2]^{2+}$	3.45 + 0.01	2.08 ± 0.02(2)	$\log \beta_{LM2(OH)2}$
$2Cu^{2+} + L + 3OH^- = [Cu_2(L)(OH)_3]^{2+}$	-	-8.58 ± 0.04(4)	$\log \beta_{LM2(OH)3}$
$Cu^{2+} + L + = [Cu(L)]^{2+}$	12.79 ± 0.03	11.97 ± 0.02(2)	$\log \beta_{LM}$
$Cu^{2+} + L + H^+ = [Cu(L)H]^{3+}$	21.17 ± 0.03	20.37 ± 0.02(2)	$\log \beta_{LMH}$
$Cu^{2+} + L + 2H^+ = [Cu(L)(H)_2]^{4+}$	28.62 ± 0.02	27.72 ± 0.02(2)	$\log \beta_{LMH2}$
$Cu^{2+} + L + 3H^+ = [Cu(L)(H)_3]^{5+}$	-	34.32 ± 0.03(3)	$\log \beta_{LMH3}$
$Cu^{2+} + L + OH^- = [Cu(L)(OH)]^+$	2.62 ± 0.05	2.13 ± 0.02(2)	$\log \beta_{LM(OH)}$

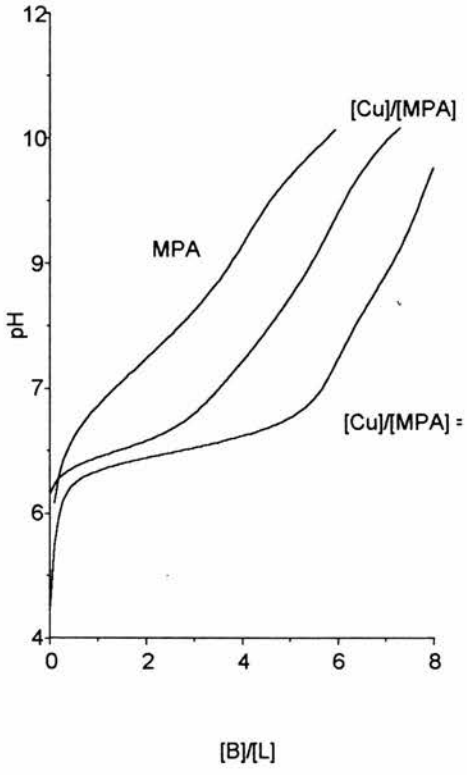

Figure 3

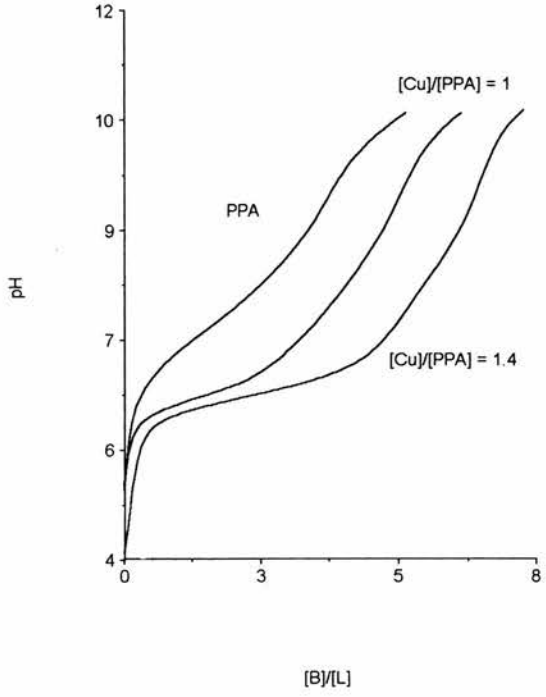

Figure 4

Protonated species of 1,5,9,18,22,26-hexaaza[11.11]paracyclophane (PPA)

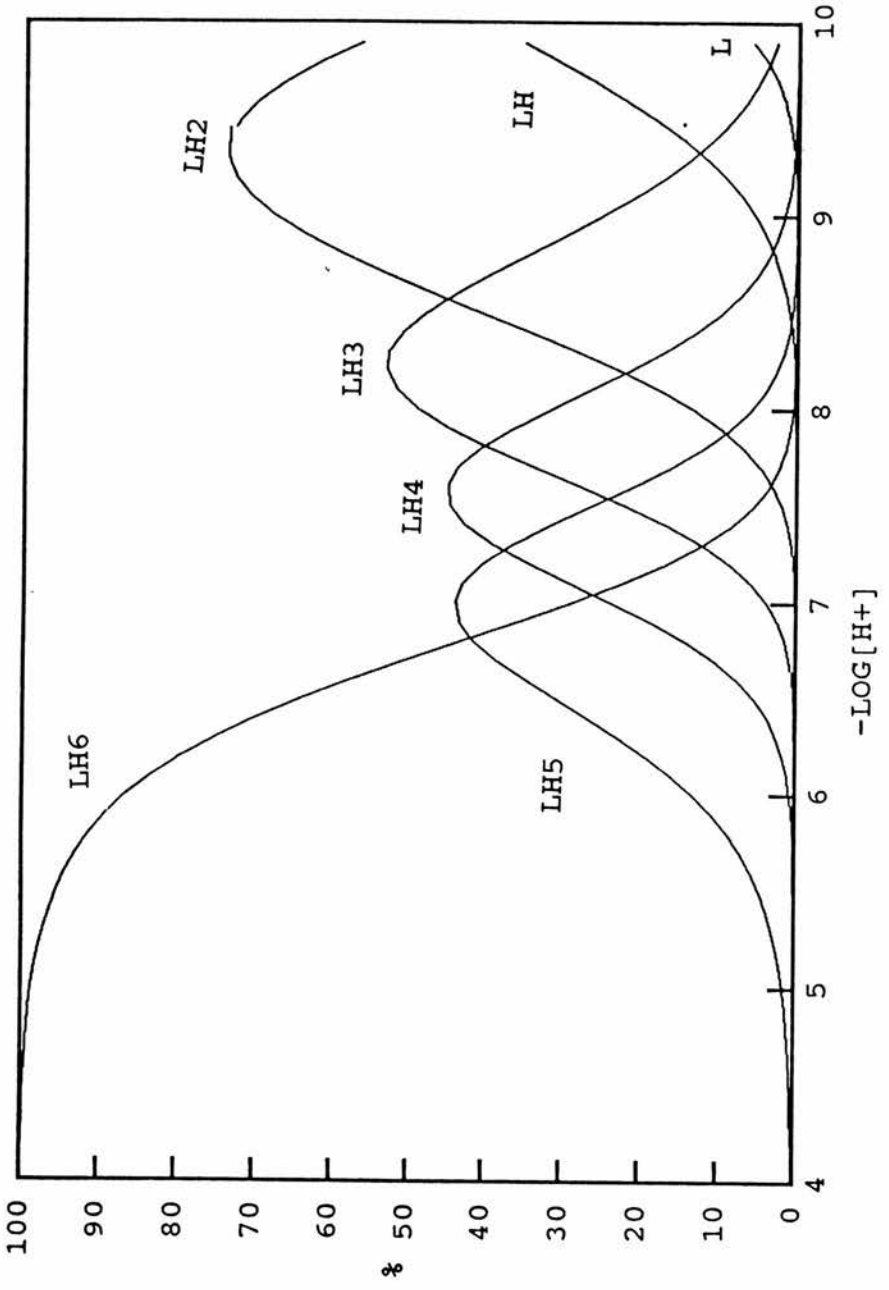

Protonated species of 1,5,9,18,22,26-hexaaza[11.11]metacyclophane (MPA)

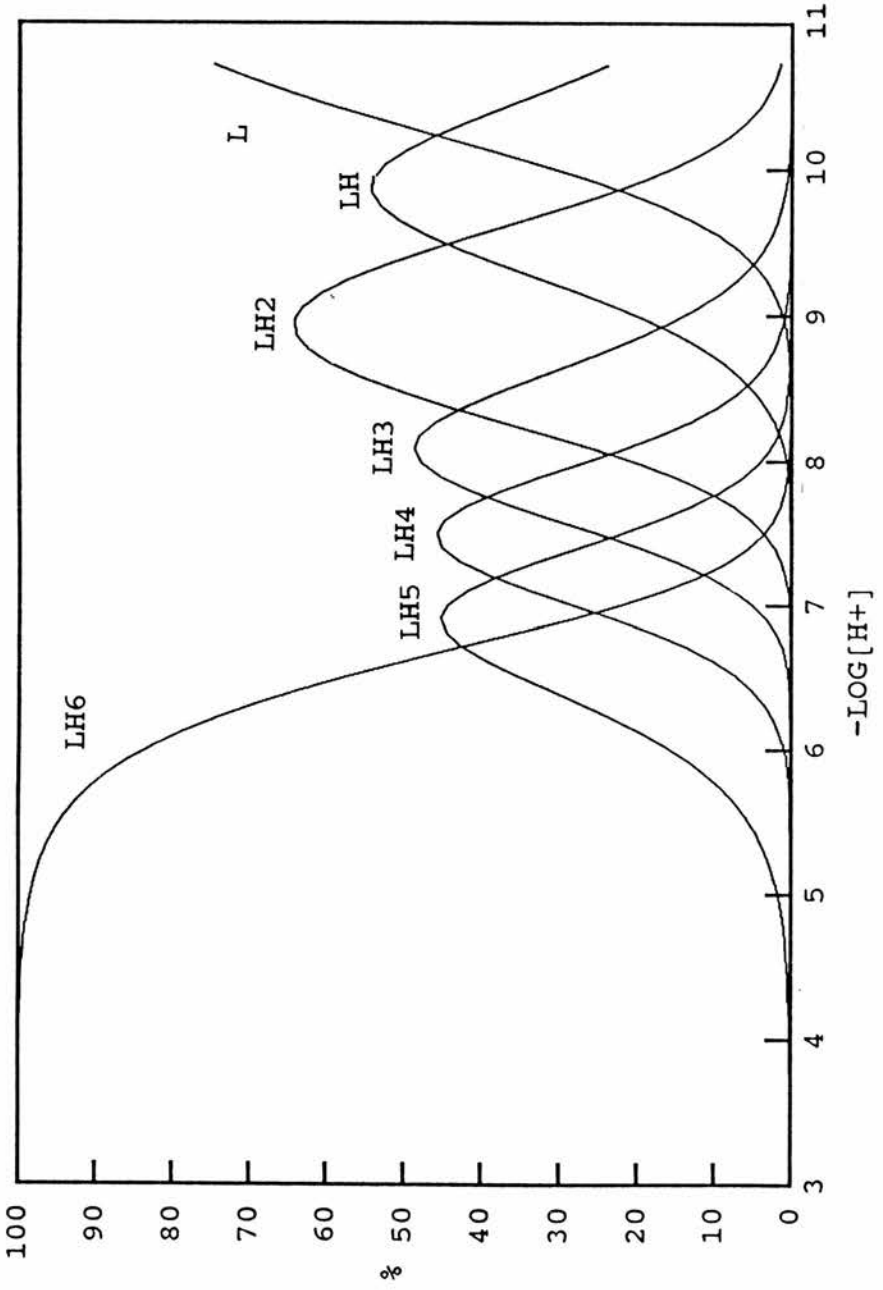

Copper Complexation. Titrations made in the presence of one or two equivalents of copper(II) were used to calculate stability constants for both mononuclear and dinuclear complexes using SUPERQUAD. The pH vs [B]/[L] plots in Figure 3 and Figure 4 show that the ligands both behave as dinucleating complexating agents and that the presence of a buffer region at greater than six equivalents of base indicate hydroxy complexes are formed. The best model included protonated mononuclear, dinuclear and hydroxy complexes of mono and dinuclear complexes. The calculated stability constants for the two systems are given in Table 2.

Speciation curves for the copper(II) complexes of 1,5,9,18,22,26-hexaaza[11.11]metacyclophane (MPA) in the presence of one equivalent of copper(II)

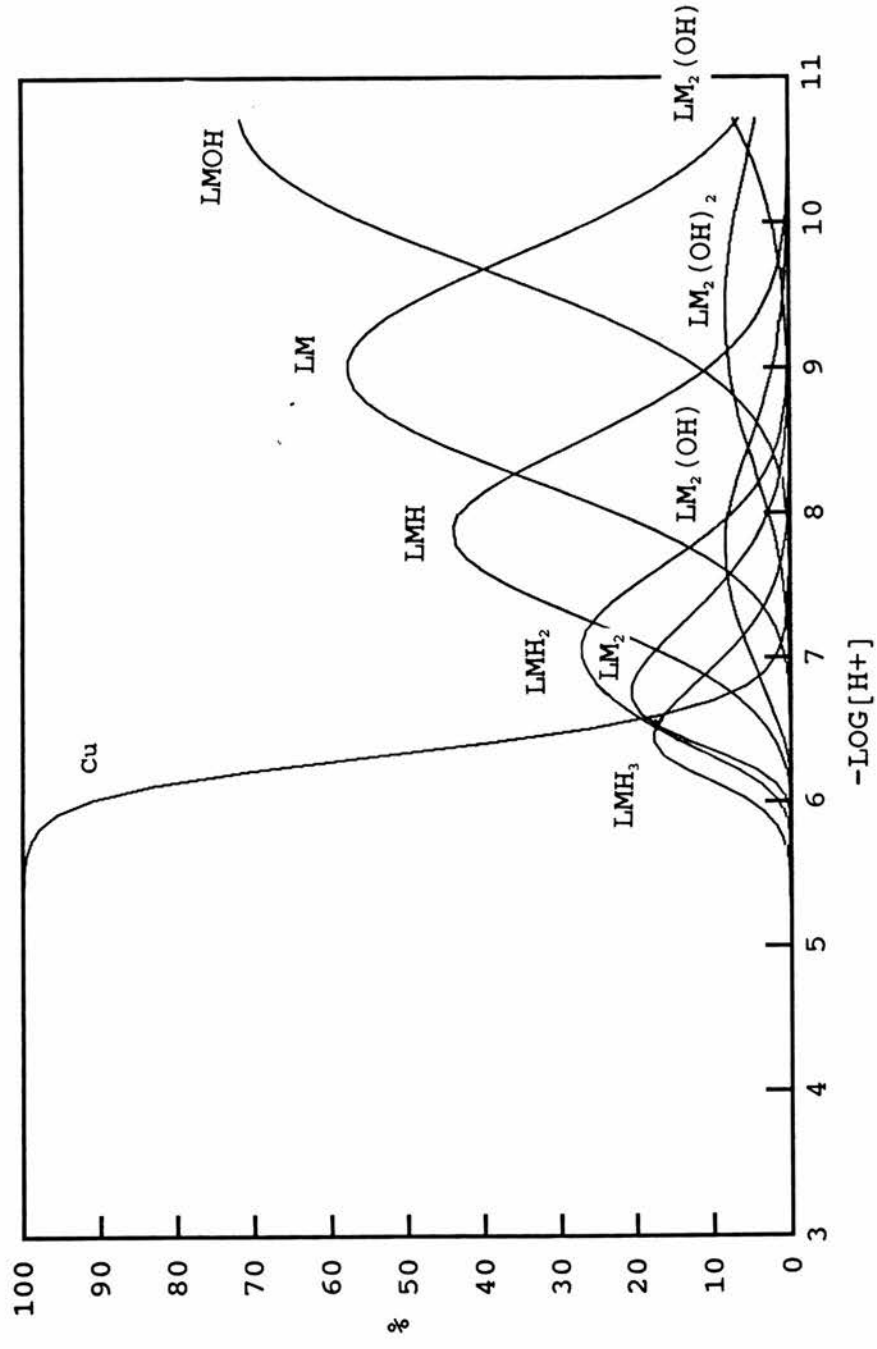

Speciation curves for the copper(II) complexes of 1,5,9,18,22,26-hexaaza[11.11]metacyclophane (MPA) in the presence of two equivalents of copper(II).

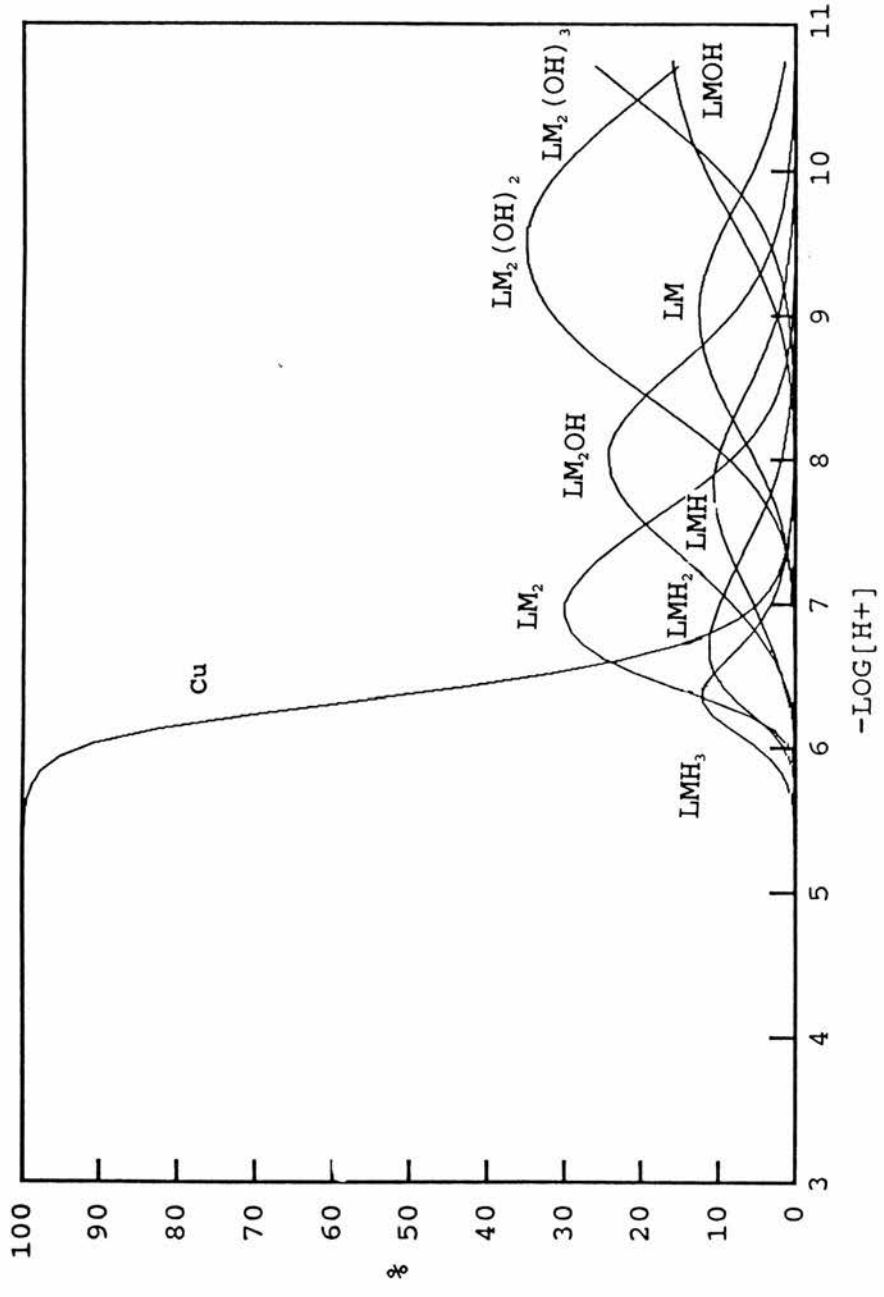

Speciation curves for the copper(II) complexes of 1,5,9,18,22,26-hexaaza[11.11]paracyclophane (PPA) in the presence of one equivalent of copper(II)

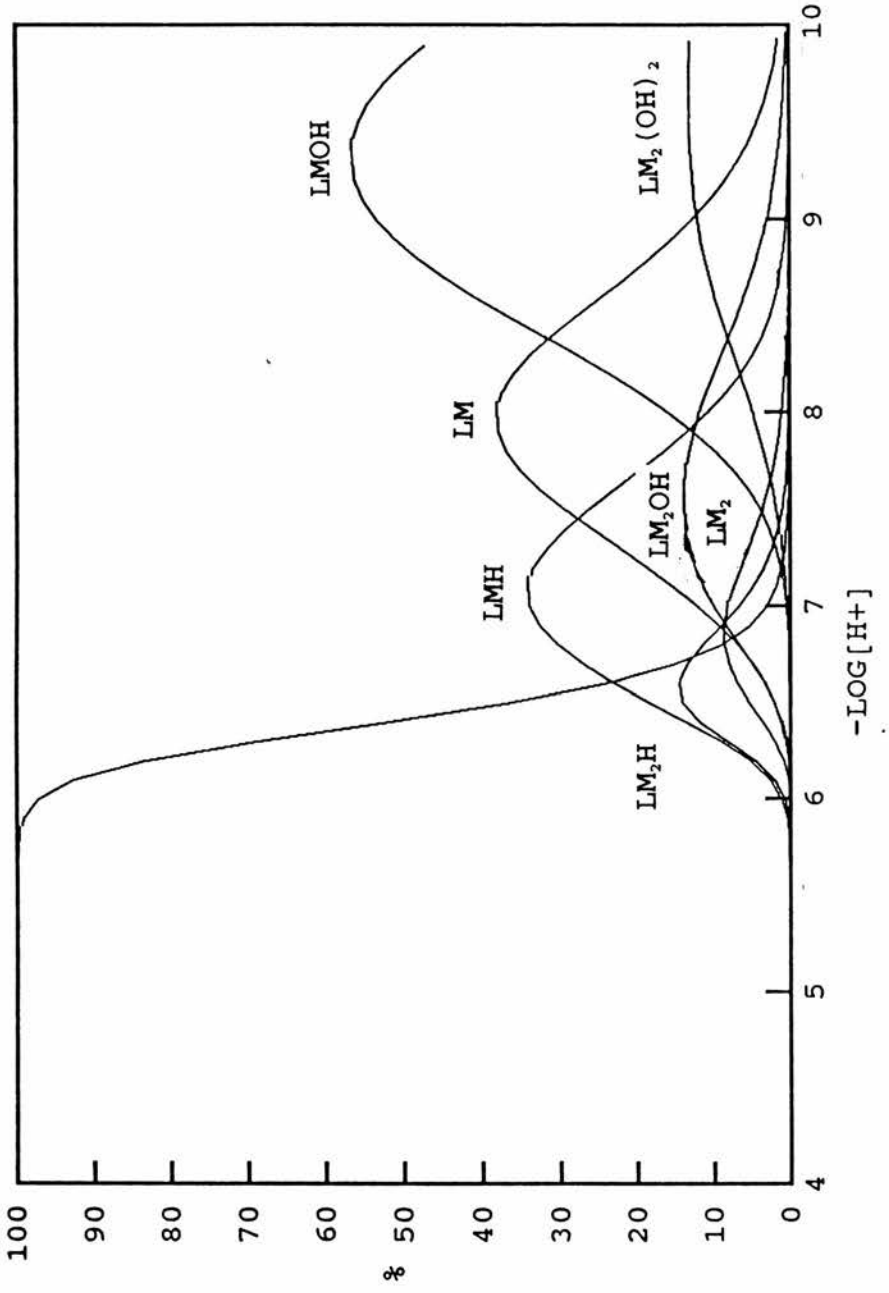

Speciation curves for the copper(II) complexes of 1,5,9,18,22,26-hexaaza[11.11]paracyclophane (PPA) in the presence of two equivalents of copper(II)

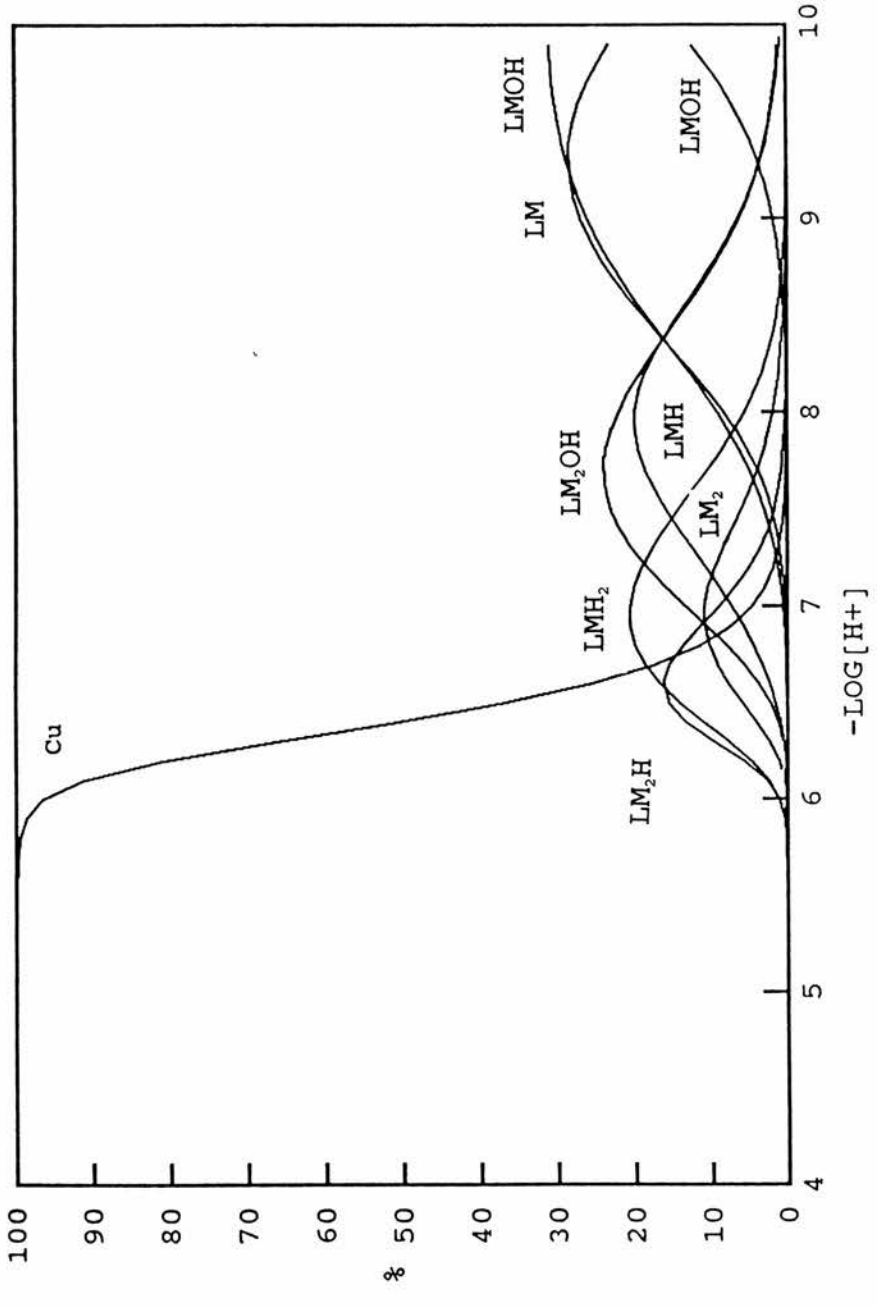

Since this work was completed Martell[7] has published a paper dealing with the solution chemistry of the complexes of MPA. In general terms our results are in good agreement with those of Martell (Table 3), however we found that hydroxy complexes of the mononuclear complexes could be detected. This observation enabled us to compare the pK values for the formation of the hydroxy complex of the mononuclear copper complex with that found for the dinuclear complex:

$[Cu(MPA)]^{2+} + OH^- = [Cu(MPA)(OH)]^+$ pK = 9.84 ± 0.03

$[Cu_2(MPA)]^{4+} + OH^- = [Cu_2(MPA)(OH)]^{+3}$ pK = 7.66 ± 0.09

$[Cu(PPA)]^{2+} + OH^- = [Cu(PPA)(OH)]^+$ pK = 10.17 ± 0.06

$[Cu_2(PPA)]^{4+} + OH^- = [Cu_2(PPA)(OH)]^{+3}$ pK = 6.91 ± 0.09

Martell has proposed[11] that these types of complexes form μ–hydroxy bridges (Figure 5) in a similar way to BISDIEN[12]. The greater acidity of the water molecules coordinated to the dinuclear complex as opposed to the mononuclear one could be explained by μ–hydroxy bridge formation. However it may be dangerous to simply assume this. The bridging of the copper complex of a flexible dinucleating ligand, such as BISDIEN, may be correct, but the presence of aromatic rings in MPA leads to a more rigid molecule. The formation of μ-

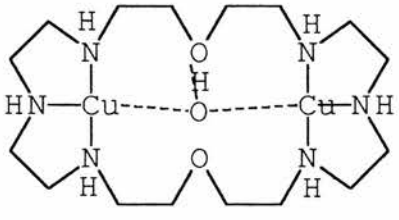

Figure 5. Hydroxo-bridged binuclear Cu(II) O-Bisdien Complex

hydroxy bridged complexes may accur for MEA, but is less likely for the larger macrocycle MPA and even less so for the paracyclophanes PPA and PEA.

Table 3 Comparison of stability constants of copper(II) complexes of MPA with those found by Martell

Reaction	Martell[7]	This work	
$2Cu^{2+} + L = [Cu_2(L)]^{4+}$	19.74	$18.31 \pm 0.03(3)$	$\log \beta_{LM2}$
$2Cu^{2+} + L + H^+ = [Cu_2(L)H]^{5+}$	-	–	$\log \beta_{LM2H}$
$2Cu^{2+} + L + OH^- = [Cu_2(L)OH]^{3+}$	10.89	$10.65 \pm 0.03(3)$	$\log \beta_{LM2OH}$
$2Cu^{2+} + L + 2OH^- = [Cu_2(L)(OH)_2]^{2+}$	1.28	$2.08 \pm 0.02(2)$	$\log \beta_{LM2(OH)2}$
$2Cu^{2+} + L + 3OH^- = [Cu_2(L)(OH)_3]^{2+}$	-	$-8.58 \pm 0.04(4)$	$\log \beta_{LM2(OH)3}$
$Cu^{2+} + L + = [Cu(L)]^{2+}$	11.46	$11.97 \pm 0.02(2)$	$\log \beta_{LM}$
$Cu^{2+} + L + H^+ = [Cu(L)H]^{3+}$	20.31	$20.37 \pm 0.02(2)$	$\log \beta_{LMH}$
$Cu^{2+} + L + 2H^+ = [Cu(L)(H)_2]^{4+}$	28.40	$27.72 \pm 0.02(2)$	$\log \beta_{LMH2}$
$Cu^{2+} + L + 3H^+ = [Cu(L)(H)_3]^{5+}$	34.67	$34.32 \pm 0.03(3)$	$\log \beta_{LMH3}$
$Cu^{2+} + L + OH^- = [Cu(L)(OH)]^+$	-	$2.13 \pm 0.02(2)$	$\log \beta_{LM(OH)}$

References

[1] a) D.E.Fenton, *Adv.Inorg.Bioinorg.Mech.*, 1983, **2**, 187; (b) T.Sorrel, *Tetrahedron*, 1989, **45**, 3; (c) D.E.Fenton and H.Okawa in R.W.Hay, J.R.Dilworth and K.B.Nolan (Eds.) *Perspectives in Bioinorganic Chemistry*, JAI Press, Connecticut, 1993.

[2] H.Tin-That and K.A.Magnus, *J.Inorg.Biochem.*, 1993, **51**, 65.

[3] A.L. van den Brenk, K.A.Bryrel, D.P.Fairlie, L.A.Ghan, G,R.Hanson, C.J.Hawkins, A.Jones, C.H.L.Kennard, B.Boubaraki and K.S.Murray, *Inorg.Chem.*,1993, **33**, 3549

[4] P.A.Clark, and D.E.Wilcox, *Inorg.Chem.*, 1989, **28**, 1326; R.E.Blakely and B.Zerner, *J.Molec.Catal.*, 1984, **23**, 263; N.E.Dixon, G.Gazzola, R.J.Blakely and B.Zerner, *J.Am.Chem.Soc.*, 1975, **97**, 4130; N.E.Dixon, P.W.Riddles, G.Gazzola, R.L.Blakely and B.Zerner, *Can.J.Biochem.*, 1980, **58**, 1335.

[5] B.C.Antanaitis and P.C.Aisen, *J.Biol.Chem.*, 1982, **257**, 5330; B.C.Antanaitis, P.C.Aisen and H.R.Lilienthal, *J.Biol.Chem.*, 1983, **258**, 3166.

[6] XIX International Symposium on Macrocyclic Chemistry, The University of Kansas, June 12th-17th 1994.

[7] A.Llobet, J.Reibenspies and A.E.Martell, *Inorg.Chem.* 1994, **33**, 5946.

[8] R.W.Hay, D.T.Ritchens, G.Wyllie, A.Danby and T.Clifford;*Trans.Met.Chem.*, 1995 **20**, 220.

[9] H.C.Nelson, S.H.Simonsen, and G.W.Watt, *J.C.S. Chem. Commun.*, 1979, 632.

[10] S.S.Tandon, L.K.Thompson, J.N.Bridson V.McKee and A.J.Downard, *Inorg.Chem.*, 1992, **31**, 4635.

[11] R.Menif, A.E.Martell, P.J.Squattrito and A.Clearfield, *Inorg.Chem.*, 1990, **29**, 4723.

[12] R.J.Motekatis, A.E.Martell, J.P.Lecomte and J.M.Lehn, *Inorg.Chem.* 1983, **22**, 609.

Binucleating Hexaaza Macrocycle (1,4,7,16,19,22-hexaaza[9.9]paracyclophane (PEA) and its Methylated Derivative 1,4,7,16,19,22-Hexamethyl-1,4,7,16,19,22-hexaaza[9.9]paracyclophane (Me_6PEA) and its Copper(II) and Zinc(II) Complexes; Synthesis, and Solution Chemistry of the Copper complex.

Abstract

The synthesis of the ligand 4,7,16,19,22-hexaaza[9.9]paracyclophane (PEA) and a new facile synthetic route to the previously published[1] fully methylated derivative 1,4,7,16,19,22-hexamethyl-1,4,7,16,19,22-hexaaza[9.9]paracyclophane (Me_6PEA) is described. The copper and zinc complexes have been prepared and the stability constants determined in aqueous solution by potentiometry (pK_1, pK_2, pK_3, pK_4, pK_5, pK_6 determined as 9.53(3), 8.84(3), 8.23(2), 7.36(4), 2.89(4), 3.57(8) respectively and 25.35(1), -8.17(4), -8.42(5), 11.16(3) for the stability constant for the binuclear complex, pK_a of the first water molecule, pK_a of the second water molecule and the stability constant for the formation of a mononuclear diprotonated species, respectively). The protonation sites of PEA have been identified for the protonated ligand species by nmr titration. The crystal structure of the complex $[Cu(PEA)Cl_2]Cl_2.5H_20.CH_3CN$ has been solved and shows a similar conformation to that of the complex $[Cu_2(Me_6PEA)Cl_2](ClO_4)(BPh_4).CH_3CN$

Experimental Section

Experimental

Measurements.-Infrared spectra were recorded on a Perkin Elmer 1710 Infrared Fourier Transform Spectrometer as KBr pellets. Melting points were obtained using a Gallenkamp melting point apparatus. UVis spectra were recorded on a Lambda 14P Spectrometer. The NMR spectra were obtained using a 200MHz Varian Gemini in D_2O (reference sodium 2,2 dimethyl-2-sila-pentane-5-sulphonate) or $CDCl_3$ (reference TMS).

Materials.-High purity potassium chloride, 1,5-diamino-3-azapentane (dien), copper salts, and sodium borohydride were obtained from Aldrich and used without further purification. Terepthalaldehyde was obtained from Avocado.

The concentration of copper nitrate stock solution was determined by EDTA complexometric titration. Carbonate free stock solutions of NaOH were prepared by dilution of a Rhone Poulenc Volucon ampoule with distilled, boiled out water and then standardised potentiometrically by titrating known weights of potassium hydrogen phthalate. A stock solution of HNO_3 was prepared by diluting concentrated HNO_3 .All sample solutions were prepared in freshly boiled out distilled water.

Synthesis.-The ligand was prepared by a nontemplate [2+2] condensation of 1,5-diamino-3-azapentane with the dialdehyde terepthalaldehyde to form a tetramine followed by a sodium borohydride reduction.

Preparation of (a) tetraimine. Under a nitrogen atmosphere, a filtered acetonitrile solution ($50cm^3$) of terepthalaldehyde (3g, 22.4mmol) was added dropwise (3h) to a rapidly stirred acetonitrile solution ($100cm^3$) of dien (2.93g, 22.4mmol). After approximately half of the dialdehyde had been added, a fine white precipitate formed. The mixture was left stirring overnight before the solid was collected by filtration and dried at reduced pressure at 50°C (yield 4.15g, 80%).

The tetramine Schiff base could be recrystallized from toluene or ethylacetate (if the temperature did not exceed 70°C) but the crude product could be used directly in the reduction step.

(b) 4,7,16,19,22-hexaaza[9.9]paracyclophane (PEA). The Schiff base produced above (4.15g, 8.96mmol) was dissolved in ethanol ($100cm^3$) and cooled in an ice bath. With rapid stirring, sodium borohydride (6g) was added in 0.5g quantities. The mixture was left stirring over night.

The mixture was acidified with concentrated hydrochloric acid (pH < 2) and ethanol added ($30cm^3$). The white precipitate of crude PEA was filtered off and dried at 50°C under reduced pressure.

The solid was redissolved in water ($100cm^3$) and basified with sodium hydroxide (a white precipitate forms immediately). The mixture was extracted with dichloromethane ($4x20cm^3$) and the extracts combined and dried over anhydrous sodium sulphate. The solid residue obtained after removal of solvent was recrystallized from hot (70°C) toluene giving fine white needles (yield 3.42g, 82%). (Found: C, 70.21; H, 9.35; N, 20.44%. Calcd. for $C_{24}H_{38}N_6$: C, 70.20; H, 9.33; N, 20.47%); i.r.(KBr): 3340s, broad(O-H ν); 3293, 3227, 2942, 290s (N-H ν); 2873, 2800, 273s (C-H ν); 1503, 1471(N-H δ); 1447, 1434, 1139, 1122, 1113, 1018(C-N δ); 998, 969, 945, 926, 817, 800, 485.

(c) 1,4,7,16,19,22-Hexamethyl-1,4,7,16,19,22-hexaaza[9.9]paracyclophane.6HCl. 1.5H₂O (Me₆PEA.6HCl.1.5H₂O). Formic acid, ($8cm^3$, 98%), formaldehyde ($7cm^3$, 35% aqueous solution) and PEA (1.519g, 3.205mmol) were refluxed under argon for 18 hours. The solution was cooled and basified with sodium hydroxide (9g) in water ($10cm^3$) then extracted with dichloromethane ($3x20cm^3$). The combined extracts were dried over $MgSO_4$. Removal of the solvent at reduced pressure gave a the crude product as a pale yellow oil. The oil was dissolved in ethanol (*ca.* $20cm^3$) and concentrated HCl (37%) added until the solution became turbid. The white precipitate formed was filtered off washed with isopropanol then diethylether. The product was recrystallized from aqueous methanol and dried at reduced pressure (yield 2.42g, 91%). (Found: C, 48.80; H, 7.96; N, 11.26%. Calcd. for $C_{30}H_{56}N_6.(1.5H_2O)Cl_6$: C, 48.66; H, 8.03; N, 11.35%); i.r.(KBr): 3453s br (O-H ν); 2975s (C-H ν); 2663, 2380s br (N^+-H ν); 1664s (N^+-H δ); 1537, 1474, 1439, 1230 (C-N ν); 1113, 947, 791, 567.

(d) [Cu₂(PEA)Cl₄].3H₂O.MeOH. Copper(II) chloride dihydrate (0.832g, 4.88mmol) was dissolved in ethanol ($20cm^3$) and added dropwise to a boiling ethanol solution ($20cm^3$) of PEA (1.0g, 2.44mmol). After half of the copper chloride had been added to the rapidly stirred amine solution, a fine pale blue-green precipitate formed. The complex was filtered off, washed with ethanol ($3x10cm^3$) then diethylether ($1x10cm^3$) and dried at reduced pressure at 50°C. The complex was further purified by dissolving in aqueous methanol (*ca.* 50%) then adding a equal volume of acetonitrile to give blue plate like crystals which were washed with

ethanol and air dried (yield 1.65g, 88%). (Found: C, 39.10; H, 5.52; N, 11.06. Calcd. for $C_{25}H_{48}N_6Cu_2Cl_4O_4$: C, 39.22; H, 6.32; N, 10.98); i.r.(KBr)cm^{-1}: 3404s (O-H ν), 3182s (N-H ν); 2879s (C-H ν); 1617m (N-H δ); 1520, 1451, 1065, 1019 (C-N ν); 871, 837, 803 (CH_2 γ); 656, 478. λ_{max}/nm (ε_{max}/$dm^3mol^{-1}cm^{-1}$) 617 (238), water; Λ_M/ S cm^2mol^{-1} 391 (water);

(e) [Zn(PEA)Cl_2]3.5H_2O. Anhydrous zinc(II) chloride (0.665g, 2.34mmol) was dissolved in ethanol (20cm^3) and added dropwise to a boiling ethanolic solution of PEA (1.0g, 2.44mmol). A flocculant white precipitate immediately formed which cleared after half of the PEA had been added. On near complete addition of PEA, the solution again became cloudy and a white solid separated from the cooled solution. The solid was filtered off, washing with ethanol (3x10cm^3) then ether (1x10cm^3). The powder was dried *in vacuo* for 24h at 50°C (yield 1.52, 98%). (Found: C, 47.58; H, 7.04; N, 12.91. Calcd. for $C_{24}H_{38}N_6ZnCl_2.3.5H_2O$: C, 47.26; H, 7.44; N, 13.78.); i.r.(KBr): 3406s (O-H ν); 3230s (N-H ν); 2925, 2875, 2801s (C-H ν); 1636s (N-H δ); 1515, 1447, 1347 (C-N ν); 1051, 990, 947, 847 (CH γ). Λ_M / S cm^2mol^{-1} 274 (water).

(f) [Ni_2(PEA)Cl_4].$CH_3OH.H_2O$. Nickel(II) chloride hexahydrate (1.16g, 4.88mmol) was dissolved in methanol (20cm^3) and added dropwise to a refluxing methanol solution (30cm^3) of PEA (1g, 2.44mmol) over a 10 min period. the mixture was refluxed for a further 15 min to give a pink-red solution with a small amount of solid. the solution was filtered and reduced in volume to ca. 15cm^3. Pale green crystals formed over night. After a fortnight the crystals were filtered off and washed with cold ethanol (2x10cm^3) and dried *in vacuo* 24h, 50°C (yield 1.06g, 60%).(Found: C, 41.74; H, 5.68; N, 11.67. Calcd. for $C_{24}H_{44}N_6O_2Ni_2Cl_4$: C, 41.71; H, 6.16; N, 11.67; i.r.(KBr): 3405 (O-H ν); 3227 s (N-H ν); 2928, 2847s (C-H ν), 1616s (N-H δ); 1457, 1078 (C-N ν); 992, 938, 817 (CH2 γ). λ_{max}/nm(ε_{max}/$dm^3mol^{-1}cm^{-1}$) 369 (22), 603 (12), 773 (sh) large rise in abs. above 850nm, water; Λ_M/ S cm^2mol^{-1} 431 (water);

(g) [Co_2(PEA)Cl_4].0.5MeOH.1.5H_2O. Anhydrous cobalt(II) chloride (1.36g, 5.72mmol) was dissolved in methanol (20cm^3) and added dropwise to a boiling methanol solution of PEA (1.0g, 2.44mmol), under argon. The solution deposited a pale brown precipitate. The solid was filtered off, washed with ethanol (3x10cm^3) then ether (1x10cm^3) and dried *in*

vacuo for 24h at 50°C. The complex was found to be insoluble in all solvents apart from water (in which it was only slightly soluble) (yield 1.36g, 78%). (Found: C, 41.45; H, 5.41; N, 11.84. Calcd. for $C_{24}H_{38}N_6Co_2Cl_4.1.5H_2O.0.5MeOH$: C, 41.27; H, 6.08; N, 11.79; i.r.(KBr): 3405s (O-H ν); 3255(N-H ν); 2940, 2801s (C-H ν); 1647, 1636 (N-H δ); 1509, 1457, 1434, 1341 (C-N ν); 1112, 1069, 1049, 1026, 922, 845, 797, 628. λ_{max}/nm(ε_{max}/dm^{3}mol^{-1}cm^{-1}) 523 (103) water; Λ_M/ S cm^{2}mol^{-1} 315 (water);

X-ray Determination of the Crystal structure of $[Cu_2(PEA)Cl_4]MeCN\ 5H_2O$.- A single crystal of $[Cu_2(PEA)Cl_4]MeCN.\ 5H_2O$ was grown by the diffusion of acetonitrile into an aqueous methanolic solution of the complex to give well formed dark blue blocks. The crystals were found to be efflorescent and it was necessary to obtain the diffraction at low temperature (120K).

Crystal Data. $C_{26}H_{38}N_7Cu_2Cl_4O_5$, M = 797.53, Orthorhombic, a = 14.971(8), b = 42.25(4), c = 25.32(3) Å, U = 16012(21) Å^3 (by least-squares refinement on diffractometer angles for 25 automatically centred reflections, in the range $19.41<2\theta<24.90°$ λ = 0.71069 Å), space group *Ibca*(#73), Z = 16, D_c = 1.323 g cm^{-3}, F(000) = 6544.00. Blue block crystal. Approximate crystal dimensions 0.50 x 0.40 x 0.35 mm, μ(Mo-K$_\alpha$) = 13.68 cm^{-1}.

Data Collection and Processing. Rigaku AFC7S diffractometer, ω-2θ scan type with ω scan width = (1.68 + 0.35 tan θ)°, ω scan speed 16.00° min-1 (up to 4 scans), graphite monochromated MoKα radiation; 6222 reflections measured (max 2θ = 50.0°), 3532 unique (R_{int} = 0.005). Decay correction (8.26% decline), and absorption correction (trans. factors: 0.4247 - 1.0000)were required. Corrections were made for Lorentz and polarisation effects.

Structure Analysis and Refinement. Direct methods[2] were employed and expanded using Fourier techniques[3] Some non-hydrogen atoms were refined anisotropically, while the rest were refined isotropically. Hydrogen's were included but not refined. The final cycle of full-matrix least-squares refinement[4] was based on 1827 observed reflections ($I>3.00\sigma(I)$) and 248 variable parameters and converged (largest parameter shift was 0.19 times its esd) with unweighted agreement factors of:

$$R = \sum \| Fo| - |Fc| \| / \sum |Fo| = 0.112$$

$$R_w = \sqrt{\left(\sum \left(|Fo| - |Fc| \right)^2 / \sum wFo^2 \right)} = 0.099$$

The standard deviation of an observation of unit weight[5] was 7.22. The weighting scheme was based on counting statistics and included a factor (p = 0.003) to downweight the intense reflections. Plots of $w(\Sigma |Fo| - |Fc|)^2$ versus $|Fo|$, reflection order in data collection, sin θ/λ and various classes of indices showed no unusual trends. The maximum and minimum peaks on the final difference Fourier map correspond to 1.23 and -0.85 $e^-Å^{-3}$, respectively. Considerable difficulty was encountered in modelling the disordered solvent present in the structure. Unfortunately the ease with which solvent was lost from the crystals prevented the determination of degree of solvation by microanalysis of fresh samples. A freshly recrystallized sample was found to give a stable weight after 15 min. Micro analysis of this sample indicated the presence of at least three water molecules. IR spectra of fresh samples showed no CN stretch attributable to acetonitrile however one molecule of acetonitrile had to be included in the structure to give a reasonable fit. All calculations were performed using the teXsan[6] crystallographic software package of Molecular Structure Corporation.·

NMR titrations.- Duterated compounds were obtained from Aldrich. NMR spectra were obtained in D_2O, the required pH obtained by adjustment with NaOD (30% wt. in D_2O) or DCl (37% in D_2O). Quoted ^{13}C chemical shifts are relative to sodium 2,2-dimethyl-2-sila-pentane-5-sulphonate (Aldrich) dissolved in dioxane and sealed into a capillary. The ligand concentration was approximately 0.01M. Spectra were recorded on a Varian Gemini 200 MHz Spectrometer.

Potentiometric Titrations.- Potentiometric pH measurements and computation of the protonation constants and Cu(II) binding constants were carried out by procedures described in detail in Appendix I. Solutions were made up with boiled out water and the ionic strength adjusted to 0.1mol dm^3 with KCl. Approximately 1:1 or 1:2 PEA:Cu molar ratios were used. Details of the concentrations of components in the titration are given in Table 1. Potasium chloride rather than KNO_3 was chosen as supporting electrolyte as protonated PEA forms water insoluble salts with nitrate.

Table 1 Summary of experimental parameters for the potentiometric study of the system Cu(II),-PEA **Summary of experimental parameters for the potentiometric study of the system Cu(II),-PEA**

Solution composition	
$[T_L]$ range/mol dm^{-3}	$7.5x10^{-4}$ - $8.0x10^{-4}$
$[T_{Cu}]$ range/mol dm^{-3}	$1.5x10^{-3}$ - $8.0x10^{-4}$
I/mol dm^{-3}, electrolyte	0.1, KCl
pH Range	3-10.5
Experimental method	pH Titration, calibrated by standard buffers
T/°C	25±0.1
Total number of data points	
Protonation	327 (8 curves)
Copper complexation	205 (6 curves)
Method of Calculation	SUPERQUAD

The glass electrode was calibrated and checked for linearity with borax and potassium hydrogen phthalate buffers in aqueous solution. The presence of CO_3^{2-} was checked using a Gran plot.

Spectrophotometric Titration.- Under approximately the same conditions as for the potentiometric titrations, a visible spectrum (wavelength range 850-400 nm) was taken after each aliquot of standard sodium hydroxide was added. The data were processed using the

HYPERQUAD suite of programs. Experimental parameters for the experiment are given in Table 2 and details of the computation of the Cu(II) binding constants, were carried out by procedures described in detail (appendix I).

Table 2. Summary of experimental parameters for the spectrophotometric study of the system Cu(II)-PEA

Solution composition	
$[T_L]$ range/mol dm^{-3}	1.5×10^{-3} ; 1.2×10^{-3}
$[T_{Cu}]$ range/mol dm^{-3}	2.7×10^{-3} ; 1.1×10^{-3}
I/mol dm^{-3}, electrolyte	0.1, KCl
pH Range	3-10.5
Experimental method	Spectrophotometric Titration (400-900nm)
T/°C	25±0.1
Total number of data points	
Copper complexation	2x[spectra at 28 H+ concentrations 26 wavelengths] = 1456 points
Method of Calculation	HYPERQUAD

DNPDEP hydrolysis kinetics. - The hydrolysis of the triester DEPDNP was measured spectrophotometrically at 360nm. Solutions at various pH's were prepared by the adjustment of a 4.65×10^{-3} mol dm^3 solution with respect to Cu(II), 2.52×10^{-3} mol dm^{-3} to PEA and 0.1 mol dm^{-3} to KCl to the required pH with NaOH or HCl. The reaction was initiated by the addition of a 2µl acetonitrile stock solution of DEPDNP to a 2cm^3 sample of the solution in a 1 cm pathlength cuvette. The final DEPDNP concentration was 2×10^{-4} mol dm^{-3}. For slow reactions (< pH 7) data were collected over one half life only. The infinity value was obtained after two weeks at room temperature. Above pH 7 data could be collected for three half lives. The absorbence versus time curves were fitted to a first order rate equation using a linear least squares method. The quoted rate constants are the average of two runs. The duplicate showed that the rate constants could be replicated to within 5%.

Results and Discussion

Synthesis.- The reaction of 1,5-diamino-3-azapentane (dien), with *p*-phthalaldehyde in acetonitrile gives the macrocyclic Schiff base in reasonable yield and purity to allow $NaBH_4$ reduction to the amine without further purification. Although this [2+2] addition reaction has been of great utility in recent years to prepare large macrocycles, Pietraszkiewicz and Gasiorowski[7] have reported that the reaction in THF solvent results in the formation of polymeric material. Clearly that these reactions are very solvent dependant. The amine is readily purified by recrystallisation from ethyl acetate to give analytically pure crystalline material. The amine can be permethylated by the standard Eschweiler-Clarke[8] procedure and is a distinct improvement, in terms of yield and ease of synthesis, to that of described by Paoletti[1].

The binuclear complexes of PEA with cobalt(II), nickel(II), and copper(II) are hydrated and even after prolonged periods of drying at reduced pressure, the microanalytical data showed the presence of solvent of crystallisation. The presence of solvent, have been noted in similar complexes[9]. Surprisingly the binuclear zinc complex could not be prepared. The microanalysis could only be fitted to a mononuclear zinc complex. The rather low conductivity of the zinc complex when compared to the other metal(II) complexes confirms the mononuclear nature of this complex. All the other complexes have molar conductivities greater than 300 S cm^2mol^{-1} which, although rather low for a 1:4 electrolyte[10] it may be due to the bulky nature of the complex. Low ionic mobility has been used to explain the unusually low conductivities of tetraphenylborate salts[11]. The visible spectrum of the copper(II) (ε = 119 per copper centre at λ_{max}= 617) is consistent with a d^9 five co-ordinate metal ion The nickel complex has two main bands in the visible region and a third >900nm all of low intensity indicative of an octahedral d^8 ion.

Description of the crystal structure of $[Cu_2(PEA)Cl_4]MeCN\ 5H_2O$.-The copper centres have an N_3Cl_2 donor set, with square pyramidal geometry. Three nitrogens from the macrocycle and one of the chlorides make up the base of the pyramid with the copper somewhat displaced above the plane towards the apical chloride (as is commonly found with

square pyramidal complexes). The apical chloride is directed away from the macrocycle cavity to form a bridge to copper centre in an adjacent macrocycle. The bridging occurs throughout the structure to form chains of chloro-bridged complexes running parallel to the *b* axis, Figure 1.The copper to nitrogen distances are not unusual (the mean distance found for five co-ordinate secondary amine complexes in the Daresbury database is 2.029Å). The copper to chloride distance is normal for the basal chloride, but the apical chloride to copper distance is a little longer than expected, and may be due to a small degree of electron withdrawal in bridge formation. The Cu-Cu distance is 7.02 Å.

The complex has *C2* symmetry with the reflection plane bisecting the Cu-Cu axis. The nitrogen donor ends of the ligand are folded back-to-back giving a basket like structure with the benzene rings forming the base of the basket and one unbound chloride within the cavity.

Table 3. Assorted bond lengths (Å), angles and Cu...Cu separation for PEA complex

Cu(1)-Cl(2)	2.732(7)	Cl(1)-Cu(1)-Cl(2)	96.5(2)
Cu(1)-Cl(1)	2.241(8)	N(1)-Cu(1)-Cl(2)	88.6(6)
Cu(1)-N(1)	2.02(2)	N(2)-Cu(1)-Cl(2)	62.4(6)
Cu(1)-N(2)	1.99(2)	N(3)-Cu(1)-Cl(2)	88.9(6)
Cu(1)-N(3)	2.00(3)	N(1)-Cu(1)-N(2)	84.7(8)
Cu(2)-Cl(5)	2.658(7)	N(1)-Cu(1)-N(3)	170.2(9)
Cu(2)-Cl(3)	2.265(9)	Cl(3)-Cu(2)-Cl(5)	97.0(3)
Cu(2)-N(4)	2.02(2)	N(6)-Cu(2)-Cl(5)	84(1)
Cu(2)-N(5)	1.99(3)	N(5)-Cu(2)-Cl(5)	91.4(7)
Cu(2)-N(6)	2.05(2)	N(4)-Cu(2)-Cl(5)	94.1(6)
Cu(1)....Cu(2)	7.02	N(6)-Cu(2)-N(5)	84(1)
		N(6)-Cu(2)-N(4)	167(1)

Figure 1. ORTEP drawings of $[Cu_2(PEA)Cl_4]MeCN.5H_2O$ and ball and stick drawing showing chloro bridging.

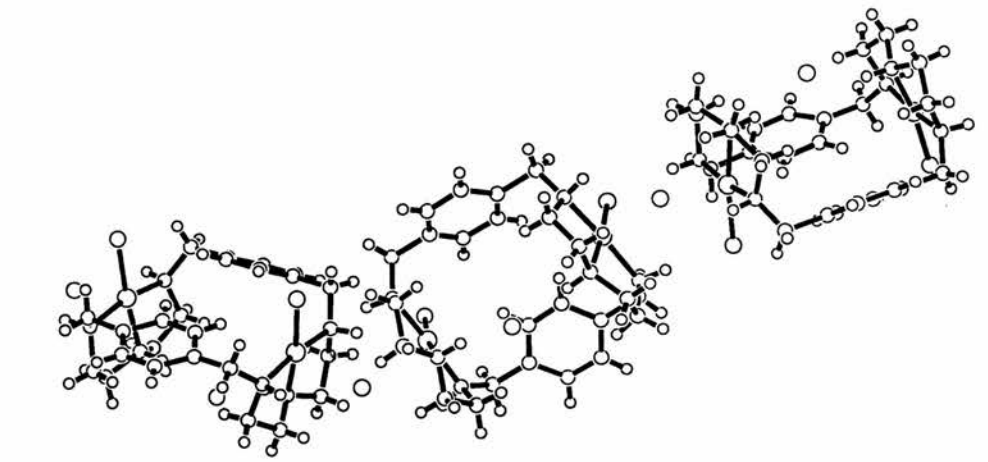

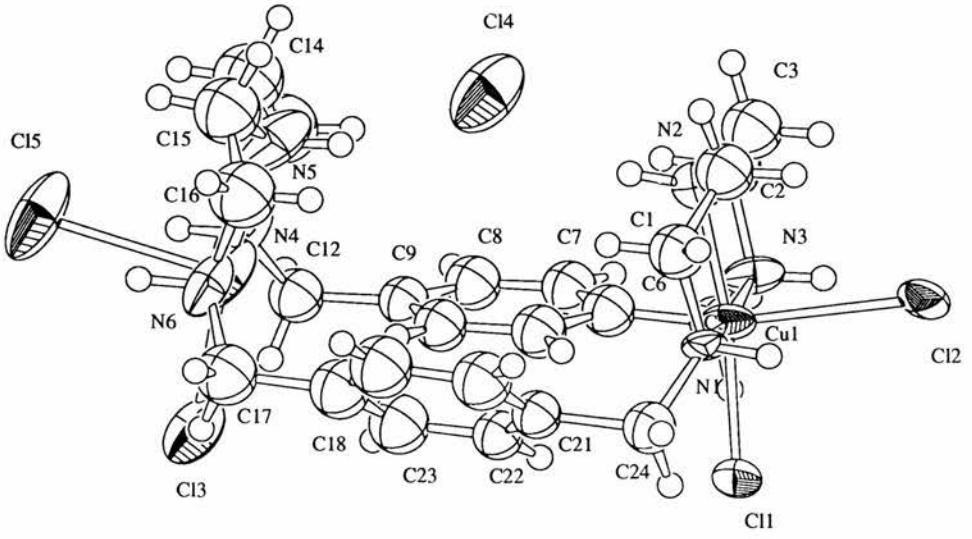

Potentiometric titration.-

Table 4. Protonation Constants and Cu(II) Stability Constants of 4,7,16,19,22-hexaaza[9.9]paracyclophane (PEA)

Ion	Reaction	Log β	symbol
H+	$L + H^+ = [LH]^+$	9.48 ± 0.01	β_1
	$L + 2H^+ = [LH_2]^{2+}$	18.355 ± 0.009	β_2
	$L + 3H^+ = [LH_3]^{3+}$	26.58 ±0.01	β_3
	$L + 4H^+ = [LH_4]^{4+}$	33.95 ± 0.01	β_4
	$L + 5H^+ = [LH_5]^{5+}$	36.87 ± 0.02	β_5
	$L + 6H^+ = [LH_6]^{6+}$	40.44 ± 0.01	β_6
Cu	$L + 2Cu^{2+} = [LM_2]^{2+}$	25.24 ± 0.03	β_{LM2}
	$L + 2Cu^{2+} + OH^- = [LM_2OH]^{3+}$	16.96 ± 0.02	β_{LM2OH}
	$L + 2Cu^{2+} + 2OH^- = [LM_2(OH)_2]^{2+}$	8.13 ± 0.06	$\beta_{LM2(OH)2}$
	$L + Cu^{2+} + 2H = [LMH_2]^{4+}$	29.75 ± 0.05	β_{LM2H2}

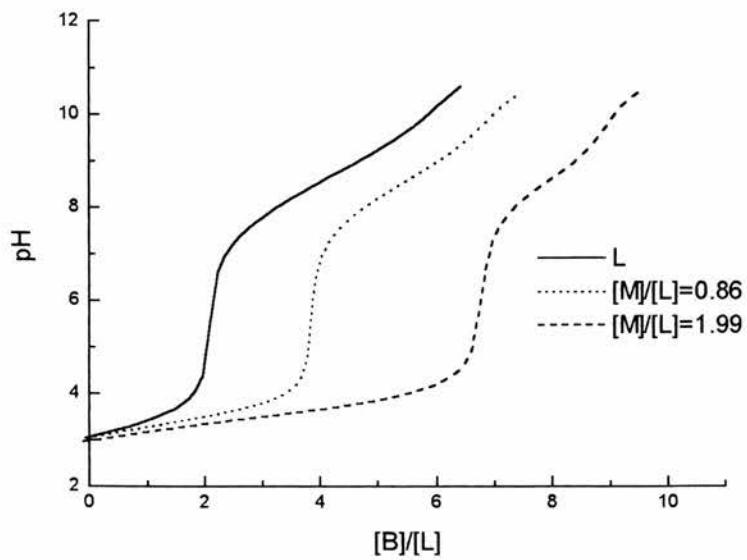

Figure 2. Titration curves for PEA. PEA in the presence of one equivalent of copper(II) and two equivalents of copper(II).

The titration curves and speciation plots are shown in Figures 1, 2 and 3 respectively. As for the similar ligand studied by Martell *et al*[12] the weakly basic nitrogens may be assigned to the central amino groups. Coulombic repulsion from the two adjacent protonated nitrogens favours the deprotonation of the central nitrogen.

NMR Measurements

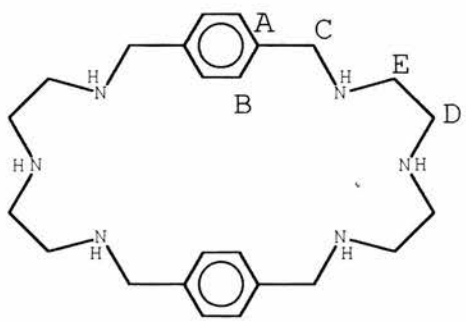

Figure 3. ^{13}C NMR Resonance assignments.

Measurements of the chemical shift of the ^{13}C resonances over the pH range 2.5 to 11 shows the greatest movement for the signals of the carbons adjacent to the central amino groups at low pH. At progressively higher pH the benzyl carbons shift.

Plots of the ^{13}C resonances versus pH are shown in Figure 4. The resonances are assigned on the basis of shifts observed in similar compounds (N-benzylmethylamine[13] and dimethylethylenediamine[14]). Interestingly the aromatic carbon resonances (Figure 5) also show considerable movement over the pH range studied, with a plateau coincident with the first inflexion point found in the titration curve. This observation indicates little conformational change on removal of the second proton and a steady change on the removal of subsequent protons.

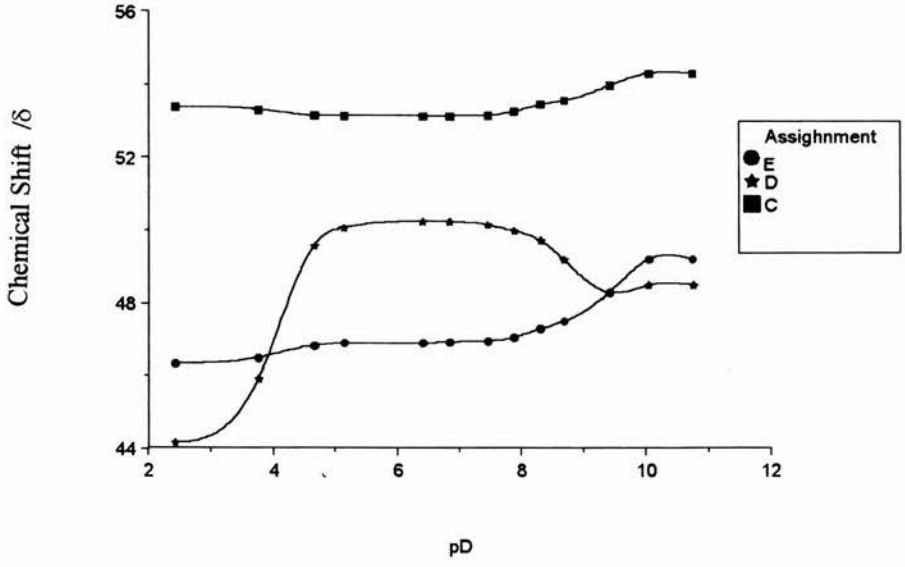

Figure 4 Variation of ^{13}C NMR chemical shifts of the alkyl resonances with pH.

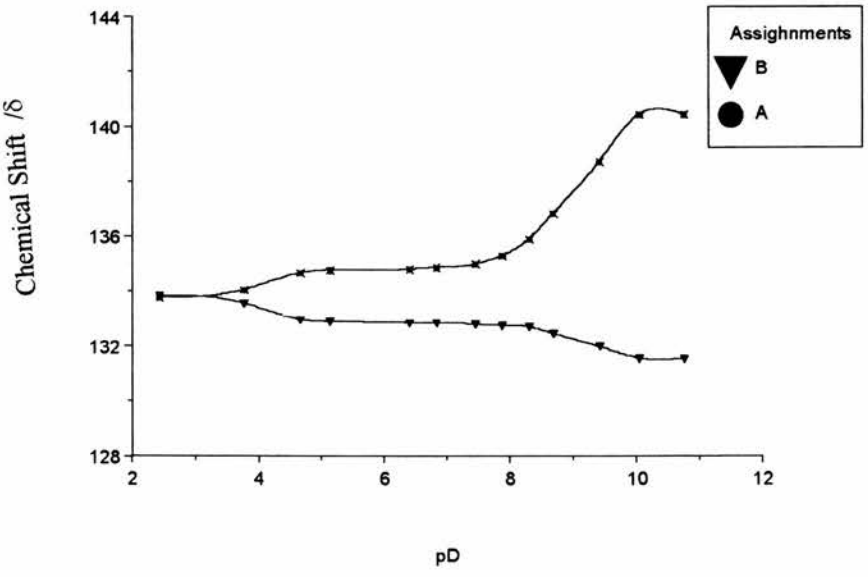

Figure 5. Variation of ^{13}C NMR chemical shifts of the aromatic resonances with pH.

Protonated species of the ligand 4,7,16,19,22-hexaaza[9.9]paracyclophane (PEA).

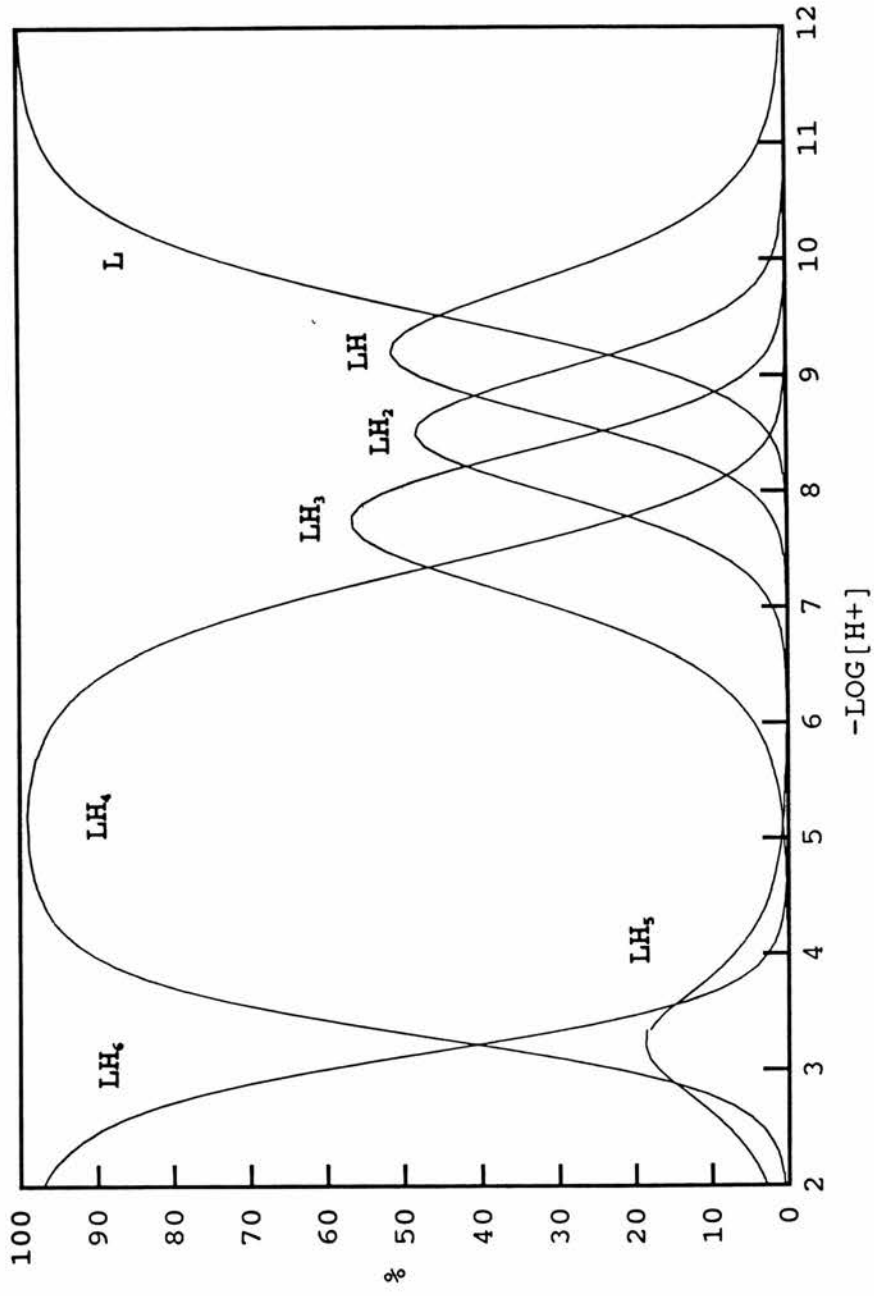

Titration in the presence of copper indicated the formation of binuclear complexes and the formation of hydroxo complexes at higher pH. The pKa's of the coordinated water molecules can be derived from the log β values quoted in Table 4:

$[Cu_2(PEA)(OH_2)_2]^{4+} + OH^- = [Cu_2(PEA)\ (OH_2)(OH)]^{3+} + H_2O$ $\log K_1 = 8.28 \pm 0.04$

$[Cu_2PEA(OH)_2(OH)]^{3+} + OH^- = [Cu_2PEA(OH)_2]^{2+} + H_2O$ $\log K_2 = 8.83 \pm 0.06$

Although previous potentiometric studies of similar binucleating ligands have demonstrated significant amounts of mononuclear species, PEA appears to form exclusively binuclear complexes. The initial model for SUPERQUAD included a number of hydroxo and protonated mononuclear complexes. The first minimisation at 1:1 Cu/ligand ratios gave reasonably low error values. However, the introduction of the stability constants of the binuclear complexes resulted in the rejection of the hydroxo and neutral species. The mononuclear species left (protonated copper complexes) had poor standard deviation and their presence did not significantly decrease sigma. Apart from the minor complex, 1 1 2 these were removed from the model and the final calculated equilibrium constants derived for the equilibria shown in table 1.

The system was also studied spectrophotometrically to check the results obtained by potentiometry.

Speciation curves of the complexes of 4,7,16,19,22-hexaaza[9.9]paracyclophane (PEA) in the presence of one equivalent of copper(II).

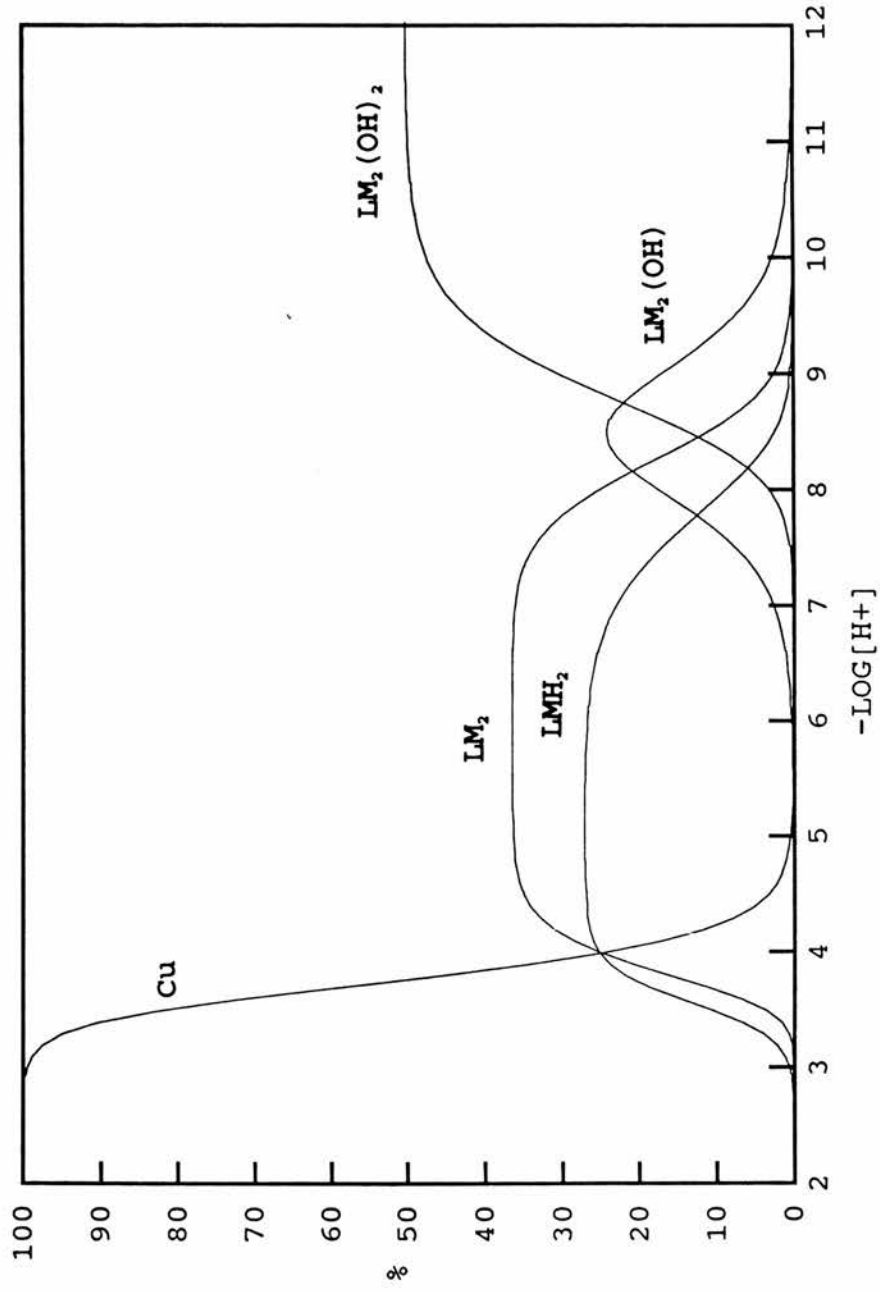

Speciation curves of the complexes of 4,7,16,19,22-hexaaza[9.9]paracyclophane (PEA) in the presence of two equivalents of copper(II).

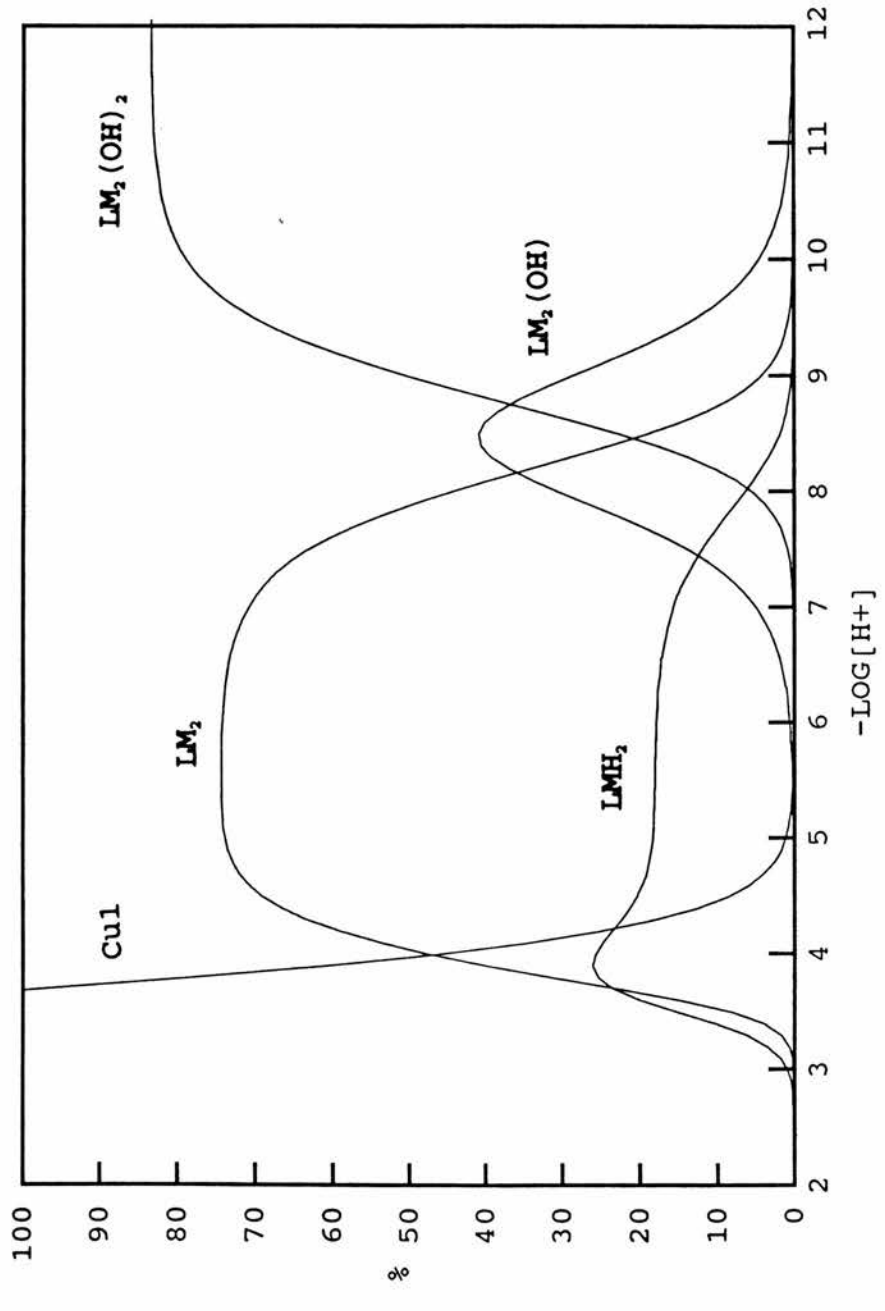

Spectrophotometric titration of PEA

Table 5 Cu(II) Stability Constants of 4,7,16,19,22-hexaaza[9.9]paracyclophane (PEA) determined spectrophotometrically.

Ion	Reaction	Log β	symbol
Cu	$L + 2Cu^{2+} = [LM_2]^{2+}$	25.27 ± 0.04	β_{LM2}
	$L + 2Cu^{2+} + OH^- = [LM_2OH]^{3+}$	19.11 ± 0.10	β_{LM2OH}
	$L + 2Cu^{2+} + OH^- = [LM_2(OH)_2]^{2+}$	8.77 ± 0.12	$\beta_{LM2(OH)2}$
	$L + Cu^{2+} + 2H^+ = [LMH_2]^{4+}$	29.37 ± 0.13	β_{LM2H2}

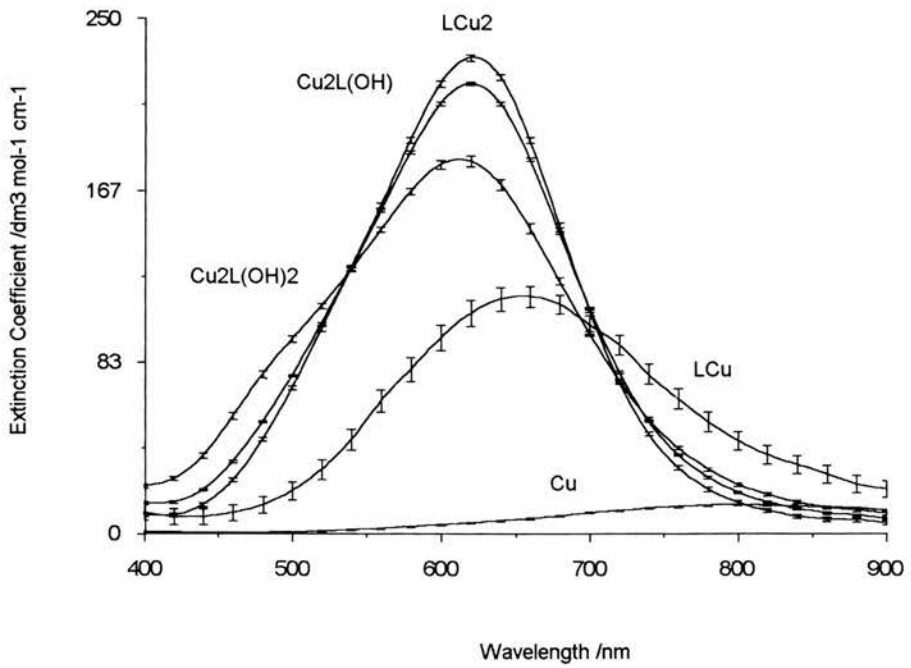

Figure 6 Calculated visible spectra of the species $LCuH_2$, LCu_2, $LCu_2(OH)$, and $LCu_2(OH)_2$

The species model for the copper PEA system determined spectrophotometrically compares exceedingly well with the potentiometric method and confirms the hypothesis that the introduction of a rigid spacer increases the tendency of this molecule to form binuclear complexes. Similar arguments, to those used to account for the instability of mononuclear

complexes, of MPA and PPA can be applied to PEA. The presence of a "free" and coordinated site in the molecule makes the coordinated site more strained, resulting in the destabilisation of the mononuclear complex. When a binuclear complex is formed a lower energy conformation is produced, resulting in extra stabilisation of the binuclear complex. Large macrocycles with greater flexability are able to form more stable mononuclear complexes by the similtaneous coordination of both donor sets to a single metal centre (OBISDIEN for example).

The calculation of absorption coefficients for the species found in solution by HYPERQUAD shows that the absorption coefficients of the mononuclear species, *per copper centre*, is nearly the same as that of the dinuclear species suggesting that the coordination geometry of both metal centres is the same. The magnitude suggests five coordinate geometry. The hydroxo complexes are blue shifted as one might as OH^- exerts a stronger ligand field than H_2O

DNPDEP hydrolysis kinetics.- The pseudo first order rate constants for the hydrolysis of DEPDNP are shown in Table 6 and illustrated in Figure 7. The low activity of the copper complex is consistent with the view that the active species is an hydroxo complex. The pH-rate profile is sigmoidal and is consistent with a pK=8.8 for the catalytically active complex. This figure is very similar to that observed for the ionisation $[Cu_2(PEA)(OH)(OH_2)]^{3+}$ = $[Cu_2(PEA)(OH)(OH)]^{2+} + H^+$ (pK=8.83). Possible mechanisms are shown in (I) and (II). Mechanism (II) appears unlikely due to the large Cu-Cu separation.

Table 6. pH dependence of the hydrolysis of DEPDNP

pH	$k_{obs}/10^5\ s^{-1}$
2.71	2.37
3.24	0.64
4.24	0.71
5.57	0.78
6.52	2.5
7.49	3.5
8.44	19.1
9.53	45.8
10.62	54.0

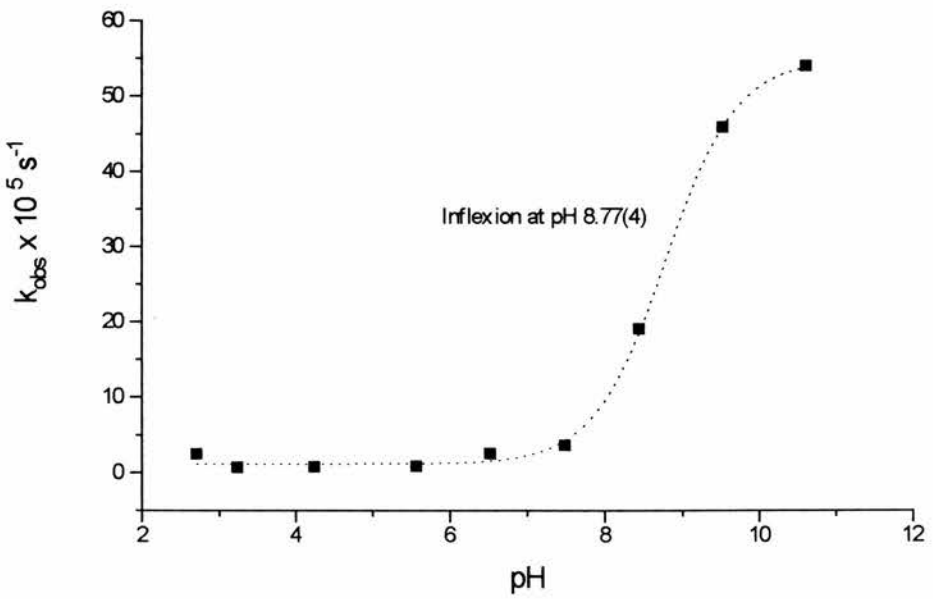

Figure 8 The pH-rate profile for the $[Cu_2(PEA)]^{2+}$ catalysed hydrolysis of 2,4-dinitrophenyl diethyl phosphate.

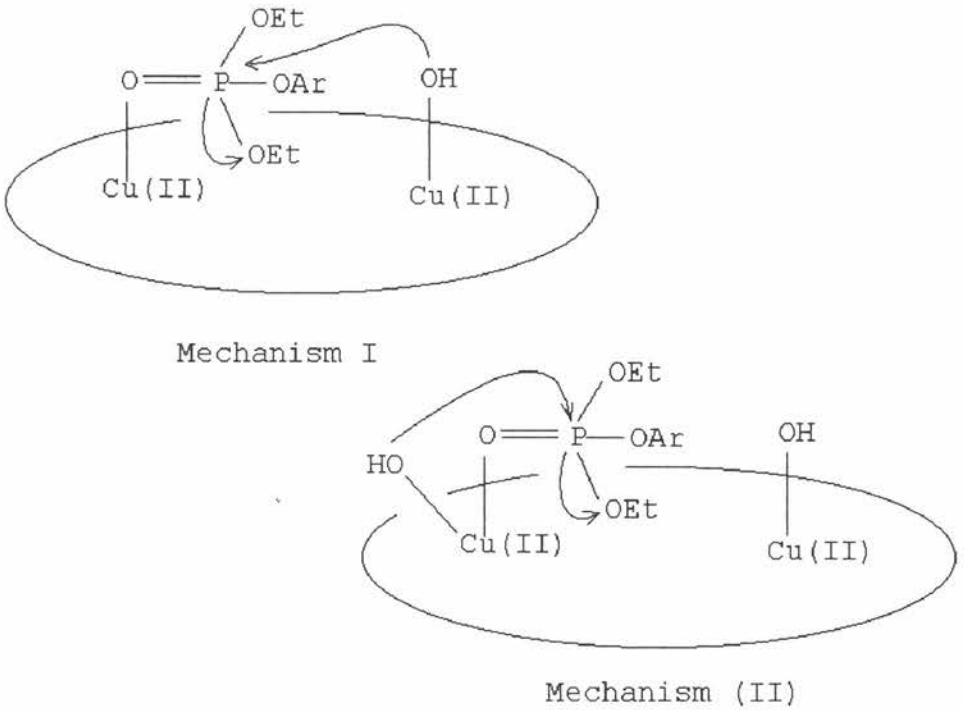
OEt
O
P
OAr
OH
OEt
Cu(II)
Cu(II)
Mechanism I
OEt
O
P
OAr
OH
HO
OEt
Cu(II)
Cu(II)
Mechanism (II)

Figure 9

References

[1]C.Bazzicalupi, A.Bencini, A.Bianchi, V.Fusi, C.Giorgi, P.Paoletti, A.Stefani and B.Valtancoli, *Inorg.Chem.*, 1995, **34**, 552.

[2]*SIR92:* A.Altomare, M.C.Burla, M.Camalli, M.Cascarano, C.Giacovazzo, A.Guagliardi and G.Polidori, 1994, *J.Appl.Cryst.*, in preparation.

[3]DIRDIF94: P.T.Beurskens, G.Admiraal, G.Beurskens, W.P.Bosman, R. de Gelder, R.Israel and J.M.M.Smits, 1994. *The DIRDIF-94 program system,* Technical Report of the Crystallography Laboratory, University of Nijmegen, The Netherlands.

[4]Least-Squares:

Function minimised: $\Sigma w(\frac{1}{2}Fo\frac{1}{2}-\frac{1}{2}Fc\frac{1}{2})^2$ where $w = 1/s^2(Fo) = 4Fo^2/s^2(Fo^2)$

$s^2(Fo^2) = S^2(C+R^2B)+(pFo^2)^2/Lp^2$

S = Scan speed

C = Total integrated peak count

R = Ratio of scan time to background counting time

B = Total background count

Lp = Lorentz-polarization factor

p = p-factor

[5]Standard deviation of an observation of unit weight:

$$\sqrt{\sum w\left(|Fo|-|Fc|\right)^2 / (No-Nv)}$$

where: No = number of observations

Nv = number of variables

[6]*Crystal Structure Analysis Package,* Molecular Structure Corporation (1985& 1992)

[7] M.Pietraskiewics and R.Gasiorowski, *Chem.Ber.,* 1990, **123**, 405.

[8] W.Eschweiler, *Chem.Ber.*, 1905, **38**, 880.

[9]C.J.McKenzie, H.Toftlund, M.Pietraszkiewics, Zb.Stojec and K.Slowinski, *Inorg.Chim.Acta.*, 1993, **210**, 143.

[10] M.Sneed and J.Maynard, *General Inorganic Chemistry,* Van Nostrand, New York, 1942, 813

[11] J.F.Coetzee and G.P.Cunningham, *J.Am.Chem.Soc.* 1969, **91**, 568.

[12] R.Menif, A.E.Martell, P.J.Squattrito and A.Clearfield, *Inorg.Chem.*, 1990, **29**, 4723.

[13] PhCH_2 56.1, methyl 35.9, quaternary aromatic 141.1 and other aromatic 126.7 and 128.2 d, LeRoy F.Johnson and W.C.Janokowski, *13C NMR Spectra* (pub J.Wiley & Sons)

[14] Aldrich NMR database

Synthesis of the 24-Membered Binucleating Hexaaza Macrocycle (1,4,7,16,19,22-hexaaza[9.9]metacyclophane (MEA) and The Characterisation of its Copper(II), Nickel(II), Cobalt(II) and Zinc(II) Complexes, and the Copper(II) Complex Promoted Hydrolysis of the Phosphotriester 2,4-Dinitrophenyl diethylphosphate.

Abstract

A variety of transition metal complexes of the 22-membered hexaazamacrocycle, 1,4,7,16,19,22-hexaaza[9.9]metacyclophane (MEA) have been prepared and characterised. The crystal structure of the binuclear copper (II) complex shows that it exists in two forms. One form (type I) with an inversion centre, has both copper atoms in essentially square pyramidal stereochemistry with an N_3Cl_2 donor set and a Cu-Cu distance of 5.82Å. The other form (type II) has one square pyramidal copper (N_3Cl_2 donor set) and one square planar copper with an N_3Cl donor set. The Type II Cu-Cu distance is 6.13Å The structure is best described as $[Cu_2(MEA)Cl_4]_{0.5}[Cu_2(MEA)Cl_3]ClO_4.0.67DMF$. The copper(II) complex catalyses the hydrolysis of the phosphotriester 2,4-dinitrophenyl diethyl phosphate. The complex is moderately active in catalysing the hydrolysis of the ester to give diethyl phosphate and the mechanism of the reaction is discussed.

Experimental

Measurements.-Infrared spectra were recorded on a Perkin Elmer 1710 Infrared Fourier Transform Spectrometer as KBr pellets. Melting points were obtained using a Gallenkamp melting point apparatus. U.V./Visible spectra were recorded on a Lambda 14P Spectrometer.

Materials.-Potassium chloride, 1,5-diamino-3-azapentane (dien), copper(II) salts, and sodium borohydride were obtained from Aldrich and used without further purification. Isophthalaldehyde was obtained from Avocado.

Synthesis.-The ligand was prepared by a nontemplate [2+2] condensation of 1,5-diamino-3-azapentane with isophthalaldehyde to give a macrocyclic tetramine which was then reduced with

sodium borohydride[1]. Purification was achieved by recrystallization (three times) of the HBr salt from aqueous methanol.

HBr Salt (Found: C, 29.57; H, 3.67; N, 8.35; Br, 48.83 Calcd. for $C_{24}H_{38}N_6.6HBr.5H_2O$: C, 29.23; H, 65.52; N, 8.52; Br, 48.62).

(d) $[Cu_2(MEA)Cl_4](Cu_2Cl_4)_{0.33}(EtOH)_{0.167}$. Copper(II)chloride dihydrate (0.993g, 4.82mmol) was dissolved in ethanol (20cm^3) and added dropwise to a boiling ethanol solution (20cm^3) of MEA (1.20g, 2.93mmol). When half of the copper(II) chloride has been added to the rapidly stirred amine solution, a fine blue green precipitate began to form. The complex was filtered off, washed with ethanol (3x10cm^3) then diethylether (1x10cm^3) and dried *in vacuo* at 50°C. (1.70g, 75%). (Found: C, 37.49; H, 5.07; N, 10.78. Calcd. for $C_{24}H_{38}N_6Cu_2.(Cu_2Cl_4)_{1/3}.(EtOH)_{1/6}$: C, 37.60; H, 5.06; N, 10.81); i.r. (KBr) cm^{-1}: 3434s (O-H ν), 3186s (N-H ν); 2944, 2875s (C-H ν); 1614m (aromatic ν); 1448 (C-N ν); 1050s, 968m; 857m, 784m (Ar-H δ oop); 741m, 706m, 669w. λ_{max}/nm (ε_{max}/dm^{3}mol^{-1}cm^{-1}) 692 (304), 437 (116) DMF; Λ_M/ S cm^{2}mol^{-1} 46 (DMF).

(e) $[Zn(MEA)Cl_2]2H_2O$. Anhydrous zinc(II) chloride (0.857g, 6.29 mmol) was dissolved in ethanol (20cm^3) and added dropwise to a boiling ethanolic solution of the ligand (1.29g, 3.14 mmol). A flocculant white precipitate formed immediately, but dissolved when half of the ligand had been added. On complete addition of ligand, the solution became cloudy and a white solid separated on cooling. The complex was filtered off, washed with ethanol (3x10cm^3) then ether (1x10cm^3) and dried *in vacuo* for 24h at 50°C (yield 1.65, 73%). (Found: C, 40.15; H, 5.43; N, 11.16. Calcd. for $C_{24}H_{38}N_6ZnCl_2.2H_2O$: C, 40.08; H, 5.89; N, 11.68.); i.r. (KBr): 3475s (O-H ν); 3217s (N-H ν.); 2936, 2875s (C-H ν.); 1615s (Aromatic ν); 1450, 1342, 1162 (C-N ν); 1079s, 1044s, 1001s, 883vw, 852w, 799m (ArH δ oop); 753m, 704m. Λ_M/ S cm^{2}mol^{-1} 30 (DMF).

(f) $[Ni_2(MEA)Cl_4].(NiCl_2)_{1/6}.H_2O$. Nickel chloride hexahydrate (1.23g, 5.17mmol) was dissolved in ethanol (20cm^3) and added dropwise to a refluxing ethanol solution (30cm^3) of MEA (1.07g, 2.44mmol) over a 10 min period. A pale green precipitate formed during the addition. The precipitate was collected by filtration from the cooled solution and washed with ethanol (2x10cm^3) and dried *in vacuo* 24h, 50°C (yield 1.35g, 73%). (Found: C, 40.47; H, 5.69; N, 11.49. Calcd. for $C_{24}H_{44}N_6O_2Ni_2Cl_4$: C, 40.64; H, 5.68; N, 11.84); i.r. (KBr): 3434-3194 (O-H

and N-H ν); 2951, 2936, 2878 s (C-H ν), 1637s (aromatic ν and O-H δ); 1458, (C-N ν); 1045w, 976s, 791w, 743m (Ar-H δ oop); 706 w. λ_{max}/nm (ε_{max}/dm^{3}mol^{-1}cm^{-1}) 390 (33), 628 (20), DMF; Λ_M/ S cm^{2}mol^{-1} 67 (DMF);

(g) $[Co_2(MEA)Cl_2].(CoCl_4)_{0.25}(Cl)_{1.5}$. Anhydrous cobalt(II) chloride (0.646g, 4.98mmol) was dissolved in ethanol (20cm^3) and added dropwise to a boiling solution of the ligand (1.02g, 2.49mmol), in ethanol (20cm^3) under argon. A blue precipitate formed and was filtered off and washed with ethanol (3x10cm^3) then ether (1x10cm^3). The complex was dried *in vacuo* for 24h at 50°C. (yield 1.308g, 75%). (Found: C, 41.45; H, 5.41; N, 11.84. Calcd. for $C_{24}H_{38}N_6Co_2Cl_2.(CoCl_4)_{0.25}(Cl)_{1.5}$: C, 41.02; H, 5.45; N, 11.96); i.r.(KBr): 3399s (O-H ν); 3235 (N-H ν); 2922, 2873s (C-H ν); 1616 (aromatic ν), 1440s, 1340m (C-N ν); 1078m, 1003, 947w, 942s, 887w, 850w, 801w (Ar-H δ oop), 750m, 698m. λ_{max}/nm (ε_{max}/dm^{3}mol^{-1}cm^{-1}) 524(112), 609(122), 661 (143), 802 (18) DMF; Λ_M/ S cm^{2}mol^{-1} 3.4 (DMF).

Crystal structure of $[Cu_2(MEA)Cl_4]_{0.5}[Cu_2(MEA)Cl_3]ClO_4.2/3DMF$.- Crystals suitable for X-ray diffraction were grown by the diffusion of diethyl ether into a DMF solution of the chloro complex, containing added sodium perchlorate. Small dark blue blocks were obtained. The diffraction measurements were carried out at low temperature (120K).

Crystal Data. $C_{39}H_{62.5}N_{10}Cu_3Cl_6O_5$, M = 770.22, Primitive monoclinic, a = 10.504(4), b = 38.68(2), c = 12.962(6) Å, U = 4937(3) Å^3 (by least-squares refinement on diffractometer angles for 25 automatically centred reflections, in the range 20<2θ<25° λ = 0.71069 Å), space group $P2_1/c$(#14), Z = 4, D_c = 1.554 g cm^{-3}, F(000) = 2383.98. Blue block crystal. Approximate crystal dimensions 0.30 x 0.20 x 0.15 mm, μ(Mo-K$_\alpha$) = 16.57 cm^{-1}.

Data Collection and Processing. Rigaku AFC7S diffractometer, ω-2θ scan type with ω scan width = (0.79 + 0.35 tan θ)°, ω scan speed 16.00° min-1 (up to 4 scans), graphite monochromated MoKα radiation; 8688 reflections measured (max 2θ = 45.1°), 6275 unique (R_{int} = 0.045). No decay correction was required. Correction for absorption (trans. factors: 0.7596 - 1.0000) were required. Corrections were made for Lorentz and polarisation effects.

Structure Analysis and Refinement. Direct methods[2] and were expanded using Fourier techniques[3]. Some non-hydrogen atoms were refined anisotropically, while the rest were refined isotropically. Hydrogen's were included but not refined. The final cycle of full-matrix least-squares refinement[4] was based on 4241 observed reflections ($I>3.00\sigma(I)$) and 568 variable parameters and converged (largest parameter shift was 0.04 times its esd) with unweighted agreement factors of:

$$R = \sum \| Fo| - |Fc| \| / \sum |Fo| = 0.048$$

$$R_w = \sqrt{\left(\sum \left(|Fo| - |Fc| \right)^2 / \sum wFo^2 \right)} = 0.055$$

The standard deviation of an observation of unit weight[5] was 3.03. The weighting scheme was based on counting statistics and included a factor (p = 0.027) to downweight the intense reflections. Plots of $w(\Sigma |Fo| - |Fc|)^2$ versus $|Fo|$, reflection order in data collection, sin θ/λ and various classes of indices showed no unusual trends. The maximum and minimum peaks on the final difference Fourier map correspond to 0.68 and -0.49 $e^-Å^{-3}$, respectively. All calculations were performed using the TEXSAN[6] crystallographic software package of Molecular Structure Corporation.

Catalytic Activity. - The hydrolysis of the phosphotriester 2,4-dinitrophenyl diethyl phosphate (DNPDEP) (obtained from CBDE, Porton Down) was studied spectrophotometrically at 360nm. Solutions of various pH's were prepared by the adjustment of a 4.65×10^{-3} mol dm^3 solution with respect to Cu(II) which contained 2.52×10^{-3} mol dm^{-3} MEA and 0.1 mol dm^{-3} KCl to the required pH with either NaOH or HCl. The reaction was initiated by the addition of 2µl of an acetonitrile stock solution of DNPDEP to a $2cm^3$ sample of the solution in a 1 cm cuvette. The final DNPDEP concentration was 2×10^{-4} mol dm^{-3}. For slow reactions (below pH 7) data were collected over one half-life only, and the infinity value obtained after two weeks at room temperature. Above pH 7 data could be collected for up to three half-lives. The absorbance versus time curves were fitted to the first order rate equation using a linear least squares method, (the quoted rates constants are the average of two runs). Duplicate runs showed that the rate constants could be replicated to within 5%.

Results and Discussion

Synthesis.- The macrocycle did not form a solid which could be readily recrystallized so purification was effected by the recrystallization of the hydrobromide salt. The free base was prepared by addition of KOH to the HBr salt followed by extraction into dichloromethane. The free base was used for the preparation of the complexes.

Micro-analytical data did not fit for simple binuclear chlorido complexes. The percentage of C H and N was consistently lower than expected. A similar problem was encountered with the metacyclophane ligand (MPA) studied previously. Chloride analysis indicated greater than expected percentage for some of the complexes which could be explained by the presence of bridging metalchloro clusters or the presence of tetrachlorometalate anions present in the product. In view of the large size of the cation it is not surprising that large anions are required to stabilise the structure.

The low absorption coefficients for the nickel complex in DMF suggests a pseudo octahedral environments for the two nickel centres. Only two of the $^3A_2$ -> $^3T_2$, $^3A_2$ -> $^3T_1$ and $^3A_2$ -> $^3T_1$, bands are observed over the wavelength range studied. The low intensity for the cobalt complex rules out tetrahedral geometry (*ca.* 50 dm^3 mol^{-1} cm^{-1} per metal centre) but fits well for trigonal bipyramidal geometry (*c.f.* $Co(Et_4dien)Cl_2$ which exhibits three bands between[7] 950 and 520nm (ε in the 20 to 100 dm^3 mol^{-1} cm^{-1} range). The low conductivity observed for the complex also suggests that two chlorides are bound to each cobalt. The copper(II) chloride complex is green in the solid state and in DMF solution due to a broad band above 500nm and a band at 437 with strong absorption below 420nm. This latter band is not present in the chloro perchlorate derivative and disappears on addition of water to the DMF solution of the chloride complex. It is probably due to ligand to copper charge transfer in a metal chloride cluster.

Description of the crystal structure of $[Cu_2(MEA)Cl_4]_{0.5}[Cu_2(MEA)Cl_3]ClO_4.2/3DMF$

The crystal structure shows the presence of two different binuclear copper complexes. Two thirds of the complex has the type I structure and one third forms the type II structure (see the ORTEP diagram). The two structures will be discussed separately.

Figure 1. ORTEP diagram showing two structural forms of the dicopper complex of 1,4,7,16,19,22-hexaaza[9.9]metacyclophane

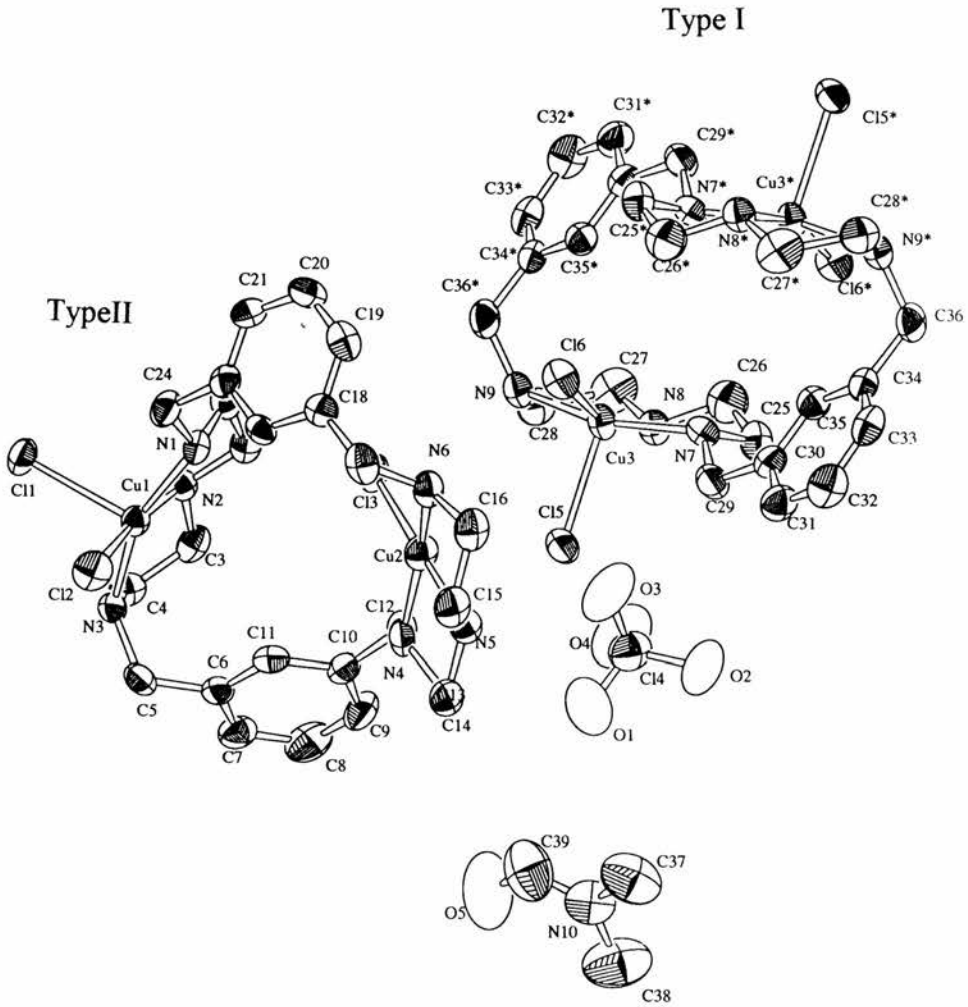

Type I. The complex lies on a crystallographic centre of inversion (at 1, 0, 1/2) and displays *Ci* symmetry. The bond lengths and angles of half of this molecule relate to the other half by virtue of this centre of symmetry. The copper centres may best be described as square pyramidal, three nitrogens from the macrocycle and one of the chlorides make up the base of the pyramid with the copper somewhat displaced above the plane towards the apical chloride (as is commonly found with square pyramidal complexes). The apical chloride is directed away from the macrocycle cavity to form a long bond with a copper centre in the type II structure. The copper nitrogen distances are not unusual (the mean distance found for five co-ordinate secondary amine complexes in the Daresbury database is 2.029Å). The copper to chloride distance is normal for the basal chloride, but the apical chloride to copper distance is a little longer than expected, and may be due to a small degree of electron withdrawal from the bond to form a bridge to the type II structure. The Cu-Cu distance is 5.82 Å.

Type II. Like the Type I structure one of the copper centres is square pyramidal but the other copper is best described as square planar or Jahn Teller distorted square pyramidal (the apical chloride belonging to the apical chloride of the type I structure). The bond distances are close to those for the Type I, apart from the rather shorter bond distances for the Jahn Teller distorted copper centre. The planar character of this copper is reflected in the donor-copper-donor angle close to the ideal 90 or 180° required for a this geometry. The Cu-Cu distance for type II is 6.13 Å.

Unfortunately both structures show the chloride ligands to be directed away from each other. The MPA system does not provide sites on the same face for the attachment of nucleophiles and substrates and thus the complex may not be a good catalyst as a result. The Cu-Cu distances are also rather long for an interaction between hydroxide on one copper and the substrate on the other.

The structure also includes two thirds of a DMF to each macrocyclic complex and one half of a perchlorate (balancing the four co-ordinate copper in Type II) to each complex. The DMF is not hydrogen bonded to any of the components of the structure and bond lengths and angles are quite normal.

Table 1. Assorted bond lengths(/Å), angles(°) and Cu...Cu separation for Type I MEA complex

Cu(3)-Cl(6)	2.287(2)	Cl(6)-Cu(3)-Cl(5)	102.95(8)
Cu(3)-Cl(5)	2.491(2)	N(7)-Cu(3)-Cl(6)	90.6(2)
Cu(3)-N(8)	2.031(6)	N(8)-Cu(3)-Cl(5)	96.1(2)
Cu(3)-N(7)	2.043(6)	N(8)-Cu(3)-Cl(6)	160.8(2)
Cu(3)-N(9)	2.045(6)	N(9)-Cu(3)-Cl(6)	97.0(2)
Cu(3)...Cu(3)*	5.82	N(7)-Cu(3)-N(8)	83.3(2)
		N(8)-Cu(3)-N(9)	84.1(2)
		N(7)-Cu(3)-N(9)	162.0(2)

Table 2. Assorted bond lengths, angles and Cu...Cu separation for Type II MEA complex

Cu(1)-N(1)	2.033(6)	N(1)-Cu(1)-N(2)	83.8(2)
Cu(1)-N(2)	2.015(6)	N(1)-Cu(1)-N(3)	158.1(2)
Cu(1)-N(3)	2.040(6)	N(4)-Cu(2)-N(5)	83.7(3)
Cu(1)-Cl(1)	2.543(2)	N(6)-Cu(2)-N(4)	161.9(2)
Cu(1)-Cl(2)	2.256(2)	N(6)-Cu(2)-N(5)	83.7(3)
Cu(2)-N(4)	2.063(6)	N(1)-Cu(1)-Cl(1)	105.0(2)
Cu(2)-N(6)	2.093(6)	N(1)-Cu(1)-Cl(2)	96.5(2)
Cu(2)-Cl(3)	2.257(2)	N(2)-Cu(1)-Cl(1)	88.0(2)
Cu(2)-Cl(5)	2.845(2)	N(6)-Cu(2)-Cl(3)	98.6(2)
Cu(1)....Cu(2)	6.13	Cl(1)-Cu(1)-Cl(2)	96.5(2)

Hydrolysis of 2,4-dinitrophenyl diethyl phosphate (DNPDEP).- The observed first order rate constants for the hydrolysis of DNPDEP are shown in Table 3 and illustrated in Figure 2. The pH-rate profile is similar to that of the paracyclophane analogue, PEA. The pH-rate profile is sigmoidal indicating a catalytically active complex with a pK of ca 9.0 This would correspond to the formation of $[CuMEA(OH)_2]^{2+}$. The monohydroxo complex is also probably active. Since the

crystal structure indicates that the two metal centres are not correctly aligned for attack of coordinated hydroxide on one copper on the substrate bound to the other, it seems probable that the substrate and the attacking OH^- are bound to the same copper centre.

Table 3. pH dependence of the hydrolysis of DNPDEP

pH	$k_{obs}/10^5\ s^{-1}$
5.05	1.88 ± 0.2
5.52	2.54 ± 0.45
6.01	2.20 ± 0.08
6.52	1.85 ± 0.3
7.00	2.15 ± 0.08
7.50	2.54 ± 0.05
8.00	6.29 ± 0.4
8.50	8.50 ± 0.9
9.00	12.2 ± 0.9
9.48	23.6 ± 0.8
10.06	24.3 ± 1.4
10.50	26.8 ± 3.0

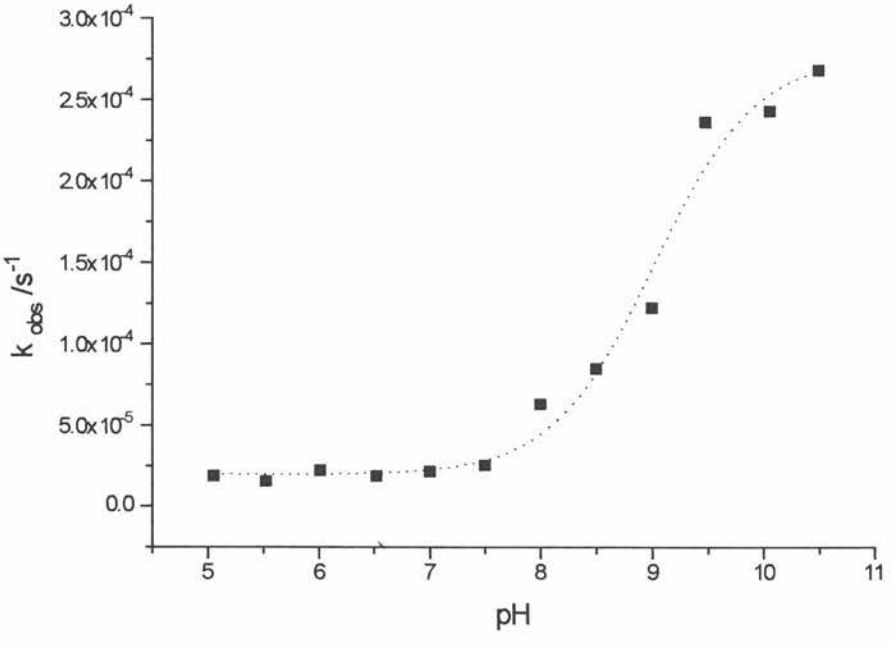
3.0x10-4
2.5x10-4
2.0x10-4
1.5x10-4
1.0x10-4
5.0x10-5
0.0
k obs /s-1
5
6
7
8
9
10
11
pH

Figure 2

Speciation curves for the complexes of MEA in the presence of two equivalents of copper(II). Data taken from Martell's work[8].

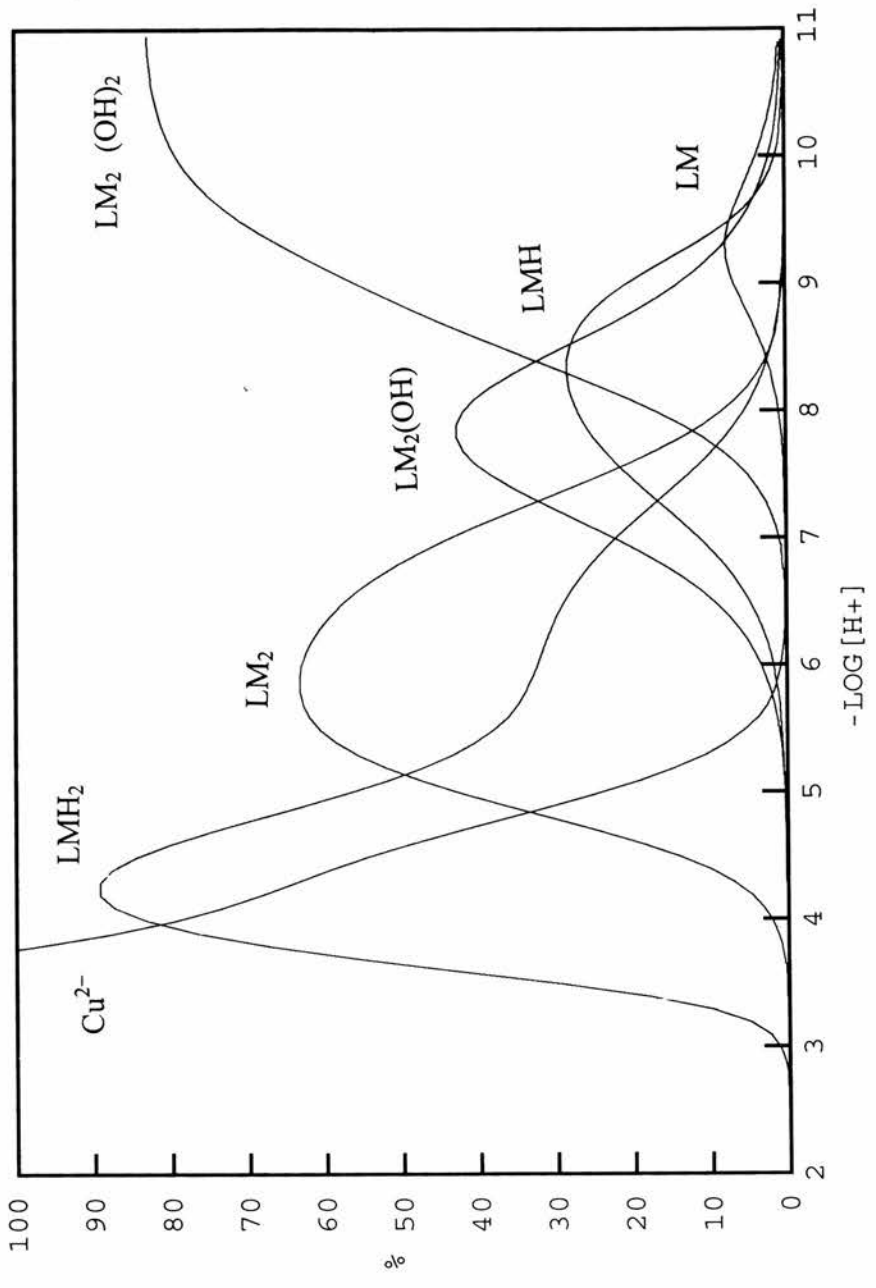

References

[1] R.Menif and A.E.Martell, *J.Chem.Soc.,Chem.Commun.*, (1989), 1522.

[2] *SIR92:* A.Altomare, M.C.Burla, M.Camalli, M.Cascarano, C.Giacovazzo, A.Guagliardi and G.Polidori, (1994), *J.Appl.Cryst.*, in preparation.

[3] DIRDIF94: P.T.Beurskens, G.Admiraal, G.Beurskens, W.P.Bosman, R. de Gelder, R.Israel and J.M.M.Smits **(1994)**. *The DIRDIF-94 program system,* Technical Report of the Crystallography Laboratory, University of Nijmegen, The Netherlands.

[4] Least-Squares:

Function minimised: $Sw(½Fo½-½Fc½)^2$ where $w = 1/s^2(Fo) = 4Fo^2/s^2(Fo^2)$

$s^2(Fo^2) = S^2(C+R^2B)+(pFo^2)^2/Lp^2$

S = Scan speed

C = Total integrated peak count

R = Ratio of scan time to background counting time

B = Total background count

Lp = Lorentz-polarization factor

p = p-factor

[5] Standard deviation of an observation of unit weight:

$$\sqrt{\sum w\left(|Fo| - |Fc|\right)^2 / (No - Nv)}$$

where: No = number of observations

Nv = number of variables

[6] *Crystal Structure Analysis Package,* Molecular Structure Corporation (1985& 1992)

[7] Z.Dori and H.B.Gray, *Inorg.Chem.*, (1968), **7**, 889.

[8] R.Menif, A.E.Martell, P.J.Squattrito and A.Clearfield, *Inorg.Chem.*, (1990), **29**, 4723.

Chapter 5

Computer Aided Ligand Design

The Rational Design of Novel Ligand Systems for Transition Metal Catalysed Hydrolysis of Phosphate Triesters. Bispidine Complexes, Copper(II) and Zinc(II) Complexes of N,N'-Dimethyl Bispidine (DMB) and the Crystal Structure of the Copper Complex [Cu(DMB)Cl_2] (Bispidine = 3,7-Diazacyclo[3.3.1]nonane)

Abstract

The ligand N,N'-dimethyl-3,7-diazabicyclo[3.3.1]nonane (DMB) has been prepared by a Mannich reaction of methylpiperidone with methylamine followed by a Wolff-Kishner reduction of the carbonyl function. Complexes with copper(II) and zinc(II) have been characterised and the crystal structure of [$CuLCl_2$]0.5MeOH determined. $C_{9.5}H_{20}N_2O_{0.5}Cl_2Cu$, tetragonal, space group I42d, a = 19.086(7), c = 7.157(6), Z = 8. The copper centre has tetrahedral stereochemistry with two nitrogen and two chloride donors, Cu-Cl = 2.47(1) and Cu-N = 1.987(3) Å. The ligand acts as a "proton sponge" forming very strong complexes with the hydrogen ion. As a result the mono complex with copper(II) decomposes quite readily in aqueous solution.

Introduction

The copper(II) complex $[Cu(tmen)(OH)(OH_2)]^+$ (1) (tmen = N,N'-tetramethyl ethylenediamine) is an excellent catalyst for the hydrolysis of phosphate esters and is particularly active in the hydrolysis of phosphate triesters[1-3]. The zinc complex of hydroxyethylethylenediamine [1], and the copper (II) complex of 2,2'-pyridylamine[2] (the imino nitrogen is non-coordinating), are also potent catalysts for the base hydrolysis of phosphate esters Figure 1.

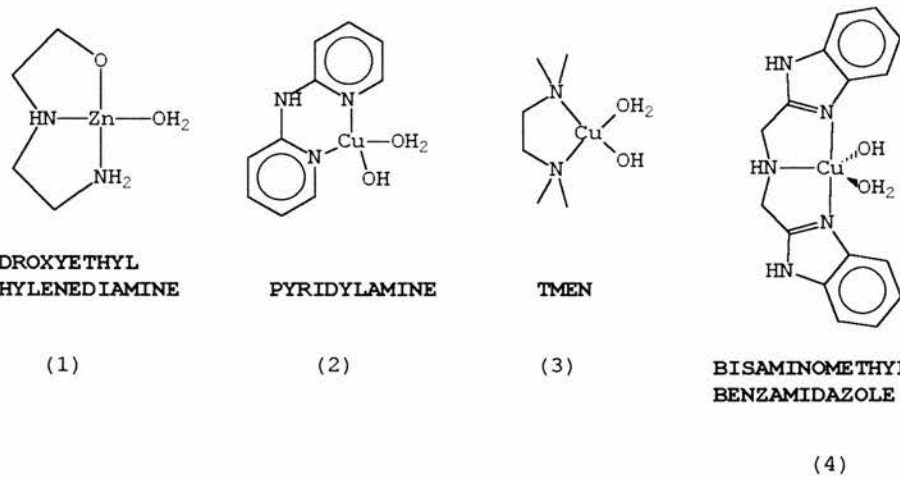

Figure 1

It has been proposed that these catalysts operate by the coordination of phosphate at a labile aquo site, followed by nucleophilic attack by a coordinated *cis*-hydroxide . Figure 2 shows

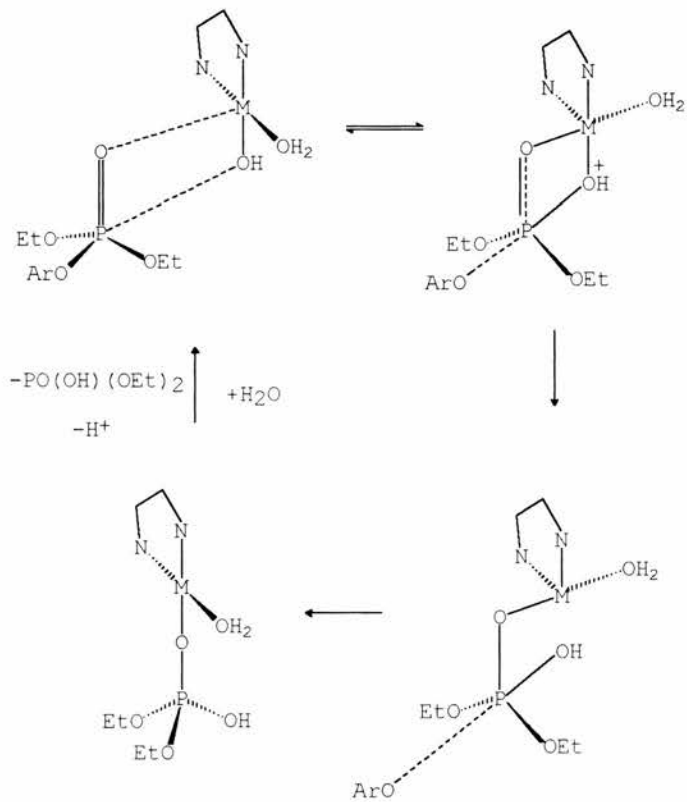

Figure 2

the possible series of events leading up to the hydrolysis of the ester.

Complex [3] was chosen by Menger because steric constraints of the tetra methylated ligand prevents the formation of *bis*-complexes with copper (II). Potentiometric titration studies, and kinetic investigations have shown that inhibition of the ester hydrolysis can still occur by formation of binuclear hydroxo complexes complexes.

Chin[1] has also used a ligand based on benzimidazole, Figure 1, [4] where the steric bulk has been increased. However, the copper complex is almost inactive as a catalyst for the hydrolysis of DNPDEP.

It would be desirable to have a more rational way to design new coordination catalysts. To this end we have used the molecular modelling package MM+ in HYPERCHEM (expanding Allingers parameter set to include coordination complexes). Our aim was to study potential catalysts on the computer, and synthesise the most promising ligand system of the set. Dimethylbispidine was found to be the most promising ligand, both from a synthetic and molecular mechanics point of view. The synthesis *via* a ketone may allow further functionalisation of the organic framework of the ligand (Figure 3).

Complexes of N,N'-dimethyl bispidine (2) (bispidine = diazabicyclo[3.3.1]nonane) are of interest and the present work describes the preparation of the ligand and the characterisation of its copper (II) and zinc(II) complexes. The acid of the copper(II) complex have also been studied and the activation parameters obtained.

Experimental

Synthesis.-The ligand was prepared essentially as previously reported[2]. A Mannich reaction of methylpiperidone and methylamine to form the bicyclic intermediate, followed by Wolff-Kischner reduction of the ketone to an alkane.

3,7-Dimethyl-3,7-diazabicyclo[3.3.1]non-9-one. Under argon, a mixture of 1-methylpiperidone (50g, 0.44mol), acetic acid (26.5g, 0.44mol) and methanol (220cm^3) were added dropwise into a 2 litre flask containing methylammonium chloride(29.9g, 0.44mol) and paraformaldehyde (26.54g, 0.92mol), suspended in refluxing methanol

(500cm^3). The dropwise addition continued over a three hour period and then the

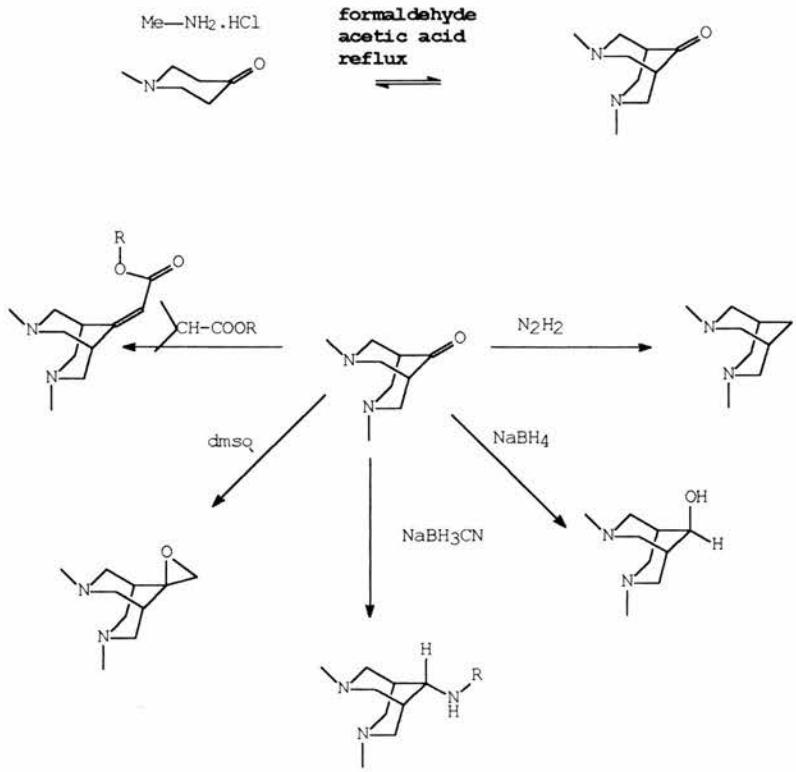

Figure 3

solution was refluxed for a further 3 hours after complete addition.

Most of the solvent was removed under reduced pressure to leave a viscous oil. The oil was basified (200g KOH in 150 cm^3 water) with cooling in an ice-water bath. The mixture was filtered and extracted with dichloromethane (4x70cm^3). The combined extracts were dried over $MgSO_4$, filtered and the solvent removed to give a colourless oil which solidified on standing (44.5g, 60%). (Found: C, 64.25; H, 10.40; N, 16.81. Calc. for $C_9H_{16}N_2O$: C, 64.25; H, 9.59; N, 16.65%); i.r.(thin film)/cm^{-1}, 2950, 2894, 2840, 2802, 2756s (C-H ν); 1741s (C=O ν); 1711m (C-N δ); 1468m, 1450m (C-H δ). δ_H (200MHz; solvent $CDCl_3$; standard reference TMS) 3.05 (dd H4a [4H]), 2.73(dd H4e[4H]), 2.50 (tt H1[2H]), 2.28 (s Me's [6H]).; δ_C 215.00 (carbonyl, 61.00 [c1,c5]), 46.69 (c6,8,2,4), 45.14(Me's).

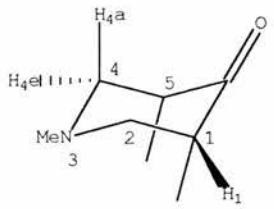

Figure 4

3,7 Dimethyl-3,7-diazabicyclo[3.3.1]nonane.H_2O (DMB). Potassium hydroxide (34g), 3,7 dimethyl-3.7diazabicyclo[3.3.1]non-9-one (44.5g, 0.265mol) and hydrazine (26cm^3, 0.795mol) were dissolved in triethyleneglycol (600cm^3) and refluxed for 4 hours. A Dean and Stark trap was fitted and the mixture heated until ~17cm^3 of aqueous hydrazine was collected. The hydrazine was discarded and the reaction mixture acidified with conc. HCl. The precipitates were filtered off and retained. Under reduced pressure the filtrate was reduced to ~ 100cm^3 and allowed to cool. Further crystals formed overnight and were collected and combined with the filtrates collected previously.

Concentrated KOH solution (100g in 150cm^3) and KCl (123g) was added to the combined precipitates, and the mixture extracted with dichloromethane (3x100cm^3).

The combined extracts were dried over $MgSO_4$ filtered and the solvent removed to give a pale yellow oil. This was distilled (80°C ~0.5mmHg) twice (bulb to bulb) to give a colourless oil (yield 22.7g, 53%). (Found: C, 63.55; H, 11.55; N, 17.22. Calc. for $C_9H_{18}N_2OH_2$: C, 11.70; H, 11.76; N, 18.16%); i.r.(thin film)/cm^{-1}, 3414s br (H-OH ν); 2918s, 2884s, 2859s, 2772s, 2737s,2778s, 2969s (C-H ν); 1635m (H-O δ); 1460m, 1446m (C-N).

Cu(DMB)Cl_2. To DMB (1g, 6.5mmol) in boiling methanol (15cm^3) was carefully added copper(II) chloride dihydrate (1.2g, 6.5mmol) in methanol (15cm^3). When the mixture had cleared, the green solution was allowed to cool. Long green crystals formed overnight. These were filtered off, washed with ethanol and dried *in vacuo* (yield 1.64g, 87%) (found: C, 37.77; H, 6.28; N, 9.70. Calcd. for $C_9H_{18}N_2Cl_2Cu$: C, 37.44; H, 6.28; N, 9.70); i.r.(KBr) cm^{-1} 2949, 2922, 2863s, 2819m (C-H ν.); 1454s (C-N ν); 831, 808, 736 m (CH_2 rock).

λ_{max}/nm (ε_{max}/dm^{3}mol^{-1}cm^{-1}) 901(170), 357(*ca.* 3500) DMF, 728 (88), 840 sh H_2O; Λ_M / S cm^{2}mol^{-1} 3 (DMF).

Zn(DMB)Cl$_2$ To DMB (1.17g, 6.8mmol) in boiling methanol (15cm^3) was carefully added zinc(II) chloride (0.93g, 6.8mmol) in methanol (15cm^3). When the mixture had cleared, the colourless solution was allowed to cool. Colourless needles formed overnight. The crystals were filtered off, washed with ethanol and dried *in vacuo* (yield 1.73g, 87%). (Found: C, 37.05; H, 6.23; N, 9.57. Calcd. for $C_9H_{18}N_2Cl_2Zn$. C, 37.21 H, 6.24 N, 9.64); i.r.(KBr) cm^{-1} 2951, 2927, 2904, 2860s, 2826m (C-H ν.); 1463s (C-N ν); 1088, 831, 808, 735m (CH_2 rock). Λ_M / S cm^{2}mol^{-1} 0 (DMF);

Crystal Data.-- $C_{9.5}H_{20}N_2CuCl_2O_{0.5}$, M = 304.73, Primitive orthorhombic, a = 19.086(7), c = 7.157(6) Å, U = 2607(2) Å^3 (by least-squares refinement on diffractometer angles for 25 automatically centred reflections, in the range 21.88<2θ<24.75° λ = 0.71069 Å), space group *I42d*(#122), Z = 8, D_c = 1.553 g cm^{-3}, F(000) = 1264.0. Lime green block crystal (grown by slow cooling of a methanol solution of the complex). Approximate crystal dimensions 0.20 x 0.40 x 0.30 mm, μ(Mo-K$_\alpha$) = 20.60 cm^{-1}.

Data Collection and Processing.--Rigaku AFC7S diffractometer, ω-2θ scan type with ω scan width = (0.89 + 0.35 tan θ)°, ω scan speed 16.00° min^{-1} (up to 4 scans), graphite monochromated MoKα radiation; 1070 reflections measured (max 2θ = 50.0°). No decay correction required but a correction for secondary extinction was applied (coefficient = 2.35533e^{-7}). Corrections were made for Lorentz and polarisation effects.

Structure Analysis and Refinement.-- Direct methods[2] were employed and expanded using Fourier techniques[3] The non-hydrogen atoms were refined anisotropically. Hydrogen's were included but not refined. The final cycle of full-matrix least-squares refinement[4] was based on 910 observed reflections (I>3.00σ(I)) and 77 variable parameters and converged with unweighted agreement factors of:

$$R = \sum \| Fo | - | Fc \| / \sum | Fo | = 0.025$$

$$R_w = \sqrt{\left(\sum \left(| Fo | - | Fc | \right)^2 / \sum w Fo^2 \right)} = 0.028$$

The standard deviation of an observation of unit weight[6] was 1.80. The Weighting scheme was based on counting statistics and included a factor (p = 0.009) to downweight the intense reflections. Plots of $w(\Sigma | Fo | - | Fc |)^2$ versus $| Fo |$, reflection order in data collection, sin θ/λ and various classes of indices showed no unusual trends. The maximum and minimum peaks on the final difference Fourier map correspond to 0.33 and -0.29 $e^- Å^{-3}$, respectively. All calculations were performed using the TEXSAN[7] crystallographic software package of the Molecular Structure Corporation.

Dissociation Kinetics. Dissociation of $[Cu(DMB)Cl_2]$ at 25°C and I = 0.1M (KNO_3) monitored at 278nm with a Phillips PU8720 Spectrometer. $[Cu(DMB)Cl_2]$ was injected into the acidic solution as a 10μL DMF solution (DMF stock solution 6.4×10^{-3} M) giving a cuvette concentration of 2×10^{-6}M with a DMF % (vol) of 0.3%.

Absorbence versus time data was collected for greater than 3 half lives and entered into the PC program Grafit.

Results and Discussion

Molecular Mechanics.- The reaction scheme shown in Figure 2 assumes that both the phosphorous centre and the copper centre pass through a five co-ordinate geometry in the transition state. Since Westheimer's initial proposal[8], much evidence has accumulated to support a five co-ordinate phosphorane intermediate or transition state in the hydrolysis of triesters[9].

Stabilisation of a five co-ordinate phosphorane, has been used to explain the unexpectedly high rates of hydrolysis of cyclic phosphates. We were interested to see if a ligand that would tetrahedrally distort the normally square planar geometry of these complexes, could be designed. It is proposed that a ligand that favoured a tetrahedral geometry may be better able to rearrange itself to the required five co-ordinate transition state than the commonly found square planar geometry. It is interesting to note that the $[Cu(tmen)Cl_2]$[10] is square pyramidal

with a distorted N_2Cl_2 basal plane, and $[Cu(bpa)Br_2]$ is tetrahedral[11]. Cram's rule of preorganisation[12] introduces the concept that the free ligand should be in the right conformation to complex to the metal ion.

MM calculations have allowed the inspection of a number of possible ligands. The ligand tmen was first inspected first to gain some knowledge of an active catalyst. The minimum

energy structures are given in and Figure 6.

Figure 5. 12.55 kcal mol^{-1}

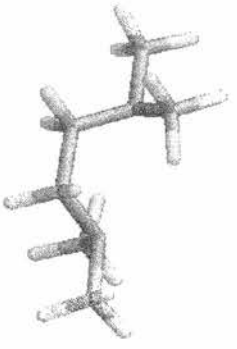

Figure 6. 10.68 kcal mol^{-1}

Interestingly the conformation closest to that found in the chelated ligand is the lowest energy form of the two. Molecular dynamics indicates the energy barrier for interconversion is not very high. Starting from the conformation required for complexation Figure 7 shows the switch from bent to linear conformation as a change in N-N distance. The plot also indicates that there is no movement out of this energy well during the run.

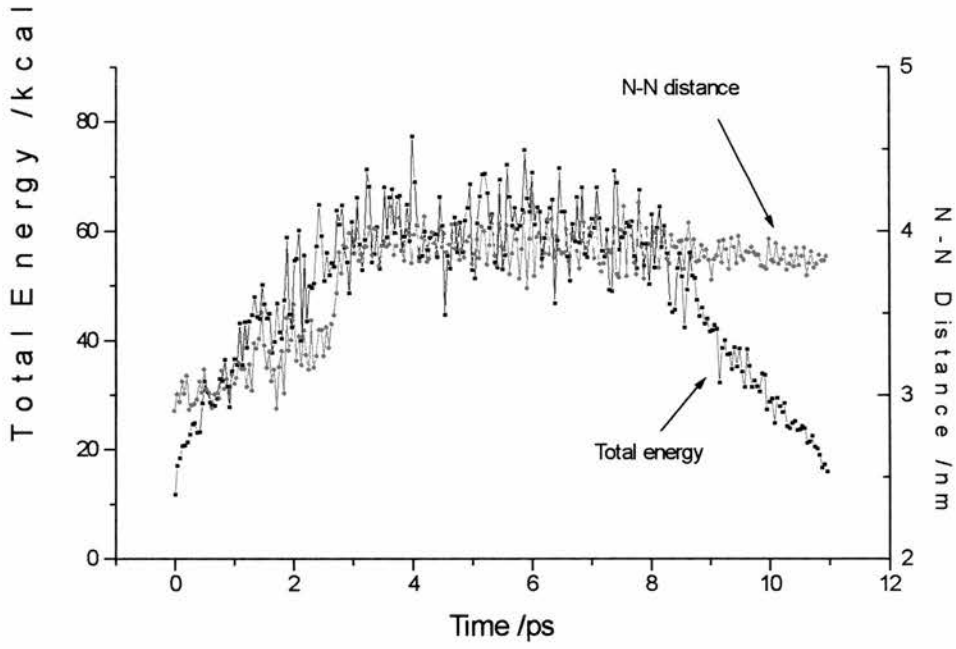

Figure 7

It would be interesting to model a molecule that has a minimum energy form preorganised for complexation but a higher energy barrier to conversion to conformations less suitable for coordination. The restriction of conformations may be best made by incorporating bridged structures into the molecule. For example the donor nitrogens might be incorporated into a cyclic structures as shown in Figure 8. DMB (3) 3,7-diazabicyclo[3.3.1]nonane (dimethyl bispidine), dmbipy (4) 6,11-dimethylbipyridine, DMDACH (2) N,N'-dimethyl-1,4-diazacyclohexane, and DMDACO (1) N,N'-dimethyl-1,5-diazacyclooctane.

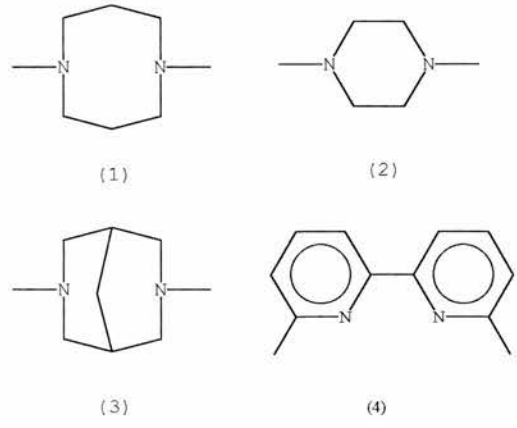

Figure 8

The minimum energy form and next highest conformation of each of the cyclic amines (1-3) were found are shown below (figures 9 to 14)

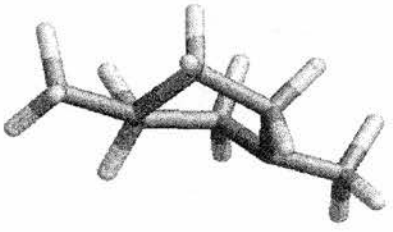

Figure 9. 15.71 kcal mol^{-1}

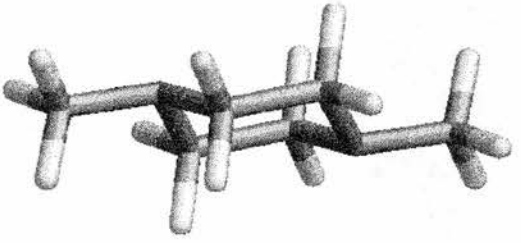

Figure 10. 8.33 kcal mol-1

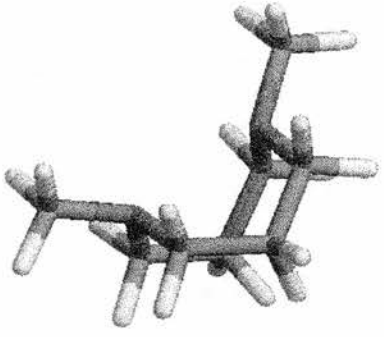

Figure 11. 24.48 kcal mol-1

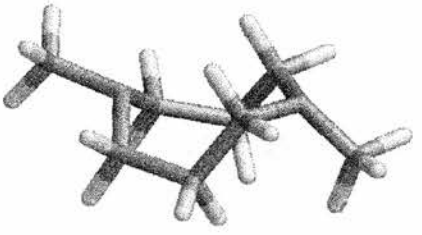

Figure 12. 28.30 kcal mol-1

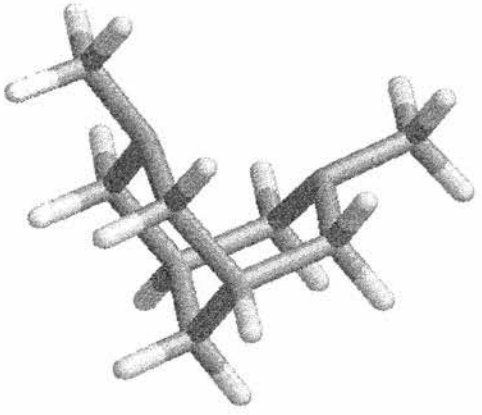

Figure 14. 18.71 kcal mol-1

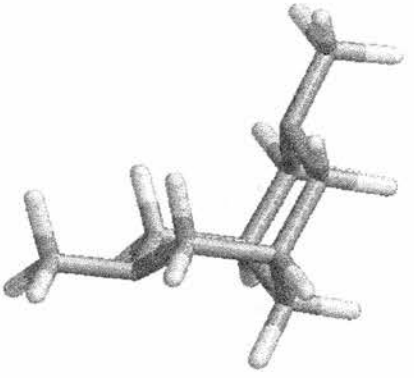

Figure 13. 25.25 kcal mol-1

It is interesting to note that all the candidate ligands apart from dimethyldiazacyclohexane, have their lowest energy conformation corresponding to that required for complexation. The energy difference between the two conformations is most pronounced for diazabicyclooctane (DMB) (-6.54 Kcal mol^{-1}) Table 1.

Table 1. Energies required in the conformational change for decomplexation.

Ligand Candidate	Δ^* /Kcal mol^{-1}
TMEN	-1.87
DMDACH	7.38
DMDACO	-3.82
DMB	-6.54

* $\Delta = U_{com}-U_{dcom}$ where U_{com} is the energy of the conformation closest to that required for complexation, and U_{dcom} is the next highest conformation with an inverted nitrogen.

To gain more information on the ligands complexing ability of the ligands, a study on the best fit of metal ion to the chelate ring formed by each was made. The complexes were given tetrahedral geometry (two nitrogen donors from the candidate ligand and the other two to chloride) and the structure minimised at a number of different N-M distances. These

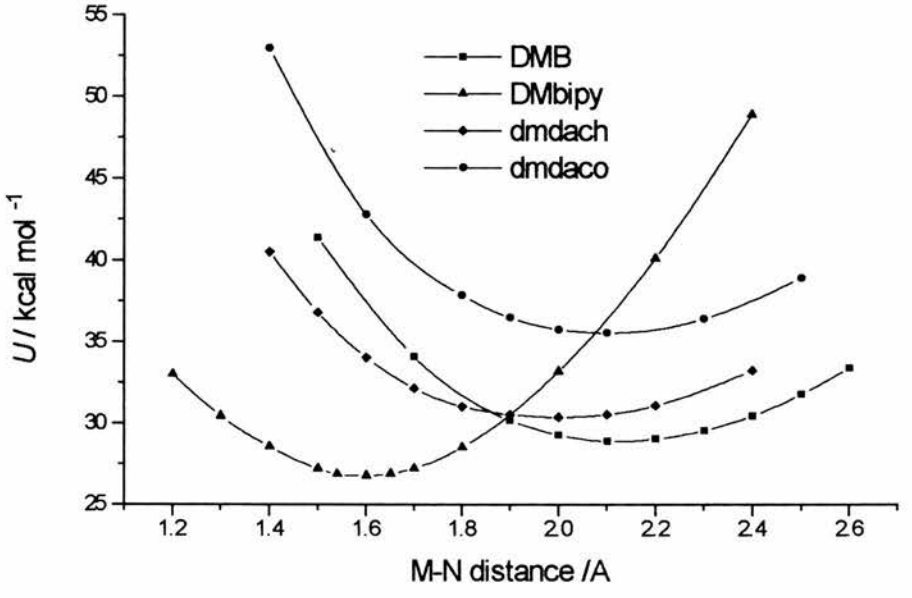

Figure 15

distances were plotted versus the minimised energy of the system, Figure 15, to give a series of curves, the minimum of each corresponding to the optimum M-N bond distance.

Table 2. Optimum M-N distances (Å), N-M-N angle and N, N Bite distance for the candidate ligand systems complexed to copper in tetrahedral stereochemistry.

Ligand	M-N Distance /A	N-M-N angle	N, N bite distance/ A
DMBipy	1.589	92.92	2.45
DMDACH	2.004	65.04	2.50
DMDACO	2.105	81.24	3.05
DMB	2.120	86.09	3.03

The bipyridyl derivative was also examined to allow a comparison with a planar five membered chelate ring system. Dimethyl bispidine shows the largest N-M-N angle of the cyclic systems. Presumably this is mainly due to the additional steric crowding in the propyl bridges, opening up the M-C-C and C-C-C angles of the chelate rings. Comparison with the bipy derivative indicates there are significant non-bonding interactions between the ligand organic framework due to steric crowding caused by an N-Me and the metal atom in DMDACH, DMDACO, and DMB. The large N-M-N angle for the bispidine complex make this ligand the most promising for further investigation.

Description of the Crystal Structure of [Cu(DMB)Cl_2]0.5MeOH.

An inspection of the bond angles around the copper centre show the metal atom to be of tetrahedral geometry with the Cl-Cu-Cl bond angle close to the ideal (109.5°) and the N-Cu-N distorted to give the more acute angle of 89.8°. Bond distances are close to mean Cu-Cl distances extracted from the Cambridge Crystallographic Data Base [2.25(3) Å] for four co-ordinate copper however the Cu-N bond length is shorter than that expected [2.06(4) Å].

Table 3. Selected bond lengths (Å) and angles of*[Cu(DMB)Cl_2]0.5MeOH.*

Cu(1)-N(1)	1.987(3)	N(1)-Cu(1)-Cl(1)*	124.62(9)
Cu(1)-Cl(1)	2.247(1)	N(1)-Cu(1)-N(1)*	89.8(2)
Cl(1)-Cu(1)-N(1)-C(1)	55.0(3)	Cl(1)-Cu(1)-Cl(2)*	110.09(6)
N(1)*-Cu(1)-N(1)-C(1)	-179.2(3)	N(1)-Cu(1)-Cl(1)	104.10(9)

ORTEP diagram of the complex $[Cu(DMB)Cl_2].0.5MeOH$

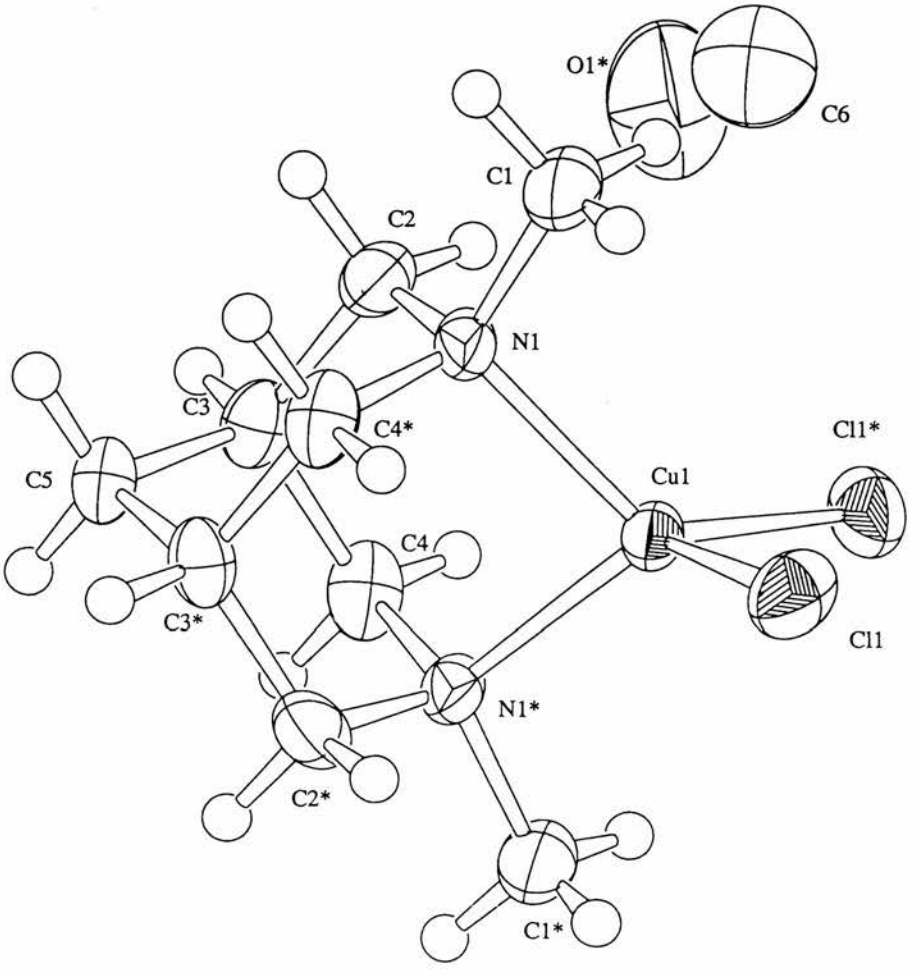

Dissociation Kinetics.- The copper(II) complex [Cu(DMB)Cl_2] dissociates readily in acidic solution and a brief study was made of the kinetics of this process. Values of k_{obs} as a function of the acidity are summarised in Table 1.

Table 4. Acid dissociation of [Cu(DMB)Cl_2] at 25°C and I=0.1M (KNO_3)

[HNO_3] (M)	$10^3 k_{obs}$ /s^{-1}
0.1	5.92
0.09	5.92
0.07	5.75
0.05	5.79
0.03	5.77
0.01	5.83
0.007	5.77
0.004	5.82
0.002	5.68
0.001	5.63

mean k_{obs}=5.79(0.09)

The observed activation parameters have also been determined, the temperature dependence of the acid dissociation of [$Cu(DMB)^{2+}$] is shown in Table 2.

Table 5. Temperature dependence of the acid dissociation of $[Cu(DMB)^{2+}]$ in 0.1M HNO_3[a]

Temperature/°C	$10^3 k_o$ /s^{-1}
25.5	6.54(0.13)
27.8	8.45(0.15)
30.0	10.03(0.43)
32.5	12.12(0.23)
35.0	15.77(0.14)
40.0	19.45(0.24)

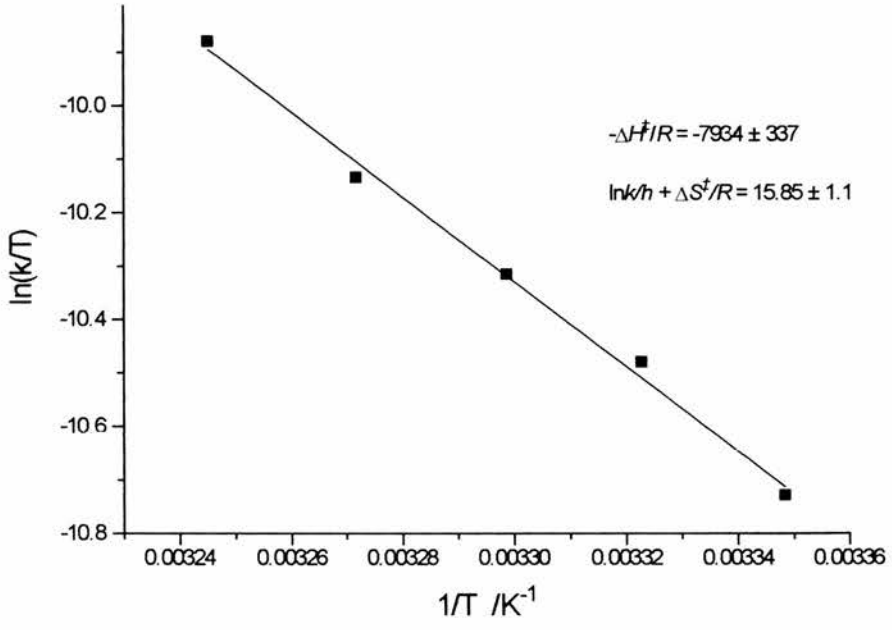

Figure 16

[a] H =56.6 KJ/mol; S =-96.8 KJ/mol

The reaction is first order in the complex and is independent of the concentration of the hydrogen ion, Table 4. Over the acidity range 0.001 to 0.1 mol dm^{-3} $[H^+]$ the mean value of

k_{obs} = 5.79 ± 0.09 s^{-1} at 25°C and I = 0.1mol dm^{-3}. Activation parameters were determined using the rate constants obtained in the temperature range 25.5°C to 40°C, Table 5. The Eyring plot is shown in Figure 16 giving ΔH = 56.6 ± 0.5kJmol^{-1} and ΔS = -96.8 ± 4 (correlation coefficient 0.9884)

It is interesting that the acid dissociation of the complex is quite slow and occurs on the "normal" spectrophotometric time scale rather than in the stopped flow range. Its behaviour is

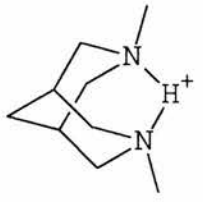

Figure 17

similar to that observed with a number of macrocyclic complexes. A similar effect has also been observed in a pyridyl derivative of bispidine.

The pseudo-adamantane structure of the protonated ligand is highly stable. All six membered

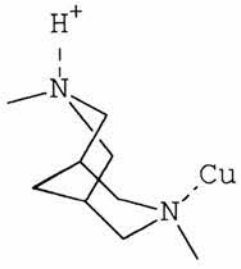

Figure 18

rings are locked in chair conformations. A protonated copper complex would have a chair boat conformation (Figure 18), a rather high energy conformation.

References

[1] D.Wahnon, R.C.Hynes and J.Chin; *J.C.S. Chem. Commun.*, 1994, 1441

[2] J.E.Douglas and T.B.Ratcliff, *J.Org.Chem.*, 1968, **33**, 355.

[3] *SIR92:* A.Altomare, M.C.Burla, M.Camalli, M.Cascarano, C.Giacovazzo, A.Guagliardi and G.Polidori, 1994, *J.Appl.Cryst.*, in preparation.

[4] DIRDIF94: P.T.Beurskens, G.Admiraal, G.Beurskens, W.P.Bosman, R. de Gelder, R.Israel and J.M.M.Smits 1994. *The DIRDIF-94 program system,* Technical Report of the Crystallography Laboratory, University of Nijmegen, The Netherlands.

[5] Least-Squares:

Function minimised: $\Sigma w(|Fo| - |Fc|)^2$ where $w = 1/\sigma^2(Fo) = 4Fo^2/\sigma^2(Fo^2)$

$\sigma^2(Fo^2) = S^2(C+R^2B)+(pFo^2)^2/Lp^2$

S = Scan speed

C = Total integrated peak count

R = Ratio of scan time to background counting time

B = Total background count

Lp = Lorentz-polarization factor

p = p-factor

[6] Standard deviation of an observation of unit weight:

$$\sqrt{\sum w\left(|Fo| - |Fc|\right)^2 / \left(No - Nv\right)}$$

where: No = number of observations

Nv = number of variables

[7] *Crystal Structure Analysis Package,* Molecular Structure Corporation (1985& 1992)

[8] F.H.Westheimer, *Acc.Chem.Res.*, 1968, **1**, 70.

[9] T.Koike and E.Kimura, *J.Am.Chem.Soc*, 1991, **113**, 8935.

[10] E.D.Estes, W.E.Estes, W.E.Hatfield and D.Hodgson, *Inorg.Chem.*, 1975, **14**, 106.

[11] N.Ray, S.Tyagi, and B.Hathaway, *J.Chem.Soc.Dalton Trans.*, 1982, 143.

[12] D.J.Cram, T.Kaneda, R.C.Helgeson, S.Brown, C.B.Knobler, E.Maveric and K.N.Trueblood, *J.Am.Chem.Soc.*, 1985, **7**, 3645.

Chapter 6

Oxidation Catalysts for the Destruction of *bis*-(2-chloroethyl)sulfide (HD)

Investigation of Two Transition Metal Oxidation Catalysts, $[Mn_2(III)L_2(CH_3CO_2)_2\mu(O)](ClO_4)_2$ and $VO(Acac)_2$ for the Detoxification of *bis*-(2-chloroethyl)sulfide (HD).

Abstract

A manganese based catalyst using 1,4,7-trimethyl-1,4,7-triazacyclononane (Me_3tacn) as the ligand has been developed for the oxidation of mustard [*bis*-(2-chloroethyl)sulfide] to the sulfoxide. This catalyst is too active, oxidising the substrate to the still toxic sulfone. The use of vanadyl acetylacetonate ($VO(acac)_2$) in the presence of a peroxide (*t*-butylhydroperoxide) has been found to provide a rapid and satisfactory method for the oxidation of mustard to the non-toxic sulfoxide. The mechanism of the reaction is discussed. The low water solubility of mustard can be overcome by using microemulsion techniques.

Introduction

For a such simple molecule, *bis*-(2-chloroethyl)sulfide (HD) has a complicated chemistry and particularly unpleasant physiological effects[1]. The chloroethyl arms may undergo substitution or elimination of the chloro group by intramolecular nucleophilic attack and the presence of the thioether moiety enables intramolecular attack of sulfur to form a three membered sulfonium ring. The sulfide moiety can be oxidised to the sulfoxide or sulfone, either of which can undergo nucleophilic attack (Figure 1).

Both nucleophilic attack or oxidation may be utilised in the detoxification however HD reacts slowly with nucleophiles such as hydroxide. We have been interested in oxidative processes as a speedier way of decontamination. Some easily available oxidants are i) bleach (ii) peroxides (iii) oxygen. Bleach is fast, but it is too corrosive for regular use on fabrics, paints, metalwork, rubber and skin. Dilute peroxides or atmospheric oxygen are less

corrosive but the rates of reaction are too slow. Catalysts are required to enhance the rates of reaction for their use as decontaminants.

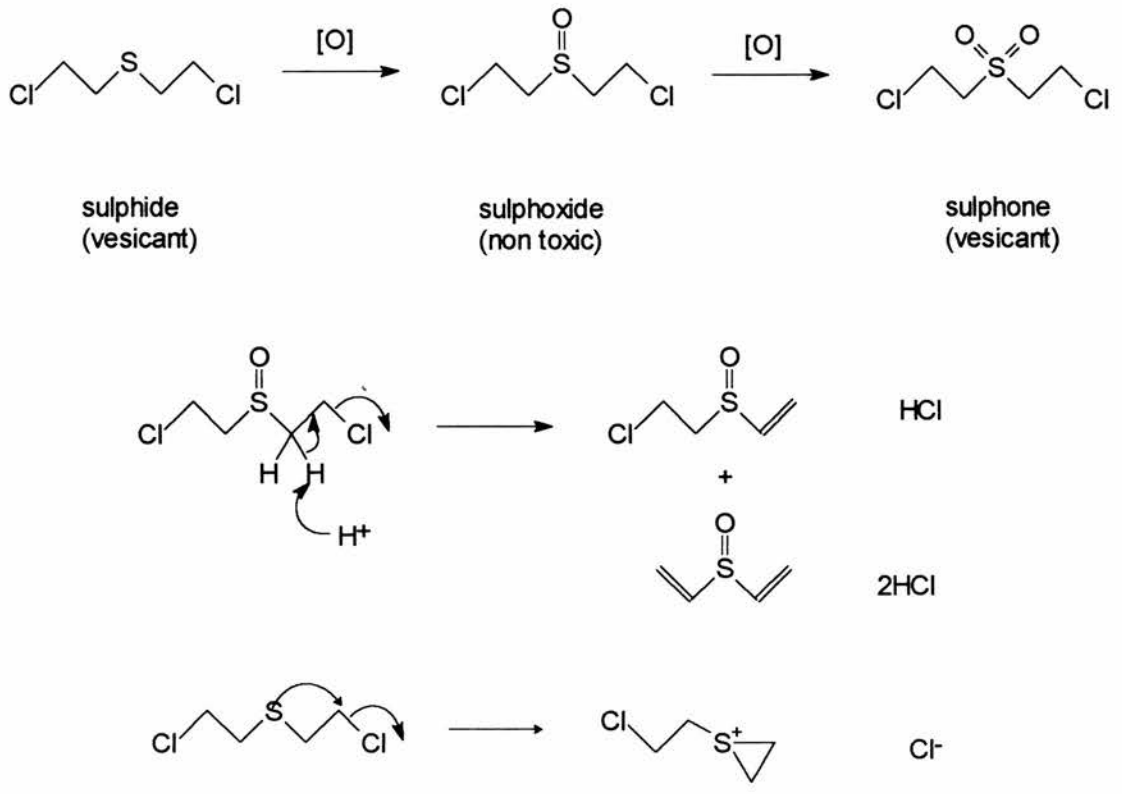

Figure 1

A serious difficulty with the decontamination of HD is its low solubility in water. Since water is the solvent of choice in any emergency, ways must be developed to overcome this problem. One approach is to use mixed solvent systems, either as miscible mixtures (ie. ethanol and water) or as miscible solvent systems stabilised as emulsions or microemulsions. Emulsion systems are attractive as it may be possible to formulate emulsions with a much greater proportion of water, relative to mixed solvent systems, thus reducing the weight of

concentrated decontaminant. We studied oil-in-water microemulsions as a solvent for carrying out oxidation reactions of sulfides in addition to using alcohol-water mixtures.

Microemulsions.- A microemulsion is an isotropic and optically transparent dispersion of oil-in-water (O/W) or water-in-oil (W/O) (oil= hydrocarbon). Microemulsions form spontaneously when water, a hydrocarbon, a surfactant and a co-surfactant (generally a low molecular weight alcohol) are mixed in specific proportions. The solutions contain dispersed droplets averaging 50-500 Å in diameter and will remain clear indefinitely. Some example oil in water microemulsions are (weight percentages):

Table 1.Typical Oil in Water Microemulsions weight percentage

1. 3% cyclohexane in 82% water stabilised by 5% sodium dodecyl sulfate and 10% *n*-butanol.
2. 4% n-hexadecane in 60% water stabilised by 24% Brij-96 and 12% 1-butanol.
(Brij-96 is a nonionic poly(oxyethylene) ether surfactant $CH_3(CH_2)_7CH{=}CH(CH_2)_8(OCH_2CH_2)_{10}OH$

Fast reactions in microemulsions are related, in part, to the large interfacial contact area between the oil droplet and the continuous aqueous phase.

A major problem with the investigation of the reactions of HD is the lack of available spectroscopic "handles" on this compound. Most investigations have resorted to sampling techniques or NMR to determine substrate and product concentrations. These techniques are unfortunately only of use for slow reactions which are of little value for decontamination use.

The development of IR spectrometer total internal reflectance (TIR) cells where the IR beam is passed through a test solution through a wave guide, has enabled the study of the IR spectrum in solvents initially thought to be far to strongly absorbing for IR techniques. Using TIR IR spectroscopy we have been able, not only qualitatively, but semi quantitatively, to

study the formation of sulfoxide and sulfone products (Figure 2) of the oxidation of HD and di-*n*-butylsulfide in O/W micellar media.

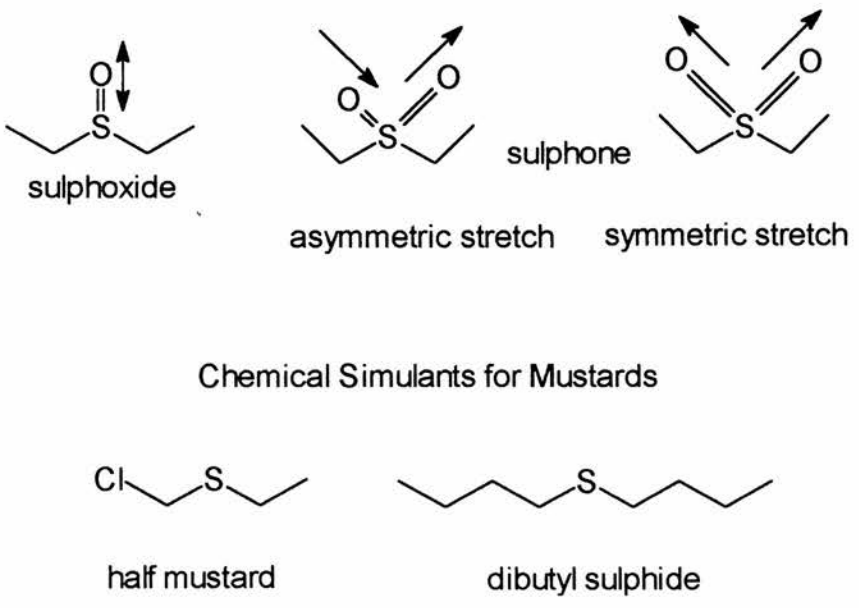

Figure 2

We are investigating the oxidation of the sulfide moiety of mustard so di-*n*-butyl sulfide was chosen as the simulant. The solubility characteristics of so di-*n*-butyl sulfide are silmilar to those of mustard.

Experimental

Measurements.-Ir spectra were measured with a REACTIR FT spectrometer fitted with a diamond probe.

Materials.-1,4,7-trimethyl-1,4,7-triazacyclononane (Me_3tacn) was prepared by the methylation of 1, 4, 7-triazacyclononane which was prepared by a standard Richman-Atkins[2]

procedure (Figure 3). Methylation was carried out by a Eschweiler-Clark procedure (by a modification of the method for preparing 1,4,8,11-tetramethyl-1,4,8,11-tetraazacyclotetradecane[3]). $VO(acac)_2$ was prepared as previously described[4]. Tosyl chloride was obtained from Lancaster Synthesis. 1,5-diamino-3-azapentane, 1,2-ethanediol, formaldehyde, and formic acid were bought from Aldrich and acetylacetone and sodium metal from Fisons. *n*-Butyl sulphide, *t*-Butyl hydroperoxide, hydrogenperoxide and the surfactants SDS and BRIJ 97 were bought from Sigma. *bis*-(2-Chloroethyl)sulfide obtained from CBDE, Porton Down. Manganese(II) acetate and vanadium pentoxide were obtained from BDH.

Synthesis

Preparation of 1,4,7-trimethyl-1,4,7-triazacyclononane, (L). (a) N,N-*bis(*p-*tolylsulfonamidoethyl)*-p-*tolylsulfonamide[1].* 1,5-diamino-3-azapentane (51g, 0.5mol), and NaOH (60g, 1.5mol) were dissolved in water (400cm^3), cooled in an ice bath and solid tosyl chloride (152g, 0.66mol) was slowly added to the vigorously stirred solution. A large quantity of white precipitate was filtered off, washed with water. The product was recrystallized from methanol and dried *in vacuo* at 60°C.(285g, 97%)

(b)Disodium-N,N-*bis(*p-*tolylsulfonamidoethyl)*-p-*tolylsulfonamide[2].* Sodium metal (4.1g, 0.178mol) was carefully added to ethanol (100ml) then added to a hot, stirred slurry of [1] (50g, 0.089mol) over a 15min period. Overnight a mass of white crystals formed. These were filtered off, washed with ethanol (2x20cm^3) and dried *in vacuo*.

(c) 1,2-Bis(toluenesulfonyl)ethane[3]. 1,2-Ethanediol (31g, 0.1mol) in pyridine (100cm^3) was added dropwise to a cooled (NaCl-ice bath) solution of toluene sulfonamide chloride (286g, 1.5mol) in pyridine (400cm^3) over 2h. Colourless crystals and were filtered off, washed with water then dilute H_2SO_4 (0.1mol dm^3), $NaHCO_3$ solution and finally with water. The filtrate was added to water (500cm^3), chilled in ice and refiltered. The product was washed in the same way as above and then combined with the first crop.

*(d) 1,4,7-Tri(*p*-toluenesulfonamide)-1,4,7-triazacyclononane[4].* [3] (35.5g, 0.096mol) in DMF (480cm^3) was added dropwise over 2h to a solution of [2] (58.2g, 0.096mol) in DMF (960cm^3) heated to 100°C. Most of the DMF was removed from the mixture and water added until crystals started to form. After cooling for 5h the mass of white crystals were filtered off and washed with MeOH. The product was further purified by reprecipitation from dichloromethane by the addition of MeOH. (37.5g, 76%).

(e) 1,4,7-Triazacyclononane3/2SO_4[5]. [4] (37.5g, 68mmol) in sulfuric acid (80%, 113cm^3) was heated to 150°C with stirring for 5h. The cooled mixture was added slowly, dropwise to a vigorously stirred methanol/ether (1:1, 400cm^3) cooled in an ice bath. The white precipitate was filtered off, washed with ethanol and dried in vacuo (22.42g, 45%).

(f) 1,4,7-triazacyclononane[6]. [5] (22.42g, 40mmol) was dissolved in water (50cm^3) and NaOH added until pH > 12. The solvent was removed and the residue azeotropically dried with ethanol and then distilled at reduced pressure (bulb to bulb) (4.24g, 40%).

(f) 1,4,7-trimethyl-1,4,7-triazacyclononane[7]. [6] (4.24g), formic acid (96% 34cm^3, 0.732mol) and formaldehyde (35%, 33cm^3, 0.388mol) were refluxed for 18h. The solution was cooled, NaOH added until pH>12, the mixture extracted with dichloromethane (6x20cm^3), and dried over $MgSO_4$. Removal of solvent gave a brown oil which was distilled at reduced pressure to give a colourless oil which solidified on standing.

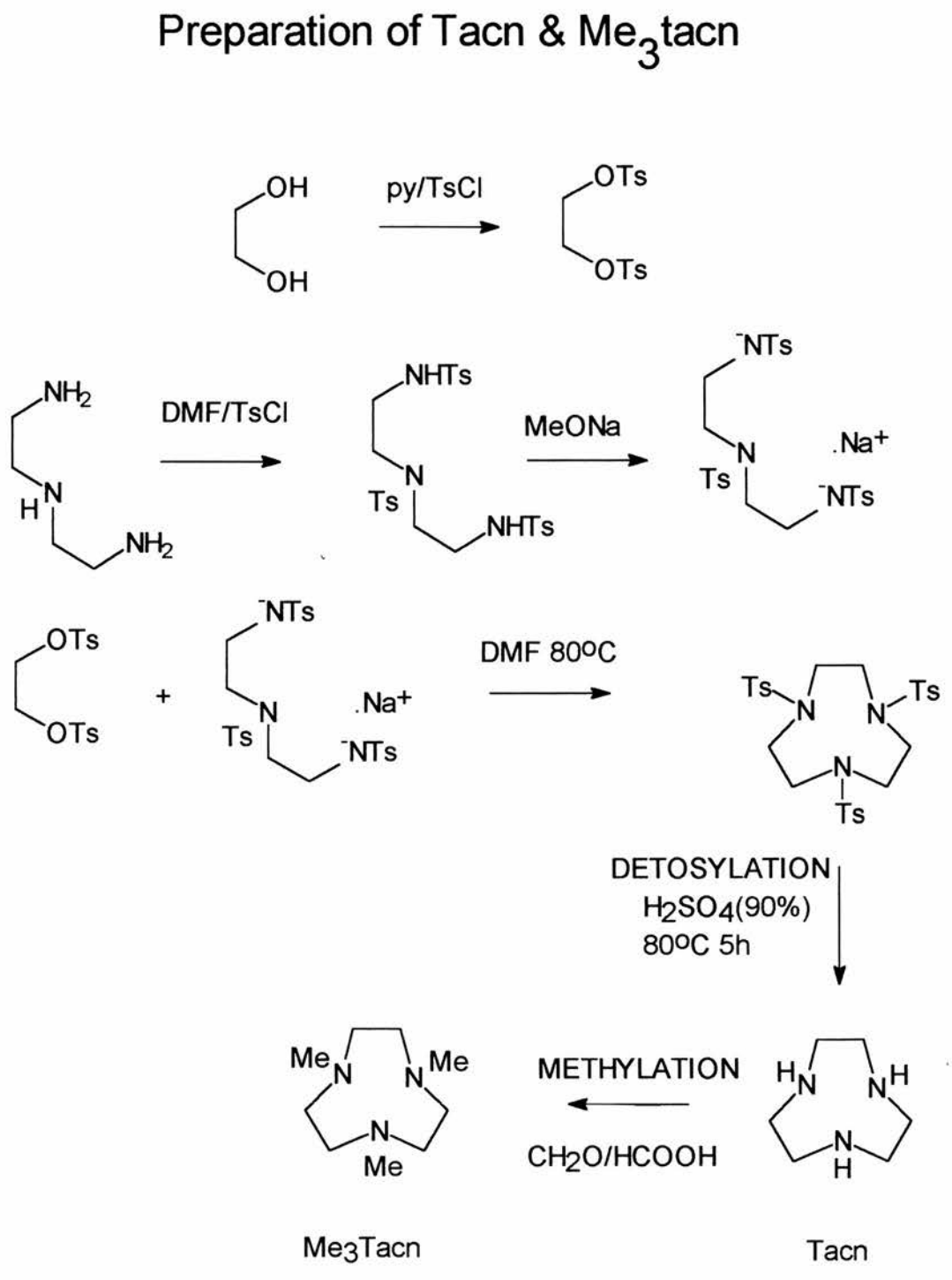

Figure 3

(g) $[Mn_2(III)L_2(CH_3CO_2)_2\mu(O)](ClO_4)_2$.- The complex was prepared by an alternative route to that described by Wieghardt *et al*[5]. Me_3tacn (1g, 5.85mmol) in acetonitrile ($10cm^{-3}$)

was added to manganese (II) acetate (1.43g, 5.85mmol) under argon to give a light straw coloured solution. Oxygen was gently bubbled through a course frit into the solution and immediately gave a dark brown solution. Addition of $NaClO_4$ (4.14g, 29.2 mmol) and slow evaporation gave dark brown blocks, which were filtered off and recrystallised from methanol to give feathery maroon crystals. (1.64g, 74%) (Found: C, 33.38; H, 5.86; N, 10.22. Calcd. for $C_{22}H_{48}N_6O_{13}Cl_2Mn_2$: C, 33.64; H, 6.16; N, 10.70); i.r.(KBr): 1571 $\nu_{asym}(COO^-)$, 1468 $\nu_{sym}(COO^-)$, 1423 $\nu_{sym}(COO^-)$, [lit[5]. 1570, 1450, 1415] λ_{max}/nm(ε_{max}/dm^{3}mol^{-1}cm^{-1}) 486.1(663), 521.6(633), 718.4(110) [lit.[5] 486 and 521] MeCN;

(h)VO(acac)$_2$. Vanadium pentoxide (5g, 0.03mol) was refluxed with acetylacetone (100cm^3, 0.98mol) for 24h. The suspension was filtered hot and the filtrate cooled. Small blue-green crystals formed overnight. These were filtered off, washed with acetone then ether and dried at 110°C.

Kinetics.- The course of the reactions were followed by TIR IR spectroscopy, collecting absorbance data over the 1600 to 400 cm^{-1} range. Rate constants were calculated from absorbancies centered on the sulfoxide band (996 cm^{-1} [di-*n*-butyl sulfoxide] 1011 cm^{-1} [*bis*-(2-chloroethyl)sulfoxide]) or sulfone band (1131 cm^{-1}[di-*n*-butyl sulfone]). In a typical run ca. 1cm^3 of alkyl sulfide was added to 10cm^3 of solvent (microemulsion or *tert*-butyl alcohol) containing the catalyst and two equivalents of peroxide. The background spectrum was taken prior to addition of alkyl sulfide. The reactor vessel was not thermostatted (ambient temperature was 18-21°C) for ease of decontamination of the cell after use.

Results and Discussion

Synthesis.-The acetate bridged complex may be prepared from the Mn(II) salt, presumably via a peroxo bridged dimer. The presence of *bis*-acetato bridging is evident from the characteristic electronic spectrum[6] and C-O stretching frequency in the IR spectrum. IR assignments were based upon the work of Deacon and Suzuki *et al*[7]

Kinetics.- activity of $[Mn_2(III)L_2(CH_3CO_2)_2\mu(O)](ClO_4)_2$ towards sulfides

The oxidation of di-*n*-butyl sulfide in microemulsion media with *t*-butyl hydroperoxide revealed that the manganese catalyst catalyses both the oxidation to sulfone and sulfoxide. The appearance of sulfoxide and sulfone bands are shown in Figure 4. The absorbance versus time data for the sulfoxide and sulfone bands enable the measurement of the rates of formation of these compounds.

The system can be considered as an irreversible biphasic reaction (equation 1) :

$$A \xrightarrow{k_1} B \xrightarrow{k_2} C \qquad (1)$$

In this reaction A= di-*n*-butyl sulfide, B = di-*n*-butyl sulfoxide, C = di-*n*-butyl sulfone. Only the sulfone and sulfoxide may be measured in this experiment. The rate equations for these two components are:

$$-\frac{d[A]}{dt} = k_1[A] \qquad (2)$$

$$-\frac{d[B]}{dt} = k_1[A] - k_2[B] \qquad (3)$$

$$-\frac{d[C]}{dt} = k_2[B] \qquad (4)$$

the integrated rate equations for [B] and [C]

$$[B] = \frac{[A]_0 k_1}{k_2 - k_1}\left[\exp(-k_1 t) - \exp(-k_2 t)\right] \qquad (5)$$

$$[C] = [A]_0\left[1 - \frac{k_2}{k_2 - k_1}\exp(-k_1 t) + \frac{k_1}{k_1 - k_2}\exp(-k_2 t)\right] \qquad (6)$$

The absorbance of the sulfoxide and sulfone band *versus* time was fitted to equation 5 and 6 respectively. The experimental points and the fitted curves are shown in Figure 5 and the kinetic parameters determined from the curve fitting are shown in Table 2.

Table 2. Rate/catalyst rate profile for the oxidation of di-*n*-butylsulfide with *t*-butyl hydroperoxide*

curve parameter	Sulfoxide band	Sulfone band
k_1/s^{-1}	0.0025	0.0021
k_2/s^{-1}	0.0027	0.0023
A_0	0.0773	0.101
error	0.006	0.006

* concentrations a stated in Figure 4

Although the shape of the curves fit well the biphasic model, the error in the fit indicates that there is considerable uncertainty in the absolute magnitude of the rate constants. This uncertainty can be linked to the conditions used to obtain the rate data. High concentrations of sulfide were required to observe the weak absorbance bands (ca. 10%v/v). In addition, the use of stoichiometric quantities of oxidant and multiple-phase nature of the medium all contribute to difficult experimental conditions. However, the results definitely establish that the sulfoxide is further oxidised to the sulfone in the presence of the manganese(III)catalyst. In view of the toxicity of the sulfone, these results indicate that the $[Mn_2(III)L_2(CH_3CO_2)_2\mu(O)]^{2+}$ is unsuitable as a decontaminant for HD.

Figure 4. Oxidation of di-*n*-butyl sulfide (0.459mol dm^{-3}) by *t*-butyl hydroperoxide (0.914 mol dm^{-3}) catalysed by $[Mn_2(III)L_2(CH_3CO_2)_2\mu(O)]^{2+}$ (2.18x 10-3 mol dm^{-3}) in SDS microemulsion (10cm^3, [3% cyclohexane in 82% water stabilised by 5% sodium dodecyl sulfate and 10% *n*-butanol, w/w%]).

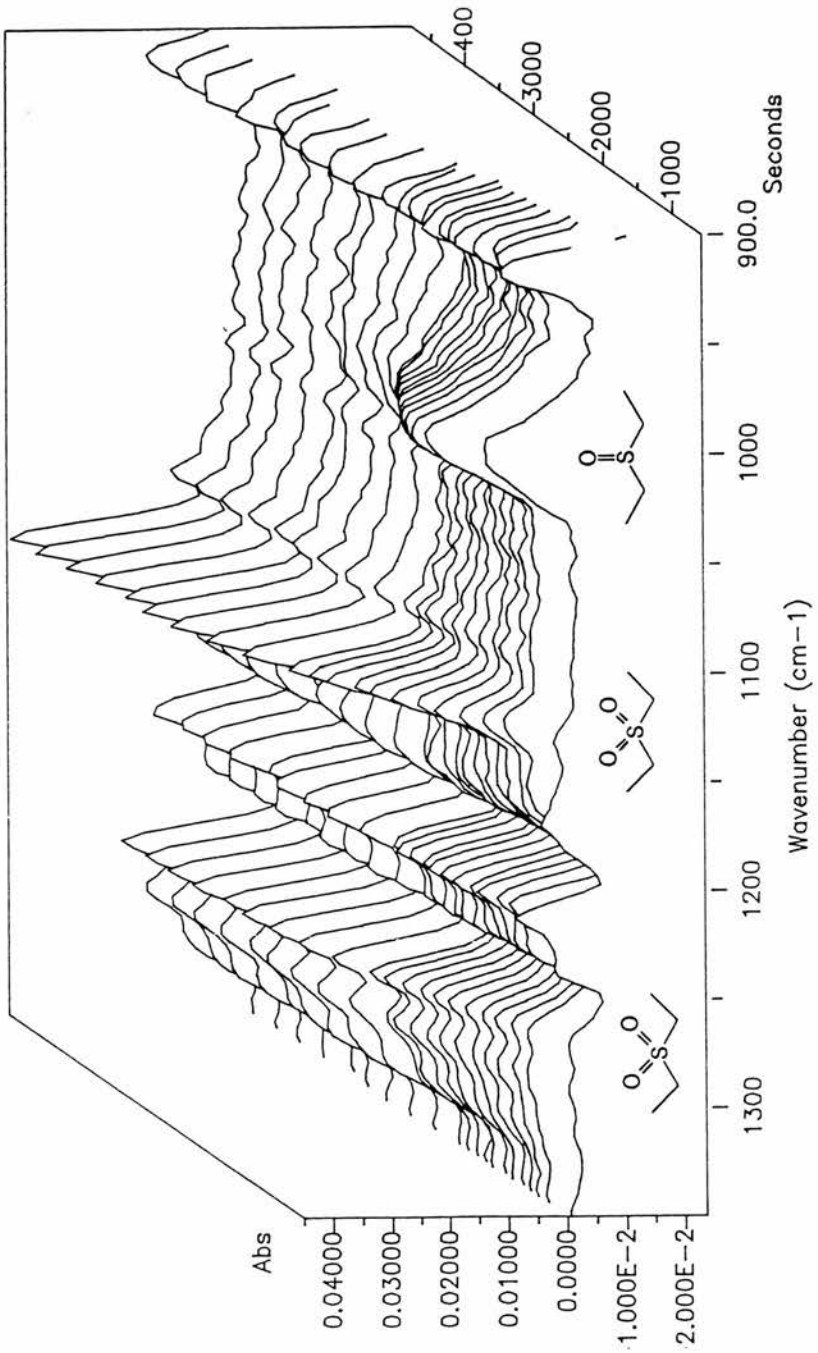

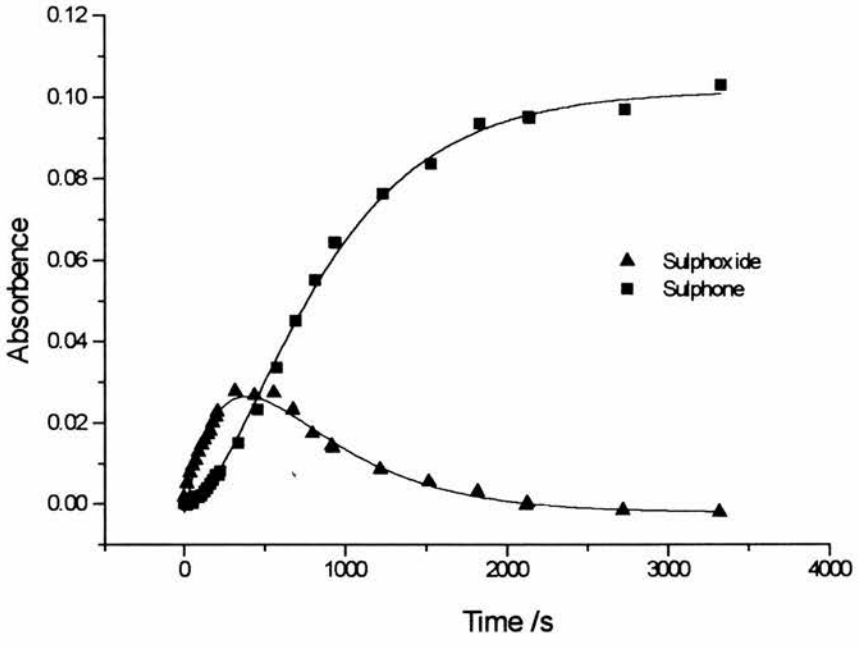

Figure 5

Graph showing appearance of sulfone and sulfoxide in the oxidation of *n*-butyl sulfide by *t*-butyl hydroperoxide catalysed by $[Mn_2(III)L_2(CH_3CO_2)_2\mu(O)]^{2+}$ di-*n*-butylsulfide at 0.459 mol dm^{-3}, *t*-butyl hydroperoxide 0.914 mol dm^{-3} in 10 cm^3 SDS microemulsion (82% water, 3.2% cyclohexane, 4.9% SDS, 9.8% *n*-butanol) and catalyst concentration at 2.18 $x10^{-3}$ mol dm^{-3}.

Activity of VO(acac)$_2$ towards sulfides. Work by Menger[8] has indicated that$VO(acac)_2$ Figure 6, could be utilised to promote the selective oxidation of HD to the sulfoxide, by peroxides.

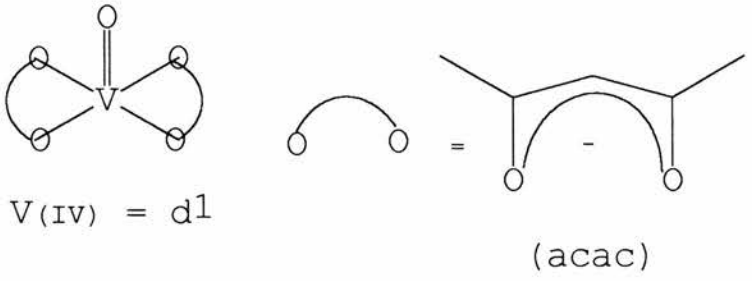

Figure 6

The UVis spectrum of the green $VO(acac)_2$ in ethanol has two bands at 775 and 580 nm due to d-d transitions (EtOH as solvent) to give a green solution. Bands disappear on adding t-butyl hydroperoxide [due to oxidation to d^0, Vanadium(V)]. A strong charge transfer band tailing in from the UV gives the solution a strong yellow colour.

The mechanism[9] for the reaction is thought to involve the formation of a V^0 peroxide adduct which is then attacked by the sulfide to form a sulfoxide (Figure 8).

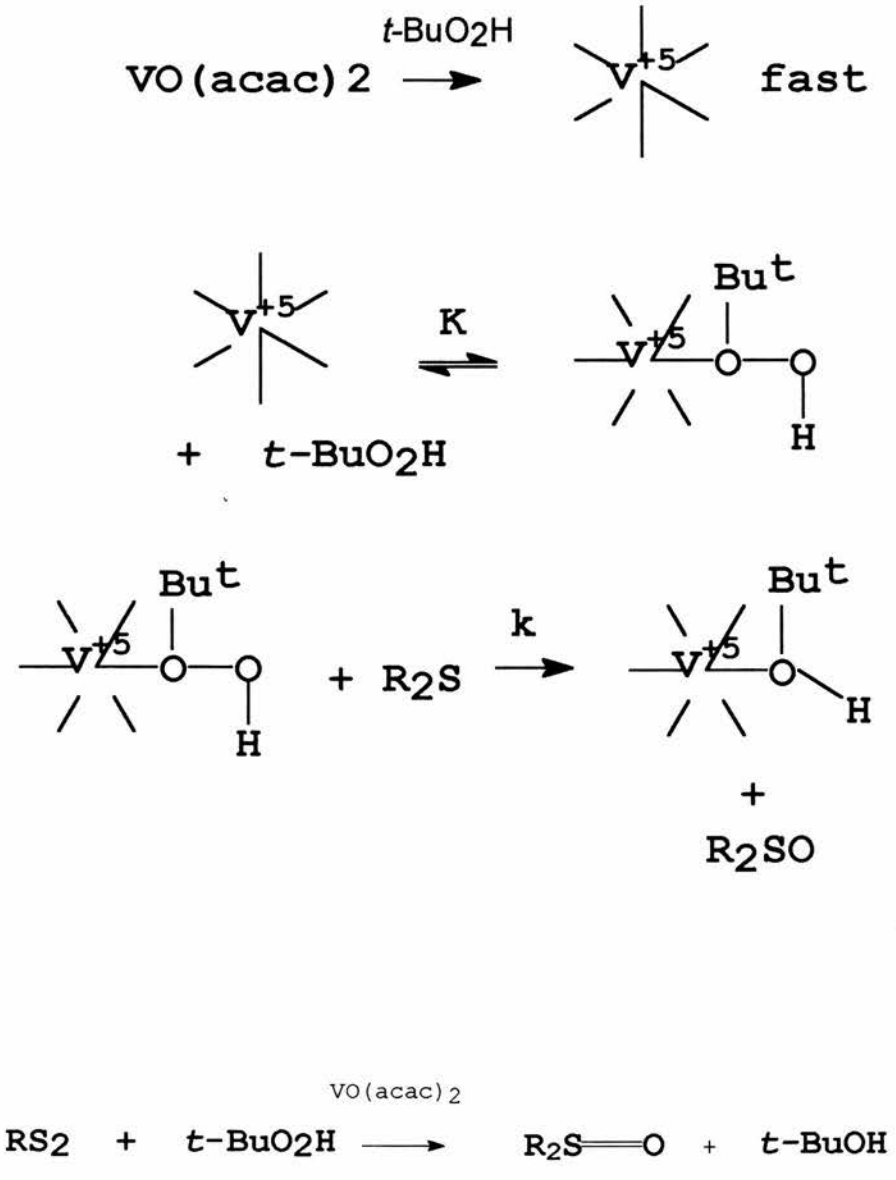
t-BuO2H
VO(acac)2
V+5
fast
K
But
H
+ t-BuO2H
k
+ R2S
+
R2SO
VO(acac)2
RS2 + t-BuO2H
R2S=O + t-BuOH

Figure 7

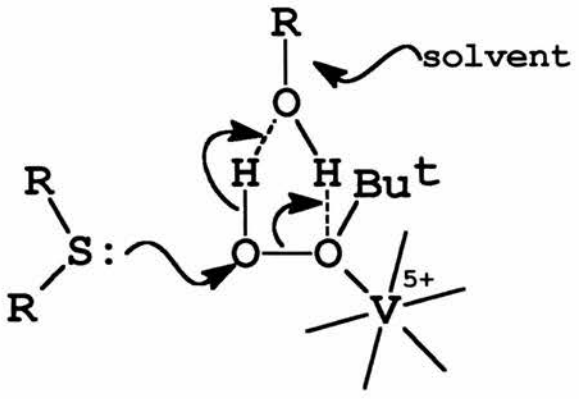

Figure 8

Evidence for the equlibrium constant (K) in the proposed catalytic cycle is supported by the observation of saturation kinetics for the catalysed oxidation of sulfides. A number of oxidations of *n*-butyl sulfide by *t*-butyl hydroperoxide were monitored in the presence of various concentrations of the vanadyl catalyst. The rate constants were obtained by curve fitting the first order rate increase with the intensity of the sulfoxide IR band, Table 3. The datapoints and fitted curves are presented in Figure 9.

Table 3. Values of k_{obs} as a function of the $VO(acac)_2$ concentration

$VO(acac)_2$ /mol dm^{-3}	k_{obs} /s^{-1}	$t_{1/2}$ /s
0.034	0.0357 ± 0.0015	19.4
0.023	0.0348 ± 0.0015	19.9
0.0132	0.0105 ± 0.0015	35.4
0.0043	0.0105 ± 0.0015	66
0.0013	0.00692 ± 0.0015	100

di-*n*-butylsulfide at 0.459 mol dm^{-3}, *t*-butyl hydroperoxide 0.914 mol dm^{-3} in 10 cm^3 BRIJ microemulsion (60% water, 4% hexadecane, 23.6% BRIJ97, 12.4% *n*-butanol w/w%)

Considering the complexity of the mixture and high concentration of substrate employed the curves fit remarkably well to a simple first order equation. A plot of the pseudo first order rate constant versus the concentration of catalyst, Figure 10, indicates that over the catalyst concentration range employed, saturation kinetics were not observed. There is no evidence for the formation of the sulfone. Further studies at even higher catalyst

concentrations will be required to investigate the pre-equilibrium. The vanadyl catalyst proves to be an effective, cheap, and selective catalyst for the decontamination of HD.

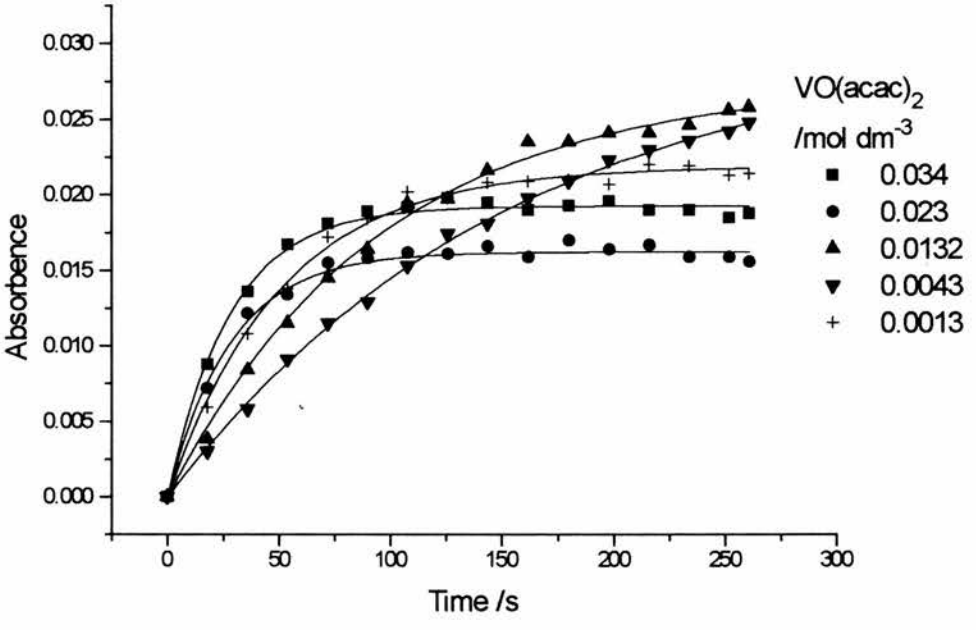

Figure 9

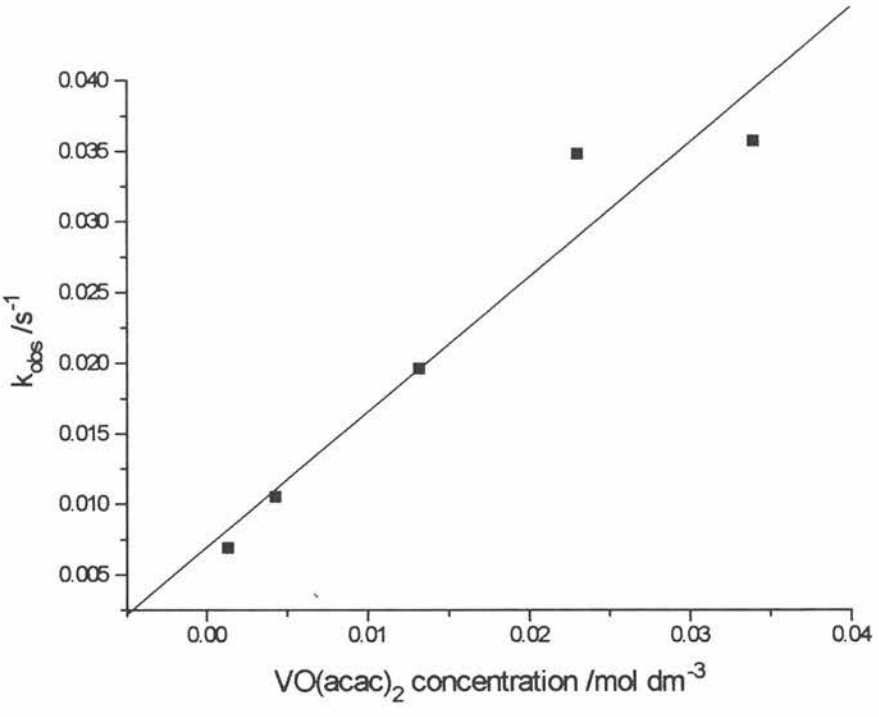
0.040
0.035
0.030
0.025
0.020
0.015
0.010
0.005
k_{obs} /s^{-1}
0.00
0.01
0.02
0.03
0.04
$VO(acac)_2$ concentration /mol dm^{-3}

Figure 10

Figure 11. Oxidation of di-*n*-butyl sulfide (0.459mol dm^{-3}) by *t*-butyl hydroperoxide (0.914 mol dm^{-3}) catalysed by $VO(acac)_2$ (2.18x 10^{-3} mol dm^{-3}) in BRIJ 97 microemulsion (10cm^3, [60% water, 4% hexadecane, 23.6% BRIJ 97, 12.4% *n*-butanol, w/w%]).

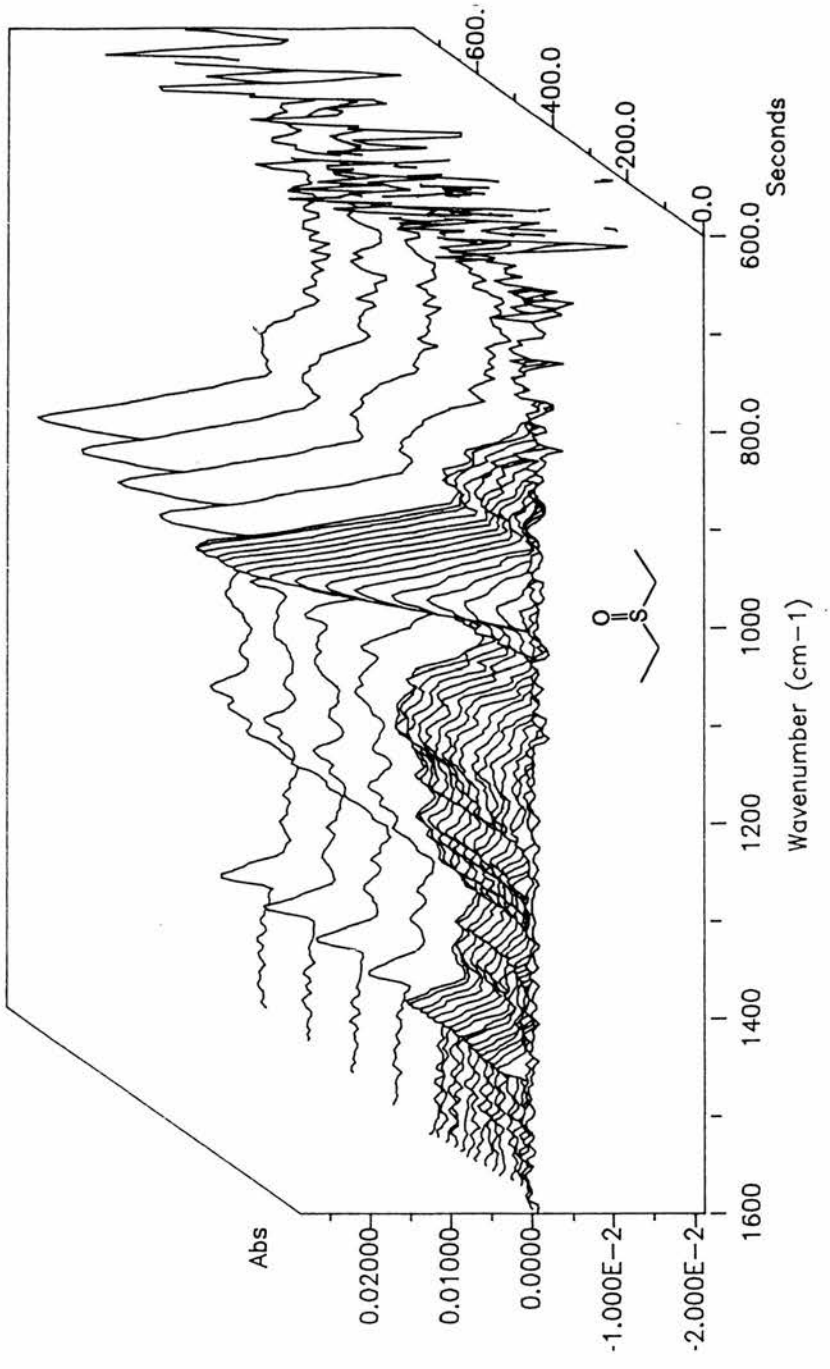

$VO(acac)_2$ promoted oxidation of HD. The oxidation of HD was investigted as described for di-*n*-butyl sulfide. Problems with phase separation were encountered with the BRIJ microemulsion so a number of other formulations were investigated. It was found that the SDS surfactant based micelles gave the best microemulsions with high HD loadings. The results of a typical oxidation run is shown in Figure 12. The plot shows considerable deviation from the pseudo first order plots encountered with the di-*n*-butylsulfide. There is an initial lag phase, which is associated the cloudy non-microemulsion solution. When this clears to give a microemulsion the formation of sulfoxide is extremely rapid. The maximum on the graph indicates that a solution saturated with sulfoxide has formed. After this point colourless crystals formed in the solution. The decrease in absorbance is due to the loss of sulfoxide from the supersaturated solution to give solid sulfoxide.

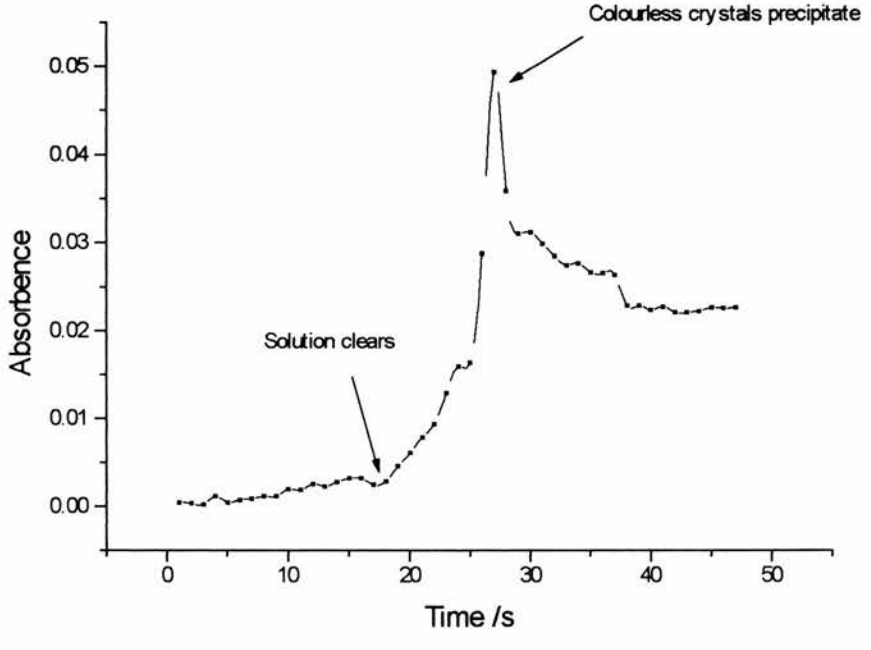

Figure 12. Reaction of *t*-butyl hydroperoxide with mustard in an SDS emulsion with $VO(acac)_2$ as catalyst. A microemulsion forms after some 20 seconds and rapid oxidation occurs.

Figure 13. Oxidation of mustard (0.37mol dm^{-3}) by hydrogen peroxide (0.55mol dm^{-3}) catalysed by $VO(acac)_2$ ($18x10^{-3}$mol dm^{-3}) in SDS microemulsion ($10cm^3$, [3% cyclohexane in 82% water stabilised by 5% sodium dodecyl sulfate and 10% *n*-butanol, w/w%]).

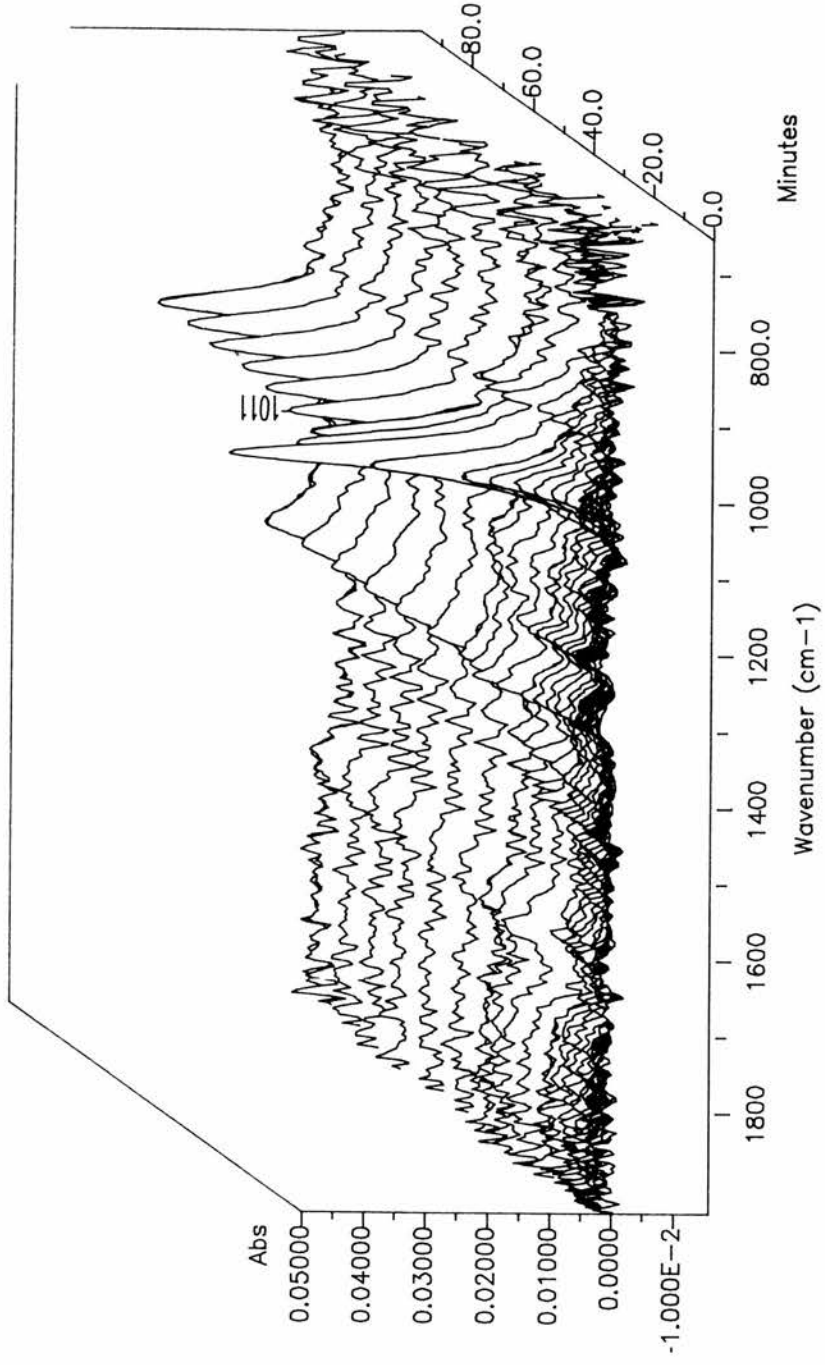

Figure 14. Ir spectrum of *bis*-(2-chloroethyl)sulfoxide and *bis*-(2-chloroethyl)sulfone in *t*-butanol (5cm^3) and water (5cm^3)

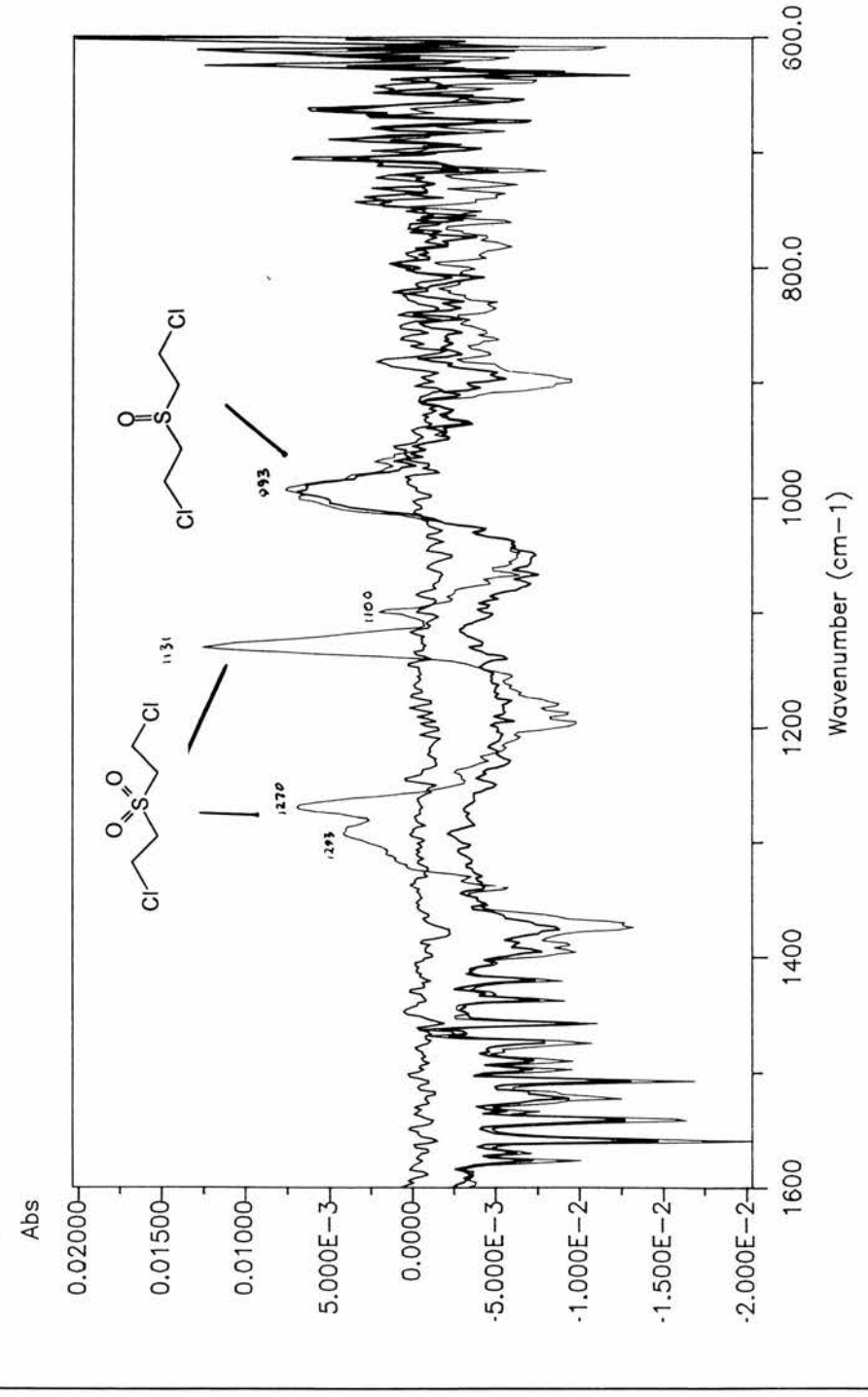

Figure 15. Ir spectrum of di-*n*-butyl sulfoxide and di-*n*-butyl sulfone in *t*-butanol (5cm^3) and water (5cm^3)

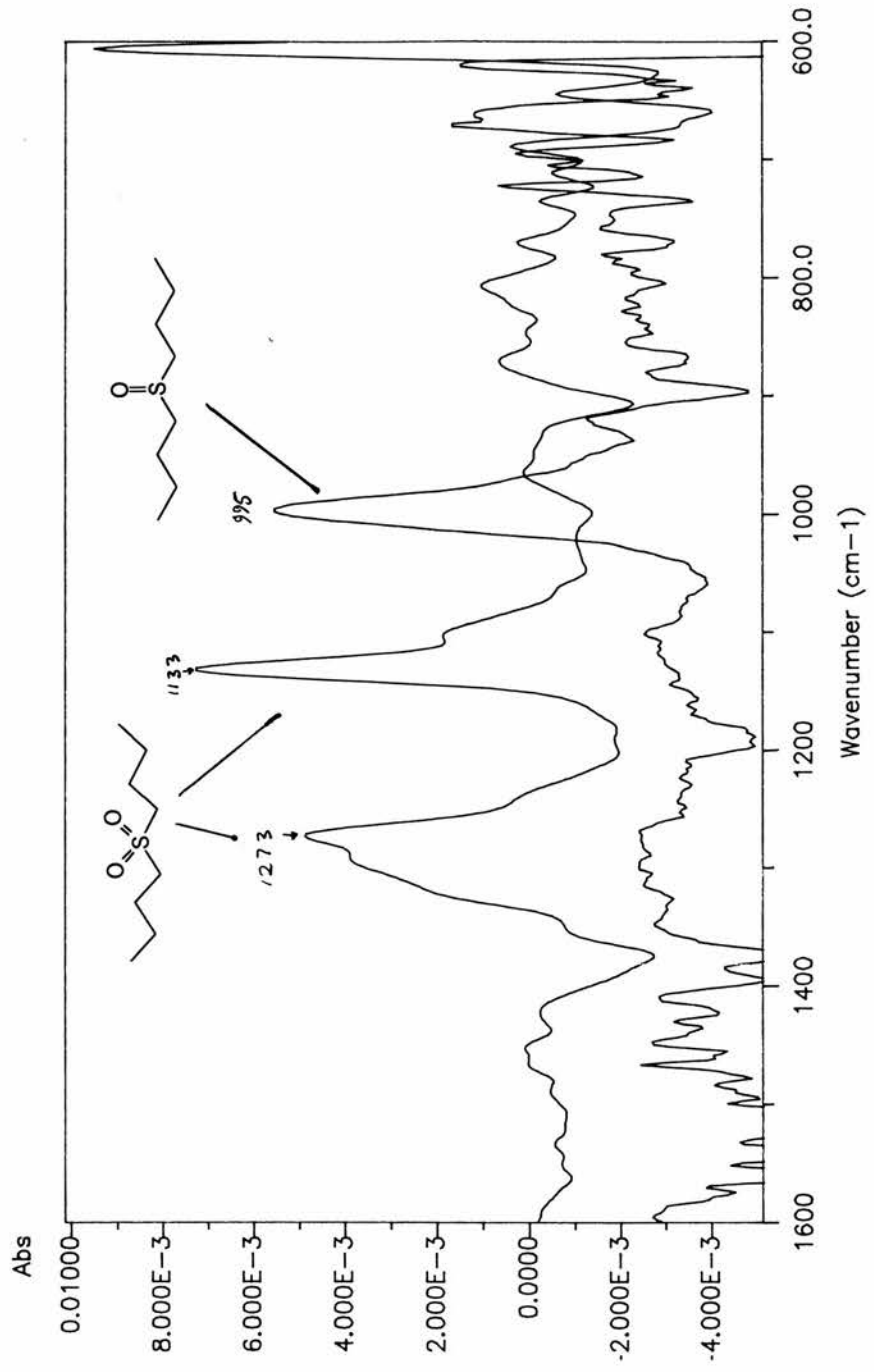

References

[1] K.E.Jackson, *Chem.Rev.*, 1934, **15**, 425.

[2] J.E.Richman and T.J.Atkins, *J.Am.Chem.Soc,* 1974, **96**, 2268.

[3] E.K.Barefield and F.Wagner, *Inorg.Chem.*, 1973,**12**, 2435.

[4] B.E.Bryant and W.C.Fernelius, *Inorg.Syn.*, 1957, **5**, 115.

[5] K.Wieghardt, U.Bossek, D.Ventur and J.Weiss, *J.Chem.Soc.Chem.Commun.*, 1985, 347.

[6] K.Weighardt, *Angew.Chem.Int.Ed.Engl.*, 1989, **28**, 1162.

[7] G.B.Deacon and R.J.Phillips, *Coord.Chem.Rev.*, 1980, **23,** 227; M.Suzuki, M.Mikuriya, S.Murato, A.Uchara, H.Oshio, S.Kida and K.Saito, *Bull.Chem.Soc.Jpn*, 1987, **60**, 4305.

[8] F.M.Menger and A.R.Elrington, *J.Am.Chem.Soc.*, 1991, **113**, 9621.

[9] R.Curci, F.D.Furia, R.Testi and G.Modena., *J.C.S, Perkin II*, 1974, 752.

Appendix I

Potentiometric Procedures

Procedures For Potentiometric Titrations

Introduction

A good introduction to solution equilibria can be found in Albert and Serjeant's book[1]. A modern guide to potentiometric work can be found in Martell's book, "*Determination and Use of Stability Constants*"[2].

Ionic Equilibria.- To take an example, the ionisation of an acid is defined below.

$$HA = H^+ + A^- \qquad (1)$$

For instance ammonium bromide will dissociate in water to give ammonia, protons and bromine ions.

$$NH_4^+Br^- = NH_3 + H^+ + Br^- \qquad (2)$$

Strong acids, bases and their salts, by definition will dissociate completely. These electrolytes first stimulated interest in ionization phenomena and resulted in the first theory of ionization of electrolytes by Arrhenius which was later developed by Bronsted, Lowry and Debye. The theory is based upon the assumption that electrolytes such as sodium chloride, ionize to form sodium cations and chloride anions, in aqueous solution. The realization that in some cases there may not be complete ionization [as in (2)] leads to the proposal that there must be an equilibrium between the associated and dissociated species.

The Law of Mass Action may be used to describe the state of ionic equilibrium. For our example (2) the ratio of products to reactants are fixed:

$$Q = \frac{a_{H+}.a_A}{a_{HA}} \qquad (3)$$ where Q = the equilibrium quotient

It can be seen that since Q is fixed, perturbation of the equilibrium by the external addition of acid or base will change the degree of ionization of the system resulting in the consumption of added acid or base to restore Q to its original value. A comparison of the known H^+ content of a system with the measured free H^+ concentration then provides a way of studying and determining of the equilibrium constant.

Equation (3) is composed of activities of the species involved, as the Law of Active Mass is based on the concept of active masses not concentrations. However, in dilute solutions the component concentrations approaches the value for the activity of the component. Since the determination of the activity of species at infinite dilution and with real solutions is time-consuming, a compromise has to be made. The compromise is to use constant ionic strength. Although the magnitude of the stability constants will not be the same as those found at infinite dilution without supporting electrolyte, the equilibrium constants determined from data at finite concentration in a supporting electrolyte, will be close to equilibrium constants determined at infinite dilution in the supporting electrolyte. The activity coefficients show little concentration dependence in the supporting electrolyte. In practical terms

a_c = [c] at constant ionic strength.

Where [c] is a components molar concentration and ac is the components activity

Molar concentrations may now be substituted directly into the mass balance equations. Provided comparisons are made between equilibria constants determined at the same ionic strength, useful information about the relative stability of complexes can be determined. It

is important to state the ionic strength when reporting the equilibrium constants for a given system. In most modern work the ionic strength used is 0.1 mol dm^{-3} with a 1:1 electrolyte (KCl, KNO_3, $NaClO_4$, $[NBu_4][ClO_4]$ are some common examples) For In our work we have used 0.1 mol dm^{-3} KNO_3 as the supporting electrolyte.

Determination of $[H^+]$, the glass electrode[3].-Under constant ionic strength conditions

$aA + bB = cC + dD$ $K_c = \frac{[C]_c [D]_d}{[A]_a [B]_b}$ since $Q \cong K_c$

The activity of H^+ may be measured by isolation of the H_2/H^+ couple by surrounding one electrode with a glass, which is selectively permeable to H^+, and measurement of the potential relative to the silver/silver chloride couple of the reference electrode in the test solution. The output from the cell is found to vary linearly with the log of the hydrogen ion activity (Nernst equation).

$$E = E_o + S\log a_H$$

Where E is the measured voltage, Eo is a combination of several constants within the system (e.g. reference potentials, junction potentials, etc.), S is the slope of the electrode (RT/nF), and a is the activity of the H^+ ion. At a fixed and constant ionic strength activity is proportional to concentration:

$$E = E_o + S\log C$$

Where C is the concentration and S is slope of the electrode.

By measuring the electrodes potential in both a standardizing solution (C_{std}) and a sample solution, it is possible to calculate the unknown concentration (C_x):

$$E_{std} = E_o + S\log C_{std}$$

$$E_x = E_o + S\log C_x$$

Assuming E_o and S are the same for both solutions (valid in a supporting electrolyte):

$$\log C_x = -\Delta E/S + \log C_s$$

ΔE is the difference between observed potentials in the standardizing and sample solutions. For the measurement of H^+, the quantity pH is commonly used. pH is defined as

$$pH = -\log a_{H+}$$

Assuming that, under the conditions of the experiment, the hydrogen ion activity is equal to hydrogen ion concentration the equation becomes:

$$pH = p[H^+] = -\log[H^+]$$

where $[H^+]$ is the molar concentration of H^+

If a glass electrode is used, $[H^+]$ may be measured:

$$-\log[H_x^+] = \Delta E/S + \log[H_s^+]$$

where $[H_x^+]$ is the sample $[H^+]$ molar concentration and $[H_s^+]$ is the standard solution of $[H^+]$.

Some workers prefer to make up the standard $[H^+]$ solution from known amounts of standard acid. However, we prefer to use buffers for which the pKa's are very accurately known. In this way the pH meter may he calibrated directly in pH units using two standard buffers enabling the slope of the electrode to be determined. A further check on the

linearity of electrode response with $\log[H^+]$ is made by titrating standard acid with standard base, from which the calculated acid concentration may be plotted against $[H^+]$ from electrode measurement. This plot must be linear and is known as a Gran plot The Gran plot and may also be used to assess the CO_3^{2-} content of the standard base (CO_3^{2-} will always be present to a greater or lesser extent in standard alkali solutions, and only becomes a problem when present at over 2% of the total moles of hydroxide).

pH standards used for the calibration of the glass electrode at 25°C

Solution	Buffer substance*	Molality	pH
Phthalate	$KHC_8O_4H_4$	0.05	4.008
borax	$Na_2B_4O_7.10H_2O$	0.01	9.180

*Prepared as described in Vogel[4]

Conventions for Equilibrium Symbols[5].

Ligand protonation Constants.-Consecutive protonation constants are given the symbol K with the subscript defining the protonation step:

$H^+ + L = HL$

$$\log K_1 = \log\left(\frac{[HL]}{[H^+][L]}\right)$$ for the first step, and for subsequent steps

$H^+ + H_{h-1}L_l = H_hL_l$

$$\log K_{lh} = \log\left(\frac{[H_hL]}{[H^+][H_{h-1}L]}\right) \qquad where \quad h \geq 2 \text{ normally } l = 1$$

The cumulative or gross protonation constant is expressed as:

$hH^+ + lL = H_hL_l^{n+}$ where l is normally equal to 1

$$\log \beta_{lh} = \log\left(\frac{[H_hL_l]}{[H^+]^h[L]^l}\right)$$

For example, the protonation of ethylenediamine ($H_2NCH_2CH_2NH_2$):

$H^+ + H_2NCH_2CH_2NH_2 = H_2NCH_2CH_2NH^+_3$

and

$H^+ + H_2NCH_2CH_2NH^+_3 = H_2NCH_2CH_2NH^+_3$

$$\log K_{lh} = \log K_1 = \log\left(\frac{\left[H_2NCH_2CH_2(NH_3)^+\right]}{\left[H^+\right]\left[H_2NCH_2CH_2NH_2\right]}\right) \quad \text{first protonation}$$

$$\log K_{lh} = \log K_{12} = \log\left(\frac{\left[^+(H_3N)CH_2CH_2(NH_3)^+\right]}{\left[H^+\right]\left[H_2NCH_2CH_2(NH_3)^+\right]}\right) \quad \text{second protonation}$$

and the cumulative equilibrium constant is:

$$\log \beta_{12} = \log\left(\frac{\left[^+(H_3N)CH_2CH_2(NH_3)^+\right]}{\left[H^+\right]^2\left[H_2NCH_2CH_2NH_2\right]}\right)$$

Equilibria with metal ions.- The same nomenclature can be expanded to include equilibria involving metal ions:

$$\log \beta_{lmh} = \log\left(\frac{\left[L_l M_m H_h\right]}{\left[L\right]^l\left[M\right]^m\left[H\right]^h}\right)$$

The species model is entered into SUPERQUAD in the form of cumulative constants. To prevent confusion the stability constants for equilibria involving metal ions are tabulated as cumulative constants. These constants are then rationalized as consecutive constants in the discussion. The equilibrium equation is shown explicitly.

Measurements and Materials

Throughout, titrant was added by a microprocessor controlled (VIT90 video titrator) piston burette (ABU91 Radiometer autoburette). Chloride (Orion 9717B) and bromide (Orion9435) selective electrodes were used to detect halide consumption in Ag^+ titrations for the analysis of the halide content of the amine salts. Complexometric titrations to determine ligand concentration were monitored by a copper(II) selective electrode (Orion 9429) The voltage output from the selective electrodes were measured relative to SCE (Orion 900200 reference electrode). pH measurements were made with an Orion Ross Combination electrode (Model 8102). The data were passed from the VIT90 video titrator to a 386 PC by the program TITRAFILE. Conversion of the data to SUPERQUAD format was made using the Fortran program VITOQUAD. The data were processed with SUPERQUAD to give the equilibrium constants. Speciation curves of % species (relative to ligand in speciation curves for protonated ligand species and relative to one equivalent of metal ion in complex species plots) versus pH were calculated by Martell's program SPE and were printed on a HP series III laser printer using the program SPEPLOT.BAS.

Solutions of metal(II) salts were standardised against standard 0.1M edta (Aldrich) in a complexometric titration, monitoring by a copper (II) selective electrode (Cu(II) added as an indicator where necessary). Standard sodium hydroxide was made by dilution of concentrated sodium hydroxide ampoules (Rhone-Poulenc). The standard solution was protected against atmospheric CO_2 by calcium oxide (carbosorb, BDH), and was standardised by titration against accurately weighed samples of potassium hydrogen phthalate. Stock solutions of hydrochloric acid and nitric acid were standardised against standard sodium hydroxide. All aqueous solutions were made up with distilled and boiled out water (kept over a stream of argon whilst cooling). Methanol used in the mixed solvent study was distilled before use over magnesium methoxide in an argon atmosphere.

During the titration, the titration vessel was partially sealed and protected against the ingress of atmospheric CO_2 by blowing nitrogen gas over the solution surface. The temperature was maintained at 25.0°C using a Heto thermostated circulating water jacketed cell.

Unless otherwise stated all measurements were obtained from solutions with ionic strengths adjusted to 0.1 mol dm^{-3} with KNO_3 (Aldrich 99.99%)

The Titration Method.-First a solution containing ligand and acid was titrated, and the protonation constants calculated. Second, titrations are made in the presence of the metal ion, and the metal formation constants calculated.

The test solution can be made up in two possible ways

1) by the dilution of a volume of stock solution of approximately 0.1 mol dm^{-3} in ligand, usually as the hydrobromide or hydrochloride salt

2) addition of an accurately weighed amount of solid ligand directly into the titration vessel.

The first method is to preferred since the halide content of the solution, can be checked by silver nitrate titration. If the amount of available ligand is small addition of the solid directly is preferred.

Determination of the halide content provides an independent check on the acid content (as moles of Br^- or Cl^- mols equals moles of H^+ in the hydrobromide or hydrochloride salt). Halide analysis was made by the titration of a known volume of stock solution with silver nitrate, and monitoring the voltage output from a chloride sensitive electrode. A sudden change in potential signifies that the end point has been reached (the use of a computer controlled piston burette with a end-point analysis program automates this time consuming procedure). The same experimental technique was used in the complexometric titration. In this case the halide selective electrode was replaced with a Cu-selectrode. The end point signifies complete formation of the copper(II) EDTA complex and the presence of free copper(II) in solution. A good end point requires the formation of a complex species with a high formation constant and it should be born in mind that the ligand may also form bis or binuclear complexes. In these circumstances the titration with copper(II) may well give important information on the complexing properties of the ligand even before the potentiometric titration proper has begun.

When it is not possible to make up a 0.1 mol dm^{-3} solution of the ligand for reasons of low solubility or availability, the solutions are made up by the addition of an accurately known

weight of ligand to a volume of electrolyte. If required acid is added and the solution titrated. The solution can then be reacidified and titrated for a second time. The first titration enables not only the determination of protonation constants of the ligand, but a check on the molar concentration of acid and ligand present in solution. Often the concentrations are as expected, but for the large macrocycles, inaccuracies on the order of only 0.5% may be sufficient to cause SUPERQUAD calculation to stall. In these cases the acid and ligand molar concentration were varied to get a good fit. These values were then used as the input for the determination of metal ion constants for the second titration. Generally the concentrations needed less than 0.5% adjustment. As the second titration is on a solution with known ligand and acid contents the computation of equilibrium constants was made with no further adjustments of ligand and hydrogen ion concentration, apart from that required to account for added hydroxide and re-acidification.

Potentiometry using mixed solvent systems.- The electrode was calibrated as for a purely aqueous system with the same standard buffers (borax and potassium hydrogen phthalate). The electrode was checked in the mixed solvent system by titrating standard acid (H_2SO_4, Aldrich, 0.1008 mol dm^{-3})in the presence of electrolyte. A Gran plot gave an indication of CO_3^{2-} contamination and any deviations from linear behaviour. The $logK_w$ for the solvent conditions could also be determined from the inflexion point, and entered into the SUPERQUAD calculations as the 00-1 species.

For example, in the benzimidazole system 50%wt MeOH was used as the solvent. A value of 7.058 pH units was obtained indicating a pK_w of -14.12. In purely aqueous systems at 0.1 mol dm^{-3} ionic strength, pK_w is 13.86 (i.e. an inflexion point at pH 6.93). This equates to a pH increase of 0.128 when pH measurements are made in 50%wt MeOH using a glass electrode calibrated in water. This result compares favorably with the correction value of 0.124 pH units which Bates *et al*[6] found necessary to subtract from pH values determined in 50% methanolic solutions (**Figure 1**).

There have been discussions on the utility of "Universal pH scales" and conversion factors to enable a comparison of the activity of the hydrogen ion under a wide variety of experimental conditions. It seems likely that calibration of the glass electrode with aqueous buffers will always remain the technique of choice in laboratories where the vast majority

of situations require pH determination in purely aqueous solution. The pH values used are those that would be obtained if the pH electrode was calibrated in water. The practical pH (aH*) may be found by the subtraction of 0.124 after the manner of Bates *et al* for comparison with wholly aqueous systems.

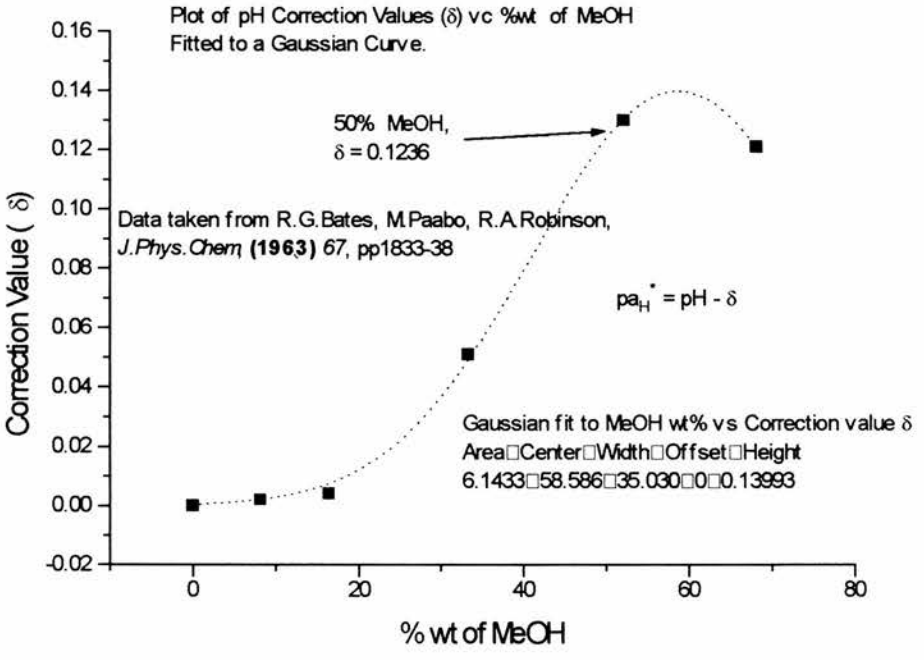

Figure 1

Computation

All equilibrium constants were computed using the program SUPERQUAD. The protonation constants were first determined from titrations in the absence of metal ions. These were entered as constants (along with K_w) in the species model for titrations in the presence of metal ions. The calculation of protonation constants is reasonably easy, since the number of protonation sites are known for the ligand and for HBr salts analytical data

gives the stiochiometry of titratable protons to be expected so the formulation of a species model is simple. Finding the species model for the complexed species is much more problematical. A careful look at the the titration curves (plotted as [B]/[L] vs pH) helps to identify the presence of protonated species and hydroxo complexes. Titrations at differing [L]:[M] concentrations must be made to see if there are any *bis* or *tris* complexes in solution. Evidence for dimerisation can be found if good agreement of stability constants is found for runs at one concentration, but at higher concentration show significant differences in the equilibrium constants.

Initially the titrations are processed individually to get reasonable estimates of logβ and some feel for the species model. Equilibrium constants for species that may only be minor components are entered as constants. When a good fit is found the titration curves are combined and all of the species minimized. This usually results in a larger σ and X^2 value for the minimization, and some of the minor species may be lost, but it will provide a more realistic estimation of error and a more realistic model of the system.

Potentiometric/Spectrophotometric titrations and HYPERQUAD.

Introduction.-The potentiometric technique has proven to be a useful tool for studying the solution chemistry of a wide range of systems. However, as more complicated applications are investigated, more complicated models have to be entered into SUPERQUAD. Unfortunately as the number of possible equilibria in a given system increases so does the possibility of picking the wrong model. It may even be possible to have (on grounds of error inspection only) more than one model to describe the system. For this reason it is important to determine stability constants with more than one experimental technique. The program HYPERQUAD uses spectrophotometric data to determine stability constants.

Titration method.-As for the potentiometric titrations, an acidic mixture of metal ions and ligand are titrated with base, but at intervals during the titration the spectrum of the solution is taken the and quantity of NaOH added noted.

Computation.-Computation and processing of the spectra are made using the suite of programs called HYPERQUAD writen by P.Gans. Below is a brief summary of the prrocedure for processing spectra.

The error in the absorbances has to be determined. Spectra over the wavelength and absorbance range of the test solution are collected from a suitable standard (holmium filter or a blue Whatman filter for copper(II) solutions). Ten spectra were used in our calculations. These spectra are then converted to ASCCI format and used as the input for HABER which allows the trial and error fitting of an exponential or quadratic function to the error versus absorbence data (it is assumed that error does not vary significantly with wavelength). The titration spectra are collected and converted to HYPERQUAD format by HEDIT. The program HEDIT outputs an organisation file (.CON) which contains directions for the other programs for the spectrum data (.BAD) and the model and mmole concentrations of the components (.PAR). The spectra are initially processed at single wavelength in HYDRASP. The program HYDRASP contains a number of data manipulation functions to aid the picking the model, estimation of the stability constants and preparation of the files (.PAD) for an "all wavelengths" calculation. Once the .PAD file is prepared the adjustment of the species model is the same as for SUPERQUAD.

References

[1] A.Albert and E.P.Serjeant, *Ionisation Constants of Acids and Bases*, Methuen & Co Ltd, London, 1st edition, 1962.

[2] A.E.Martell and R.J.Motekaitis, *Determination and Use of Stability Constants*, VCH 1988.

[3] Powell, *Analytical Chem.*, 1971, **43,** 1206.

[4] A.I.Vogel, *Text Book of Quantitative Inorganic Analysis*, Fourth Ed., Longman Group Ltd. 1978, 587.

[5] L.G.Sillen and A.E.Martell, *Stability Constants of Metal-ion Complexes*, The Chemical Society, London,1964, p xi.

[6] R.G.Bates, M.Paabo and R.A.Robinson, *J.Phys.Chem.*, 1963, **67**, 1833.